Non-linear behavioural New Keynesian models: Design and estimation

Arioli, R.

Publication date
2022

Document Version
Final published version

PhD Thesis

Non-Linear Behavioural New Keynesian Models: Design and Estimation

Author:
Rodolfo Arioli

Supervisors:
Prof. Dr. Cars Hommes
Prof. Dr. Paul Levine

A thesis submitted in fulfillment of the requirements for the degree of Doctor of Philosophy

University of Surrey
University of Amsterdam

ExSide Programme

Non-Linear Behavioural New Keynesian Models: Design and Estimation

ACADEMISCH PROEFSCHRIFT

ter verkrijging van de graad van doctor
aan de Universiteit van Amsterdam
op gezag van de Rector Magnificus
prof. dr. ir. P.P.C.C. Verbeek
ten overstaan van een door het College voor Promoties ingestelde commissie,
in het openbaar te verdedigen in de Agnietenkapel
op woensdag 21 december 2022, te 16.00 uur

door Rodolfo Arioli
geboren te Aprilia

Promotiecommissie:

Promotores:	prof. dr. C.H. Hommes	Universiteit van Amsterdam
	prof. dr. P.L. Levine	University of Surrey
Overige leden:	prof. dr. C.G.H. Diks	Universiteit van Amsterdam
	prof. dr. J. Tuinstra	Universiteit van Amsterdam
	dr. K. Mavromatis	De Nederlandsche Bank
	prof. dr. M. Ben-Gad	City University of London
	prof. dr. R. Dennis	University of Glasgow
	dr. H. Joo	University of Surrey

Faculteit Economie en Bedrijfskunde

Dit proefschrift is tot stand gekomen in het kader van het Marie Skłodowska-Curie Actions Innovative Training Network 'Expectations and Social Influence Dynamics in Economics' (ExSIDE), met als doel het behalen van een gezamenlijk doctoraat. Het proefschrift is voorbereid in de Faculteit Economie en Bedrijfskunde van de Universiteit van Amsterdam en in de School of Economics van de University of Surrey.

This thesis has been written within the framework of the Marie Skłodowska-Curie Actions Innovative Training Network 'Expectations and Social Influence Dynamics in Economics' (ExSIDE), with the purpose of obtaining a joint doctorate degree. The thesis was prepared in the Faculty of Economics and Business at the University of Amsterdam and in the School of Economics at the University of Surrey.

Declaration of Authorship

I, Rodolfo Arioli[1], declare that this thesis titled, "Non-Linear Behavioural New Keynesian Models: Design and Estimation" and the work presented in it are my own. I confirm that:

- This thesis and the work to which it refers are the results of my own efforts. Any ideas, data, images or text resulting from the work of others (whether published or unpublished) are fully identified as such within the work and attributed to their originator in the text, bibliography or in footnotes.
- This thesis has not been submitted in whole or in part for any other academic degree or professional qualification.
- I agree that the University has the right to submit my work to the plagiarism detection service TurnitinUK for originality checks. Whether or not drafts have been so assessed, the University reserves the right to require an electronic version of the final document (as submitted) for assessment as above.
- This work has received funding from the European Union's Horizon 2020 research and innovation programme under the Marie Skłodowska-Curie grant agreement No 721846, Expectations and Social Influence Dynamics in Economics (ExSIDE)
- The views expressed do not reflect the official position of the European Central Bank or the Eurosystem.

Date: 23 August 2022
Signed:

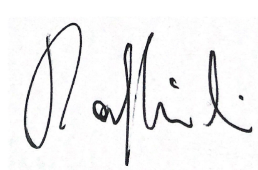

[1]rodolfoarioli@gmail.com

Abstract

This thesis studies empirical Behavioural New Keynesian (NK) DSGE models that incorporate *heterogeneous expectations* and *reinforcement learning* (Brock and Hommes, 1997) to endogenise the distribution of agent types, with a specific focus on the use of higher-order estimation methods to capture the highly non-linear features of the learning mechanism. The thesis is composed of three chapters.

Chapter 1 investigates the properties of efficient local Gaussian-based filters for Bayesian posterior inference on the parameters of non-linear DSGE models. A variety of filters is assessed estimating artificial data generated from the simulation of the fifth-order Taylor expansion of a Real Business Cycle (RBC) model: the second-order Extended Kalman filter, a linear Kalman filter applied on the stochastic steady state resulting from a higher-order approximation of the model, and sigma-point filters - such as the Unscented Kalman filter and the Cubature Kalman filter. Results show these filtering techniques represent a valid alternative to the particle filter for problems requiring highly computational efforts.

Chapter 2 develops a Behavioural NK model enriched with portfolio adjustment costs to study long-term asset purchases. Adjustment costs on the composition of the households' financial portfolio allow for bond-market segmentation by introducing a wedge on the yields paid by bonds with different duration. *Reinforcement learning* combined with bounded-rational agents introduces state-dependent asset-purchases multipliers, by linking policy measures to the sentiment prevailing in the economy. In this framework, policy experiments support the role of asset purchase programs as counter-cyclical measures and emphasize the importance of Central Bank credibility for monetary policy transmission.

Chapter 3 estimates a small Behavioural NK model with trend inflation. A formal test for parameters identification shows that core *reinforcement learning* parameters can only be jointly identified using higher-order approximations of the model while expanding the information set with a measure of the share of agents adopting a specific expectations mechanism. Thus, a proxy for the share of *näive* agents based on the *Survey of Consumer Expectations* by the University of Michigan is exploited for estimating the *intensity of choice* and the *memory* parameters with the Bayesian non-linear filtering technique selected in Chapter 1 - the second-order Extended Kalman filter. Model estimates outperform a rational expectation counterpart in matching higher-order empirical moments.

Abstract

Deze dissertatie bestudeert empirische Behavioural New Keynesian (BNK) DSGE-modellen gebruikmakend van heterogene verwachtingen en versterkingsleren (Brock en Hommes, 1997) om de verdeling van agententypen te endogeniseren, met de nadruk op hogere-orde schattingsmethoden om de niet-lineaire kenmerken van het leermechanisme vast te leggen.

Hoofdstuk 1 onderzoekt de eigenschappen van efficiënte lokale Gaussiaanse filters voor Bayesiaanse posterieure inferentie van de parameters van niet-lineaire DSGE-modellen. Een verscheidenheid aan filters wordt beoordeeld door het schatten van kunstmatige gegevens: het tweede-orde extended Kalman filter, een lineaire Kalman filter toegepast op de stochastische steady state die voortvloeit uit een hogere-orde benadering van het model, en sigma-punt filters. De resultaten laten zien dat deze filtertechnieken kunnen helpen bij empirische problemen die grote rekeninspanningen vergen.

Hoofdstuk 2 ontwikkelt een BNK-model verrijkt met aanpassingskosten voor de studie van lange-termijnaankopen van activa. Aanpassingskosten voor de samenstelling van de financiële portefeuille van de huishoudens maken segmentatie van de obligatiemarkt mogelijk door een wig te introduceren tussen het rendement van obligaties van verschillende duur en?. Versterkingsleren in combinatie met gebonden rationele agenten wordt gebruikt om toestandsafhankelijke multiplicatoren van activa-aankopen te bestuderen, door beleidsmaatregelen te koppelen aan het endogene economische sentiment.

Hoofdstuk 3 schat een klein BNK-model met trendmatige inflatie. Een formele test voor de identificatie van de parameters toont aan dat de kernparameters van het versterkingsleren alleen gezamenlijk kunnen worden geïdentificeerd met behulp van hogere orde benaderingen van het model, terwijl de informatieverzameling wordt uitgebreid met een proxy voor het aandeel van agenttypes op basis van enquêtegegevens van consumenten. Modelramingen op basis van niet-lineaire filtertechnieken presteren beter dan een tegenhanger van de rationele verwachting bij het matchen van empirische momenten van hogere orde.

Acknowledgements

I am grateful to Paul and Cars, my supervisors, for their constant support along the way and for sharing their passion for research with me. To Paul, for always being positive also in the difficult moments, and Cars, for his pragmatism when things got complicated, without this complementarity I would not have succeeded in completing this journey.

I also would like to thank Thomas Dumitru Holden for his guidance during our time at the University of Surrey.

A special thank to my friends Son and Alessandro for their constant presence, especially in hard times.

Thanks to my ECB Management at the PAC Division, allowing me to pursue this project and, in particular, to Chiara for pushing me forward.

Thanks to my friends at the University of Surrey and at the University of Amsterdam for the fruitful discussions and the fun we had together, and to the Korego Theater Group for being my family in Amsterdam.

This thesis has also benefited from many discussions and correspondences, especially with faculty members from University of Surrey, University of Amsterdam, and the ExSIDE consortium.

Last but not least, I am grateful to Susanna, a central pillar of my life, for her continuous encouragement and comprehension.

A mio nonno, Rodolfo, e mio padre, Roberto, grazie ai quali ho avuto tante opportunità.

Contents

List of Figures

List of Tables

Introduction

Dynamic Stochastic General Equilibrium (DSGE) models reproduce dynamic optimal decision making of households, firms, and government, and represent a well established laboratory for policy evaluation. Policy actions enter these models as random shocks influencing the evolution of macroeconomic variables such as GDP, consumption, and inflation over time. In this framework, the way agents form expectations is crucial to determine the magnitude and persistence of the transmission of policy shocks to the economy. The majority of DSGE models assume agents behave under *fully informed rational expectations* (FIRE) hypothesis, i.e. agents know the exact structure of the economy and are able to consider timely and complete information when taking decisions.

This dissertation studies empirical Behavioural DSGE models which incorporate heterogeneous expectations and *reinforcement learning* (Brock and Hommes, 1997) to endogenise the distribution of agent types, with a specific focus on the use of higher-order estimation methods to capture the highly non-linear features of the learning mechanism. In these models, agents can gradually adjust the way they form expectations on the basis of the past performance of a specific forecasting rule and a random component. The possibility of switching across rules introduces highly non-linear dynamics, which can only be fully captured with higher-order approximations of the model.

Consequently, non-linear estimation methods become essential for estimating model parameters. The choice of this expectation formation mechanism is motivated by its ability to reproduce the higher-order moments observed in macroeconomic time-series, while being consistent with empirical findings based on survey data and laboratory experiments. Therefore, they can usefully complement FIRE DSGE models in assessing newly designed policies and helping public bodies in taking more aware decisions.

The thesis is composed of three chapters.

The first chapter investigates the properties of *local* Gaussian-based filters for Bayesian posterior inference on the parameters of non-linear DSGE models. These filtering techniques are known to be more efficient than *global* filters, based on Sequential Monte Carlo simulations. *Local-Gaussian* filters represent an alternative to estimate models incorporating heterogeneous expectations and reinforcement learning as these features lead to a quick increase of the state-space representation of the model. A variety of *local-Gaussian* filters is assessed by estimating artificial data generated from the simulation of the fifth-order Taylor expansion of a Real Business Cycle (RBC) model: the second-order extended Kalman filter, a linear Kalman filter applied on the stochastic steady-state resulting from a higher-order approximation of the model, and sigma-point filters - such as the Unscented Kalman filter, the Cubature Kalman filter and an application of the latter on a sparse grid of points (i.e. Gaussian Particle filter). The accuracy and efficiency of these filters are compared against a standard particle filter with resampling.

Results show *local-Gaussian* filters represent a relatively reliable alternative to the particle filter when computational costs become excessive.

In an environment characterised by realistic non-linearities, accuracy was higher for the examined *local-Gaussian* filters than for a particle filter.

With more extreme non-linearities, accuracy deteriorates for all filters, showing the difficulty of these tools in dealing with highly volatile systems. Nonetheless, the Cubature Kalman filter and the second-order Extended Kalman filter were, on average, as accurate as the particle filter while confirming their superior efficiency.
As a result, these filtering techniques are a useful device for estimating medium-scale non-linear models and can be applied for an initial estimation of higher-order models featuring heavily non-Gaussian latent variables before moving to more computationally intensive methods.

In the following chapters, *reinforcement learning* is applied under different degrees of *bounded rationality*. In the second chapter, agents are assumed to be either backward-looking or *fundamentalists*, whereas, in the third chapter, the latter are substituted by *fully rational* agents. While *fundamentalists* know the fundamental steady state of the model, but are not aware of the existence of other agent types and do not consider the possibility of persistent shocks, *fully rational* agents know the full system, but have to pay a persistent random cost to benefit of this knowledge. This difference offers alternative analytical elements. *Fundamentalists* lead to a fully backward-looking system of equations which can be solved recursively as deterministic models; thus it allows to consider the direct effects of a fully non-linear *reinforcement learning* mechanism for model dynamics. By contrast, although requiring an approximation of the non-linearities, the presence of *fully rational* agents (i.e. forward-looking) introduces precautionary behaviour thereby easing comparisons against standard FIRE models.

The second chapter develops a New Keynesian model enriched with heterogeneous expectations, reinforcement learning and portfolio adjustment costs to study long-term asset purchases. Adjustment costs on the composition of the households financial portfolio allow for bond-market segmentation by introducing a wedge on the yields paid by bonds with different duration. Thanks to this friction, the Central Bank can influence consumption decisions by lowering long-term interest rates through the purchase of long-term assets.

Reinforcement learning combined with bounded-rational agents are exploited to introduce state-dependent asset-purchases multipliers. In such framework, the share of agents adopting a specific forecasting rule dynamically determines the level of economic confidence and trust in the Central Bank target in each period. Thus, the transmission of standard and non-standard monetary policy shocks varies with the economic sentiment prevailing in the economy. A Monte Carlo exercise shows that this set-up can provide interesting insights on the robustness of long-term asset purchase programs. Even though the effects of asset purchases across different simulations are on average similar to those from standard FIRE DSGE models, *reinforcement learning* highlights the importance of economic sentiment for the success of a policy. In fact, the positive short-term pass-through of asset purchases is stronger when confidence is either extremely high or extremely low. Considering the robust empirical link between output gap and sentiment indicators, structurally reproduced by the model, asset purchases are promoted as a valid counter-cyclical measure. Moreover, the effectiveness of asset purchases is stronger with elevated Central Bank credibility, thus providing a further layer of complexity to test these instruments. Finally, the chapter sheds light on the adequate policy mix to reduce economic uncertainty under *reinforcement learning*, emphasising the role of the *Taylor principle* as a necessary condition for stability, and stresses the importance of output-gap stabilization in reducing the frequency of high-volatility episodes.

The third chapter estimates a small Behavioural New Keynesian model with trend inflation characterised by *reinforcement learning* where agents can be either backward-looking or fully rational. In particular, this estimation targets the core parameters of the heuristic switching learning mechanism: the *intensity of choice* parameter, ruling agents sensitivity to changes in relative utility linked to the performance of forecast rules, the *cost of being rational*, describing the effort of gaining deep and timely knowledge of model dynamics, and *memory parameters*, weighting the importance of past forecast errors for the selection of a forecast rule. A formal test for local identification of parameters in non-linear DSGE models confirms that higher-order approximations are needed for identifying *reinforcement learning* parameters, and that observing the share of agents adopting a specific forecasting rule is useful for disentangling the value of the *intensity of choice* parameter. Thus, the information set is augmented with a proxy for the share of *näives* based on the qualitative questions on business activity from the "*Survey of Consumer Expectations*" held by the *University of Michigan*. Relying on results from *Chapter 1*, direct inference based on the second-order Extended Kalman filter in a Bayesian framework suggests higher values of the *intensity of choice* parameter relative to what assumed in previous studies. Moreover, a validation exercise provide evidence that the Behavioural NK model can outperform its fully rational counterpart in matching empirical higher-order moments, even in the small departure analysed in this paper.

Chapter 1

Non-linear Estimation of DSGE Models: Assessing Gaussian Filters

Abstract

This paper assesses the performance of novel methods for the estimation of non-linear DSGE models. Given the well-known curse of dimensionality issue affecting particle filters, alternative methods -more suitable for the estimation of medium-scale DSGE models- are considered. For this purpose, a range of *local-Gaussian* filtering techniques is compared to the particle filter in terms of accuracy and computational efficiency. In particular, the paper evaluates the performance of sigma-point filters, as the Cubature Kalman filter (Arasaratnam and Haykin, 2009), the Unscented Kalman filter (Julier and Uhlmann, 2004), the second-order extended Kalman filter (Gustafsson and Hendeby, 2012) and risky linear approximations *à la* Meyer-Gohde (2014b). Results from a Monte Carlo exercise based on artificial data suggest that *local-Gaussian* filters represent a valid candidate to estimate medium-scale non-linear DSGE models. All filters analysed showed to be a reasonable alternative to the particle filter in a context characterized by limited non-linearities. When dealing with higher volatility, the second-order Extended Kalman filter and the Cubature Kalman filter were as accurate as the particle filter while being evidently more efficient.

JEL Classification: [C11 E1]
Keywords: Nonlinear DSGE - Cubature Kalman Filter - Unscented Kalman filter - Gaussian Filters - Extended Kalman Filter - Risky Linear Approximations - Particle Filter

1.1 Introduction

The last financial crisis proved that linear DSGE models were not well-equipped for modelling the complexity of the economic environment. A linear framework, in fact, could not include relevant non-linear modelling elements that would instead better capture actual economic dynamics.

As a direct consequence, a new flourishing stream of non-linear DSGE models developed over the last decade. Non-linearities such as those generated by asymmetric shocks, stochastic volatility and occasionally binding constraints have thus become recurrent elements in the DSGE literature.

Standard applications of DSGE models rely on the linearisation of the model around the non-stochastic steady state. This approach allows to efficiently solve the model, to the detriment of relevant non-linear features. For instance, in a linear world, it is not possible to capture the role of uncertainty on agents' behaviour (Schmitt-Grohé and Uribe, 2004b). Moreover, some dynamics cannot be reproduced in a linear framework, and -for example- it is not possible to model the evolution of the proportion of rational agents in a Behavioural DSGE model with reinforcement learning (Deák et al., 2017a). Some of the parameters characterising the reinforcement learning mechanism *à la Brock and Hommes (1997)* are not identifiable with a linear approximation of the model and the shares of agents become constant. Thereof, the role of higher-order approximations gain relevance.

Unfortunately, the non-linear features bring about complex computational problems when estimating model parameters. First, finding solutions to models characterised by significant non-linearities represents a cumbersome task. Secondly, when a solution is obtained, it results in a non-linear state-space representation which cannot efficiently be treated with traditional linear tools like the standard Kalman filter.

Although the application of higher-order perturbation methods allowed to solve non-linear models relatively quickly (Schmitt-Grohé and Uribe, 2004b; Andreasen et al., 2018), non-linear estimation of DSGE models is not yet regularly employed for policy decision-making because standard techniques - such as particle filters (Fernández-Villaverde and Rubio-Ramírez, 2005) or moment-based estimators (Ruge-Murcia, 2012) - are instead not efficient enough. For the sake of computational efficiency, recent research has concentrated its attention on *local-Gaussian* filters (Ivashchenko, 2014; Binning and Maih, 2015; Holden, 2017; Noh, 2019).

Although these techniques rely on the strong assumption that latent states are normally distributed, it was demonstrated that they can challenge particle filters in terms of accuracy, while notably reducing computational efforts (Andreasen, 2013; Kollmann, 2015, 2017; Noh, 2019).

This study contributes to the literature on estimation of non-linear DSGE models by computationally evaluating the performance of a variety of *local-Gaussian* filters measured in terms of efficiency and accuracy. The assessment results from an estimation exercise based on simulated data which were generated from a small Real Business Cycle model.

Specifically, the paper will analyse the properties of two *local-Gaussian* sigma-point filters - the Cubature Kalman filter (Arasaratnam and Haykin, 2009) and the Unscented Kalman filter (Julier et al., 1995) - and will compare them with recently developed alternatives, such as the second-order extended Kalman filter (Gustafsson and Hendeby, 2012) and risky-linear approximations (Meyer-Gohde, 2014b). These results will be evaluated against more global methods like the Gaussian Particle filter (Kotecha and Djuric, 2003) - a *semi-Global* filter applying the Cubature Kalman filter on a sparse matrix of nodes - and a standard particle filter with resampling (Andrieu et al., 2001).

Three questions are asked: are *local-Gaussian* filters reliable? Which *local-Gaussian* filter is the most efficient? Which filter provides the best estimates of latent variables and parameters?

Following similar studies (Fernández-Villaverde and Rubio-Ramírez, 2005; Noh, 2019), this paper tries to provide an answer by means of two Monte Carlo exercises estimating models parameters on artificial data simulated from a fifth-order approximation of the model. In the *Benchmark* exercise, data is generated by parametrizing the model to reproduce realistic non-linearities whereas, in the second exercise, a *Risky* parametrization was chosen to produce highly non-linear dynamics with the purpose to evaluate the filters under different degrees of non-linearity.

The results of the exercise show that *local-Gaussian* filters, applied on a second-order Taylor expansion of the model, represent a good alternative to the particle filter in terms of accuracy.

Accuracy, measured in terms of Average Relative Parameters biases (ARB) evaluated at the posterior mode and Root Mean Squared Errors (RMSE) on filtered latent variables (non-observed states and exogenous shocks), was higher for *local-Gaussian* filters than for a particle filter in an environment characterised by realistic non-linearities.

Increasing model non-linearities, all filters become, on average, less accurate. Nonetheless, the Cubature Kalman and the second-order Extended Kalman filter were as accurate as the assessed particle filter.

In terms of efficiency, all *local-Gaussian* filters were more efficient than the particle filter in spite of the limited number of particles used for this exercise thereby showing their usefulness for applications considering medium-scale models.

The rest of the paper is organised as follows: Section 1.2 introduces the reader to estimation methods for non-linear DSGE models and reviews some of the relevant DSGE literature. Section 1.3 will shed light on methods to apply the Kalman filters in a non-linear framework. Section 1.4 presents the features of the baseline model and the solution method. Section 1.5 presents the metrics for evaluating accuracy and efficiency and the results of the paper. Finally, 1.6 proposes some conclusions.

1.2 Estimation Methods

Estimating non-linear DSGE models generally relies on two approaches: direct inference and the method of moments. Direct inference applies filtering techniques to track the evolution of latent variables (i.e. shocks and non-observed endogenous variables) and recover parameters by minimizing the loss function generated by the model. The method of moments singles out the parameters minimizing the distance between selected empirical moments and the respective ones associated to the model.

Filtering techniques have been extensively applied for the estimation of both linear and non-linear DSGE models (Smets and Wouters, 2007; Fernández-Villaverde and Rubio-Ramírez, 2007). Given a set of observable variables, these methods allow to approximate the likelihood of latent states and, ultimately, apply Bayesian inference to estimate model parameters.

In a linear context, DSGE models solutions can be represented by linear state-space systems of equations with Gaussian random variables. As linear combinations of Gaussian variables are generally still Gaussian, it is possible to use the Kalman filter to recursively compute their sample likelihood. By contrast, higher-order approximations do not benefit of this property as Gaussian variables in a non-linear state-space representation originate non-Gaussian distributions. Therefore, it is no longer possible to apply the standard Kalman filter to map the path of latent variables.

A solution to this problem is offered by *global* and *local-Gaussian* non-linear filters. *Global* filters try to approximate the full sample likelihood using genetic algorithms, as Sequential Monte Carlo (SMC) simulations. *Local-Gaussian* filters assume that the predictive and filtering densities of the filter are Gaussian and uses a non-linear approximation of the model to shape these density functions, which in practical terms means tracking their mean and variance.

Global filters can deliver unbiased estimates of the sample likelihood and can theoretically reproduce its complete structure.

Fernández-Villaverde and Rubio-Ramírez (2005) introduced the particle filter in combination with the Metropolis-Hasting algorithm (PF-MH algorithm) to recover the deep parameters of a non-linear DSGE model with Bayesian methods.

Since then, many variants of the Sequential Importance Sampling (SIS) algorithm were deployed to increase the accuracy of estimates. The Sequential Importance Sampling with Resampling (SISR) algorithm, embedding systematic resampling after every iteration of the SIS algorithm, was developed to overcome the issue that most of the likelihood density was assigned to a single particle, also called *particle degeneracy* issue. The Auxiliary Particle filter (Pitt and Shephard, 1999) was introduced to improve efficiency and better deal with fat-tailed distributions by adding a resampling step on past particles only when the predictive density is more informative about the value of observed states than the transition density. In a similar vein, conditional particle filters, embedding a non-linear Kalman filter to compute the predictive densities, were also applied on DSGE models (Amisano and Tristani, 2010; Murray et al., 2012). In order to better address problems with multi-modal posteriors, Chopin et al. (2013) developed the SMC^2 algorithm by introducing a particle filter iteration in the correction and mutation steps of the SMC algorithm. Iiboshi et al. (2020, 2022) recently applied it in a model with the zero-lower bound.

Herbst and Schorfheide (2019) developed a particle filter algorithm based on tempering, that is sequentially adding data to the likelihood function in order to reduce the number of evaluations. The algorithm is initialised with large measurement errors to help the particle filter better explore the likelihood surface and iteratively converge to a good tempering level in terms of efficiency and unbiasedness.

Although these alternatives allowed to speed up the estimation process, the computational burden is still too high. In fact, these algorithms are subject to a *curse of dimensionality* problem: the number of iterations directly increases with the number of states, particles and observations. Moreover, each endogenous variable needs to be predicted and filtered using numerical integration for every particle, and eventually a resampling step is executed after these operations. As accuracy depends on the number of particles, there exists an important trade-off between computational tractability and the quality of estimates, especially with large models.

Local-Gaussian filters enable the application of linear filtering techniques to non-linear models under the assumption of Gaussian prediction and filtering distributions. This reduces computational efforts and provide higher precision compared to particle filters. In an exercise similar to this one, Noh (2019) showed that Gaussian-mixture filters can outperform particle filters in estimating a Neo-Classical model with stochastic volatility. Comparably, both a Kalman filter applied on a second-order approximation based on pruning (Kollmann, 2015) and the Divided Difference Kalman filter (Andreasen, 2013) could challenge a sequential Monte Carlo algorithm based on 500'000 particles. I extend these findings to a wider set of *local-Gaussian* filters trying to compare them on a common ground.

The engineering literature proposes a wide range of *local-Gaussian* filters differing for the way of characterising the shape of the Gaussian distribution (i.e. approximating its mean and variance) assumed for the predictive and filtering densities of latent variables.[1]

Standard *local-Gaussian* filters are usually grouped in Extended Kalman filters and sigma-point filters. Extended Kalman filters approximate non-linearities with Taylor Expansions and deliver closed form solutions for the moments of the Gaussian distributions. Sigma-point filters select a set of nodes and deterministically propagate them through the non-linear transition and measurement equations, thereby being able to better track non-linearities when computing moments.

In this paper, the *Cubature Kalman filter* (Arasaratnam and Haykin, 2009) and the *Unscented Kalman filter* (Julier and Uhlmann, 2004) were chosen to represent sigma-point filters. The Cubature Kalman filter assumes the posterior distribution

[1] See Särkkä (2013) for a complete survey and technical explanation.

of states to take *a priori* a Gaussian form, and applies non-product monomial cubature rules of integration to recover information on latent variables.[2] The Unscented Kalman filter (UKF) (Julier and Uhlmann, 2004) is conceptually similar to the Cubature Kalman filter except for the different way of selecting nodes and of integrating over states. Compared to the CKF, this filter allocates extra weight on nodes at the center of the distribution leading to unstable estimates when distributions are extremely non-Gaussian. Nonetheless, the UKF can be parametrised to replicate the weighting scheme of the CKF.

The interesting feature of this family of filtering techniques is the high accuracy obtained with few nodes.[3] The latter are compared to the second-order extended Kalman filter developed by Gustafsson and Hendeby (2012), relying on a complete second-order Taylor approximation of the state-space representation, which allows to analytically extrapolate the mean and variances over time and compute the predictive and filtering distributions with full precision up to the second order.[4]

Following Meyer-Gohde (2014b), we consider an application of *risky linear approximations* by applying the linear Kalman filter in a neighborhood of either the stochastic steady state or the erogodic mean. Using Meyer-Gohde (2014b)'s algorithm one can compute the solution of the third-order approximation of the model. Then, the slope of the first-order Taylor expansion of the model in this fixed point will contain information on the constant and time-varying effects of risk on agents' behaviour (e.g. the precautionary motive). Therefore, one can assume latent variables to be normally distributed and apply the linear Kalman filter to efficiently estimate model parameters.

Gaussian filters can notably reduce estimation time while guaranteeing acceptable precision compared to particle filters with a limited number of particles. However,

[2]Holden (2017) extends this approach by matching third and fourth-order approximations. Arasaratnam and Haykin (2009) propose a square-rooted version of the Cubature Kalman filter to improve the numerical stability of the Kalman filter.

[3]Another sigma-point filter which was applied on DSGE models is the Central Difference Kalman filter, assessed in Andreasen (2013) and in Noh (2019). Moreover, Binning and Maih (2015) presents an application and assessment of these filters on Markov-switching DSGEs.

[4]A variant of the Extended Kalman filter is the Kalman-Q filter developed by Kollmann (2015) to deal with explosiveness of higher-order DSGE approximations. The latter exploits pruned state space representations efficiently solved with perturbation methods to compute the mean and covariance matrices in closed-form. As for Extended Kalman filters, the KQF relies on the assumption of Gaussian errors and it might lose accuracy when dealing with highly non-Gaussian distributions.

each of these filtering techniques deals with non-linearities in a different way and an evaluation exercise is needed to understand their strengths and weaknesses.[5]

Local filters: ALL relies on the assumption of Gaussian distributed latent states

Filter	Approximation	Pros/Cons
Extended Kalman filter	Taylor approximation (up to second order)	+ Exact first and second moments - Local approximation, not for high non-linearities - Both transition and measurement equations must be differentiable;
Sigma-points (Cubature, Unscented, Central Difference, Hermite/quadrature)	NUMERICALLY approximate 1st and 2nd moments around nodes DETERMINISTICALLY propagated with NL transition equation	- Exact 2nd moment approximation most of the times + More global than EKF + No need to be differentiable - More computationally intensive than EKF
Risky linear Approximations (Ergodic Mean or Stochastic SS)	Linear Kalman filter in a point different from the deterministic steady state	- Higher order dynamics are linearly approximated + Follow the mean of the process + fast - function must be continuous and differentiable

FIGURE 1.1: Characteristics of *local-Gaussian* filters.

Since the seminal work of Kim (2002), the Simulated Method of Moments (SMM) and the Generalised Method of Moments (GMM) were often applied for the estimation of highly non-linear DSGE models. Relevant applications of the SMM are Christiano et al. (2005), who introduced impulse responses matching in a linear environment, followed by recent applications in a non-linear context (see Ruge-Murcia (2012); Mumtaz and Zanetti (2013); Castelnuovo and Pellegrino (2018)).

Born and Pfeifer (2014) introduced a two-step approach: first, they estimated parameters of the shock-processes with sequential Monte Carlo methods, then, these were imposed while estimating the deep parameters of the model with the method of moments. Finally, Kim and Ruge-Murcia (2019) used the SMM for estimating a model with non-Gaussian shocks to capture the effects of extreme events.[6] As this method requires simulating the model many times in order to find the set of parameters minimising the distance between simulated and empirical moments, it was recently replaced by GMM methods. In fact, thanks to the work on pruned state-space systems presented in Andreasen et al. (2018), it is now possible to compute

[5]Deák et al. (2018) provides an illustration based on simulated data without running a complete assessment exercise.

[6]See Scalone (2018) and Deák et al. (2018) for a recent survey.

theoretical moments exploiting the solution of the model computed with perturbation methods, thereby speeding up the estimation process.

The main advantage of the method of moments resides in the estimation of model parameters without the need of recovering information on current state variables. Additionally, GMMs seem to perform relatively well when models are strongly mis-specified. However, this estimation method is subject to some implementational problems. Specifically, one should try to match as many moments as possible to guarantee the validity of estimates (Mumtaz and Zanetti, 2013). Unfortunately, this is not a straightforward task. In fact, matching a moment of a specific order might deteriorate the the ability of matching moments of different orders. Thus, the econometrician needs to make an arbitrary choice on which moments should be assigned with higher priority; furthermore, repeating the minimisation step for many different moments is quite costly in computational terms. Finally, when the sample is short, the actual distribution of moments might heavily differ from its asymptotic one.[7]

1.3 Likelihood Based Filtering

The set of first-order conditions describing agents' optimal choices takes the form of a system of non-linear stochastic equations:

$$E_t \left[e \left(k_{t+1}, k_t, k_{t-1}, \theta, \varepsilon_t \right) \right] = 0 \tag{1.1}$$

where the E_t represents the expectation operator, $\mathbf{e}$, defines a system of known non-linear equations describing how the structural parameters of the model, θ, shape the relationships between the endogenous variables, k_{t+1}, k_t, k_{t-1}, in equilibrium. Finally, ε_t are exogenous structural shocks.

In order to estimate deep parameters, the model is specified in state-space form so to link equilibrium conditions to data. The system of equations (1.1) is rearranged

[7]Friedman and Woodford (2010) use the likelihood of moments to update the prior distribution in a Bayesian estimation setting – Bayesian Limited information. This method allows to better exploit information from data. However, it has the drawback not to perform well when the distribution of moments presents irregularities and when the sample is short, because asymptotic properties are not reliable with few observations. Creel and Kristensen (2011) solved this issue by approximating moments density with kernel techniques. Such method has also the advantage of skipping the minimisation step of the objective function in the GMM, thus speeding up the computation. Scalone (2018) improved the small sample properties.

to build the state transition function, f, describing the evolution of state variables, $s_t \in S_t := \{s_0, ..., s_T\}$, over time:

$$s_t = f\left(s_{t-1}, \varepsilon_t; \theta\right) \tag{1.2}$$

where exogenous i.i.d. structural shocks, $\varepsilon_t \sim \mathcal{N}\left(\mathbf{0}, \mathbf{\Omega}_\varepsilon\right)$. Then, this system is augmented with measurement equations defining the simultaneous relationships between observable variables, $z_t \in Z_t := \{z_0, ..., z_T\}$, and states, s_t:

$$z_t = g\left(s_t, v_t; \theta\right) \tag{1.3}$$

where measurement errors are i.i.d. following $v_t \sim \mathcal{N}\left(\mathbf{0}, \mathbf{\Omega}_\mathbf{v}\right)$. The state-space representation of the model is composed by systems (1.2) and (1.3) which respectively provide the "predictive" density and "filtering" distribution.[8]

Assuming the state-space model to be Markovian, it describes the joint density of observations z_t and latent states s_t conditional on the DSGE model parameters θ:[9]

$$\begin{aligned} p(Z_{1:T}, S_{1:T}|\theta) &= \prod_{t=1}^{T} p(z_{1:t}, s_{1:t}|Z_{1:t-1}, S_{1:t-1}; \theta) \\ &= \prod_{t=1}^{T} p(z_t|s_t; \theta) p(s_t|s_{t-1}; \theta) \end{aligned} \tag{1.4}$$

where $Z_{1:T} = z_1, ..., z_T$ and $S_{1:T} = s_1, ..., s_T$.

Bayesian inference aims at estimating the structural parameters of the model, θ, by maximising the posterior density of states conditional to the observed data (i.e. for a fixed sample) over the parameter space Θ.[10]

[8]The predictive density is also defined "transition density" whereas the "filtering density" from the measurement equation is also referred to as "updating density".

[9]State variables are defined to be Markovian if the value of the states in t conditional to the value in t-1 is independent from older lags of both states and measurements, $p(s_t|S_{1:t-1}, Z_{1:t-1}; \theta) = p(s_t|S_{1:t-1}; \theta)$, and current value of measurements conditional to current value of states is conditionally independent from from history, $p(z_t|S_{1:t}, Z_{1:t-1}; \theta) = p(z_t|S_{1:t}; \theta)$.

[10]This usually consists of computing an estimator - i.e. the mode or the mean - which maximises the posterior distribution. This can be done in various ways. However, DSGE literature has been mainly focusing on numerical integration techniques like Markov Chain Monte Carlo sampling, sequential Monte Carlo sampling, importance sampling, etc.

For this purpose, one needs to compute the marginal posterior density of the model:

$$p(\theta|Z_{1:T}) = \frac{p(z_{1:T}|\theta)p(\theta)}{p(z_{1:T}|Z_{1:T-1};\theta)} \propto \overbrace{p(z_{1:T}|\theta)}^{\substack{\text{marginal}\\ \text{likelihood}}} \overbrace{p(\theta)}^{prior} \tag{1.5}$$

where $p(\theta)$ is the prior distribution - embodying *a priori* knowledge about the parameters.

The marginal likelihood $p(z_{1:t}|\theta)$ is extrapolated from (1.4) by filtering out the states, s_t, and results in:

$$p(Z_{1:T}|\theta) = \prod_{t=1}^{T} p(z_t|Z_{1:t-1};\theta) \tag{1.6}$$

Filtering techniques are used to recursively calculate the marginal likelihood (or the marginal posterior density in a Bayesian framework).

Starting from a known initial value for the state density conditional to the information set, $p(s_{t-1}|z_{1:t-1};\theta)$, it is possible to use the transition density to predict the density of latent states at time t given the information up to time $t-1$:

$$\begin{aligned} p(s_t|Z_{1:t-1};\theta) &= \int p(s_t, s_{t-1}|Z_{1:t-1};\theta)\, ds_{t-1} \\ &= \int p(s_t|s_{t-1}, Z_{1:t-1};\theta)p(s_{t-1}|Z_{1:t-1};\theta)\, ds_{t-1} \end{aligned} \tag{1.7}$$

and

$$p(z_t|Z_{1:t-1};\theta) = \int p(z_t|s_t, Z_{1:t-1};\theta)p(s_t|Z_{1:t-1};\theta)\, ds_t \tag{1.8}$$

The Bayes rule is then used to update the filtering distribution by extending the information set, $Z_{1:t}$, through the observation density as defined in the measurement equation, $p(z_t|s_t;\theta)$:

$$p(s_t|Z_{1:t};\theta) = p(s_t|z_t, Z_{1:t-1};\theta) = \frac{p(z_t|s_t, Z_{1:t-1};\theta)p(s_t|Z_{1:t-1};\theta)}{p(z_t|Z_{1:t-1};\theta)} \tag{1.9}$$

At this point, the filtering density (1.9) is substituted to the initial value of the conditional state density in the prediction density (1.7). Repeating these steps over time, allows to recursively calculate the posterior distribution of states.

The Bayesian filter provides a generalised framework to estimate latent states of both linear and non-linear dynamic systems by recursively extrapolating information from noisy observations given the states.

Unfortunately, applying the Bayesian filter is not always straightforward. Under the specific assumptions of a linear system of equations with Gaussian shocks, one can use the Kalman filter to recursively compute the mean and covariance of the distribution and use them for recovering past states and the likelihood function. However, when one of the two conditions does not hold, the standard Kalman filter cannot be used to recover the likelihood and non-linear methods relying on approximations are needed.

The literature offers two approaches to approximate the likelihood function: *Global* filters, aiming at fully reproducing the likelihood function by sequential Monte Carlo sampling, or *local-Gaussian* filters, assuming latent variables to be normally distributed to then extrapolate the first and second moment.

The idea underpinning *local-Gaussian* filters consists in *a priori* assuming that the distribution of latent states is Gaussian at each point in time. Thanks to this assumption, it is possible to approximate the filtering density in the updating step - see equation (1.9) - by only predicting the mean and covariance matrix of the distribution. As the state transition density is non-linear, the integral in the prediction step is not easy to be evaluated and some form of approximation is needed.

Depending on the approximation method employed in the prediction-step of equation (1.7), it is possible to distinguish among the various non-linear versions of the Kalman filter. Some methods try to approximate the non-linear function, whereas others try to directly recover the mean and the covariance of the distribution. For instance, the Extended Kalman filter exploits Taylor approximations to handle non-linearities, whereas the Unscented Kalman filter uses the unscented transform to straightly provide estimates of the mean and covariance.

Among the filters directly gauging the first two moments of the distribution, another distinction is made with respect to the approximation technique. In particular, this varies on the basis of how the nodes (i.e. sigma-points) where the approximation takes place are chosen and on the methodology used to compute the prediction step. Concerning the choice of the nodes, this usually happens through deterministic rules aiming at guaranteeing a high level of accuracy. For instance, the Central Difference

Kalman filter selects the points with a Sterling interpolation method whereas the *Cubature Kalman filter* chooses them through non-product monomials which provide an exact accuracy for polynomials of a desired order.[11]

The rest of the section will present a selection of *local-Gaussian* filters, including the Cubature Kalman filter (CKF), the Unscented Kalman filter (UKF), the Second-order Extended Kalman filter (EKF) and a Kalman filter applied at the stochastic steady-state (MG-S) or at the ergodic mean (MG-M) to capture higher-order effects in a linear slope. The section concludes presenting a *Global* filter, a Particle Filter (PF) with systematic resampling which will be used for benchmarking.

1.3.1 Cubature Kalman Filter

The *Cubature Kalman* filter (Arasaratnam and Haykin, 2009) assumes the filtering distribution is Gaussian, $p(\mathbf{s_t}|\mathbf{z_{1:t}}) \simeq N\left(s_t|\mathbf{m_t}, \mathbf{\Sigma_t}\right)$ to compute its mean and variance with Gaussian moment matching

$$\int \mathbf{f}(\mathbf{s}) N(\mathbf{s}|\mathbf{m}, \mathbf{\Sigma})\, \mathbf{ds} \tag{1.10}$$

where the above integral is calculated by non-product monomial cubature rules to compute the above expectations in an efficient way.

The key advantage of assuming Gaussian densities resides in the possibility of riformulating (1.10) in terms of expectations over unit Gaussian distributions, $\int \mathbf{f}(\eta^{(i)})\mathbf{N}(\eta^{(i)}|\mathbf{0}, \mathbf{I})$, evaluated in efficiently selected nodes. The latter are treated as “local states" characterised by a Gaussian distribution. As a result, it is possible to apply cubature rules for approximating the integral with weighted sums:[12]

$$\int \mathbf{f}(\mathbf{s}) N(\mathbf{s}|\mathbf{m}, \mathbf{\Sigma})\, \mathbf{ds} \approx \frac{\mathbf{1}}{\mathbf{2d}} \sum_{\mathbf{i=1}}^{\mathbf{2d}} \mathbf{f}(\mathbf{m} + \sqrt{\mathbf{\Sigma}}\eta^{(i)}) \tag{1.11}$$

where for each of the $2d$ evaluation points $\eta^{(i)}$ is determined by means of “non-product monomial cubature rules”:[13]

[11] For further details on these methods, Särkkä (2013) provides a rich methodological explanation and an extension to non-additive measurement errors and Ivashchenko (2014) provides a computational comparison against a particle filter.

[12] Cubature rules are quadrature rules in a multi-dimensional space.

[13] These techniques of integration are known as “non-product monomial cubature rules” and consist in building weighted sums of functions in specific evaluation points. The main advantage of

$$\eta^{(i)} = \begin{cases} \sqrt{d}\mathbf{j_i} & i = 1, ..., d \\ -\sqrt{d}\mathbf{j_{i-d}} & i = d+1, ..., 2d \end{cases} \tag{1.12}$$

with $\mathbf{j}$ being a unit vector in the direction of the unit axis i.[14]

The Cubature Kalman filter introduces the approximation of Gaussian moment matching into the Bayesian filter algorithm to obtain efficient estimates of the mean and covariance matrices of the filtering distribution and can be summarised by the following steps.

The algorithm is initialised by choosing initial guesses for the mean, $\mathbf{m_{t-1}}$, and the covariance matrix, $\mathbf{\Sigma_{t-1}}$. The prediction step starts from the selection of evaluation points, λ:

$$\lambda^{(i)}_{t-1} = \mathbf{m_{t-1}} + \sqrt{\mathbf{\Sigma_{t-1}}}\eta^{(i)} \text{ i=1,....,2d} \tag{1.13}$$

where $\eta^{(i)}$'s are determined as in (1.12).

Evaluation points are deterministically propagated ahead by means of the non-linear transition equation of the model:

$$\lambda^{(i)}_{t|1:t-1} = \mathbf{f}(\lambda^{(i)}_{t-1}) \text{ i=1,....,2d} \tag{1.14}$$

the predicted mean and covariance of the model are approximated with cubature rules

$$\mathbf{m}_{\bar{t}} = \frac{1}{2d}\sum_{i=1}^{2d}\lambda^{(i)}_{t|1:t-1} \tag{1.15}$$

$$\mathbf{\Sigma}_{\bar{t}} = \frac{1}{2d}\sum_{i=1}^{2d}\left(\lambda^{(i)}_{t|1:t-1} - \mathbf{m}_{\bar{t}}\right)\left(\lambda^{(i)}_{t|1:t-1} - \mathbf{m}_{\bar{t}}\right)' + \mathbf{\Omega}_{k-1} \tag{1.16}$$

where $\bar{t} = t|t-1$.

this technique is that approximations are exact for polynomials up to a given order while using the minimum possible number of evaluation points. This is different from the unscented transform which is exact only for polynomials up to order three.

[14]Unit vectors represents vectors with coordinates falling on the unit circle, thus, this specific quadrature rule is called spherical.

In the updating step of the Bayesian filter, new information enters into the filtering density of the states. Similarly, in the *Cubature Kalman* filter, additional information from observables is used to update evaluation points. Substituting (1.15) and (1.16) into (1.13), the selected points are

$$\lambda_{t|1:t-1}^{(i)} = \mathbf{m}_{\bar{\mathbf{t}}} + \sqrt{\mathbf{\Sigma}_{\bar{\mathbf{t}}}}\eta^{(i)} \text{ i=1,....,2d} \tag{1.17}$$

which are propagated through the measurement equation:

$$\hat{Z}_t^{(i)} = \mathbf{g}\left(\lambda_{t|1:t-1}^{(i)}\right) \text{ i=1,....,2d} \tag{1.18}$$

At this point, one can approximate the predicted mean $\hat{\mathbf{m}}_{\mathbf{t}}$ and covariance $\hat{\mathbf{\Sigma}}_t$ of the measurement, and the cross-covariance $\hat{\mathbf{\Omega}}_{\mathbf{t}}$ of the state and the measurement:

$$\hat{\mathbf{m}}_{\mathbf{t}} = \frac{1}{2d}\sum_{i=1}^{2d}\hat{Z}_t^{(i)} \tag{1.19}$$

$$\hat{\mathbf{\Sigma}}_t = \frac{1}{2d}\sum_{i=1}^{2d}\left(\hat{Z}_t^{(i)} - \hat{\mathbf{m}}_{\mathbf{t}}\right)\left(\hat{Z}_t^{(i)} - \hat{\mathbf{m}}_{\mathbf{t}}\right)' + \mathbf{Q}_t \tag{1.20}$$

$$\hat{\mathbf{\Omega}}_{\mathbf{t}} = \frac{1}{2d}\sum_{i=1}^{2d}\left(\hat{Z}^{(i)} - \mathbf{m}_{\bar{t}}\right)\left(\hat{Z}_t^{(i)} - \hat{\mathbf{m}}_{\mathbf{t}}\right)' \tag{1.21}$$

The Kalman gain $\mathbf{K}_{\mathbf{t}}$, the filtered state mean, $\mathbf{m}_{\mathbf{t}}$, and the covariance, $\mathbf{\Sigma}_{\mathbf{t}}$, conditional on the measurement, $\mathbf{z}_{\mathbf{t}}$, can be derived :

$$\mathbf{K}_{\mathbf{t}} = \hat{\mathbf{\Omega}}_{\mathbf{t}}\hat{\mathbf{\Sigma}}_{\mathbf{t}}^{-\mathbf{1}} \tag{1.22}$$

$$\mathbf{m}_{\mathbf{t}} = \mathbf{m}_{\bar{\mathbf{t}}} + \mathbf{K}_{\mathbf{t}}\left[\mathbf{z}_{\mathbf{t}} - \hat{\mathbf{m}}_{\mathbf{t}}\right] \tag{1.23}$$

$$\mathbf{\Sigma}_{\mathbf{t}} = \mathbf{\Sigma}_{\bar{\mathbf{t}}} - \mathbf{K}_{\mathbf{t}}\hat{\mathbf{\Sigma}}_{\mathbf{t}}\mathbf{K}_{\mathbf{t}}' \tag{1.24}$$

1.3.2 Unscented Kalman Filter

The Unscented Transform Kalman filter (UKF) (Julier et al., 1995; Julier and Uhlmann, 2004) belongs to the family of sigma-point filters. As for the Cubature

Kalman filter, aims at directly estimating the first two moments of the target distribution by choosing deterministically some nodes and propagating them using model non-linear approximations. Then, the mean and the covariance matrices are computed from these nodes and plugged into a normal distribution.

As illustrated in Wan and van der Merwe (2001), the *unscented transform* is a numerical method for approximating the joint distribution of random variables $\mathbf{x_1}$ and $\mathbf{x_2}$ defined as

$$\mathbf{x_1} \sim \mathcal{N}(\mathbf{m}, \mathbf{P}) \qquad \mathbf{x_2} = \mathbf{T}(\mathbf{x_1})$$

by applying the following algorithm:

1. Select a set of $2d + 1$ nodes with the below rule:

$$\eta_1^{(0)} = \mathbf{m} \tag{1.25}$$

$$\eta_1^{(i)} = \mathbf{m} + (d+q)^{\frac{1}{2}} \left[\sqrt{\mathbf{P}}\right]_i \tag{1.26}$$

$$\eta_1^{(i+d)} = \mathbf{m} - (d+q)^{\frac{1}{2}} \left[\sqrt{\mathbf{P}}\right]_i i = 1, ..., d \tag{1.27}$$

   where $\sqrt{\mathbf{P}}\sqrt{\mathbf{P}}^T = \mathbf{P}$, $[.]_i$ denotes the i-th column of the matrix, and q is defined by

$$q = \alpha^2 (d+k) - d \tag{1.28}$$

   with α and k allowing for controlling the spread of the nodes.

2. Propagate the nodes using $T(.)$

$$\eta_2^{(i)} = \mathbf{T}(\eta_1^{(i)}) \qquad i = 0, ..., 2d \tag{1.29}$$

3. Compute the mean and covariance of the transformed variable η_1 from the nodes η_2:

$$E[\mathbf{T}(\mathbf{J_1^{(i)}})] \simeq \mathbf{m_U} = \sum_{i=0}^{2d} W_i^{(m)} \eta_2^{(i)} \tag{1.30}$$

$$Cov[\mathbf{T}(\mathbf{J_1^{(i)}})] \simeq \mathbf{S_U} = \sum_{i=0}^{2d} W_i^{(C)} (\eta_2^{(i)-\mathbf{m_U}})(\eta_2^{(i)-\mathbf{m_U}})^T \tag{1.31}$$

with constant weights defined as:

$$\begin{array}{rlrll} W_0^{(m)} &= \frac{q}{d+q} & W_i^{(m)} &= \frac{1}{2(d+q)} & i = 1, ..., 2d \\ W_0^{(c)} &= \frac{q}{d+q} + (1 - \alpha^2 + \beta) & W_i^{(c)} &= \frac{1}{2(d+q)} & i = 1, ..., 2d \end{array}$$

where β can be used to adjust the weight of the covariance matrix.

The UKF applies the unscented transform to estimate the mean and covariance matrix the filtering distribution under the assumption of Gaussianity:

$$p(\mathbf{s}_t|\mathbf{z}_{1:t}) \simeq \mathcal{N}(\mathbf{s}_t|\mathbf{m}_t, \mathbf{\Sigma}_t)$$

where $\mathbf{m}_t$ and $\mathbf{\Sigma}_t$ are computed at every measurement step t = 1, 2, ... with the following algorithm:

1. Select initial nodes for the prediction step

$$\lambda_{t-1}^{(0)} = \mathbf{m}_{t-1} \tag{1.32}$$

$$\lambda_{t-1}^{(i)} = \mathbf{m}_{t-1} + (d+q)^{\frac{1}{2}} \left[\sqrt{\mathbf{\Sigma_{t-1}}} \right]_i \tag{1.33}$$

$$\lambda_{t-1}^{(i+d)} = \mathbf{m}_{t-1} - (d+q)^{\frac{1}{2}} \left[\sqrt{\mathbf{\Sigma_{t-1}}} \right]_i i = 1, ..., d \tag{1.34}$$

Propagate the nodes using transition function

$$\lambda_{t|1:t-1}^{(i)} = \mathbf{f}(\lambda_{t-1}^{(i)}) \text{ i=1,....,2d} \tag{1.35}$$

and use them to compute the mean and covariance matrices

$$\mathbf{m}_{\bar{t}} = \sum_{i=1}^{2d} W_i^m \lambda_{t|1:t-1}^{(i)} \tag{1.36}$$

$$\mathbf{\Sigma}_{\bar{t}} = \sum_{i=1}^{2d} W_i^c \left(\lambda_{t|1:t-1}^{(i)} - \mathbf{m}_{\bar{t}} \right) \left(\lambda_{t|1:t-1}^{(i)} - \mathbf{m}_{\bar{t}} \right)' + \mathbf{\Omega}_{t-1} \tag{1.37}$$

2. Form the nodes for the updating step:

$$\lambda^{(i)}_{t|1:t-1} = \mathbf{m}_{\bar{t}} \tag{1.38}$$

$$\lambda^{(i)}_{t|1:t-1} = \mathbf{m_{\bar{t}}} + \sqrt{(\mathbf{d}+\mathbf{q})}\left[\sqrt{\mathbf{\Sigma_{\bar{t}}}}\right]_{\mathbf{i}} \tag{1.39}$$

$$\lambda^{(i+d)}_{t|1:t-1} = \mathbf{m_{\bar{t}}} - \sqrt{(\mathbf{d}+\mathbf{q})}\left[\sqrt{\mathbf{\Sigma_{\bar{t}}}}\right]_{\mathbf{i}} \text{ i=1,....,2d} \tag{1.40}$$

which are propagated through the measurement equation:

$$\hat{Z}^{(i)}_t = \mathbf{g}\left(\lambda^{(i)}_{t|1:t-1}\right) \text{ i=1,....,2d} \tag{1.41}$$

At this point, one can approximate the predicted mean $\mathbf{\hat{m}_t}$, and covariance of the measurement, $\hat{\mathbf{\Sigma}}_t$, and the cross-covariance of the state and the measurement, $\mathbf{\hat{\Omega}_t}$

$$\mathbf{\hat{m}_t} = \sum_{i=1}^{2d} W_i^{(m)} \hat{Z}^{(i)}_t \tag{1.42}$$

$$\hat{\mathbf{\Sigma}}_t = \sum_{i=1}^{2d} W_i^{(c)}\left(\hat{Z}^{(i)}_t - \mathbf{\hat{m}_t}\right)\left(\hat{Z}^{(i)}_t - \mathbf{\hat{m}_t}\right)' + \mathbf{Q}_t \tag{1.43}$$

$$\mathbf{\hat{\Omega}_t} = \sum_{i=1}^{2d} W_i^{(c)}\left(\hat{Z}^{(i)} - \mathbf{m}_{\bar{t}}\right)\left(\hat{Z}^{(i)}_t - \mathbf{\hat{m}_t}\right)' \tag{1.44}$$

The Kalman gain $\mathbf{K_t}$, the filtered state mean, $\mathbf{m_t}$, and the covariance, $\mathbf{\Sigma_t}$, conditional on the measurement, $\mathbf{z_t}$, can then be derived as follows

$$\mathbf{K_t} = \mathbf{\hat{\Omega}_t}\mathbf{\hat{\Sigma}_t^{-1}} \tag{1.45}$$

$$\mathbf{m_t} = \mathbf{m_{\bar{t}}} + \mathbf{K_t}\left[\mathbf{z_t} - \mathbf{\hat{m}_t}\right] \tag{1.46}$$

$$\mathbf{\Sigma_t} = \mathbf{\Sigma_{\bar{t}}} - \mathbf{K_t}\mathbf{\hat{\Sigma}_t}\mathbf{K_t'} \tag{1.47}$$

1.3.3 Kalman Filter by means of Risky Linear Approximations

In a series of papers, Meyer-Gohde (2014a,b) designed an algorithm to efficiently evaluate the stochastic steady-state and build a linear approximation of the state-space representation which is corrected for risk. Thanks to this *risky linear approximation* and assuming latent variables to be normally distributed, it is possible to apply the linear Kalman filter to estimate model parameters while taking into account for the implication of agents' *precautionary behaviour* for model dynamics. As this technique does not rely on a non-linear filter *per se* but its ability to capture non-linearities is the result of an extremely powerful solution method, the aim of this section intends to provide an intuition of how the latter works. For a more comprehensive description of the method and the derivation of the ergodic mean, Meyer-Gohde (2014a,b) present the solution method, based on the representation developed in Lan and Meyer-Gohde (2013b), its Dynare implementation and an estimation exercise on simulated data whereas Kliem and Meyer-Gohde (2022) show an empirical application.

As a consequence of certainty equivalence, a linear approximation of agents' behaviour in the deterministic steady state is neither influenced by current shocks nor by expected future ones. By contrast, although current shocks are shut off in the stochastic steady state, agents expect them to materialise in the future with a given probability distribution and, therefore adjust their behaviour accordingly (*precautionary motive*). Meyer-Gohde (2014b) presents an algorithm to evaluate the stochastic steady state by exploiting the intrinsic structure of a higher-order policy function computed with perturbation methods without the need of using non-linear equilibrium conditions to recursively determine fixed points through fully non-linear solution methods. In particular, this method allows to take into account for the implications risk through the higher-order derivatives obtained at the deterministic steady state to characterise a policy function which is linear in states but non-linear in risk while avoiding heavy computational costs. Then, latent variables are assumed to be normally distributed and a first-order Taylor expansion is computed to estimate model parameters with the Kalman filter. As a result, the slope of the linear approximation at the stochastic steady state will be influenced by the non-linear effects of risk on model dynamics.

The set of equilibrium conditions stated in equation (1.1) can be expressed in function of the risk parameter σ,

$$E_t \left[e \left(k_{t+1}, k_t, k_{t-1}, \theta, \sigma \varepsilon_t \right) \right] = 0 \tag{1.48}$$

Using this notation, models solutions can be represented as:

$$k_t = f \left(k_{t-1}(\sigma \epsilon_t, \sigma), \sigma \epsilon_t, \sigma \right) \tag{1.49}$$

with a deterministic steady state defined as $f\left(\tilde{k}(0,0), 0, 0\right)$ and the stochastic steady state as $f\left(\tilde{k}(0,1), 0, 1\right)$.

The algorithm starts from the computation of a Taylor approximation of order $\mathcal{C}$ at the deterministic steady state:

$$k_t \approx \sum_{c=0}^{\mathcal{C}} \frac{1}{c!} \left[\sum_{d=0}^{\mathcal{C}-c} f_{s^c \sigma^c} \sigma^d \right] (s_t - \bar{s})^{\otimes [c]} \tag{1.50}$$

where $f_{s^c \sigma^c}$ is the partial derivative of the system computed c times with respect to the state vector $s_t = [k'_{t-1} \quad \sigma \epsilon_t]'$ and d times with respect σ. As pointed out in Meyer-Gohde (2014b), the term $\sum_{d=0}^{\mathcal{C}-c} f_{s^c \sigma^c} \sigma^d$ in equation (1.50) shows that the deterministic steady state and the stochastic steady state do not coincide even with linear approximations. As agents take into account for the presence of future shocks when choosing their optimal allocations in the stochastic steady state, one must consider the expectation operator in (1.48) when computing this fixed point.

For this purpose, the recursive representation of the policy function developed in Lan and Meyer-Gohde (2013b) is constructed by rearranging higher-order derivatives obtained when solving for the deterministic steady state as:

$$k_t \approx \sum_{c=0}^{\mathcal{C}} \frac{1}{c!} \sum_{d_1=0}^{\infty} \sum_{d_2=0}^{\infty} ... \sum_{d_c=0}^{\infty} \left[\sum_{g=0}^{\mathcal{C}-c} \frac{1}{g!} k_{\sigma^g, d_1, d_2, ..d_c} \sigma^g \right] \left(\epsilon_{t-i_1} \otimes \epsilon_{t-i_2} \otimes ... \otimes \epsilon_{t-i_c} \right) \tag{1.51}$$

with $k_{\sigma^g, d_1, d_2, ..d_c} \sigma^g$ being the derivative with respect to the Kronecker products computed c-times for the d exogenous shocks and g times with respect to σ.

This representation allows to express the stochastic steady state by shutting off the the whole shock history while keeping $\sigma = 1$ to consider the effects of risk up to the $\mathcal{C}$-th order:

$$\tilde{k}\left(0,1\right) \approx \sum_{g=0}^{\mathcal{C}} \frac{1}{g!} k_{\sigma^g} \tag{1.52}$$

Once the stochastic steady state is determined, it is possible to compute the first-order derivatives with respect to states and shocks and use them to build a risky linear approximation:

$$k_t \approx \tilde{k}(\sigma\epsilon_t, \sigma) + \tilde{k}_k(\sigma\epsilon_t, \sigma)(k_{t-1} - \tilde{k}(\sigma\epsilon_t, \sigma)) + \tilde{k}_\epsilon(\sigma\epsilon_t, \sigma)\epsilon_t \tag{1.53}$$

where $\tilde{k}_k(\sigma\epsilon_t, \sigma)$ and $\tilde{k}_\epsilon(\sigma\epsilon_t, \sigma)$ are first-order derivatives varying with the chosen risky point.

At this point, one can assume that the shocks are normally distributed with zero-mean and known diagonal covariance matrix and use the Kalman filter for recovering information on latent states.[15]

1.3.4 Extended Kalman Filter

The Extended Kalman filter is based on the approximation of the non-linear transition equation with a Taylor series expansion along under the assumption that the filtering density is Gaussian - $p(\mathbf{s_t}|\mathbf{z_{1:t}}) \simeq N\left(s_t|\mathbf{m_t}, \mathbf{Q_t}\right)$.[16]

The version exposed here is based on the second-order extended Kalman filter with additive errors in the measurement equation (Gustafsson and Hendeby, 2012; Särkkä, 2013). The algorithm used for the evaluation exercise is based on the work presented in Holden (2018) who implemented the second-order Extended Kalman filter in Dynare.[17]

The main advantage of this approach is the possibility of computing an exact closed form representation of mean and variance in a similar fashion to the linear Kalman filter. This should help both in terms of accuracy and in terms of speed

[15] In the case of the ergodic mean, on average the linear transition equation will follow the ergodic mean of the model.

[16] Alternatively, the non-linear dynamic can be approximated by means of statistical linearisation (Stengel, 1994). This technique has the advantage of providing a more global approximation of the distribution but it often encounters issues due to very complex expectations to be computed in the prediction step of the filter (see Särkkä (2013) book for further details).

[17] Särkkä (2013) generalises this algorithm to the case of non-additive noise. Holden (2018) fine-tuned the algorithm to handle with non-stationary shock processes.

of the algorithm. Given the generalised non-linear state space representation with additive noise,

$$s_t = f\left(s_{t-1};\theta\right) + \varepsilon_t \qquad \varepsilon_t \sim N(0,\Sigma_\varepsilon) \tag{1.54}$$

$$z_t = g\left(s_t;\theta\right) + v_t \qquad v_t \sim N(0,\Sigma_v) \tag{1.55}$$

one can derive the moments characterising the prediction and updating steps.

The mean and the covariance matrix of the prediction step are:

$$\mathbf{m_{\bar{t}}} = \mathbf{f}(\mathbf{m_{t-1}}) + \frac{\mathbf{1}}{\mathbf{2}}\sum_{\mathbf{i}} \mathbf{e_i tr}\left(\mathbf{F_{SS}^{(i)}}(\mathbf{m_{t-1}})\mathbf{Q_{t-1}}\right) \tag{1.56}$$

$$\mathbf{Q_{\bar{t}}} = \mathbf{F_S}(\mathbf{m_{t-1}})\mathbf{Q_{t-1}}\mathbf{F_S^T}(\mathbf{m_{t-1}}) \tag{1.57}$$

$$+\frac{\mathbf{1}}{\mathbf{2}}\sum_{\mathbf{i,i'}} \mathbf{e_i e_{i'}^T tr}\left(\mathbf{F_{SS}^{(i)}}(\mathbf{m_{t-1}})\mathbf{Q_{t-1}}\mathbf{F_{SS}^{(i')}}(\mathbf{m_{t-1}})\mathbf{Q_{t-1}}\right) + \Sigma_{\epsilon,t-1} \tag{1.58}$$

These can be used to build all the elements needed to recover the filtering distribution in the updating step:

$$\mathbf{h_t} = \mathbf{z_t} - \mathbf{g}(\mathbf{m_{\bar{t}}}) - \frac{\mathbf{1}}{\mathbf{2}}\sum_{\mathbf{i}} \mathbf{e_i tr}\left(\mathbf{G_{SS}^{(i)}}(\mathbf{m_{\bar{t}}})\mathbf{Q_{\bar{t}}}\right) \tag{1.59}$$

$$\mathbf{X_t} = \mathbf{G_S}(\mathbf{m_{\bar{t}}})\mathbf{Q_{\bar{t}}}\mathbf{G_S^T}(\mathbf{m_{\bar{t}}}) \tag{1.60}$$

$$+\frac{\mathbf{1}}{\mathbf{2}}\sum_{\mathbf{i,i'}} \mathbf{e_i e_{i'}^T tr}\left(\mathbf{G_{SS}^{(i)}}(\mathbf{m_{\bar{t}}})\mathbf{Q_{\bar{t}}}\mathbf{G_{SS}^{(i')}}(\mathbf{m_{\bar{t}}})\mathbf{Q_{\bar{t}}}\right) + \Sigma_{v,t} \tag{1.61}$$

$$\mathbf{K_t} = \mathbf{Q_{\bar{t}}}\mathbf{G_S^T}(\mathbf{m_{\bar{t}}})\mathbf{X_t^{-1}} \tag{1.62}$$

$$\mathbf{m_t} = \mathbf{m_{\bar{t}}} + \mathbf{K_t h_t} \tag{1.63}$$

$$\mathbf{Q_t} = \mathbf{Q_{\bar{t}}} - \mathbf{K_t X_t K_t^T} \tag{1.64}$$

with:

$$\mathbf{F_S}(\mathbf{m}) = \frac{\partial \mathbf{f_j}(\mathbf{x}, \varepsilon)}{\partial \mathbf{s_j}}\bigg|_{[\mathbf{s}=\mathbf{m}, \varepsilon=0]} \tag{1.65}$$

$$\mathbf{G_S}(\mathbf{m}) = \frac{\partial \mathbf{g_j}(\mathbf{s}, \mathbf{v})}{\partial \mathbf{s_j}}\bigg|_{[\mathbf{s}=\mathbf{m}, \mathbf{v}=\mathbf{0}]} \tag{1.66}$$

$$\mathbf{F_{SS}}(\mathbf{m}) = \frac{\partial^2 \mathbf{f_i}(\mathbf{s})}{\partial \mathbf{s_j} \partial \mathbf{s_{j'}}}\bigg|_{[\mathbf{s}=\mathbf{m}]} \tag{1.67}$$

$$\mathbf{G_{SS}}(\mathbf{m}) = \frac{\partial^2 \mathbf{g_i}(\mathbf{s})}{\partial \mathbf{s_j} \partial \mathbf{s_{j'}}}\bigg|_{[\mathbf{s}=\mathbf{m}]} \tag{1.68}$$

1.3.5 Sequential Importance Filtering with Resampling

Sequential Monte Carlo filtering relies on the concept of importance sampling to approximate the posterior density, $p(\theta|Z_{1:T})$, by sampling from an easy-to-handle distribution, $\pi(\theta)$. In this framework, the algorithm assigns increasing weights to the draws depending on how close they are to the actual posterior density.

Importance sampling builds on the theoretical approximation of the posterior distribution with:[18]

$$E_p[\Omega(\theta)] = \int_{-\infty}^{\infty} \Omega(\theta)\, p(\theta|Z_{1:T})\; d\theta = H^{-1} \int_{\Theta} \Omega(\theta)\, W(\theta)\, \pi(\theta)\; d\theta \tag{1.69}$$

[18]Where $H = \int_\Theta \frac{q(\theta)}{\pi(\theta)} \pi(\theta)\; d\theta$ is a constant of proportionality normalising the expected value to meet $p(\theta|Z_{1:T}) = \frac{q(\theta)}{p(z_{1:T}|Z_{1:T-1};\theta)} \propto \frac{q(\theta)}{H}$.

where the "population" importance weight $W(\theta) = \frac{q(\theta)}{\pi(\theta)}$ are used to weigh the draws from $\pi(\theta)$. In practical terms, one samples i.i.d. $(\theta^i)_{i=1}^N$ from $\pi(\theta)$ and construct the "sample" importance weights $w(\theta^i) = \frac{q(\theta^i)}{\pi(\theta^i)}$. Finally, these can be used to approximate $E_p[\Omega(\theta)]$ with $\bar{\Omega}_N = \frac{1}{N}\sum_{i=1}^N w(\theta^i)\Omega(\theta^i)$.

Given the generalised non-linear state space representation

$$s_t = f(s_{t-1};\theta) \qquad \varepsilon_t \sim N(0,\Sigma_\varepsilon) \tag{1.70}$$

$$Z_t = g(s_t;\theta) \qquad v_t \sim N(0,\Sigma_v) \tag{1.71}$$

where measurement errors v_t enter the system additively, the particle filter algorithm can be summarised by the following steps.

For each state variable, s, and exogenous shock, ε, define N_s particles $\{s_t^i, w_t^i\}$ with $i \in \{0,...,N_s\}$ and w_t^i being the weight assigned to particle i at time t.[19]

1. At period t=0, draw N_s i.i.d. particles $\left\{s_{0|0}^i, w_0^i\right\}_{i=1}^{N_s}$ using the prior distribution, $p(s_0;\theta)$, and uniform weights, $w_0^i = 1/N_s$

2. In each period $t \in \{0,...,T\}$ repeat the following step for each particle $i \in \{0,...,N_s\}$:

   (a) Predict s_t. Draw state variables $\hat{s}_t^{(i)}$ from the importance distribution, $\pi(\hat{s}_t|s_{t-1}^{(i)})$, relying on information up to period t-1 and build the corresponding weights $w^{(i)} = \frac{p(\hat{s}_t^{(i)}|s_{t-1}^{(i)})}{\pi(\hat{s}_t^{(i)}|s_{t-1}^{(i)})}$.

   Approximate $E[h(s_t)|Z_{1:t-1};\theta]$ by means of

$$\hat{h}_{t,N_s}^{(i)} = \frac{1}{N_s}\sum_{i=1}^{N_s} h\left(\hat{s}_t^{(i)}\right) w_t^{(i)} W_{t-1}^{(i)} \tag{1.72}$$

[19]This version of the algorithm by Andrieu et al. (2001) is the Sequential Importance Resampling algorithm and it has the advantage of reducing the probability of the degeneracy problem of particles.

(b) Predict observable variables by approximating the predictive density with importance sampling:

$$\hat{p}\left(z_t|Z_{t|t-1}^{(i)};\theta\right) = \frac{1}{N_s}\sum_{i=1}^{N_s} w_t^{(i)} \tag{1.73}$$

(c) Update particle i with an additional information from the observables:

$$E[h(s_t)|Z_{1:t};\theta] = \hat{h}_{t,N_s}^{(i)} = \frac{1}{N_s}\sum_{i=1}^{N_s}\hat{W}_t^{(i)}h(\hat{s}_t^{(i)}) \tag{1.74}$$

where

$$\hat{W}_t^{(i)} = \frac{\hat{w}_t^{(i)}W_{t-1}^{(i)}}{\frac{1}{N_s}\sum_{i=1}^{N_s}\hat{w}_t^{(i)}}W_{t-1}^{(i)} \tag{1.75}$$

(d) When some particles become too important compared to others, the algorithm encounters a degeneracy problem which leads to accuracy losses. For this reason a resampling step is introduced in the algorithm and activated every time the number of propagated particles is smaller than $\hat{N}_s = \frac{N_s}{\frac{1}{N_s}\sum_{i=1}^{N_s}\left(\hat{W}_t^{(i)}\right)^2}$. In this case, N_s states are systematically resampled from $s_{t|t}^{(i)} \in \left\{s_{t|t-1}^{(1)}, ..., s_{t|t-1}^{(i)}, ..., s_{t|t-1}^{(N_s)}\right\}$ with probability proportional to rescaled weights $\frac{w_t^i}{\sum_{i=1}^{N_s}}$. Then, $E[h(s_t)|Z_{1:t};\theta]$, can be approximated with $\hat{h}_{t,N_s} = \frac{1}{N_s}\sum_{i=1}^{N_s}\hat{W}_t^{(i)}h(s_t^{(i)})W_t^{(i)}$

3. At time T, approximate the likelihood function as:

$$log\left(\hat{p}\left(Z_{1:T}|\theta\right)\right) \simeq \sum_{t=1}^{T} log\left(\frac{1}{N_s}\sum_{t=1}^{N_s}\hat{w}_t^{(i)}W_{t-1}^{(i)}\right) \tag{1.76}$$

The above algorithm highlights the sources of the *curse of dimensionality* problems affecting particle filters. Computationally speaking, integrals computed in step (a) and (c) require Monte Carlo integration and solving the model needs to be solved many times. Overall, computational time increases quite rapidly with the number of iterations being N_s x $N_{observables}$ x $(N_{endogenous} + N_{exogenous})$. For instance, estimating a small model with 10 variables, 100 observations and 40 000 particles would require 40 000 000 iterations thereby resulting in a quite heavy computational problem.

1.3.6 Gaussian Particle Filter

This section introduces the Gaussian Particle filter developed by Kotecha and Djuric (2003) and applied on DSGE models by Adjemian and Karame (2016). The idea underlying this filter consists in approximating particles proposal distribution with the Gaussian posterior obtained from one of the *local-Gaussian* filters presented above. Then, the distribution of current states is approximated by Gaussian sparse grids.

$$\tilde{s}_t^{(i)} \sim \mathcal{N}(s_t|\bar{s}_{t|t}, P_{s_{t|t}}) \qquad\qquad i = 1, .., N$$

with associated weights:

$$\begin{aligned} \hat{w}_t^{(i)} &\propto \hat{w}_{t-1}^{(i)} \frac{p(y_t|\tilde{s}_t^{(i)})p(\tilde{s}_t^{(i)}|s_{t-1}^{i})}{q(\tilde{s}_t^{(i)}|s_{t-1}^{(i)}, y_t)}) \\ &= \frac{1}{N} \frac{p(y_t|\tilde{s}_t^{(i)})\mathcal{N}(\tilde{s}_t^{(i)}; \bar{s}_{t|t-1}, P_{s_{t|t-1}})}{\mathcal{N}(\tilde{s}_t^{(i)}; \bar{s}_{t|t}, P_{s_{t|t}})} \end{aligned} \tag{1.77}$$

Crucially, the transition density of states is approximated by the Gaussian density obtained by a *local-Gaussian* filter. On the one hand, this speeds up computations because it is sufficient to track only the mean and variance of the distribution. On the other one, by randomly drawing particles at each step it avoids issues related to particle degeneracy and allow to avoid the resampling step. Problems might arise if the posterior is particularly non-Gaussian. Then, normalised weights (i.e. weights embedding current observed information through the conditional likelihood) makes the filtering step more efficient:

$$\begin{aligned} s_{t|t} &= \sum_{i=1}^{N} \tilde{w}_t^{(i)} \tilde{s}_t^{(i)} \\ P_{s_{t|t}} &= \sum_{i=1}^{N} \tilde{w}_t^{(i)} (\tilde{s}_t^{(i)} - s_{t|t})(\tilde{s}_t^{(i)} - s_{t|t})' \end{aligned} \tag{1.78}$$

1.4 The Model

For sake of comparability with previous studies, like Fernández-Villaverde and Rubio-Ramírez (2005), Noh (2019) and Kollmann (2015), the above direct inference methods will be tested on a stochastic Neo-classical Growth model.

1.4.1 RBC Application

A Neo-classical Growth Model with High Non-linearity

The performance of non-linear estimation techniques will be assessed on a small Real Business Cycle model designed by Brock and Mirman (1972). There are three main reasons for the choice of this model. First, it embeds the main features of modern DSGE models. Second, the nature of the Monte Carlo evaluation exercise requires to somehow contain computational time. Therefore, one needs a model that can be easily solved with higher-order perturbation methods and at the same time allowing for repeated estimations in a reasonable time. Finally, it helps comparing results from former studies using similar versions of the model as Fernández-Villaverde and Rubio-Ramírez (2005) and Noh (2019).

The model relies on a representative agent who has to allocate resources between consumption, C_t, and hours worked, H_t, subject to a resource constraint, (1.81). Agents are characterised by a CRRA separable utility function where the relative risk aversion parameter, σ, affects the *Frisch elasticity* of the labour supply and the labour utility slope ψ is strictly positive.

Households produce a single good, Y_t, by combining labour, H_t, and capital, K_t, according to the production function (1.80) with $\alpha \in (0, 1)$. Capital follows the law of motion (1.82) - where I_t are investments and δ is the depreciation rate of capital. Finally, the technology shock, A_t, and the investment specific shocks, μ_t, evolve as stationary AR(1) processes with Gaussian shocks $\epsilon_t^i \sim \mathcal{N}(m_i,\, \sigma_i^2)$ for i=A,μ.

Agents maximise expected utility by choosing C_t, H_t and K_t:

$$E_0 \sum_{t=0}^{\infty} \beta^t \left\{ log\,(C_t) + \psi \frac{(1 - H_t)^{(1-\sigma)} - 1}{1 - \sigma} \right\} \tag{1.79}$$

subject to:

$$Y_t = A_t K_{t-1}^{1-\alpha} H_t^{\alpha} \tag{1.80}$$

$$Y_t + (1-\delta)K_{t-1} = C_t + K_t \tag{1.81}$$

$$K_t = K_{t-1}(1-\delta) + \mu_t I_t \tag{1.82}$$

And the AR(1) processes for technology and investment specific shocks:

$$log(A_t) = \rho_A log(A_{t-1}) + \epsilon_t^A \tag{1.83}$$

$$log(\mu_t) = \rho_\mu log(\mu_{t-1}) + \epsilon_t^\mu \tag{1.84}$$

This maximisation problem leads to the following Lagrange equation:

$$\begin{aligned}\mathcal{L} : E_0 \sum_{t=0}^{\infty} \beta^t \{ log\left(C_t\right) + \psi \frac{\left(1-H_t\right)^{(1-\sigma)} - 1}{1-\sigma} + \\ + \lambda_t \left(A_t K_{t-1}^{1-\alpha} H_t^{\alpha} - C_t - K_t + (1-\delta)K_{t-1} \right) \}\end{aligned}$$

and the related first-order conditions with respect to C_t, H_t and K_t:

$$C_t : \frac{1}{C_t} - \lambda_t = 0 \tag{1.85}$$

$$H_t : \psi \left(1-H_t\right)^{-\sigma} + \frac{1}{C_t} \alpha A_t \left(\frac{K_{t-1}}{H_t} \right)^{1-\alpha} = 0 \tag{1.86}$$

$$K_t : -\frac{E_t\{C_{t+1}\}}{\beta C_t} + \left(1-\alpha\right) A_t \left(\frac{K_{t-1}}{H_t} \right)^{-\alpha} + (1-\delta) = 0 \tag{1.87}$$

$$\lambda_t : A_t K_{t-1}^{1-\alpha} H_t^{\alpha} - C_t - K_t + (1-\delta)K_{t-1} = 0 \tag{1.88}$$

Agents' optimal behaviour, described by first-order conditions from (1.85) to (1.88), constitutes a system of non-linear difference equations which can be solved around the non-stochastic steady state using perturbation methods - for a detailed derivation please see Section 1.4.2. The resulting solution is a policy function depending on a vector of control variables $Z_t = [C_t, H_t, I_t]$ given the set of predetermined state variables $S_t = [K_t, A_t, \mu_t]$ and a set of exogenous shocks $V_t = [\epsilon_t^A, \epsilon_t^\mu]$.

Details on the zero-growth steady state and its recursive representation are presented in Appendix A.1.

1.4.2 Solution Methods and Likelihood Evaluation

This paper assesses methods to estimate non-linearities deriving from higher-order approximations of models. All the filtering algorithms presented above require evaluating the likelihood function several times. In order to efficiently solve the model, standard perturbation methods are applied around the non-stochastic steady state. For this purpose, the second-order Taylor approximation of the model is computed with the methods introduced in Schmitt-Grohé and Uribe (2004b) and higher-order approximations by means of the techniques developed by Andreasen (2013). These methods were also applied in similar studies as Noh (2019) and Fernández-Villaverde and Rubio-Ramírez (2005; 2007). Moreover, these solution methods are nowadays implemented in standard toolkits for estimating DSGE models with rational expectations.

Once a second-order Taylor approximation of the model is computed, it is possible to build its respective state-space representation as:

$$z_t = G_s^\theta (s_t) + \frac{1}{2} G_{ss}^\theta (s_t \otimes s_t) + \frac{1}{2} f_{\sigma\sigma}^\theta + \sigma \Omega_v^{\frac{1}{2}} v_t \tag{1.89}$$

$$s_{t+1} = F_s^\theta (s_t) + \frac{1}{2} F_{ss}^\theta (s_t \otimes s_t) + \frac{1}{2} h_{\sigma\sigma}^\theta + \sigma \Omega_\epsilon^{\frac{1}{2}} \epsilon_{t+1} \tag{1.90}$$

where exogenous shocks $\varepsilon_t \sim \mathcal{N}(0, I_2)$ i.i.d. with

$$\Omega_\epsilon^{\frac{1}{2}} = \begin{bmatrix} 0 & 0 \\ \sigma_A & 0 \\ 0 & \sigma_\mu \end{bmatrix} \tag{1.91}$$

and measurement errors on the three observable variables $z_t := \{C_t, H_t, I_t\}$ are $v_t \sim \mathcal{N}(0, I_3)$ i.i.d. with covariance matrix

$$\Omega_v^{\frac{1}{2}} = \begin{bmatrix} \sigma_C & 0 & 0 \\ 0 & \sigma_H & 0 \\ 0 & 0 & \sigma_I \end{bmatrix} \tag{1.92}$$

Given the aim of this exercise is to provide results of general use, I follow the literature on non-linear estimation by including as many measurement errors as observables. As shown in sections 2.2 and 2.3 of Fernández-Villaverde and Rubio-Ramírez (2007), the latter choice reduces problems of stochastic singularity when using particle filters, and it is *de facto* a necessary condition for generalising likelihood computation to a wider range of particle filters and models. Acknowledging the presence of measurement errors might represent an issue for macroeconomic modellers (i.e. as the econometrician relies on a different information set compared to agents), the latter should be of relatively limited magnitude in order not to heavily influence model dynamics.

1.5 Evaluating Filtering Techniques

Filters properties were evaluated through a Monte Carlo exercise. The RBC model was used to generate 100 samples of data for 500 periods. The filtering techniques presented in Section 1.3 were applied on each sample. Then, descriptive statistics were calculated to assess “efficiency" and “accuracy" in terms of their ability to track latent states and recover the value of parameters.

Observability is the ability of a filter to reproduce the dynamics of non-observed state variables. This is evaluated through a root-mean-squared error (RMSE) computed in the following way:[20]

$$RMSE_j^f = \frac{1}{K}\sum_{k=1}^{K}\sqrt{\frac{1}{T}\sum_{t=1}^{T}(s_{j,t}^k - \hat{s}_{j,t|t}^k)^2} \qquad f = F \tag{1.93}$$

[20] Binning and Maih (2015) suggest a similar indicator to study filtering techniques on DSGE models with Markov-Switching mechanisms.

where $s_{j,t}$ is the true realised value of the j-th state variable at time t and $\hat{s}_{j,t|t}$ is the state variable not included in the information set as reproduced with estimated parameters with filter $f \in F : \{CKF, UKF, MGM, MGS, GF, PF\}$. In the RBC example presented in Section 1.2, these are $S = \{K_t, A_t, \mu_t\}$. Finally, $RMSE_j$ are expressed in terms of shares of the long-term average of each state variable:

$$RMSE^f = \frac{1}{J}\sum_{j=1}^{J} \frac{RMSE_j^f}{\frac{1}{T}\sum_{t=1}^{T}(s_{j,t})} \qquad f = F \tag{1.94}$$

To deal with noisy estimates, I report the average cross-sample RMSE and the 10th and 90th percentiles.

Accuracy is measured with an Average Relative Bias on estimated parameters (ARB):

$$ARB = \frac{1}{K}\sum_{k=1}^{K}\frac{1}{I}\sum_{i=1}^{I}\left(\frac{\hat{\theta}_i^k - \theta_i}{\theta_i}\right)^2 \tag{1.95}$$

where θ_i is the true value of the i-th parameter and $\hat{\theta}_i^k$ is the sample-k estimate of the i-th parameter. Furthermore, the *Laplace approximation* of the marginal posterior density evaluated at the posterior mode is reported for each non-linear filter.[21]

Although this indicator represents only an approximation of the marginal density (i.e. based on a Gaussian distribution fitted at the maximum *a-posteriori* estimate), it was chosen because filters are assessed relying on the posterior mode computed with an optimiser.[22]

This is mainly motivated by computational reasons. On the one hand, it is in fact not possible to fine-tune the acceptance ratio rate for each sample estimate and still provide a comparable indicator of computational efficiency across the different samples and filters. On the other one, algorithms for setting the scale parameter at a level ensuring a good acceptance ratio (i.e. about 0.33) are quite time consuming and would make the evaluation exercise extremely long.[23]

[21] See Appendix A.2 for details on the *Laplace approximation*.

[22] Friedman and Woodford (2010) show that the Laplace approximation is a good proxy for the posterior density obtained with the Metropolis-Hasting algorithm.

[23] This is important because this paper tests 7 filters on 100 different samples.

In case of sampling from the posterior distribution, one might use the modified harmonic mean estimator as a proxy for the marginal likelihood (Geweke, 1999).[24]

Efficiency is measured in terms of the time needed by an algorithm to find the mode of the posterior distribution. For the reasons mentioned above, it was decided not to use the *effective computational time* (i.e. the ratio between the time for simulating the posterior with MC-MC and the multivariate effective sample size. The *effective computational time* developed by Vats et al. (2019) is a measure resulting from the ratio between the MC-MC computing time and the multivariate effective sample size defined as $N\left(\frac{\Omega_\epsilon}{\Lambda}\right)^{\frac{1}{l}}$, where N is the number of simulated samples, l is the number of parameters, Ω_ϵ is the asymptotic covariance matrix based on independent draws, and Λ is the asymptotic covariance-matrix of correlated samples.).

1.5.1 Estimation and Filters Assessment

The baseline model presented in equations (1.82)-(1.88) is characterised by 11 parameters, $\theta = \{\beta, \alpha, \delta, \sigma, \rho_A, \rho_\mu, \sigma_A, \sigma_\mu, \sigma_C, \sigma_H, \sigma_I\}$. As in Ríos-Rull et al. (2012), some of the parameters were chosen to match US long-term averages for macroeconomic variables not directly influencing the likelihood function. The value of β implies an annualised net interest rate of 4%, α implies a labour share of 0.33 and δ was set to 0.025 as in Fernández-Villaverde and Rubio-Ramírez (2005). $\rho_z = 95$ and $\sigma_z = 0.007$ were calibrated to match the Solow residual of the US economy. As in Noh (2019), measurement errors were set to 50% of the standard deviation of actual data detrended with the hp-filter.

Following Fernández-Villaverde and Rubio-Ramírez (2005), data were simulated with two different model parametrisations: a “benchmark" calibration -to reproduce a realistic economic environment- and a “risky" calibration -to examine the performance of filtering techniques in dealing with a highly non-linear world-.

As explained in Noh (2019), the risk parameter σ influences the volatility of the system by controlling the *Frisch labour supply elasticity* - $\Xi = \frac{1-\bar{H}}{\sigma \bar{H}}$. Therefore, lowering the value of σ increases the volatility of hour worked, generating a non-linear behaviour of the system.

[24] The latter is used in Noh (2019) after sampling only 55000 draws with the MC-MC algorithm.

In the benchmark scenario, σ is set at 2.75 whereas this is reduced to 0.025 in the risky scenario and complemented with a technological shock five times larger in order to increase the volatility of the whole system.

		Calibrations		**Priors**	
Parameter	**Domain**	**Bench.**	**Risky**	**Flat**	**Informative**
β	(0, ∞)	0.99	0.99	U[0.7,0.995]	U[0.7,0.995]
α	[0,1]	0.67	0.67	U[0.3,1]	$\mathcal{B}$ [0.67,0.2]
δ	(0, ∞)	0.025	0.025	U[0.01, 0.05]	Γ^{-1} [0.025, 0.005]
σ	(0, ∞)	2.75	0.05	U[0,100]	Γ^{-1} [σ, 0.5]
ρ_A	[0,1]	0.95	0.95	U[0, 1]	$\mathcal{B}$[0.5, 0.2]
ρ_μ	[0,1]	0.72	0.72	U[0, 1]	$\mathcal{B}$[0.5, 0.2]
σ_A	(0, ∞)	0.007	0.035	U[0,100]	Γ^{-1} [σ_A, 0.02]
σ_μ	(0, ∞)	0.06	0.06	U[0,100]	Γ^{-1} [σ_μ, 0.02]
Measurement errors					
σ_C	[0, ∞)	0.004	0.004	U[0,100]	Γ^{-1} [σ_C, 0.02]
σ_H	[0, ∞)	0.019	0.019	U[0,100]	Γ^{-1} [σ_H, 0.02]
σ_I	[0, ∞)	0.009	0.009	U[0,100]	Γ^{-1} [σ_I, 0.02]

Table 1.1: Priors summary

The joint prior distribution of the DSGE was designed to reflect economically sensible requirements. I have tested filters with informative priors as in Ríos-Rull et al. (2012) and with flat priors as in Fernández-Villaverde and Rubio-Ramírez (2005) and Noh (2019). However, given the large sample-set, the likelihood and the posterior tend to coincide and results are very similar. In this section, I discuss results for the informative prior case. The prior for β is assumed to be flat and ranging between 0.75 and 1. Shares and persistency parameters were assigned beta distributions ranging between 0 and 1. Finally, capital depreciation and standard deviations of shocks and measurement errors were assumed to be distributed as inverse gamma.

1.5.2 Results

The data-set was generated by simulating a fifth-order Taylor approximation of the model at the deterministic steady state to reproduce its non-linear features. Filters performance is evaluated by estimating the RBC model on 100 different samples with three variables - consumption, investment and labour - observed for 500 periods and parameters were initialised at their true values (i.e. the calibrated value used for generating observable variables) to avoid algorithms converging to extreme results.

Following the literature on non-linear estimation, three measurement errors - although small in magnitude- were included for the evaluation exercise. As the model embeds two stochastic processes, the addition of one measurement error would be sufficient to guarantee system invertibility and back-out shock processes under rational expectations.[25] Nonetheless, Fernández-Villaverde and Rubio-Ramírez (2005) show the inclusion of a measurement error for each observable variable facilitates a more general application of particle filters. Moreover, this allows a better comparison with other studies.

All estimates are computed in Matlab on a standard laptop endowed with an Intel Core i9-9880H with CPU 2.3GHz and 32 GB memory. Following Kollmann (2015), measurement errors generated from a normal distribution with mean zero and standard deviation at the prior mode were added to the simulated observables.[26]

The posterior mode was computed by means of a stochastic global optimiser, the CMA-ES (Covariance Matrix Adaptation Evolution Strategy) by Hansen and Kern (2004) to allow for a better exploration of the posterior surface. In fact, the likelihood function of non-linear DSGE models is non-smooth, especially when introducing resampling. Consequently, the likelihood function is affected by discontinuities which do not allow the application of gradient-based algorithms. Non-gradient based algorithms, like symplex-algorithms or stochastic optimisers, help dealing with this issue. Following Andreasen (2010), who suggests that the CMA-ES outperforms the Simulated Annealing algorithm both in accuracy and speed, all results presented in this section refer to value of parameters at the posterior mode obtained by means of this algorithm.[27]

Unless explicitly stated, filters were applied on a second-order Taylor expansion of the model computed with perturbation methods.

In the interest of computational time, evaluations for *global* filters and for the Gaussian Particle filter rely on 500 particles. Although the number of particles is

[25] Measurement errors were chosen to be small in order to limit the divergence from the assumption of perfect information.

[26] The latter avoid estimated standard deviations to touch the zero bound and thereby producing biased estimates.

[27] For the sake of completeness, in Appendix A.6, I have tested the Symplex-Algorithm designed by the Dynare Team, but its performance was worse than the CMA-ES one.

moderate compared to empirical applications, normally using thousands of particles, this choice helps comparing results with Noh (2019) and Binning and Maih (2015). Moreover, Andreasen (2013) shows, in an estimation exercise based on 500 000 particles, that the number of particles to be used depends on the characteristics of models and data, and, as such, it still represents a grey area to be investigated.

Benchmark Calibration

This section presents results related to the Benchmark case, aiming at understanding the ability of *local-Gaussian* filters to deal with non-linearities similar to those observed during the Great Moderation in the US.

Table 1.2 presents parameter estimates as evaluated at the pseudo-posterior mode. Results show that *local-Gaussian* filters offer an higher average precision than that of *global* filters.

Accuracy, as measured by the ARB, was quite similar across the various *local-Gaussian* filters examined, with Risky Linear Approximations being marginally better that the Cubature Kalman filter (CKF) and the second-order Extended Kalman filter (EKF). Interestingly, these filters were able to almost exactly recover the magnitude of the standard deviation of shocks and measurement errors.

Root-mean-squared-errors suggest that the CKF is on average better than other filters in recovering latent variables. Nonetheless, the average performance of both *local-Gaussian* filters and the particle filter do not differ concretely. RMSE ranges show that the CKF consistently performed better than other *local-Gaussian* filters since its average RMSE is below or close to the lower bounds recorded for alternative filters. Surprisingly, the RMSEs observed for the SM-CKF (i.e. the Gaussian Particle filter) suggest that applying the CKF on a sparse grid of selected nodes might lead to biased estimates.

The above results illustrate the potential weaknesses of the PF and SM-CKF in providing unbiased estimates when the number of nodes is particularly limited. One can, in fact, notice that the range of RMSEs is particularly large for these filters. With few particles, these algorithms might assign high probability mass to wrong areas of the parameter space, thereby not being able to correctly identify parameters. This might explain the evident difficulties of these two filters in estimating the correct value of σ. Notwithstanding this, Kollmann (2015) and Andreasen (2013) provide evidence that *local-Gaussian* filters can outperform particle filters with 100 000 and 500 000 particle. Turning to the log-likelihood, EKF, RLM, RLF and the PF500 reached slightly higher density at the mode with respect to the CKF.[28]

Finally, RLM, RLS and the CKF require lower computational time compared to the other Gaussian filters. Therefore, they might be more suitable for estimating larger models.

These results are consistent with what found in Noh (2019) and Kollmann (2015) who suggest that *local-Gaussian* filters perform better than the particle filter in reproducing the dynamics of latent variables. Noh (2019) finds that the Central Difference Kalman filter, a sigma-point filter, provides a relative good performance on data simulated at the third-order under the benchmark calibration.[29] Similarly, Kollmann (2015) finds that the Kalman-Q filter, relying on a closed-form representation for the mean and variance of the predictive densities like the second-order Extended Kalman filter (Gustafsson and Hendeby, 2012), outperforms the particle filter in capturing trajectories of latent states when data is generated using a RBC model with small shocks solved at the second-order.[30]

In the Benchmark environment, all *local-Gaussian* filters provide a good compromise in terms of accuracy and efficiency.

[28]The log-likelihood obtained by the Gaussian Particle filter is biased by the peaks erroneously around some nodes while building the distribution.

[29]Noh (2019) assesses the performance of a Binomial Gaussian Mixture filter, finding it provides more accurate estimates than *local-Gaussian* filters. This family of filters relies on nodes to be propagated under the assumption predictive and filtering densities being mixtures of normal distributions. However, their computational costs directly increase with the number of states to be propagated, and it is more costly than the Gaussian filter (i.e. SM-CKF) analyzied in this paper. I have tested the Gaussian-mixture filter implemented in Dynare and presented in Adjemian and Karame (2016), using a mixture of five normal distributions and 100 nodes, but the long computational time did not allowed for a systematic exercise.

[30]Kollmann (2015) 's model specification only differs from the one used in this paper because of the investment shock is replaced with a preference shock.

Parameter	Actual	CKF	EKF	RLM	RLS	SM-CKF 500	PF 500
α	0.67	0.6694	0.668	0.6678	0.6676	0.691	0.6684
β	0.99	0.9898	0.9895	0.9895	0.9896	0.9948	0.9888
δ	0.025	0.0252	0.0255	0.0255	0.0255	0.0197	0.0262
σ	2.75	2.631	2.6044	2.5934	2.5925	13.3325	4.1497
ρ_z	0.95	0.9391	0.9384	0.9396	0.9397	0.5796	0.9145
ρ_M	0.72	0.7875	0.7192	0.7059	0.7059	0.7878	0.8262
σ_M	0.06	0.0482	0.0572	0.059	0.0588	0.0581	0.0506
σ_Z	0.007	0.0064	0.0067	0.0067	0.0067	0.0585	0.0085
σ_C	0.004	0.0041	0.004	0.0039	0.0039	0.0064	0.0039
σ_I	0.019	0.0076	0.0008	0.0021	0.0021	0.0108	0.0063
σ_H	0.009	0.0089	0.0089	0.0089	0.0089	0.0092	0.0089
ARB		13.25%	13.12%	12.44%	12.46%	173.53%	34.98%
RMSE 10%		8.7%	13.25%	14.18%	14.79%	26.74%	10.95%
RMSE 90%		20.96%	23.35%	25.62%	20.68%	76.32%	30.82%
RMSE		14.77%	18.25%	19.52%	17.22%	44.23%	20.56%
Time		00:02:05	00:03:10	00:01:36	00:01:37	00:04:20	00:18:53
Log-likelihood		-6038	-6075	-6074	-6074	-11436	-6074

Table 1.2: Benchmark calibration at order 5 with informative priors. CKF: Cubature Kalman Filter; EKF: Full Second-order Extended Kalman Filter; RL-M: Approximation around the ergodic mean; RL-S: Approximation around the stochastic steady state; SM-CKF: Gaussian filter (Sparse-matrix Cubature Kalman Filter); PF500: Particle filter with 500 particles and systematic resampling. Observables: consumption, C, hours worked, H, investment, I. The experiment was run on 100 samples of 500 observations using CMAES algorithm to compute the mode. RMSE are normalised by the sample average of state variables. [10%,90%] are RMSEs at the 10^{th} and 90^{th} percentiles.

Further robustness checks are presented in Appendices A.3 - A.6. Under flat priors, all indicators deteriorate and often parameters touch the extremes of the prior bound, showing the difficulty of identifying parameters in a non-linear environment. Similarly, fixing some of the parameters difficult to identify, such as α, β and δ, seems to create some computational difficulties. By contrast, reducing the sample size to 120 observations, a number comparable to the standard sample used for estimating DSGE models with US data, does not concretely reduce accuracy using Bayesian techniques. Overall, filters performance resulted in a rank similar to what presented in this section with sigma-point filters being slightly more reliable than others.

Table 1.3 presents an evaluation of sigma-point filters by comparing the CKF to various set-ups of the Unscented Kalman filter (UKF). As explained in Section 1.3, the UKF allows to somehow steer the selection of nodes by means of parameter α and k and to apply a correction of the weight assigned to each node through parameter β. Beside the technique used for approximating polynomials, the main difference with the CKF is the UKF generally assigns more weight to central nodes. As Gaussian distributions are symmetric, adding extra weight to central nodes might reduce its ability of approximating non-Gaussian processes. Therefore, one can use the aforementioned parameters to add prior information. Nonetheless, by selecting $\{\alpha, k, \beta\} = \{1, 0, 0\}$, the UKF can reproduce the weighting scheme of the CKF. Starting from this set-up, I have tested different weighting schemes. Parameter α directly influences the position of nodes around the central one and reduces the weight assigned to non-central weights. In this case, setting α to higher values compared to the CKF filter generate a loss in accuracy. Parameter k has a symmetric impact on both the position of nodes and weights without penalising the weight of non-central nodes. Columns 4 to 6 show varying this parameter has a marginal impact on the level of accuracy compared to column 1. Finally, parameter β does not affect the position of nodes but increases the weight assigned to the non-central ones. The combinations $\{\alpha, \beta, k\} = \{1, 2, 0\}$ and $\{\alpha, \beta, k\} = \{1, 2, -1\}$ allow to slightly improve on CKF accuracy while reducing computational costs. The possibility of fine-tuning these parameters might be useful to address specific known characteristics of likelihood function. In this application, the UKF was also more efficient than the CKF. In general applications, the non-product monomial rule underpinning the CKF has the advantage of providing positive weights for polynomial up the fifth order and this guarantees an exact approximation of the first and second moment of the predictive and filtering densities. By contrast, the unscented transform might produce negative weights while increasing the number of nodes. As a result estimates might be unstable. Additionally, this technique guarantee an exact estimate of the mean for polynomial up to the third-order and of the variance only for linear models. Therefore, if some of the moments produced by the DSGE model contains higher order polynomial the UKF might lose accuracy.

Binning and Maih (2015) does a similar exercise in a Markov-switching context comparing the behaviour of various sigma-point filters in recovering latent states in a 1000 observations sample. They find the UKF outperforms the CKF and the Divided Difference Kalman filter (DDF) when computing RMSEs on the whole sample. However, the latter behaved better when considering only the second half of the sample. Hence, these authors conclude the DDF is slower in converging but can ensure a somehow stronger accuracy. Anyhow, the different performances were not concretely different and the CKF resulted less dependent on the sample.

Risky Calibration

In this section, the data generating process is characterised by an extreme calibration of parameters with the aim of testing non-linear filters in a highly non-linear environment. This calibration is based on the same set of parameter values used in the benchmark case, with the exception of a very low σ (0.025) and a five-time larger standard deviation of the technological shock, σ_z - details in Table 1.1. This set-up leads to an almost infinite Frisch labour-supply elasticity and results in a very high volatility of hours worked. As mentioned in Noh (2019), this level of Frisch elasticity combined with a large technological shock leadS to a highly non-linear behaviour of the economy.

Accuracy decreased for all *local-Gaussian* filters compared to the Benchmark calibration, recording both higher RMSEs and ARBs.

As expected, higher volatility makes it harder to recover the dynamics of latent states. In a context characterised by higher non-linearities, the relative performance of the PF improved with respect to the benchmark case.

In terms of precision in recovering parameters, the ARB shows the EKF dominated other filters, followed by the PF. Similar to Noh (2019), the performance of the simple sigma-point filter (i.e. the CKF in this study and the Central Difference Kalman filter introduced by Andreasen (2013) in his case) deteriorated in this environment. In particular, this filter experienced some difficulties in capturing the high volatility characterising shock processes.

Average RMSEs indicates that the CKF and PF showed a similar ability in tracking latent variables in this environment. The the 10-th-percentile RMSE suggests the PF might potentially be more accurate of the CKF. However, the CKF presents a smaller 10-percent-interquantile range thereby providing a more robust stability of

Parameter UKF (α, β, k)	Actual	CKF (1,0,0)	UKF (2,0,0)	UKF (3,0,0)	UKF (1,0,1)	UKF (1,0,3)	UKF (1,0,-1)	UKF (1,2,0)	UKF (1,2,1)	UKF (1,2,-1)
α	0.67	0.6706	0.67	0.6665	0.6726	0.6731	0.6739	0.6706	0.6691	0.6739
β	0.99	0.9902	0.9901	0.9894	0.9904	0.9906	0.9908	0.9902	0.9899	0.9908
δ	0.025	0.025	0.0251	0.026	0.0249	0.0246	0.0242	0.025	0.0252	0.0242
σ	2.75	2.8435	2.92	2.8925	2.6562	2.5659	3.0152	2.8441	2.6677	3.0156
ρ_z	0.95	0.9596	0.9379	0.9354	0.9617	0.9645	0.9649	0.9596	0.9597	0.9649
ρ_M	0.72	0.7919	0.7948	0.8295	0.7864	0.7754	0.7961	0.7917	0.7848	0.7959
σ_M	0.06	0.0386	0.0364	0.0414	0.0415	0.0438	0.0369	0.0386	0.041	0.0369
σ_Z	0.007	0.0063	0.0145	0.0174	0.0062	0.0058	0.0061	0.0063	0.0062	0.0061
σ_C	0.004	0.0045	0.0051	0.0058	0.0045	0.0046	0.0045	0.0045	0.0045	0.0045
σ_I	0.019	0.0046	0.0067	0.0076	0.0044	0.0045	0.0051	0.0046	0.0044	0.0051
σ_H	0.009	0.009	0.0091	0.0091	0.009	0.009	0.009	0.009	0.009	0.009
RMSE		15.7%	13.1%	13.1%	16.0%	16.5%	15.6%	14.7%	16.3%	14.4%
RMSE 10%		13.0%	10.3%	11.6%	13.6%	14.6%	11.9%	11.8%	12.9%	10.9%
RMSE 90%		18.9%	16.6%	14.2%	19.2%	17.7%	20.8%	17.3%	18.1%	17.2%
ARB		14.6%	24.7%	29.2%	14.5%	14.9%	15.5%	14.6%	14.4%	15.5%
Time		00:03:16	00:01:43	00:01:38	00:01:47	00:01:49	00:01:58	00:01:47	00:01:57	00:02:11
Log-Likelihood		-6218	-6175	-6190	-6221	-6217	-6207	-6218	-6221	-6208

TABLE 1.3: Benchmark calibration at order 2 with informative priors evaluating sigma-points. CKF: Cubature Kalman Filter; UKF = Unscented Kalman Filter. Observables: consumption, C, hours worked, H, investment, I. In the UKF, α, β and k are parameters influencing how spread sigma-points are and influencing teir weights. RMSE are normalised by the sample average of state variables. [10%,90%] are RMSEs at the 10^{th} and 90^{th} percentiles.

results. Although other *local-Gaussian* filters show a marginally worse performance, the 10-th percentile RMSE of the EKF is comparable to that of the CKF.

Similarly, the studies of Noh (2019), Kollmann (2015) and Andreasen (2013) were characterised by a general deterioration of filters performance when increasing non-linearities. Using 500 particles on data generated with a third order approximation of the model, also Noh (2019) recorded a relative improvement of the PF on *local-Gaussian* filters. By contrast, Kollmann (2015) still finds a better performance of the Kalman-Q filter compared to a partcile filter with either 100 000 or 500 000 nodes. These results are also consistent with those of Andreasen (2013) who suggests *local-Gaussian* filters can compete with a particle filter with 500 000 nodes when non-Gaussianity of latent states is generated by either extreme model parametrisations or by introducing Laplace-distributed shocks, but not when dealing with high fluctuations introduced by stochastic volatility (i.e. modelling the variance of shock processes as an AR(1) process.

The slightly higher accuracy of the EKF in estimating parameters with respect to sigma-point filters is in contrast with the results in Andreasen (2013). However, this might be explained by the use of a second-order EKF which guarantees a more accurate description of moments compared to the standard Extended Kalman filter used in Andreasen's paper. Moreover, Andreasen (2013) evaluate the performance of *local-Gaussian* filters in extremely highly non-Gaussian conditions generated either through Laplace-distributed shocks or stochastic volatility. Consequently, it might also be that sigma-point Kalman filters are more accurate than EKFs under those conditions.

Finally, among the best performing filters the EKF and the CKF guarantee similar efficiency whereas the particle filter results about 5 times slower.

Overall, the EKF and the CKF still represent a relatively good compromise in a highly non-linear environment.

Parameter	Actual	CKF	EKF	MGM	MGS	SM-CKF 500	PF 500
α	0.67	0.6664	0.6667	0.6712	0.663	0.6543	0.6664
β	0.99	0.9896	0.9896	0.99	0.9899	0.9924	0.9898
δ	0.025	0.0252	0.0252	0.0248	0.0251	0.0228	0.0254
σ	0.05	0.0239	0.03	0.1482	0.0457	37.9711	0.0598
ρ_z	0.95	0.9503	0.9492	0.9472	0.9497	0.5707	0.9478
ρ_M	0.72	0.796	0.7419	0.7445	0.7461	0.4839	0.8015
σ_M	0.06	0.0447	0.0567	0.0689	0.0643	0.0975	0.0526
σ_Z	0.035	0.0255	0.0344	0.0371	0.0346	0.2419	0.0383
σ_C	0.004	0.0062	0.0039	0.004	0.004	0.0173	0.0039
σ_I	0.017	0.0255	0.0019	0.0048	0.0047	0.05	0.0103
σ_H	0.009	0.0104	0.0091	0.0094	0.0094	0.0216	0.0091
ARB		20.89%	15.23%	43.7%	20.81%	12014.57%	19.66%
RMSE 10%		18.34%	18.27%	20.14%	21.08%	25.8%	16.66%
RMSE 90%		25.67%	30.62%	35.93%	31.64%	65.6%	26.38%
RMSE		21.57%	24.54%	27.18%	26.21%	49.45%	21.73%
Time		00:04:24	00:04:23	00:01:05	00:01:00	00:10:56	00:23:05
Log-Likelihood		-4692	-5023	-4878	-4882	-6502	-5000

Table 1.4: Risky calibration at order 5 with informative priors. LKF: Linear Kalman Filter with measurement errors; CKF: Cubature Kalman Filter; EKF: Full Second-order Extended Kalman Filter; CKF: Cubature Kalman Filter; EKF: Full Second-order Extended Kalman Filter; RL-M: Approximation around the ergodic mean; RL-S: Approximation around the stochastic steady state; Gaussian Particle filter (Sparse-matrix Cubature Kalman Filter); PF 300: Particle filter with 300 particles and systematic resampling. Observables: consumption, C, hours worked, H, investment, I. The experiment was run on 100 samples of 500 observations using CMAES algorithm to compute the mode. RMSE are normalised by the sample average of state variables. [10%,90%] are RMSEs at the 10^{th} and 90^{th} percentiles.

1.6 Conclusions

The new generation of Dynamic Stochastic General Equilibrium (DSGE) models was enriched by many non-linear elements. Phenomena like the Global financial crisis and the upsurge of extreme climatic events showed the need of modelling uncertainty, risk, non-Gaussian shocks and bounded rationality. This encouraged the development of methods for solving and estimating higher-order approximations of DSGE models. This study focuses on direct inference methods, illustrating advantages and drawbacks of *"local-Gaussian"* filters with respect to *"global"* filters and try to shed light on the properties of these methods.

A Monte Carlo study showed that *local-Gaussian* filters represent a good alternative to standard *global* filters for applications characterised by high computational costs.

In the Benchmark calibration, all *local-Gaussian* filters outperformed a Sequential Monte Carlo filter endowed with a limited number of particles. The accuracy was quite similar among *local-Gaussian* filters, with the risky linear approximations providing slightly more accurate parameter estimates and the Cubature Kalman filter being better in tracking the dynamics of latent variables.

Even though the performance of *local-Gaussian* filters deteriorated with respect to that of particle filters when increasing non-linearity, the former still provide comparable accuracy while guaranteeing concrete computational gains. Overall, the second-order Extended Kalman filter and the Cubature Kalman filter exhibited the best balance in terms of accuracy and efficiency. The second-order Extended Kalman filter was, on average, more accurate than the particle filter and the Cubature Kalman filter could challenge it.

In conclusion, *local-Gaussian* filters can be useful for preliminary estimates before moving to a more comprehensive estimation exercise, for instance using novel efficient particle filters. Additionally, they might be used for dealing with large models when data presents Gaussian features and non-linearities are not too accentuated. The next step would be to assess these filters on models generating even higher volatility -as in the case of Behavioural DSGE models with *reinforcement learning*- so to provide further evidence on the reliability of these filtering techniques in dealing with highly non-linear problems.

Chapter 2

Asset Purchase Programs in bad and good times

Abstract

This paper studies the effects of long-term asset purchases in a canonical Behavioural New-Keynesian model with portfolio adjustment costs, bounded rational agents and reinforcement learning. The latter endogenously determines the sentiment characterizing the economy in a certain period and allows the study of the uncertainty surrounding empirical results on the pass-through of long-term asset purchases to business activity. In particular, short-run impulse responses to a central bank balance-sheet shock are stronger in periods characterised by either extreme pessimism or optimism.

Furthermore, in this framework policies are more effective when central bank credibility, defined as the share of agents believing in the inflation target, is high. Finally, it provides an assessment of the best policy mix and show, under reinforcement learning, the central bank needs to stabilise both inflation and output gap to reduce uncertainty.

JEL Classification: E32, E52, E62, E71, D83
Keywords: Long-term asset purchases, Quantitative Easing, Spending multiplier, Policy state-dependent effects, Behavioural DSGE model, Heterogeneous Expectations

2.1 Introduction

After the global financial crisis, the majority of Central Banks in developed economies enriched their policy toolbox. Due to prolonged subdued macroeconomic developments, policy rates reached their effective lower bound obliging Central Banks to design alternative strategies to meet their price stability objectives. New instruments, such as forward-guidance and various forms of quantitative easing measures, were introduced. Thus, a wide bulk of empirical and theoretical literature on the effects of quantitative easing on long-term interest rates and on the subsequent transmission to the real economy were carried out.

However, uncertainty still surrounds empirical results on the actual effects of quantitative easing. As a matter of fact, the effects of these measures differed in terms of magnitude and persistence, depending on the region and the moment in which they were implemented, thus suggesting that the pass-through of non-standard monetary policy is state-dependent (Coeré, Benoit, 2018; Altavilla and Giannone, 2017; D'Amico and King, 2013).[1]

The DSGE literature on quantitative easing modeled long-term asset purchase programs using a variety of alternative approaches, as frictions on access to credit (Gertler and Karadi, 2011, 2013) or on changes in the composition of households' assets portfolio (Chen et al., 2012; Harrison, 2012, 2017; Carlstrom et al., 2017; Sims and Wu, 2020a,b), while assuming fully rational and fully informed representative agents.[2]

[1]It seems that under bad economic conditions (e.g. usually coinciding with the first round of long-term asset purchase programs when inflation is far from the target), agents believe this measure will reduce long-term interest rates while short-term ones will remain unchanged. Consequently, the term premium narrows down thus triggering a reallocation of resources. When economic conditions improve (e.g. second round of asset purchases), new announcements do not seem to keep the term premium close. Agents observe latest macroeconomic indicators and believe short-term interest rates will rise again in the near future. Therefore, long-term rates do not decrease (or even increase) in spite of new purchases of assets (Eser and Schwaab, 2016).

[2]Bond market segmentation was introduced either in TANK model in which one of the two agents is not granted access to a certain segment of the market - see Chen et al. (2012) - or via portfolio adjustment costs - Harrison (2017). The latter enters the model either via a financial intermediary who can trade only some specific assets or, as a friction entering either households' utility function or their budget constraint. In Harrison (2012) was shown these three ways lead to the same results.

One can see portfolio adjustment costs as the loss in utility of moving away from the equilibrium allocation - *"preferred habitat theory"*. Alternatively, they can be interpreted as an extra loss in households' liquidity who decide to increase their savings to buffer the higher perceived risk on long-term assets relative to short-term ones - Andrés et al. (2004).

The assumption of fully informed rational agents underpins the bulk of theoretical literature on quantitative easing. The inability of standard rational expectations models to capture salient facts observed in empirical data, especially in the aftermath of the global financial crisis, emphasises the need for alternative strategies for modeling agents behaviour.[3] Analyses of quantitative easing under bounded rationality and heterogeneous expectations is, *de facto*, still limited. This paper departs from the mainstream literature by analyzing the effectiveness of quantitative easing measures, modeled as long-term asset purchase programs, in a Behavioural New Keynesian model endowed with portfolio adjustment costs, heterogeneous expectations and reinforcement learning *à la Brock and Hommes (1997)*. Portfolio adjustment costs endow the model with a market for long-term bonds and allow the Central Bank to influence households' behaviour by targeted purchases. The Central Bank purchases long-term assets, whose price mechanically increases due to supply absorption. Consequently, households vary their portfolio mix in favor of bonds with shorter maturity. Because of portfolio adjustment costs, short-term bonds are relatively cheaper than long-term ones. As a result, this shift will provide extra resources available for consumption.

It is assumed two types of agents populate the economy, Näives and Fundamentalists. The latter believe in the commitment of the Central Bank to meet the inflation target in every period. The former expect output-gap and inflation to coincide with their latest observation without considering eventual Central Bank interventions.[4] Agents can adjust their forecasting strategy by adopting a better performing rule based on an endogenous fitness measure. Additionally, agents are assumed to behave according to Euler equation learning, thus the two type of agents only form expectations for next period as in Hommes et al. (2018), and De Grauwe and Ji (2019)).

Moreover, the evolution of the share of agents using a given rule endogenously determines the level of optimism characterizing the overall system in each period. When the output-gap is above equilibrium, Näives believe this will happen again in

[3]Refer to (De Grauwe and Ji, 2020a; Jump and Levine, 2019; Busetti et al., 2017) for evidence based on macroeconomic data, to Assenza et al. (2021) for laboratory experiments, and to Mankiw et al. (2004); Branch (2004); Pfajfar and Santoro (2010) for survey data.

[4]Fundamentalists differ from fully rational agents as they do not know about the existence of different agents types. Moreover, they cannot take into account for persistent shock processes. In case inflation and output-gap follow a random walk, the Näive forecast rule would be the best.

the next period. In this case, they are considered to be optimistic about the future. A similar reinforcement mechanism makes them pessimistic when output-gap is below its steady state. By contrast, Fundamentalists are pessimistic (optimistic) when output-gap is above (below) equilibrium because they expect output-gap to shrink (widen) in the next period.

In such framework, the same policy can produce different multipliers depending on the sentiment prevailing in the economy. Therefore, it represents a flexible field to evaluate whether cognitive limitations can provide a possible explanation for the uncertainty surrounding empirical results.

On the basis of a Monte Carlo exercise, the baseline model supports evidence on the expansionary effect of long-term asset purchase programs, and their more pronounced pass-through to real variables compared to nominal ones. However, departing from existing literature on quantitative easing, by allowing agents to learn, the model also reveals how the magnitude and persistence of these policies are state-dependent. In particular, both the *portfolio channel*, represented by the response of long-term interest rates to asset purchases, and the *feedback channel*, capturing changes in aggregate demand due to changes in interest rates, vary with the level of optimism.

The positive short-run transmission of asset purchases to the economy is robust across different scenarios. Anyhow, the strength and persistence of these measures are more uncertain over longer horizons. In fact, the model shows asset purchases have a stronger impact when either extreme pessimism or optimism features the state of the economy. As the model also provides high correlation between economic sentiment and output-gap dynamics, it promotes asset purchases as a valid counter-cyclical measure. Additionally, similar to Hommes and Lustenhouwer (2019), this model supports the importance of Central Bank's credibility for the success of monetary policies with changes in long-term interest rates affecting inflation more concretely when a larger share of agents believes in the target of the Central Bank.

Finally, the paper sheds some light on the best policy mix to reduce economic uncertainty. In this model, quantitative easing can either help or substitute standard monetary policy in stabilizing the economy, thus advocating somehow the role of this tool to exit the zero-lower bound. The Taylor principle still represents a necessary condition for stability. Yet, this framework recommends addressing directly output-gap to reduce economic uncertainty when agents form expectations using reinforcement learning.

The paper is structured as follows: Section 2.2 discusses the relevant literature, Section 2.3 illustrates the details of the New Keynesian Behavioural model, Section 2.4 presents the results and the model dynamics. Section 2.5 concludes and outlines possible ways forward.

2.2 Literature Review

This paper belongs to the growing strand of literature assessing the impact of monetary policy under bounded rationality and, at the same time, to the theoretical literature on asset purchase programs in DSGE models. This section starts with some empirical evidence on the state-dependency of the transmission of asset purchases, then, it illustrates the main theoretical literature on quantitative easing in DSGE models to conclude with the most related studies on Behavioural DSGE models.

2.2.1 Empirical Evidence

Several studies have tried to assess the effects of quantitative easing. Although they do not always arrive to the same conclusions depending on the country or period of reference, some common patterns seem to emerge: (a) there is convincing evidence in favour of the decrease in interest rates of targeted assets; (b) the bulk of quantitative easing effects on bond prices happen at the moment of the announcement whereas those at the time of the actual implementation are likely to be minor; (c) financial distress seems to amplify the effects of these measures; (d) even though it is hard to identify the pass-through from financial to macroeconomic variables, on impact, quantitative easing seems likely to have an expansionary effect.[5]

Most of the empirical evidence on the effects of QE is based on event studies trying to gauge the short-term impact of this measure on financial variables.[6]

These studies mainly conclude that asset purchase programs managed to reduce either the yields of targeted assets, (*"narrow channel"*), or both the latter and the yield of similar assets, (*"broad channel"*). For US, D'Amico and King (2013) and

[5] Beck et al. (2019) also highlights a general improvement of financial conditions and the absence of side effects so far.

[6] See Rogers et al. (2018) for an assessment of the relationship between monetary policy, foreign exchange risk premia, and term premia in US.

Gagnon et al. (2011a) estimate a fall in interest rates on government bonds in response to the federal Reserve QE1 program. In particular, D'Amico and King (2013) highlight the importance of *local supply* effects, according to which the most pronounced yields reduction concerns the bonds targeted by the purchase program and their closest substitutes in terms of maturity.[7] More recently, Altavilla and Giannone (2017) show that FOMC announcements compressed expected bond yields of US Professional Forecasters and that these lower expected yields were expected to last for one year or longer. Similar results emerged for the UK - see Joyce et al. (2011) - and the Euro area - see Falagiarda and Reitz (2015).

Yet, Krishnamurthy and Vissing-Jorgensen (2011) found no significant impact of the second-round of purchases on asset prices except for a reduction in yields on mortgage-backed securities probably due to a signal effect for a low policy rate for an extended period of time.[8]

Former surveys on the effects of unconventional monetary policies in different regions, suggest quantitative easing can generate positive real effects which are qualitatively similar to those of conventional monetary policy and more limited ones on nominal variables - see Kuttner (2018) for USA and Dell'Ariccia et al. (2018) for Euro area, UK and Japan. However, the majority of these studies are either focusing on short-term effects as natural experiments or are subject to identification issues as long-term asset purchases were often accompanied by other measures.

Hesse et al. (2018) provide evidence in favour of positive significant effects of the first-round of asset purchase programs on macroeconomic variables both in US and England. Yet, later rounds do not seem to lead to the same results.

Similarly, analysing inflation-linked swap rates and TIPS, Krishnamurthy and Vissing-Jorgensen (2011) disentangled an increase in expected inflation thanks to both QE1 and QE2 which implied larger reductions in real than nominal rates.

[7] Similar results raised after the Security Market Program run by the ECB (Eser and Schwaab, 2016).

[8] Motto et al. (2015) find the measures of quantitative easing implemented by the ECB in 2015 have triggered a general fall in asset yields even though it happened in a moment of low financial distress. In fact, although the *local supply channel* weakens with the easing of financial conditions, they suggest this result could be motivated by spill-overs toward non-targeted assets. Altavilla and Giannone (2017) find this effect to influence both Treasury securities and corporate bonds with different credit ratings thereby providing some evidence in favour of an easing of long-term funding. Altavilla et al. (2016) convey outright monetary transactions (OMT) announced by the European Central Bank have reduced 2-year government bond yields in stressed countries - as Italy and Spain - while leaving unchanged those in France and Germany.

Using a wide range of VAR models, Kapetanios et al. (2012) estimate a raise of both inflation and GDP following the asset-purchase program run by Bank of England between 2009 and 2010. Although, these dynamics are qualitative similar, their magnitude varies depending on the econometric approach, and are thus subject to uncertainty.

Concerning longer-term effects, Beck et al. (2019) apply a narrative approach to identify the effects of APPs on a 41-country macro-panel in which short-term rates are at the ZLB.[9]

Interestingly, they find positive significant and protracted effects of quantitative easing announcements on both actual and expected inflation. However, the main driver for this result seems to reside in exchange rate depreciation rather than in stronger internal demand. Additionally, they suggest asset purchase programs affect the Central Bank balance-sheet and both short- and long-term asset prices on the medium run.

2.2.2 Theories on the Transmission of Quantitative Easing

Theoretical literature on asset-purchase programs highlighted the presence of several different channels through which these measures propagate to the real economy. Recent surveys emphasise the role of the *signalling channel*, unveiling Central Bank intentions about the path of the policy rate, a *reanchoring channel*, stating quantitative easing may help stabilizing inflation expectations at the ZLB, and the *portfolio rebalancing channel*, promoting a change in private sector bond mix from long-term assets to less risky short-term ones. In turn, the latter implies that asset purchases, by targeting long-term bonds can promote a *capital relief channel* because the value of these assets in banks' balance-sheet will increase thereby easing potential capital constraints. At the same time, the rebalancing mechanism toward short-term assets might cause further flattening of the yield-curve thanks to the reduction in private sector exposure to the risk of future changes in interest rates - *duration risk channel*.[10]

Last but not least, an improvement in banks' capitalisation along with a generalised lower level of interest rates will favour credit conditions - *credit channel*.

[9]In this way, they can isolate the marginal impact of quantitative easing while abstracting from the effects of forward-guidance announcements about low-for-long policy rates.

[10]See Breckenfelder et al. (2016) for further details.

DSGE literature has tried to account for all these features. However, there is not yet a comprehensive model able to capture all these channels at the same time.

The majority of research focused its attention on the credit channel by modelling financial intermediaries and banking frictions to describe the role of unconventional monetary policies in facilitating lending. Influential examples within this strand of literature are Gertler and Karadi (2011, 2013) and Chen et al. (2012). The former designed a TANK model with financial frictions in the loan-deposit relationship between banks and households. The latter, building on the seminal paper of Andrés et al. (2004), introduces portfolio adjustment frictions to embed bond-market segmentation in a TANK model. In this framework, quantitative easing can affect asset prices and returns by changing the relative supplies of different assets. Imperfect asset substitutability has been included in several alternative ways. For instance, Harrison (2012) models a financial intermediator who pays transaction costs on more illiquid assets. Similarly, Carlstrom et al. (2017) and Sims and Wu (2020a) developed TANK models with constrained and unconstrained households where only the latter have access to the short-term bond market while being subject to portfolio adjustment costs. Yet, Harrison (2017) and Falagiarda (2013) embody imperfect substitutability across bonds within the budget constraint in the form of adjustment costs on households' bond-mix.[11]

However, all the above mentioned methods lead to very similar results in terms of impulse responses amplitude and propagation to the economy.

I will adopt the strategy of modelling imperfect substitutability via portfolio adjustment costs in the budget constraint - as in Harrison (2017). This choice is motivated by the microfundation of aggregate expectations relying on Euler learning which requires agents to have the same consumption equation. Consequently, a TANK approach would not be suitable as it would lead to different agents' behaviour even under rational expectations.

[11] A conceptually similar approach consists in introducing adjustment costs in the utility function. However, Harrison (2012) shows that this method leads to the same first order conditions as those from a budget constraint approach.

Adjusment costs in the budget constraint have been extensively embodied into small-open economy NK models - Kabaca et al. (2020) and Cova and Ferrero (2015).

2.2.3 Behavioural DSGE Macroeconomic Models

In a NK model with heterogeneous expectations and reinforcement learning, Hommes and Lustenhouwer (2019) endogenise the credibility of Central Bank's target and assess the conditions for the occurrence of liquidity traps at the ZLB. Credibility evolves over time along with the share of forward-looking agents whose future expectations on inflation and output gap coincide with the Central Bank target for these variables. In particular, trust in the Central Bank grows when forecasts by fundamentalist agents outperform those by näive (backward-looking) ones. Within this setting, they find that instability of the fundamental steady state can be caused by excessive - positive or negative - responses of the policy rate to output gap expectations. When the ZLB is touched, the possibility to leave a liquidity trap strongly depends on how low the levels of the output gap and inflation are and on how strong Central Bank credibility is. Finally, this framework is able to generate deflationary spirals also with small shocks if the credibility of the Central Bank is low - namely, backward-looking agents systematically forecast better than fundamentalist ones, thus, leading to waves of pessimism.

Goy et al. (2020) study forward guidance in a NK model with endogenous credibility and bounded rational agents - forming expectations over a finite N-step-ahead horizon. Agents can switch from being backward- to forward-looking according to an heuristic rule à la Brock-Hommes (1997) based on forecasting performance with the former building their expectations up through an adaptive rule whereas the latter ones ("credibility believers") trusting the communication of the Central Bank. The Central Bank publishes its forecasts - based on a VAR not accounting for the possibility that agents switch from one type to another - about future inflation, output and interest rates - *Delphic forward-guidance.* Additionally, it can proclaim its commitment to keep interest rates low even if forecasts on inflation are slightly above target - *Odyssean guidance.* This set-up suggests forward-guidance increases the likelihood of exiting from a liquidity trap. Although the only use of Odyssean guidance seems to be more effective, it is likely to generate a raise in ex post macroeconomic volatility and thereby would reduce welfare.

De Grauwe and Ji (2020a, 2019) assess the role of waves of optimism in a Behavioural NK model accounting for the ZLB. When comparing their NK model against a rational expectation one, they find that the effects of the ZLB are more evident in presence of reinforcement learning with the policy rate remaining around zero for longer time. Moreover, they conclude that raising the inflation target to 3 or 4 percent might avoid the economy being stuck in recession. This is because a higher inflation target helps raising inflation expectations and, thus, breaking the reinforcing mechanism between pessimism and output-gap.[12]

Hommes et al. (2018) study fiscal consolidations in a Behavioural NK model with reinforcement learning and short-sighted agents. In contrast with RE models, their model reproduces the anticipation effects of an upcoming fiscal policy. Furthermore, they show how heterogeneous expectations can alter the economic dynamics generated by fiscal consolidations taking into account for waves of optimism and pessimism - as in De Grauwe (2011).

2.3 The Model

This section illustrates the main features of a New Keynesian model designed to study long-term asset purchase programs (APPs). In a nutshell, the model is equipped with short- and long-term bonds priced by means of geometrically decaying coupons, and it allows for bond-market segmentation through portfolio adjustment costs in the resource constraint of households - as in Harrison (2017).[13]

Thanks to this friction, the Central Bank can influence the real economy by interacting with the relative supply of long-term bonds. Compared to standard models, this paper introduces heterogeneous expectations and the reinforcement learning mechanism *à la Brock-Hommes* to capture the interaction between quantitative easing and expectations dynamics.

Section 2.3.1 presents the micro-foundation of the model with a particular focus on the formation of aggregate expectations. Readers who are interested in the policy

[12]In an open-economy setting, animal spirits have been used to model cross-country growth synchronisation in a regime with limited integration of trade (De Grauwe and Ji, 2017) In this setting, waves of optimism (or pessimism) stimulate production in the neighbouring country. Additionally, these effects are amplified within a monetary union. De Grauwe and Macchiarelli (2015) have also employed animal spirits in a DSGE model with housing markets and financial frictions.

[13]The microfundation of the rational model mainly differs from Harrison (2017) for the absence of flow adjustment costs and the preference shock on labour which was replaced by a mark-up shock and for the introduction of a quantitative easing Taylor rule similar to what used in Sims et al. (2020).

focus of the paper can directly move to sections from 2.3.2 to 2.3.4 presenting the log-linear version of the model which will be used for simulations, agents' expectations and learning mechanisms and a sentiment indicator, respectively. Finally, Section 2.3.5 describes the solution. The full derivation of the non-linear model under rational expectations and its detailed linearisation are presented in appendix B.4.

2.3.1 Microfoundation of the Behavioural Model

Household Problem

The model is characterised by a representative agent choosing consumption, $C_t^{(i)}$, labour, $L_t^{(i)}$, short- and long-term bonds to maximise discounted utility over an infinite horizon. Concerning bonds notation, $B_t^{S(i)}$ are short-term bonds and, $B_t^{LT} = B_t^{LH} + B_t^{LCB}$ is the total value of long-term bonds in real terms at time t, which is equal to the sum of long-term bonds held by households, B_t^{LH}, and by the Central Bank, B_t^{LCB}.

The utility function is separable in consumption, $C_t^{(i)}$, and labour, $L_t^{(i)}$:

$$\max_{C_t^{(i)}, L_t^{(i)}, B_t^{S(i)}, B_t^{LH(i)}} \tilde{E}_t^{(i)} \sum_{t=0}^{\infty} \beta^t \{log\left(C_t^{(i)}\right) - \frac{1}{\left(1+\frac{1}{\varphi}\right)} L_t^{(i)\left(1+\frac{1}{\varphi}\right)}\} \tag{2.1}$$

where $\tilde{E}_t^{(i)}(.)$ is a generalised expectations operator for individual (i). The peculiarity of the household problem resides in the budget constraint which was enriched with quadratic adjustment costs on the composition of households' financial portfolios as in Harrison (2017):

$$AC_t^{L(i)} = \frac{\phi^{LH}}{2}\left(k^{LH}\frac{B_t^{S(i)}}{B_t^{LH(i)}} - 1\right)^2 \tag{2.2}$$

where $k^{LH} = \frac{B^{LH}}{B^S}$ is a constant depending on ratio between long- and short-term bonds in steady state.

These adjustment costs are key to model bond-market segmentation as they generate a wedge between short- and long-term interest rates and allow for the transmission of long-term APPs to the real economy.

Most of the literature on long-term asset purchases introduced bond-market segmentation, either through TANK models or through *portfolio adjustment costs*, obtaining qualitatively similar results.

TANK models usually assume a portion of agents can trade both short- and long-term bonds whereas remaining agents are subject to transaction costs when trading the latter - see Andrés et al. (2004); Chen et al. (2012); Carlstrom et al. (2017); Sims and Wu (2020b). This friction breaks perfect substitutability across assets, with restricted households not allowed to completely counterbalance eventual changes in the risk-adjusted expected returns of a bond by adjusting the composition of their financial portfolio.

Portfolio adjustment costs introduce bond-market segmentation in representative-agents models by means of frictions on the departure from the favorite bond allocation *(preferred habitat theory)*. Alternatively, they are interpreted as a tool to buffer for eventual consumption losses caused by price fluctuations in riskier assets: as long-term bonds are perceived to be illiquid assets compared to short-term bonds, agents decide to save some extra resources when investing on them as a form of insurance against higher risk. The literature explored various solutions to include portfolio adjustment costs in DSGE models, for instance, by introducing a financial intermediary who can trade only bonds with selected maturities or, by frictions affecting either households' utility function or their budget constraint - see Harrison (2012). As these methods lead to similar model dynamics, this paper follows recent literature by embedding adjustment costs directly in the budget constraint (Harrison, 2017; Alpanda and Kabaca, 2020; Kabaca et al., 2020).

Through APPs the Central Bank can reduce the relative supply of long-term bonds available to households. Hence, the price of long-term bonds increases and mechanically their return decreases thereby pushing households to adjust their financial portfolio in favour of short-term bonds. Portfolio adjustment costs break the otherwise one-to-one relationship between bonds with different maturities. For every long-term bond sold, households get in return a short-term bond and some extra resources which can be allocated to expand consumption.

Long-term bonds are modelled as perpetuities (consol) paying geometrically decaying coupons *à la Woodford (2001)* with cash flows equal to a share, $0 \leq \chi \leq 1$, of the market price of new issues of long-term bonds, Q_t^L. Given the structure of these cash flows, selling a bond issued in period t pays a nominal coupon worth a share χ^j

of current market price in t+j where $j > 0$. Therefore, it is possible to express the price of bonds with different residual maturities in terms of current market price. Denoting the real value (i.e. the number) of new perpetuities issued at time t as CF_t, the real value of the stock of bonds from past issues can be defined as

$$B_{t-1}^{LT} = Q_t^L \bar{B}_{t-1}^{LT} = CF_{t-1} + \chi CF_{t-2} + \chi^2 CF_{t-3} + ... = \sum_{j=1}^{\infty} \chi^{j-1} CF_{t-j} \tag{2.3}$$

where $\bar{B}_t^{LT} \equiv \frac{B_t^{LT}}{Q_t^L}$ is the total volume (i.e. the number) of long-term bonds issued.

The latter can be used to express the new issue of bonds as:[14]

$$CF_t = Q_t^L \left(\bar{B}_t^{LT} - \chi \bar{B}_{t-1}^{LT} \right) \tag{2.4}$$

This allows to elicit the real budget constraint of agent i in terms of a unique price for long-term bonds, Q_t^L, by scaling current market price for bonds issued in $t-j$ by χ^j:

$$\begin{aligned} & W_t L_t^{(i)} + \frac{R_{t-1}^S}{\pi_t} B_{t-1}^{S(i)} + \bar{B}_{t-1}^{LH(i)} + GT_t^{(i)} + \Gamma_t^{(i)} - C_t^{(i)} = \\ & = B_t^{S(i)} + Q_t^L \left(\bar{B}_t^{LH(i)} - \chi \bar{B}_{t-1}^{LH(i)} \right) + \frac{\phi^{LH}}{2} \left(k^{LH} \frac{B_t^{S(i)}}{Q_t^L \bar{B}_t^{LH(i)}} - 1 \right)^2 \end{aligned} \tag{2.5}$$

where GT_t are lump-sum government transfers and Ω_t are dividends from intermediate sector firms.

Equation 2.3.1 can be rearranged as

[14] Leading forward by one period equation 2.3, $B_t^{LT} = CF_t + \chi CF_{t-1} + \chi^2 CF_{t-2} + ... = \sum_{j=1}^{\infty} \chi^{j-1} CF_{t-j+1}$, which can be rearranged as $CF_t = B_t^{LT} - \chi \left(CF_{t-1} + \chi CF_{t-2} + \chi^2 CF_{t-3} + ... \right) = B_t^{LT} - \chi B_{t-1}^{LT} = Q_t^L \left(\bar{B}_t^{LT} - \chi \bar{B}_{t-1}^{LT} \right)$.

$$W_t L_t^{(i)} + \frac{R_{t-1}^S}{\pi_t} B_{t-1}^{S(i)} + \left(1 + \chi Q_t^L\right) \bar{B}_{t-1}^{LH(i)} + GT_t^{(i)} + \Gamma_t^{(i)} - C_t^{(i)} = \\ = B_t^{S(i)} + Q_t^L \bar{B}_t^{LH(i)} + \frac{\phi^{LH}}{2} \left(k^{LH} \frac{B_t^{S(i)}}{Q_t^L \bar{B}_t^{LH(i)}} - 1 \right)^2 \tag{2.6}$$

or, collecting bond prices,

$$W_t L_t^{(i)} + \frac{R_{t-1}^S}{\pi_t} B_{t-1}^{S(i)} + \frac{R_t^L}{\pi_t} B_{t-1}^{LH(i)} + GT_t^{(i)} + \Omega_t^{(i)} - C_t^{(i)} = \\ = B_t^{S(i)} + B_t^{LH(i)} + \frac{\phi^{LH}}{2} \left(k^{LH} \frac{B_t^{S(i)}}{B_t^{LH(i)}} - 1 \right)^2 \tag{2.7}$$

where the yield to maturity $R_t^L = \frac{1+\chi Q_t^L}{Q_{t-1}^L}$ - see Chen et al. (2012) and Carlstrom et al. (2017) for further discussions.

The constraint problem of the representative household i can be solved by means of a Lagrangian auxiliary function:

$$\mathscr{L}^{(i)} : \tilde{E}_0^{(i)} \sum_{t=0}^{\infty} \beta^t \{ log \left(C_t^{(i)} \right) - \frac{z_t^u}{\left(1 + \frac{1}{\varphi}\right)} {L_t^{(i)}}^{\left(1+\frac{1}{\varphi}\right)} + \\ + \lambda_t^{(i)} (W_t L_t^{(i)} + \frac{R_{t-1}^S}{\pi_t} B_{t-1}^{S(i)} + \frac{R_t^L}{\pi_t} B_{t-1}^{LH(i)} + GT_t^{(i)} + \Omega_t^{(i)} + \\ - C_t^{(i)} - B_t^{S(i)} - B_t^{LH(i)} - \frac{\phi^{LH}}{2} \left(k^{LH(i)} \frac{B_t^{S(i)}}{B_t^{LH(i)}} - 1 \right)^2) \}$$

where λ_t is the Lagrangian multiplier and single period marginal utilities are:

$$U_t^{C(i)} = {C_t^{(i)}}^{-1} \tag{2.8}$$

$$U_t^{L(i)} = -{L_t^{(i)}}^{\left(\frac{1}{\varphi}\right)} \tag{2.9}$$

The respective first order conditions are:[15]

[15]Notice that adjustment costs are null in steady state because $k^{LH} = \frac{B^{LH}}{B^S}$ - which is the steady-state ratio of long-term bonds over short-term ones. Furthermore, k^{LH} in equations (2.12) and (2.13) shows that when the steady state quantity of short-term bonds increases, the effects

$C^{(i)}$:

$$\lambda_t^{(i)} = U_t^{C(i)} \tag{2.10}$$

$L^{(i)}$:

$$\frac{-U_t^{L(i)}}{\lambda_t^{(i)}} = W_t \tag{2.11}$$

$B^{S(i)}$:

$$1 + \phi^{LH} \frac{k^{LH(i)}}{B_t^{LH(i)}} \left(k^{LH(i)} \frac{B_t^{S(i)}}{B_t^{LH(i)}} - 1 \right) = \frac{\tilde{E}_t^{(i)} \{ \lambda_{t+1}^{(i)} \} \beta}{\lambda_t^{(i)}} \left(\frac{R_t^S}{\tilde{E}_t^{(i)} \{ \pi_{t+1} \}} \right) \tag{2.12}$$

$B^{LH(i)}$:

$$1 - \phi^{LH} \frac{k^{LH(i)} B_t^{S(i)}}{(B_t^{LH(i)})^2} \left(k^{LH(i)} \frac{B_t^{S(i)}}{B_t^{LH(i)}} - 1 \right) = \frac{\tilde{E}_t^{(i)} \{ \lambda_{t+1}^{(i)} \} \beta}{\lambda_t^{(i)}} \left(\frac{R_{t+1}^L}{\tilde{E}_t^{(i)} \{ \pi_{t+1} \}} \right) \tag{2.13}$$

λ_t:

$$\begin{aligned} W_t L_t^{(i)} + \frac{R_{t-1}^S}{\pi_t} B_{t-1}^{S(i)} + \frac{R_t^L}{\pi_t} B_{t-1}^{LH(i)} + GT_t^{(i)} + \Omega_t^{(i)} = \\ C_t^{(i)} + B_t^{S(i)} + B_t^{LH(i)} + \frac{\phi^{LH}}{2} \left(k^{LH(i)} \frac{B_t^{S(i)}}{B_t^{LH(i)}} - 1 \right)^2 \end{aligned} \tag{2.14}$$

The Supply Sector

This model embeds a standard supply-side consisting of a retail sector and an intermediate-goods sector with Calvo price setting Yun (1996). As in Calvo-Yun New Keynesian model, persistence is generated by the presence of a lottery out of which only a certain portion of firms can adjust their prices in each point in time. Intermediate producers choose input quantities to maximise profits in a monopolistically competitive environment where all firms face identical production functions. When a firm is allowed to adjust prices, these are chosen by minimizing production costs while satisfying aggregate demand from the retail sector.

of adjustment costs are reduced. When ϕ^{LH} and ϕ^F are zero, the FOC for B^S collapses to the standard first order condition for ST bonds: $\lambda_t = \beta \lambda_{t+1} \frac{R_t^S}{\pi_{t+1}}$. Finally, $\chi < 1$.

Retail sector

The retail sector is derived following standard steps as it is not affected by expectation formation processes. Retail goods result from the aggregation of a continuum of intermediate inputs by means of the aggregation technology formulated in Dixit and Stiglitz (1977):

$$Y_t = \left(\int_0^1 Y_t^{(j)\frac{\varepsilon-1}{\varepsilon}} \, dj \right)^{\frac{\varepsilon}{\varepsilon-1}} \tag{2.15}$$

where $\epsilon > 1$ is the parameter determining the elasticity of substitution across different inputs. Retailers aim at maximizing their profits by combining different quantities of intermediate goods for a given market price while being subject to the aggregation technology (2.15):

$$\max_{Y_t^{(j)}} = P_t \left(\int_0^1 Y_t^{(j)\frac{\varepsilon-1}{\varepsilon}} \, dj \right)^{\frac{\varepsilon}{\varepsilon-1}} - \int_0^1 P_t^{(j)} Y_t^{(j)} \, dj \tag{2.16}$$

which results in the following first order condition for firm j:

$$P_t \frac{\epsilon}{\epsilon - 1} \left(\int_0^1 Y_t^{(j)\frac{\varepsilon-1}{\varepsilon}} \, dj \right)^{\left(\frac{\varepsilon}{\varepsilon-1} - 1\right)} \frac{\epsilon - 1}{\epsilon} Y_t^{(j)\frac{\varepsilon-1}{\varepsilon} - 1} = P_t^{(j)} \tag{2.17}$$

out of which one can derive the relative price of the intermediate good j as:

$$\left(\frac{P_t^{(j)}}{P_t} \right)^{-\varepsilon} = \left(\int_0^1 Y_t^{(j)\frac{\varepsilon-1}{\varepsilon}} \, dj \right)^{\frac{-\varepsilon}{\varepsilon-1}} Y_t^{(j)} \tag{2.18}$$

and, the relative demand for intermediate good j:

$$Y_t^{(j)} = \left(\frac{P_t^{(j)}}{P_t} \right)^{-\varepsilon} Y_t \tag{2.19}$$

Finally, one can obtain a price index by substituting (2.18) into (2.19) and reorganizing the equations:

$$P_t = \left[\int_0^1 P_t^{(j)1-\epsilon} \, dj \right]^{1/(1-\epsilon)} \tag{2.20}$$

Intermediate goods producers

Producers of intermediate good (j) share the same firm-level production function:

$$Y_t^{W(j)} = A_t L_t^{(j)} = F(A, L^{(j)}) \tag{2.21}$$

As they are subject to Calvo pricing they maximise profits by minimizing their costs:

$$Y_t^{W(j)} = \min_{L_t^{(j)}} W_t L_t^{(j)} \tag{2.22}$$

subject to the demand for intermediate good j:

$$A_t L_t^{(j)} \geq \left(\frac{P_t^{(j)}}{P_t} \right)^{-\varepsilon} C_t^{(j)} \tag{2.23}$$

resulting in the following Lagrangian and first order condition:

$$\mathscr{L} : MC_t^{(j)} \left(A_t L_t^{(j)} - \left(\frac{P_t^{(j)}}{P_t} \right)^{-\varepsilon} C_t^{(j)} \right) - W_t L_t^{(j)} \tag{2.24}$$

$$\frac{\partial \mathscr{L}}{\partial L_t^{(j)}} : \frac{W_t}{A_t} = MC_t^{(j)} \Rightarrow \frac{W_t}{F_t^L} = MC_t \tag{2.25}$$

where $MC_t^{(j)} = MC_t$ are real marginal costs of production which are common across intermediate firms and A_t follows an AR(1) process:

$$logA_t = \rho_A \, logA_{t-1} + {\epsilon^A}_t \tag{2.26}$$

where technology shock is i.i.d. $\epsilon_t^A \sim \mathcal{N}(0, \sigma^A)$ As a result, the real flow of profits for intermediate firm j:

$$\Omega_t^{(j)} = \frac{P_t^{(j)}}{P_t} Y_t^{(j)} - W_t L_t^{(j)} = Y_t^{(j)} \left(\frac{P_t^{(j)}}{P_t} - MC_t \right) \tag{2.27}$$

Intermediate goods, $Y_t^{(j)}$, are traded in a monopolistic environment characterised by sticky-prices introduced through a Calvo lottery in discrete time. This mechanism implies that a proportion, ξ, of firms cannot adjust its nominal price to the optimal price determined by current aggregate demand.[16] At time t, reoptimizing firms choose a price, $P_t^{*(j)}$, to maximise present expected discounted profits:

$$\max_{P_t^{(j)}} \tilde{E}_t^{(j)}\{\sum_{i=0}^{\infty}(\xi\beta)^i\left(\frac{C_{t+i}}{C_t}\right)^{-1}\left(\frac{P_t}{P_{t+i}}\left[P_t^{(j)}Y_{t+i}^{(j)}-TC_{t+i}\left(Y_{t+i}^{(j)}\right)\right]\right)\} \tag{2.28}$$

subject to (2.23):

$$\tilde{E}_t^{(j)}\{Y_{t+i}^{(j)}\}=\tilde{E}_t^{(j)}\{\left(\frac{P_{t+i}^{(j)}}{P_{t+i}}\right)^{-\varepsilon}C_{t+i}^{(j)}\} \tag{2.29}$$

where $\tilde{E}_t^{(j)}\{\Lambda_{t,t+i}\}=\beta^i\frac{\tilde{E}_t^{(j)}\{\lambda_{t+i}\}}{\lambda_t}=\beta^i\left(\frac{\tilde{E}_t^{(j)}\{C_{t+i}\}}{C_t}\right)^{-1}\frac{P_t}{P_{t+i}}$ is the stochastic discount factor, $\tilde{E}_t^{(j)}\{Y_{t+i}^{(j)}\}$ is the output of firms allowed to adjust prices at time t and $TC_{t+i}(\tilde{E}_t^{(j)}\{Y_{t+i}^{(j)}\})$ is the total cost function of firm j evaluated at time t+i.

The resulting first order condition for the profit maximisation problem can be solved for the optimal reset price:

$$P_t^{*(j)}=\frac{\varepsilon}{\varepsilon-1}\frac{\tilde{E}_t^{(j)}\{\sum_{i=0}^{\infty}(\xi)^i\frac{\Lambda_{t,t+i}}{P_{t+i}}MC_{t+i}z_{t+i}^uP_{t+i}^{\varepsilon}Y_{t+i}\}}{\tilde{E}_t^{(j)}\{\sum_{i=0}^{\infty}(\xi)^i\frac{\Lambda_{t,t+i}}{P_{t+i}}P_{t+i}^{\varepsilon-1}Y_{t+i}\}}=P_t^* \tag{2.30}$$

where z_t^u is a mark-up shock evolving as $log(z_t^u)=\rho_{z^u}log\left(z_{t-1}^u\right)+\epsilon^{z^u}{}_t$ with $\epsilon_t^{z^u}\sim\mathcal{N}(0,\sigma^u)$. Defining inflation between $t-i$ and t as $\pi_t=\pi_{t-1,t}$ or $\pi_{t+1}=\pi_{t,t+1}$, the average price index of the economy,

$$P_t^{1-\varepsilon}=\xi P_{t-1}^{1-\varepsilon}+(1-\xi)P_t^{*1-\varepsilon} \tag{2.31}$$

one can divide both sides of (2.31) by $P_t^{1-\varepsilon}$ and expressed it inflation terms:

$$1=\xi\pi_t^{\varepsilon-1}+(1-\xi)\left(\frac{P_t^*}{P_t}\right)^{1-\varepsilon} \tag{2.32}$$

where:

[16] For this exercise, non-reoptimizing firms keep their price equal to t-1 prices. Normally, models include some form of indexation to previous period market price or to the long-term average of market prices.

$$\frac{P_t^*}{P_t} = \frac{\varepsilon}{\varepsilon - 1} \frac{\tilde{E}_t^{(j)}\{\sum_{i=0}^{\infty} (\xi\beta)^i C_{t+i}^{-1} \pi_{t,t+i}^{\varepsilon} Y_{t+i} MC_{t+i} z_{t+i}^u\}}{\tilde{E}_t^{(j)}\{\sum_{i=0}^{\infty} (\xi\beta)^i C_{t+i}^{-1} \pi_{t,t+i}^{\varepsilon-1} Y_{t+i}\}} \tag{2.33}$$

by firms symmetry. Finally, (2.31) and (2.33) can be written in recursive form as:

$$\frac{P_t^*}{P_t} = \frac{J_t^{(j)}}{JJ_t^{(j)}} \tag{2.34}$$

$$JJ_t^{(j)} - \xi \tilde{E}_t^{(j)}\{\Lambda_{t,t+1} \pi_{t+1}^{\varepsilon-1} JJ_{t+1}^{(j)}\} = Y_t \tag{2.35}$$

$$J_t^{(j)} - \xi \tilde{E}_t^{(j)}\{\Lambda_{t,t+1} \pi_{t+1}^{\varepsilon} J_{t+1}^{(j)}\} = (\frac{\varepsilon}{\varepsilon - 1}) Y_t MC_t z_t^u \tag{2.36}$$

$$1 = \xi \pi_t^{\varepsilon-1} + (1-\xi) \left(\frac{J_t^{(j)}}{JJ_t^{(j)}}\right)^{1-\varepsilon} \tag{2.37}$$

$$MC_t = \frac{W_t}{F_t^L} \tag{2.38}$$

$$\frac{P_t^W}{P_t} = MC_t \tag{2.39}$$

An important feature introduced by sticky prices *à la Calvo* is price dispersion. As only a share $0 < \xi < 1$ of firms can adjust prices in every period, ξ firms will apply the optimal price, P_t^*, whereas $1 - \xi$ firms will continue applying the price applied in t-1, P_{t-1}.

Starting from the relative demand for intermediate good j, (2.19), and substituting the production function for each intermediate firm and integrating over j:

$$\int_0^1 A_t N_t^{(j)} dj = Y_t \int_0^1 \left(\frac{P_t^{(j)}}{P_t}\right)^{-\varepsilon} dj \tag{2.40}$$

Then, one can define price dispersion as:

$$\Delta_t^P = \int_0^1 \left(\frac{P_t^{(j)}}{P_t}\right)^{-\varepsilon} dj \tag{2.41}$$

Price dispersion negatively affects resource allocation because all firms can adjust their production to meet demand but only a share ξ can also reset prices. Consequently, the higher is price stickiness and the lower is substitutability across intermediate products, the less output is produced with a given amount of labour.

$$Y_t^{(j)} = Y_t^{W(j)} \left(\frac{P_t^{(j)}}{P_t} \right)^{-\varepsilon} = A_t L_t^{(j)} \left(\frac{P_t^{(j)}}{P_t} \right)^{-\varepsilon} \Rightarrow Y_t = \frac{A_t L_t}{\Delta_t^P} \tag{2.42}$$

by the law of large numbers and knowing that $\int_{j=0}^{1} L_t, dj$.

The law of motion for average price dispersion can be computed as:

$$\begin{aligned} \Delta_t^P &= \int_0^{1-\xi} \left(\frac{P_t^{(*)}}{P_t} \right)^{-\varepsilon} dj + \int_{1-\xi}^{1} \left(\frac{P_{t-1}^{(j)}}{P_t} \right)^{-\varepsilon} dj \\ &= \int_0^{1-\xi} \left(\frac{P_t^{(*)}}{P_t} \right)^{-\varepsilon} \left(\frac{P_{t-1}}{P_t} \right)^{-\varepsilon} dj + \int_{1-\xi}^{1} \left(\frac{P_{t-1}^{(j)}}{P_{t-1}} \right)^{-\varepsilon} \left(\frac{P_{t-1}^{(j)}}{P_t} \right)^{-\varepsilon} dj \\ &= \xi \pi_t^{\varepsilon} \Delta_{t-1}^P + (1-\xi) \left(\frac{J_t^{(j)}}{J J_t^{(j)}} \right)^{-\varepsilon} \end{aligned} \tag{2.43}$$

This model will be linearised in a point characterised by zero inflation in steady state, so trend inflation will not affect the dynamics of the system. However, price dispersion as first-order effects when considering a positive inflation rate in steady state - see Ascari and Ropele (2009) for a complete derivation and (Ascari et al., 2011) for an application to the case of price adjustments *à la Rotemberg*.

Summing over varieties, the household budget constraint can be written as:

$$Y_t^{(j)} = Y_t^{W(j)} \left(\frac{P_t^{(j)}}{P_t} \right)^{-\varepsilon} = A_t L_t^{(j)} \left(\frac{P_t^{(j)}}{P_t} \right)^{-\varepsilon} \Rightarrow Y_t = \frac{A_t L_t}{\Delta_t^P} \tag{2.44}$$

Consolidated Government-Central Bank:

The model presents a stylised public sector consisting of a consolidated Government-Central Bank faces a budget constraint:[17]

$$B_t^S + \bar{B}_t^{LT} Q_t^L = R_{t-1}^S B_{t-1}^S + \left(1 + \chi Q_t^L\right) \bar{B}_{t-1}^{LT} + GT_t \tag{2.45}$$

[17]This is in line with Harrison (2017) and Falagiarda (2013).

or

$$B_t^S + B_t^{LT} = R_{t-1}^S B_{t-1}^S + R_t^L B_{t-1}^{LT} + GT_t \tag{2.46}$$

where, GT_t are taxes/government transfers to households and short-term bond-supply is constant for simplicity,

$$B_t^S = B^S > 0 \tag{2.47}$$

and, long-term bond supply

$$B_t^{LT} = B^{LT} = B_t^{LH} + B_t^{LCB} = B_t^{LH} + W_t^B B_t^{LT} > 0 \tag{2.48}$$

where $W_t^B \equiv \frac{\bar{B}_t^{LCB}}{\bar{B}_t^{LT}}$ is the share of total long-term bonds held by the Central Bank and B^S and B^{LT} are steady-state values for short- and long-term bonds, respectively. Then, quantitative easing enters the model in the form of long-term APPs through the following QE Taylor Rule, as in Sims et al. (2020):

$$\log W_t^B = -\left(\theta^\pi \log \tilde{E}_t\{\pi_{t+1}\} + \theta^X \left(\log \tilde{E}_t\{Y_{t+1}\} - \log \tilde{E}_t\{Y_{t+1}^F\}\right)\right) + \log z_t^B \tag{2.49}$$

where the minus sign implies that the Central Bank increases long-term asset purchases when it expects lower inflation and output-gap. The latter is defined as the percentage difference of output, Y_t, from the level of output under flexible prices, Y_t^F. As shocks to the Central Bank balance-sheet are usually persistent, these are modelled as an AR(1) process $\log z_t^B = \rho_B \log z_{t-1}^B + \epsilon^B{}_t$ with $\epsilon_t^B \sim \mathcal{N}(0, \sigma^B)$.

Moreover, the Central Bank can conduct a standard monetary policy according to a Taylor rule targeting inflation and output while smoothing for the policy rate:

$$\log R_t^S = \alpha^\pi \log \tilde{E}\{\pi_{t+1}\} + \alpha^X \left(\log \tilde{E}_t\{Y_{t+1}\} - \log \tilde{E}_t\{Y_{t+1}^F\}\right) + \epsilon_t^R \tag{2.50}$$

where the monetary policy shock is a white-noise is i.i.d. $\epsilon_t^R \sim \mathcal{N}(0, \sigma^R)$.

Finally, the standard resource constraint of the economy is augmented with portfolio adjustment costs:

$$Y_t = C_t + GT_t + \frac{\phi^{LH}}{2}\left(k^{LH}\frac{B_t^S}{B_t^{LH}} - 1\right)^2 \tag{2.51}$$

Following Falagiarda (2013), it is assumed the government adjusts transfers in relation to the real value of long-term liabilities:

$$GT_t = GT + \tau^B\left(B_t^{LT} - B^{LT}\right) = GT \tag{2.52}$$

The full list of equations composing the rational expectations model is summarised in Appendix B.1 and the detailed log-linearisation is presented in Appendix B.4.

Aggregate Demand under Euler Learning

Substituting equation (2.10) into (2.11) and log-linearizing results in the labour supply equation:

$$\hat{W} = \hat{C}_t^{(i)} + \frac{1}{\varphi}\hat{L}_t^{(i)} \tag{2.53}$$

where $\hat{.}$ variables are log-deviations from the steady state.

Similarly, by combining 2.10, 2.12 and 2.13 and log-linearizing, it is possible to obtain the consumption equation for individual (i):

$$\hat{C}_t^{(i)} = \tilde{E}_t^{(i)}\{\hat{C}_{t+1}^{(i)}\} - w_1\left(\hat{R}_t^S - \tilde{E}_t^{(i)}\{\hat{\pi}_{t+1}\}\right) - w_2\left(\tilde{E}_t^{(i)}\{\hat{R}_{t+1}^L\} - \tilde{E}_t^{(i)}\{\hat{\pi}_{t+1}\}\right) \tag{2.54}$$

where, $w_1 = \frac{1}{1+\frac{B^{LH}}{B^S}}$ and $w_2 = \frac{\frac{B^{LH}}{B^S}}{1+\frac{B^{LH}}{B^S}}$ are the weights of short-term and long-term interest rates in the aggregate demand equation, respectively. Notice that when $w_2 = 0$ equation (2.54) becomes the standard consumption equation.

The aggregate demand equation is obtained by Euler Equation Learning as in Hommes and Lustenhouwer (2019).[18]

[18] Massaro (2013) extends this approach to the case of infinite horizons.

I acknowledge the latter is based on strong assumptions on agents cognitive abilities as they can realise to be the representative agent. Nonetheless, this small departure from rational expectations allows to study model behaviour when agents simply form one-step ahead expectations thus providing new insights compared to the case of infinite-horizons planner.

Under Euler learning, it is assumed all agents share the same probability of adopting a certain forecasting rule at time t and the probability of choosing that rule is independent from their past choices. These assumptions are justified by the fact that agents are not intrinsically different and every single one has the same options in terms of forecasting rules. It is also assumed all agents are aware other agents face the same probability of choosing a certain heuristic and that consumption decisions only differs because of the way they form expectations. This implies expectations on their own individual consumption coincide with their own expectations on aggregate consumption:

$$\tilde{E}_t^{(i)}\{\hat{C}_{t+1}^{(i)}\} = \tilde{E}_t^{(i)}\{\hat{C}_{t+1}\} \tag{2.55}$$

Thus, the individual demand equation can be expressed as a function of individual expectations on aggregate expected consumption:

$$\hat{C}_t^{(i)} = \tilde{E}_t^{(i)}\{\hat{C}_{t+1}\} - w_1\left(\hat{R}_t^S - \tilde{E}_t^{(i)}\{\hat{\pi}_{t+1}\}\right) - w_2\left(\tilde{E}_t^{(i)}\{\hat{R}_{t+1}^L\} - \tilde{E}_t^{(i)}\{\hat{\pi}_{t+1}\}\right) \tag{2.56}$$

Assuming agents understand market clearing conditions, as aggregate demand and aggregate supply of output are equal in equilibrium, agents' forecasts for these variables will coincide:

$$\tilde{E}_t^{(i)}\{\hat{C}_{t+1}\} = \tilde{E}_t^{(i)}\{\hat{Y}_{t+1}\} \tag{2.57}$$

Plugging the latter into equation 2.56 and aggregating across all agents allows to express aggregate demand:

$$\hat{Y}_t = \tilde{E}_t\{\hat{Y}_{t+1}\} - w_1 \left(\hat{R}^S_t - \tilde{E}_t\{\hat{\pi}_{t+1}\}\right) - w_2 \left(\tilde{E}_t\{\hat{R}^L_{t+1}\} - \tilde{E}_t\{\hat{\pi}_{t+1}\}\right) \tag{2.58}$$

Phillips Curve Derivation under Euler Learning

For the derivation of the Phillips curve under *Euler learning*, this paper follows Hommes and Lustenhouwer (2019) by starting from log-linearised version of (2.33):

$$\begin{aligned}\hat{p}^{*(j)}_t + \hat{P}_t &= (1-\beta\xi)\left(\hat{MC}_t + \hat{z}^u_t + \hat{P}_t\right) \\ &\quad + \beta\xi\,(1-\beta\xi)\sum_{i=0}^{\infty}(\beta\xi)^i \tilde{E}^{(j)}_t\{\hat{MC}^{(j)}_{t+i+1} + z^u_{t+i+1}\hat{P}^{(j)}_{t+i+1}\}\end{aligned} \tag{2.59}$$

where $p^{*(j)}_t = \frac{P^*_t}{P_t}$ is the relative price of optimizing firms.

Rewriting (2.59) in recursive form:

$$\hat{p}^{*(j)}_t + \hat{P}_t = (1-\beta\xi)\left(\hat{MC}_t + \hat{z}^u_t + \hat{P}_t\right) + \beta\xi\tilde{E}^{(j)}_t\{\hat{p}^{*(j)}_{t+1} + \hat{P}_{t+1}\} \tag{2.60}$$

or, in inflation terms, π_t,

$$\hat{p}^{*(j)}_t = (1-\beta\xi)\left(\hat{MC}_t + \hat{z}^u_t\right) + \beta\xi\tilde{E}^{(j)}_t\{\hat{p}^{*(j)}_{t+1} + \pi_{t+1}\} \tag{2.61}$$

Under the same set of assumptions employed for aggregate demand, agents take pricing decisions based on their expectations on aggregate variables, $\tilde{E}^{(j)}_t\{\hat{p}^{*(j)}_{t+i}\} = \tilde{E}^{(j)}_t\{\hat{P}_{t+i}\}$:

$$\hat{p}^{*(j)}_t = (1-\beta\xi)\left(\hat{MC}_t + \hat{z}^u_t\right) + \beta\xi\tilde{E}^{(j)}_t\{\hat{p}^{*}_{t+1} + \pi_{t+1}\} \tag{2.62}$$

The price index is the average between the price set by firms who could maximise profits in period t and the average price set in period t-1:

$$P^{1-\varepsilon}_t = \xi P^{1-\varepsilon}_{t-1} + (1-\xi)\left(p^{*(j)}_t\right)^{\frac{1}{1-\varepsilon}} \tag{2.63}$$

which can be log-linearised:

$$\hat{P}_t = \xi\hat{P}_{t-1} + (1-\xi)\,\hat{p}^{*(j)}_t \tag{2.64}$$

and, reorganised as:

$$\hat{p}_t^{*(j)} = \frac{\xi}{1-\xi}\pi_t \tag{2.65}$$

Plugging (2.65) into (2.62), one obtains

$$\hat{p}_t^{*(j)} = (1-\beta\xi)\left(\hat{MC}_t + \hat{z}_t^u\right) + \frac{\beta\xi}{1-\xi}\tilde{E}_t^{(j)}\{\pi_{t+1}\} \tag{2.66}$$

Then, one can aggregate (2.66) expectations across firms and use again (2.65) to derive the aggregate supply equation:

$$\hat{\pi}_t = \bar{k}\left(\hat{MC}_t + \hat{z}_t^u\right) + \beta\tilde{E}_t\{\hat{\pi}_{t+1}\} \tag{2.67}$$

where $\bar{k} = \frac{(1-\beta\xi)(1-\xi)}{\xi}$.

By combining, the log-linearised definition of marginal costs, (2.25), the production function, (2.21), real wages from the household problem, (2.53), and market clearing conditions:

$$\hat{MC}_t = \hat{W}_t - \hat{A}_t = \hat{Y}_t + \frac{1}{\varphi}\hat{L}_t - \hat{A}_t \tag{2.68}$$

equation (2.67) can be expressed in terms of output:

$$\hat{\pi}_t = \bar{k}\left(\left(1+\frac{1}{\varphi}\right)\hat{Y}_t - \left(1+\frac{1}{\varphi}\right)\hat{A}_t\right) + \beta\tilde{E}_t\{\hat{\pi}_{t+1}\} + \hat{z}_t^\pi \tag{2.69}$$

where $\hat{z}_t^\pi = \bar{k}\hat{z}_t^u$

In order to derive the Phillips curve in output-gap form, one has to introduce the case of fully flexible prices. When $\xi = 0$, all firms can adjust prices and there is no price dispersion. Then, real marginal costs from equation (2.33) are constant and equal to the inverse of the price mark-up, $MC_t^F = \frac{\varepsilon-1}{\varepsilon}$, and $W_t^F = \frac{\varepsilon-1}{\varepsilon}A_t$. Through the household labour supply equation, it is possible to extrapolate labour in flexible prices, $L_t^F = \left(\frac{\varepsilon-1}{\varepsilon}\right)^{\left(\frac{1}{1+\frac{1}{\varphi}}\right)}$, and using the production function the respective output level, $Y_t^F = \left(\frac{\varepsilon-1}{\varepsilon}\right)^{\left(\frac{1}{1+\frac{1}{\varphi}}\right)} A_t$, and its log-linear representation $\hat{Y}_t^F = \hat{A}_t$. Finally, plugging the output-gap definition $\hat{X}_t = \hat{Y}_t - \hat{Y}_t^F$ in (2.69):

$$\hat{\pi}_t = \bar{k}\left(\frac{1}{\varphi}+1\right)\hat{X}_t + \beta\tilde{E}_t\{\hat{\pi}_{t+1}\} + \hat{z}_t^\pi \tag{2.70}$$

The same relationships can be used in the aggregate demand, (2.58), equation to obtain:

$$\hat{X}_t = \tilde{E}_t\{\hat{X}_{t+1}\} - w_1\left(\hat{R}^S_t - \tilde{E}_t\{\hat{\pi}_{t+1}\}\right) - w_2\left(\tilde{E}_t\{\hat{R}^L_{t+1}\} - \tilde{E}_t\{\hat{\pi}_{t+1}\}\right) + \hat{z}^X_t \quad (2.71)$$

where $\hat{z}^X_t = \hat{A}_{t+1} - \hat{A}_t$

2.3.2 A small-NK Model with Asset Purchases

The framework used for policy analyses in later sections is a canonical three-equation New Keynesian model extended with equations to for long-term interest rates, heterogeneous expectations and reinforcement learning.

The main building blocks of the model are the term structure (2.72), the Quantitative Easing Taylor Rule (2.76), the aggregate demand equation (2.73), the Phillips curve (2.74) and the Taylor Rule (2.75).[19]

The term-structure equation determines the level of long-term interest rates as a combination of current short-term interest rates and the portfolio mix

$$\hat{R}^L_{t+1} = \hat{R}^S_t - V^{LH}\left(\hat{B}^S_t - \hat{B}^{LH}_t\right) \quad (2.72)$$

Parameter $V^{LH} = \phi^{LH}\frac{\left(B^S+B^{LH}\right)}{B^S B^{LH}}$ is a composite parameter depending on the size of the overall bond-market, on the households' preferred mix of long- and short-term bonds in equilibrium and the portfolio-adjustment costs parameter. The aggregate demand equation describe the relationship of output-gap with expectations on next period output gap and a weighted impact of short and long-term rates:

$$\hat{X}_t = \tilde{E}\left(\hat{X}_{t+1}\right) - w_1\left(\hat{R}^S_t - \tilde{E}_t\left(\hat{\pi}_{t+1}\right)\right) - w_2\left(\hat{R}^L_{t+1} - \tilde{E}_t\left(\hat{\pi}_{t+1}\right)\right) + \hat{z}^X_t \quad (2.73)$$

where $w_1 \equiv \frac{1}{1+k^{LH}}$ and $w_2 \equiv \frac{k^{LH}}{1+k^{LH}}$ with $k^{LH} = \frac{B^{LH}}{B^S}$ being the ratio of long-term to short-term bonds in steady state.

The Phillips Curve (2.74) and the Taylor Rule (2.75) are standard:

[19] Details on the derivation of equations (2.73) and (2.72) are exposed in appendix (B.5).

$$\hat{\pi}_t = \beta \tilde{E}_t \left(\hat{\pi}_{t+1} \right) + b_2 \hat{X}_t + z_t^{\pi} \tag{2.74}$$

where $b_2 = \frac{(1-\xi)(1-\xi\beta)}{\xi}$.

$$\hat{R}_t^S = \alpha^{\pi} \tilde{E} \left(\hat{\pi}_{t+1} \right) + \alpha^X \tilde{E} \left(\hat{X}_{t+1} \right) + \hat{z}_t^R \tag{2.75}$$

The Central Bank follows a forward-looking Taylor rule for purchasing long-term bonds:

$$\hat{W}_t^B = -\theta^{\pi} \tilde{E}\{\hat{\pi}_{t+1}\} - \theta^X \tilde{E}\{\hat{X}_{t+1}\} + \hat{z}_t^B \tag{2.76}$$

$$\hat{B}_t^{LCB} = \hat{W}_t^B \tag{2.77}$$

where $\hat{z}_t^X$, $\hat{z}_t^{\pi}$, $\hat{\epsilon}_t^R$, $\hat{z}_t^B$ represent shock processes for demand, supply, monetary policy and QE, respectively.

Long-term bonds in the household portfolio are determined as a residual:[20]

$$\hat{B}_t^{LH} = \hat{B}_t^{LT} - \hat{B}_t^{LCB} \tag{2.78}$$

Equations from (2.79) to (2.88) presented in Section 2.3.3 complete the model by defining the way agents form expectations.

2.3.3 Heuristics

Compared to *rational expectations* models where agents know the full structure of the world including the number of agents populating the economy and shocks, this paper studies a form of *bounded rationality* in which agents cannot observe these features when forming expectations. However, agents are still able to correct their forecasting behaviour by evaluating the performance of different forecasting rules through *reinforcement learning à la Brock-Hommes*.[21]

[20] As the total supply of bonds is assumed to be constant, $\hat{B^s}_t = 0$, $\hat{B}_t^{LT} = 0$, $\hat{GT}_t = 0$ and $\hat{B}_t^{LH} = -\hat{B}_t^{LCB}$

[21] In behavioural macroeconomics literature, reinforcement learning is also known as heuristic-switching or trial-and-error.

Following the literature on *reinforcement learning*, the economy is populated by agents forming expectations on macroeconomic variables by selecting a forecast rule depending on its recent performance.[22]

Agents are assumed to be either *"fundamentalist"* or *"extrapolative"*. The former group knows the fundamental steady state of the system and believes output-gap and inflation will converge to that value in the next period.[23]

Formally, this is represented by the following equations:

$$E_t^F\left(\hat{X}_{t+1}\right) = \bar{X} \tag{2.79}$$

$$E_t^F\left(\hat{\pi}_{t+1}\right) = \bar{\pi} \tag{2.80}$$

where $\bar{\pi}$ is the inflation target stated by the Central Bank and $\bar{X}$ is the steady-state output-gap.[24]

Extrapolators (also known as chartists) are backward-looking agents who assume next period output-gap and inflation rate to be coincident to the last observation plus an error correction term. In general, their behaviour can be described with an adaptive expectation rule:

$$E_t^E\left(\hat{X}_{t+1}\right) = \hat{X}_{t-1} + \rho^E\left(\hat{X}_t - \hat{X}_{t-1}\right) \tag{2.81}$$

$$E_t^E\left(\hat{\pi}_{t+1}\right) = \hat{\pi}_{t-1} + \rho^E\left(\hat{\pi}_t - \hat{\pi}_{t-1}\right) \tag{2.82}$$

In the benchmark case, the paper focuses on *näive* agents - e.g. $\rho^E = 0$ - so, the expectation operator is defined as E^N.

[22]For Behavioural NK models see De Grauwe (2011), De Grauwe and Ji (2020a), Hommes and Lustenhouwer (2019). For applications in behavioural finance refer to Brock and Hommes (1997).

[23]Fundamentalists differ from fully rational agents because they do not take into account for the existence of the second type of agent and are not able to consider the impact of future shocks on macro-variables. However, fundamentalists' forecasts coincide with those of rational agents when shocks are white-noise as a shock in output-gap will be absorbed in next period bringing back the variable to the steady state.

[24]Applications of behavioural finance have experimented alternative definitions of *fundamentalists* for which the deviation from the steady state is persistent and the model gradually reverts to its steady state at a constant rate- see (Boswijk et al., 2007) and (Hommes and in 't Veld, 2017). However, I stick to the macroeconomic literature as *"fundamentalists"* allows to better describe credibility in the Central Bank target.

Then, aggregate expectations result from a weighted average of forecasts from the different agents:

$$\bar{E}_t\left(\hat{X}_{t+1}\right) = w_t^{x,F} E_t^F\left(\hat{X}_{t+1}\right) + \left(1 - w_t^{x,F}\right) E_t^N\left(\hat{X}_{t+1}\right) \tag{2.83}$$

$$\bar{E}_t\left(\hat{\pi}_{t+1}\right) = w^{\pi,F} E_t^F\left(\hat{\pi}_{t+1}\right) + \left(1 - w^{\pi,F}\right) E_t^N\left(\hat{\pi}_{t+1}\right) \tag{2.84}$$

where the weights are given by the share of agents of each type with w^F representing the share of fundamentalists and, $w^N = 1 - w^F$, the share of näives.

Agents evaluate their forecast performances in each point in time:

$$\begin{aligned} F_t^{Z,F} &= -\sum_{j=0}^{\infty} \rho_j^{fit}\left(Z_{t-j-1} - E_{t-j-2}^F\left(Z_{t-j-1}\right)\right)^2 \\ &= \rho^{fit} F_{t-1}^{Z,F} + \left(1 - \rho^{fit}\right)\left(Z_{t-1} - E_{t-2}^F Z_{t-1}\right)^2 \end{aligned} \tag{2.85}$$

$$\begin{aligned} F_t^{Z,N} &= -\sum_{j=0}^{\infty} \rho_j^{fit}\left(Z_{t-j-1} - E_{t-j-2}^N\left(Z_{t-j-1}\right)\right)^2 \\ &= \rho^{fit} F_{t-1}^{Z,N} + \left(1 - \rho^{fit}\right)\left(Z_{t-1} - E_{t-2}^N Z_{t-1}\right)^2 \end{aligned} \tag{2.86}$$

where $Z = x, \pi$ and $\rho_j^{fit} = (1 - \rho^{fit})\left(\rho^{fit}\right)^j$ is geometrically decaying in j.[25]

This "error forgetting factor" represents the weight given to past errors; when it is close to zero older errors have similar weight to recent ones whereas when it is close to one, recent errors receive most of the weight.

Then, the share of agents adopting a specific rule varies over time with the performance of the forecasting rule itself:

$$w_t^{Z,F} = \frac{\left(\exp \gamma^{ic} F_t^{Z,F}\right)}{\left(\exp \gamma^{ic} F_t^{Z,F} + \exp \gamma^{ic} F_t^{Z,N}\right)} \tag{2.87}$$

[25] De Grauwe and Ji (2020a) shows the derivation of the recursive form representation to compute infinite summation on a computer.

$$w_t^{Z,N} = \frac{\exp \gamma^{ic} F_t^{Z,N}}{\left(\exp \gamma^{ic} F_t^{Z,F} + \exp \gamma^{ic} F_t^{Z,N}\right)} \tag{2.88}$$

where γ^{ic} is the *intensity of choice* representing how sensitive an agent is to the fitness measure. When this is zero, agents do not pay attention to their forecasting performance and randomly choose the rule to be followed next period. In this case, the probability of choosing a specific rule is $W = 1/n^{rules} = 0.5$. The higher γ^{ic} the wider the share of agents switching toward the best performing rule.

2.3.4 Sentiment Indicator and Central Bank Credibility

At this stage, it is convenient to define some indicators which will be employed in later policy analyses to interpret the importance of state-dependency.

The possibility of tracking the share of agents adopting a specific rule over time offers the opportunity to gain extra insights on the model behaviour. In fact, the share of agents can be used to define a *sentiment indicator* and the *level of Central Bank credibility.*

The sentiment indicator allows to track the share of optimistic agents over time through the share of agents adopting a specific forecasting rule for output gap. Combining equations 2.87 and 2.88, it is defined as:[26]

$$O_t \equiv \begin{cases} w_t^{x,F} & if\ x_{t-1} < 0 \\ w_t^{x,N} = 1 - w_t^{x,F} & if\ x_{t-1} > 0 \end{cases} \tag{2.89}$$

This indicator helps understanding how expectations can generate waves of optimism or pessimism and thereby endogenously generating business cycle fluctuations. Recalling that fundamentalists believe output gap always reverts to equilibrium in the next period, one can consider this rule to be optimistic when the output gap is negative. In fact, in the latter case fundamentalist agents expect a higher output gap in the next period. By contrast, when the output gap is negative the näive rule would result as being pessimistic because when näive agents observe a negative output gap, they expect it to be negative also in the next period. As a result, their believes have a detrimental effect on economic activity as negative output gap expectations reduce

[26] In the literature, this is also known as “animal spirits" or “optimism" indicator - see De Grauwe and Ji (2020a).

aggregate demand through equation (2.73). Following the same logic under positive output-gap realisations, fundamentalists become pessimistic while näives would be optimistic.

Following Hommes and Lustenhouwer (2019), the level of Central Bank credibility is measured through the share of fundamentalists agents in inflation:

$$w_t^{\hat{\pi},F} = \frac{\left(\exp \gamma^{ic} F_t^{\hat{\pi},F}\right)}{\left(\exp \gamma^{ic} F_t^{\hat{\pi},F} + \exp \gamma^{ic} F_t^{\hat{\pi},N}\right)} \tag{2.90}$$

This indicator is endogenously determined by the evolution of the system and will be used to assess whether trust in the Central Bank ability to meet the target matters for the pass-through of long-term asset purchases to the economy.

2.3.5 Model Solution

As in De Grauwe and Ji (2020a), the model is solved in each point in time by matrix inversion. In order to solve the model, it is convenient to rearrange the aggregate demand equation as function of $\hat{X}_t, \hat{X}_{t+1}, \hat{\pi}_t, \hat{\pi}_{t+1}$ and $\hat{R}_t^S$. Substituting, the long-term interest rate equation, (2.72), and all bond supply equations, from (2.76) to (2.78), into the aggregate demand equation, (2.73), one obtains:

$$\hat{X}_t = \left(1 - w_2 V^{LH} \theta^X\right) \hat{X}_{t+1} + \left(1 - w_2 V^{LH} \theta^\pi\right) \hat{\pi}_{t+1} - \hat{R}_t^S + w_2 V^{LH} \hat{z}_t^B + \hat{z}_t^X \tag{2.91}$$

Then, equation (2.91) and the Phillips curve can be used to characterise the following system of equations in structural form:

$$\begin{aligned} \begin{bmatrix} 1 & -\bar{k} \\ 0 & 1 \end{bmatrix} \begin{bmatrix} \hat{\pi}_t \\ \hat{X}_t \end{bmatrix}' = \begin{bmatrix} \beta & 0 \\ 1 - V^{LH} w_2 \theta^\pi & 1 - V^{LH} w_2 \theta^X \end{bmatrix} \begin{bmatrix} E_t^* \hat{\pi}_{t+1} \\ E_t^* \hat{X}_{t+1} \end{bmatrix}' + \\ + \begin{bmatrix} 0 \\ -1 \end{bmatrix} \hat{R}_t^S + \begin{bmatrix} \hat{z}_t^\pi \\ \hat{z}_t^X + V^{LH} w_2 \hat{z}_t^B \end{bmatrix} \end{aligned} \tag{2.92}$$

In matrix notation, system (2.92) becomes

$$\mathbf{AZ'_t} = \mathbf{BE^*_tZ'_{t+1}} + \mathbf{CR^S_t} + \mathbf{v_t} \tag{2.93}$$

which has a solution only if $\mathbf{A}$ is invertible. Considering the forecasting rules described in Section 2.3.3, the system (2.93) is completely backward-looking and its solution coincides with the reduced form of the model:

$$\mathbf{Z'_t} = \mathbf{A^{-1}}\left(\mathbf{BE^*_tZ'_{t+1}} + \mathbf{CR^S_t} + \mathbf{v_t}\right) \tag{2.94}$$

The main advantage of this approach is the possibility to fully track the highly non-linear dynamics originated by reinforcement learning mechanisms which would need to be approximated in a stochastic environment with rational expectations.

2.4 Simulations

This section of the paper analyses the dynamics of the model using numerical methods. After presenting parameters calibration, it assesses model behaviour in the short- and long-run.

2.4.1 Calibration

The model was calibrated to match quarterly frequency data for US. Parameters for the utility function are based on Galì (2008); both the labour supply and the intertemporal-substitution in consumption elasticities are set to one. The latter is in line with papers considering a binding ELB - see Harrison (2017) and Goy et al. (2020). Following results found in Slobodyan and Wouters (2012), the calibration of the discount factor guarantees an annualised short-term interest rate of 1.2 percent in equilibrium - namely, $\beta = 0.997$. The Calvo parameter is consistent with a somewhat low frequency of price adjustment being set to, 0.847, a value similar to estimates presented in Smets and Wouters (2005) - so to obtain a Phillips Curve slope of 0.0561 as in Galì (2008). The inverse elasticity of substitution across products was set at 6; equivalent to a mark-up of about 20 percent in steady state. Finally, the parameters of the Taylor rule are taken fromSmets and Wouters (2007).

Relevant parameters for quantitative easing follow Harrison (2017) and Falagiarda (2013). The size of the asset purchase program is equal to one. This value is consistent with the magnitude of long-term asset purchases run by the FED during the QE2 program which was characterised by a 100 percent increase of the long-term assets in the FED portfolio. Finally, the persistence of asset purchases was fine-tuned to replicate a LTAP lasting for 6 years in the overall.[27]

The parameter determining the decaying speed of coupons, χ, matches the average duration of US 10-year zero coupon bonds in December 2008 - when the first long-term asset purchase program was launched in US (D'Amico and King, 2013). Portfolio adjustment-costs come from Harrison (2017) who run a sensitivity analysis test over a grid of plausible parameters in order to obtain moments in line with what estimated by D'Amico and King (2013).[28]

[27]Usually, the monetary authority announces the starting date of the program, its duration and the amount of bonds purchased in each tranche. A nuisance of simulating asset purchases by means of an AR(1) shock is that the Central Bank starts reducing the purchased amount of bonds after one period. However, this calibration allows to reproduce different reasonable exit strategies for the Central Bank. To formally study the impact of more structured announcements one can use the perfect foresight solver of Dynare at the cost of loosing the effects related to the precautionary motive of agents.

[28]Appendix B.6 shows the generalised impulse responses generated with this model and the TANK model developed in Sims et al. (2020) are qualitatively very similar.

Parameter	Name	Value	Source
σ	Intertemporal elasticity of substitution	1	Harrison (2017)
φ	Labour utility	1	Galì (2008)
ζ	Elasticity of substitution across products	6	Galì (2008)
ξ	Calvo parameter	0.847	Galì (2008)
β	Discount factor	0.997	Slobodyan and Wouters (2012)
ϕ_A	Persistence of the technology shock	0.9	Galì (2008)
ϕ_U	Persistence of the mark-up shock	0.7	
α_Π	Taylor rule - inflation	1.5	Galì (2008)
α_Y	Taylor rule - output	0.125	Galì (2008)
τ_B	Fiscal rule - LT bond	0.3	Falagiarda (2013)
Asset Purchase Programmes			
ϕ_B	Persistence of the balance-sheet shock	0.83	Falagiarda (2013)
χ	Bond long - slope of coupons	0.95	Harrison (2017)
ϕ_L	Portfolio adjustment cost - stock	0.35	Harrison (2017)
Reinforcement Learning Parameters			
γ^{ic}	Intensity of choice	2	De Grauwe and Ji (2020a)
ρ^{fit}	Weight on the latest forecast error	0.5	De Grauwe and Ji (2020a)
ρ^E	reinforcement expectations parameter	0	De Grauwe and Ji (2020a)
$\omega_0^{x,F}, \omega_0^{\pi,F}$	Fundamentalists - Share in t=0	0.5	De Grauwe and Ji (2020a)
$\bar{X}$	Fundamentalists - Output gap forecast	0	De Grauwe and Ji (2020a)
$\bar{\pi}$	Fundamentalists - Inflation forecast	0	De Grauwe and Ji (2020a)

Table 2.1: Parameters summary

2.4.2 Policy Analysis

This section shows the main policy implications of introducing heterogeneous expectations and bounded rational agents behaving as reinforcement learners.

Role of Heterogenous Expectations

Figure 2.1a shows the relationship between the sentiment indicator, defined in Section 2.3.4, and output-gap is quite strong - the contemporaneous correlation is around 70 percent.[29]

[29] This is just to show the model can replicate standard results shown in De Grauwe (2012a) and De Grauwe et al. (2020)

This feature of the model is generated endogenously by agents switching across different forecasting rules while learning from their forecast errors. Periods characterised by high optimism - corresponding to a sentiment indicator above 50% - originate a reinforcement mechanism which materialises in even higher positive output-gaps. When the extrapolative forecast rule performs better than the fundamentalist one and output-gap is above steady state, a wave optimism will pervade the economy.

On the one hand, extrapolators expect output-gap to remain positive in next period thereby pushing aggregate demand up. On the other hand, more fundamentalists will become extrapolators and this will result in higher positive output-gaps. However, it might happen that after some periods the forecasting performance of fundamentalists will outperform that of extrapolators as a result of stochastic shocks hitting the economy. Consequently, a wave of pessimism would gradually take over thereby inducing a slowdown in business activity. This occurs because fundamentalists expect output-gap to revert to its steady state. The opposite would happen when the output-gap is below the steady state, as fundamentalists would be optimists and extrapolators pessimists. Figure 2.1b highlights the model is producing periods of extreme optimism and pessimism - as the distribution of the sentiment indicator is somehow skewed and presents fat tails. This is reflected in the distribution of output-gap which is, in turn, non-normal and characterised by a slightly excessive skew and kurtosis (see Figure 2.1c).

De Grauwe (2011) and more recently Jump and Levine (2019) provide empirical evidence in favour of non-normal distribution of the output-gap in industrialised countries; they find the output-gap is highly correlated with empirical measures of sentiment while being characterised by fat tails and excess kurtosis. The non-linearities introduced by reinforcement learning seem likely to help reproducing these features of empirical data.

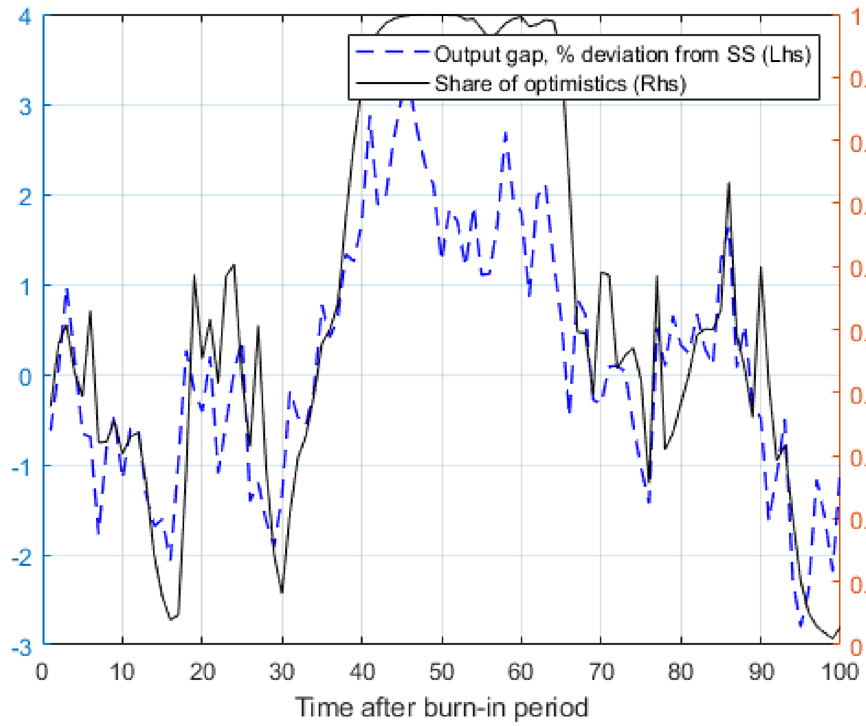

(A) Output gap and share of optimistics

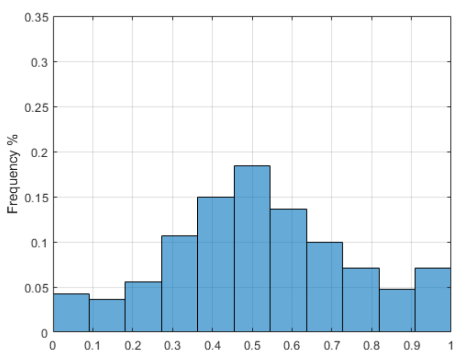

(B) Optimistics distribution

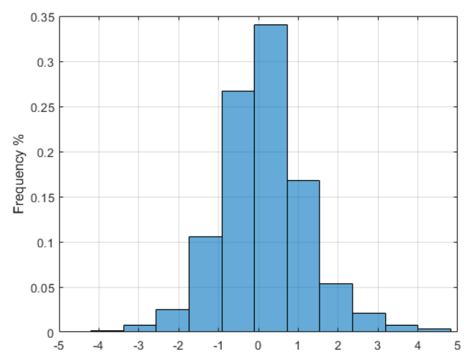

(C) Output gap distribution.

FIGURE 2.1: Relationship between output gap and optimism

Asset Purchase Programs

This section investigates the pass-through of long-term asset purchases to the economy. For this purpose, 500 scenarios only differing for the realisations of the four shock-processes were simulated. These simulations fully consider non-linearities residing in the learning process. As forward-looking agents are fundamentalists, the model was solved recursively by simple matrix inversion - see Section 2.3.5.[30]

Then, generalised impulse responses were computed to analyse the state-dependency of multipliers. As the model was simulated non-linearly, impulse responses were not generated at the deterministic steady state but at the equilibrium of the system after a burn-in of 350 periods.[31]

All graphs exhibit the average generalised impulse response across all the 500 scenarios - solid blue line - and a range represented by either adding or subtracting the standard deviation of generalised impulse responses across the different scenarios - dashed red line. As we will see, the latter will play an important role in interpreting results when heterogeneous expectations and learning are incorporated in the simulations.

First, let start by analyzing the dynamics of the model with bond-market segmentation when fundamentalists are the only agents populating the economy. Figure 2.2, shows the effects of a one-standard-deviation shock to the balance-sheet of the Central Bank. This simulation considers the standard scenario in which the shock is supposed to completely fade away after 6 years.

When the Central Bank starts purchasing long-term assets, the long-term interest rate decreases. Agents react by adjusting the mix of different bonds held in portfolio but because these are not perfect substitutes among each others, agents can expand consumption thanks to the extra resources received from the sale of long-term bonds - *portfolio channel*. The effect of higher long-term interest rates is transferred via the aggregate demand equation to the real economy (*feedback channel*), and materialises in an increase of output and inflation. The central-bank balance-sheet shock generates macroeconomic dynamics similar to those of a standard monetary policy shock. However, while output and inflation respond similarly to a monetary policy shock, the effects of a balance-sheet shock are more pronounced on output-gap than on inflation.[32]

[30]Simulations are similar to what obtained with a fully non-linear simulation under perfect-foresight but with the presence of noise.

[31]To build each generalised impulse response, the model was simulated twice using the same shock vectors: first, with a shock in period 351, then, without it. Finally, generalised impulse responses were computed as the difference between the two simulations and normalised by dividing for the magnitude of the shock.

[32]This is consistent with models presented in Sims and Wu (2020a,b) and Sims et al. (2020) and in line with empirical results showing a limited impact of QE policies on inflation.

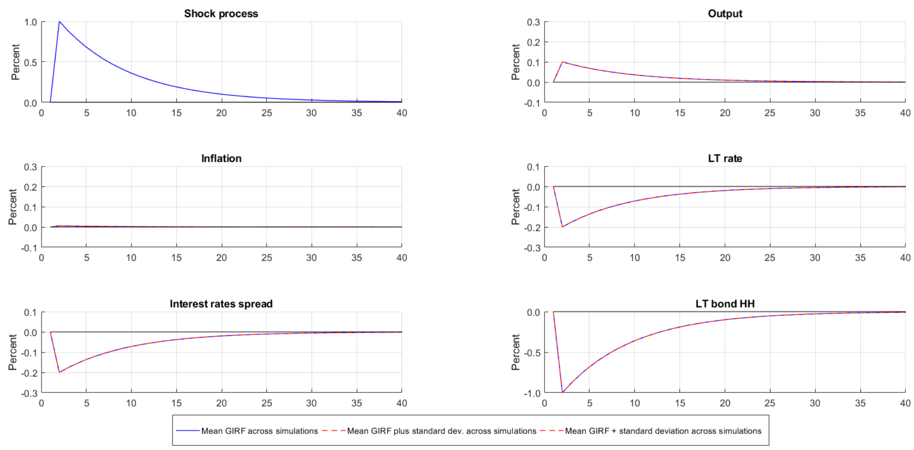

FIGURE 2.2: Balance-sheet shock - persistence, only fundamentalists. Generalised impulse responses to a one-standard-deviation balance-sheet shock. The shock is simulated after a burn-in of 350 periods on 500 different realisations of the shock processes. The blue line is the average GIRF across all scenarions. Red-dashed lines show the blue line +/- 1-standard-deviation across scenarios.

Figure 2.3 presents generalised impulse responses to the same shock as above on an economy with heterogeneous expectations and reinforcement learning. In this case, the model considers the simultaneous presence of fundamentalists and näives while allowing them to rely on reinforcement learning to form expectations. On impact, the reaction of long-term interest rates is the same as in Figure 2.2. However, the effects of the shock decay faster over the short-run - e.g. the first 4 quarters after the shock - compared to the case in which only fundamentalists populate the economy. Nonetheless, they are somewhat more persistent over the long-run. This phenomenon is reflected in the shape of the generalised impulse responses for macroeconomic variables. After the initial shock, output continues slowly growing for three periods to, then, slowly revert to equilibrium after more than 20 periods. Also the propagation of the balance-sheet shock to inflation is more evident and extended over time. After the initial impact of the shock, the magnitude of the response keeps on growing for six quarters up to three times its initial value, then, it remains somehow stable for four quarters before starting to slowly decrease. These effects vanish after about forty periods. Looking at the definition of the Phillips curve in equation (2.74), inflation behaviour is the result of two elements. On the one hand, as in standard fully rational models, the higher response and the longer persistence of output to the balance-sheet shock is transferred to inflation. On the other one, by means of reinforcement learning, the behavioural model is able to capture the *signalling effect* of quantitative easing.

The red-dashed lines can be interpreted as the uncertainty around each generalised impulse response. Impulse responses vary, on average, across different realisations of the shock processes suggesting the effect of unconventional monetary policies might be different depending on the state of the economy. The framework suggests the sign of impulse responses to be robust across simulations in the short-run. However, uncertainty about the magnitude of the effects mounts over time indicating the effects of quantitative easing might be negative in the long-run. Focusing on uncertainty on the size of the impulse response of output-gap, it seems somehow constant over time and the likelihood of observing negative effects becomes more concrete after fifteen quarters. By contrast, variability of inflation impulse responses sharply increases after four periods, reaching its maximum between around period 15 and 20 to then steadily decrease. As a result of this wide standard deviation across simulations the likelihood of observing negative impulse responses raises already after ten periods.

Figure 2.4 shows the effects of APPs are likely to be overall positive for both output-gap and inflation. Histograms 2.4a and 2.4b present some insights on the short-run impact of APP shocks on output-gap and inflation in the short-run - e.g. captured by the distribution across the different scenarios of the cumulated impact of the APP shock over the first four quarters. In fact, the distribution leans clearly on positive values and it is skewed to the upside. The situation is less evident over longer horizons - e.g. from the fifth quarter to the fortieth. For output-gap, the distribution is more dispersed. Most of the weight is on low bins and about 8 percent of realisations is in negative territory. Nonetheless, the bulk of the distribution of cumulated GIRFs for inflation is still positive and skewed to the right even though all values are close to the zero-line.

Uncertainty around the size of generalised impulse responses resides in the learning mechanism which leads agents' expectations to endogenously generate waves of pessimism and optimism. The way the system evolves during the burn-in period depends on how agents learn from past forecast errors in a stochastic environment. As GIRFs are state-dependent, the moment in which the CB launches long-term asset purchases matters. Indeed, with heterogeneous agents and reinforcement learning

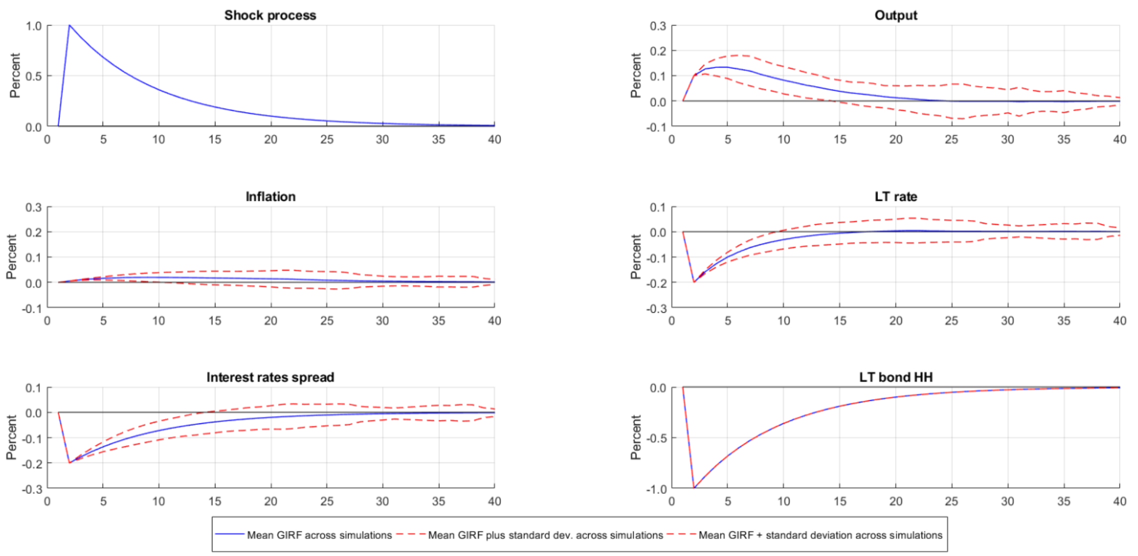

FIGURE 2.3: Balance-sheet shock - persistent shock and reinforcement learning.
Generalised impulse responses to a one-standard-deviation balance-sheet shock. The shock is simulated after a burn-in of 350 periods on 500 different realisations of the shock processes. The blue line is the average GIRF across all scenarions. Red-dashed lines show the blue line +/- 1-standard-deviation across scenarios.

the same balance-sheet shock might generate different dynamics depending on the level of optimism in the economy at the moment it happens.

To provide some evidence on this, Figure 2.5 shows the relationship between the average level of optimism, defined in (2.89), during the first four quarters after the shock and the cumulated generalised impulse responses over the same time span for both output-gap and inflation. APPs are more effective when optimism is either extremely high or extremely low. In light of the high correlation between optimism and output-gap found in Section 2.4.2, this framework seems to promote APPs as a useful counter-cyclical tool, thus, suggesting it can be used to smooth the business cycle either at its peaks or troughs.

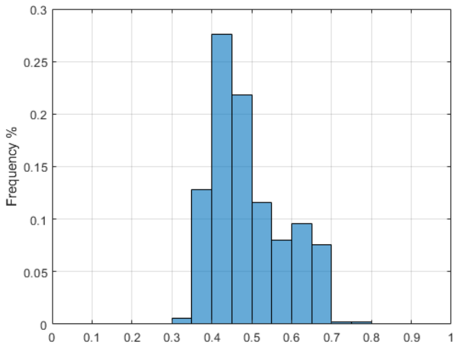

(A) Short-term output-gap

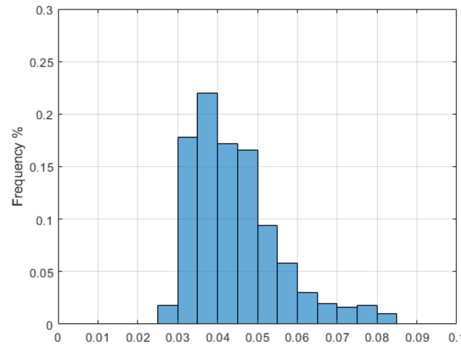

(B) Short-term inflation

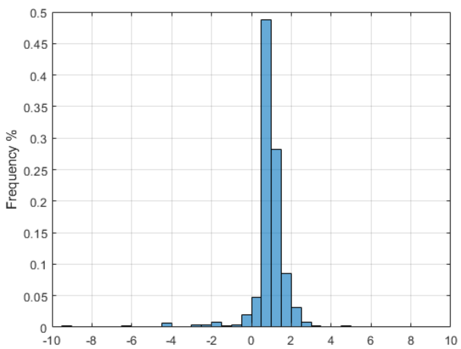

(C) Long-term output-gap

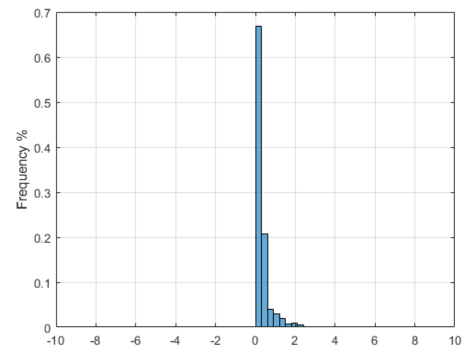

(D) Long-term inflation

FIGURE 2.4: Distribution of cumulated GIRF across different scenarios. Short-term consists of the sum of GIRFs over the first 4 quarters after the shock. Long-term starts from the 5-th quarter to 40 quarters ahead.

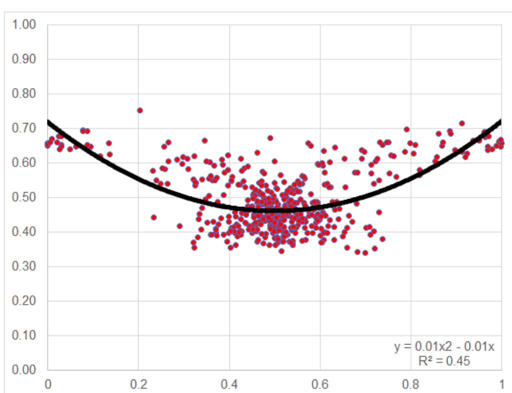

(A) Short-term output-gap

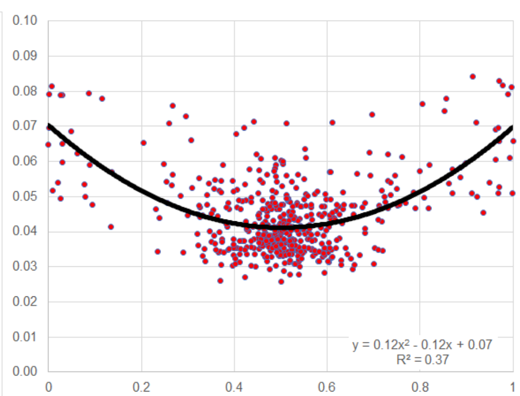

(B) Short-term inflation

FIGURE 2.5: Relationship between optimism and short-term impact of a persistent balance-sheet shock. The x-axis shows the mean share of optimistic agents over the short-term for each simulated scenario. The y-axis shows the sum of GIRFs over the first four quarters after the shock for each simulated scenario.

The model also introduces interactions between Central Bank credibility and the effectiveness of long-term asset purchases which can be used to assess state-dependency of inflation impulse responses. As fundamentalist agents expect inflation to be on target next period, their share can be considered as an endogenous measure to track CB's credibility over time, and can provide some useful insights to interpret the effectiveness of policy tools.[33]

Figure 2.6 shows a strong linear relationship between the average share of fundamentalists during the first four quarters after a CB balance-sheet shock and the respective cumulated inflation GIRFs. Therefore, the model implies strong CB credibility can amplify the APPs effectiveness.

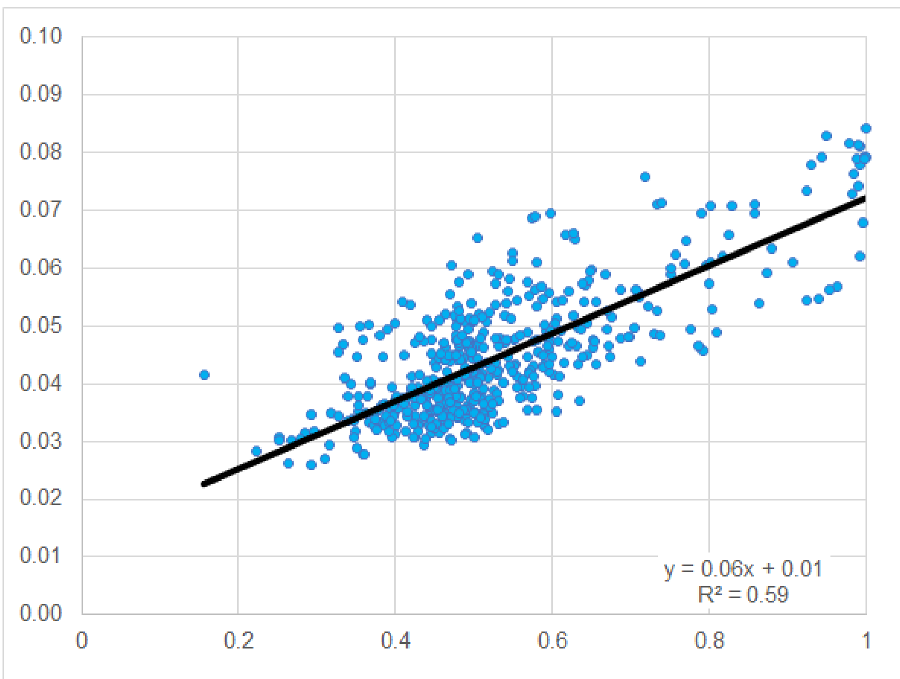

FIGURE 2.6: Relationship between central credibility and short-term impact of a persistent balance-sheet shock on inflation. The x-axis shows the mean share of inflation targeters over the short-term for each simulated scenario. The y-axis shows the sum of inflation GIRFs over the first four quarters after the shock for each simulated scenario. Each scenario is simulated over 10000 periods.

[33]Fundamentalists are also referred as "credibility-believers" or "inflation-targeters" in behavioural macroeconomics literature - see Hommes and Lustenhouwer (2019) and Goy et al. (2020).

Analysis of the Parameter Space and Optimal Policy

Following De Grauwe and Ji (2020a, 2021), model behaviour for different combinations of conventional and unconventional monetary policies was analysed through a Monte Carlo exercise. Specifically, repeated simulations for different parametrisations of the standard Taylor rule (2.75) and QE rule (2.76) were employed to assess the sensitivity of model stability, in terms of convergence and volatility, to different CB reaction functions.

Figure 2.7 presents stability regions for different configurations of the Taylor Rule while keeping QE Taylor Rule parameters fixed. In this graphical representation, model is considered to be unstable (U) when at least one endogenous variable is explosive, stable (S) when variables fluctuate around their steady states and highly volatile (HV) when the system is still stable but stochastic processes cause endogenous variables to widely oscillate around their steady states.[34]

Panel 2.7a illustrates the case in which the Central Bank uses only standard monetary policy to steer the economy. Results are similar to those of De Grauwe and Ji (2020a): the inflation parameter seems driving the stability of the stochastic system. However, *reinforcement learning* seems to oblige the CB to react at least softly to output-gap developments to avoid episodes of high volatility. On the contrary, intervening only on output-gap is not sufficient to stabilise the system and this measure would need to be accompanied by some inflation containment. Panels 2.7b to 2.7d present combinations of standard monetary policy with inflation QE rules. In this framework, QE can help standard monetary policy in stabilizing the economy. Furthermore, a heavy QE reaction to inflation can stabilise the system also when monetary policy does not react to inflation ($\alpha^{\pi} = 0$), as for instance while at the ZLB.[35]

Yet, some interventions on the output-gap are needed to avoid high volatility episodes. Similarly, Figure 2.8 confirms output-gap stabilisation is not sufficient to stabilise the system although it is critical to avoid high-uncertainty periods.

[34] These cases are characterised by a variance at least 5 times larger than the variance of stochastic processes.

[35] To interpret sensitivity of stability areas to the magnitude one has to keep in mind the specification of the Euler Equation in which the weight of long-term interest rates directly depends on the size of the overall financial sector and on the relative exposure of households to long-term bonds.

This is in line with De Grauwe and Ji (2020a), showing that episodes of high volatility in behavioural models are mainly due to the sentiment indicator reaching extreme values because of agents tangibly reacting to output-gap variations.

	0	0.1	0.2	0.3	0.4	0.5	0.6	0.7	0.8	0.9	1	...	1.5	...	3	...	3.5
0	U	U	U	U	U	U	U	U	U	U	HV	HV	HV	HV	HV	HV	HV
0.1	U	U	U	U	U	U	U	U	U	U	S	S	S	S	S	S	S
0.2	U	U	U	U	U	U	U	U	U	U	S	S	S	S	S	S	S
0.3	U	U	U	U	U	U	U	U	U	U	S	S	S	S	S	S	S
0.4	U	U	U	U	U	U	U	U	U	U	S	S	S	S	S	S	S
0.5	U	U	U	U	U	U	U	U	U	U	S	S	S	S	S	S	S
0.6	U	U	U	U	U	U	U	U	U	HV	S	S	S	S	S	S	S
0.7	U	U	U	U	U	U	U	U	U	HV	S	S	S	S	S	S	S
0.8	U	U	U	U	U	U	U	U	U	S	S	S	S	S	S	S	S
0.9	U	U	U	U	U	U	U	U	U	S	S	S	S	S	S	S	S
1	U	U	U	U	U	U	U	U	U	S	S	S	S	S	S	S	S
1.1	U	U	U	U	U	U	U	U	U	S	S	S	S	S	S	S	S
1.2	U	U	U	U	U	U	U	U	U	S	S	S	S	S	S	S	S
1.3	U	U	U	U	U	U	U	U	U	S	S	S	S	S	S	S	S
1.4	U	U	U	U	U	U	U	U	HV	S	S	S	S	S	S	S	S
1.5	U	U	U	U	U	U	U	U	HV	S	S	S	S	S	S	S	S
1.6	U	U	U	U	U	U	U	U	HV	S	S	S	S	S	S	S	S
1.7	U	U	U	U	U	U	U	U	HV	S	S	S	S	S	S	S	S
1.8	U	U	U	U	U	U	U	U	HV	S	S	S	S	S	S	S	S
1.9	U	U	U	U	U	U	U	U	S	S	S	S	S	S	S	S	S
2	U	U	U	U	U	U	U	U	S	S	S	S	S	S	S	S	S

(A) $\theta^{\pi} = 0$, $\theta^{X} = 0$

	0	0.1	0.2	0.3	0.4	0.5	0.6	0.7	0.8	0.9	1	...	1.5	...	3	...	3.5
0	U	U	U	U	U	U	U	U	U	HV	HV	HV	HV	HV	HV	HV	HV
0.1	U	U	U	U	U	U	U	U	U	S	S	S	S	S	S	S	S
0.2	U	U	U	U	U	U	U	U	U	S	S	S	S	S	S	S	S
0.3	U	U	U	U	U	U	U	U	S	S	S	S	S	S	S	S	S
0.4	U	U	U	U	U	U	U	U	S	S	S	S	S	S	S	S	S
0.5	U	U	U	U	U	U	U	U	S	S	S	S	S	S	S	S	S
0.6	U	U	U	U	U	U	U	U	S	S	S	S	S	S	S	S	S
0.7	U	U	U	U	U	U	U	HV	S	S	S	S	S	S	S	S	S
0.8	U	U	U	U	U	U	U	HV	S	S	S	S	S	S	S	S	S
0.9	U	U	U	U	U	U	U	S	S	S	S	S	S	S	S	S	S
1	U	U	U	U	U	U	U	S	S	S	S	S	S	S	S	S	S
1.1	U	U	U	U	U	U	U	S	S	S	S	S	S	S	S	S	S
1.2	U	U	U	U	U	U	HV	S	S	S	S	S	S	S	S	S	S
1.3	U	U	U	U	U	U	HV	S	S	S	S	S	S	S	S	S	S
1.4	U	U	U	U	U	U	HV	S	S	S	S	S	S	S	S	S	S
1.5	U	U	U	U	U	U	HV	S	S	S	S	S	S	S	S	S	S
1.6	U	U	U	U	U	U	S	S	S	S	S	S	S	S	S	S	S
1.7	U	U	U	U	U	HV	S	S	S	S	S	S	S	S	S	S	S
1.8	U	U	U	U	U	HV	S	S	S	S	S	S	S	S	S	S	S
1.9	U	U	U	U	U	HV	S	S	S	S	S	S	S	S	S	S	S
2	U	U	U	U	U	HV	S	S	S	S	S	S	S	S	S	S	S

(B) $\theta^{\pi} = 1.5$, $\theta^{X} = 0$

	0	0.1	0.2	0.3	0.4	0.5	0.6	0.7	0.8	0.9	1	...	1.5	...	3	...	3.5
0	U	U	U	U	U	HV	HV	HV	HV	HV	HV	HV	HV	HV	HV	HV	HV
0.1	U	U	U	U	U	S	S	S	S	S	S	S	S	S	S	S	S
0.2	U	U	U	U	U	S	S	S	S	S	S	S	S	S	S	S	S
0.3	U	U	U	U	U	S	S	S	S	S	S	S	S	S	S	S	S
0.4	U	U	U	U	U	S	S	S	S	S	S	S	S	S	S	S	S
0.5	U	U	U	U	U	S	S	S	S	S	S	S	S	S	S	S	S
0.6	U	U	U	U	U	S	S	S	S	S	S	S	S	S	S	S	S
0.7	U	U	U	U	HV	S	S	S	S	S	S	S	S	S	S	S	S
0.8	U	U	U	U	HV	S	S	S	S	S	S	S	S	S	S	S	S
0.9	U	U	U	U	S	S	S	S	S	S	S	S	S	S	S	S	S
1	U	U	U	U	S	S	S	S	S	S	S	S	S	S	S	S	S
1.1	U	U	U	U	S	S	S	S	S	S	S	S	S	S	S	S	S
1.2	U	U	U	U	S	S	S	S	S	S	S	S	S	S	S	S	S
1.3	U	U	U	HV	S	S	S	S	S	S	S	S	S	S	S	S	S
1.4	U	U	U	HV	S	S	S	S	S	S	S	S	S	S	S	S	S
1.5	U	U	U	HV	S	S	S	S	S	S	S	S	S	S	S	S	S
1.6	U	U	U	HV	S	S	S	S	S	S	S	S	S	S	S	S	S
1.7	U	U	U	HV	S	S	S	S	S	S	S	S	S	S	S	S	S
1.8	U	U	U	S	S	S	S	S	S	S	S	S	S	S	S	S	S
1.9	U	U	U	S	S	S	S	S	S	S	S	S	S	S	S	S	S
2	U	U	HV	S	S	S	S	S	S	S	S	S	S	S	S	S	S

(C) $\theta^{\pi} = 5$, $\theta^{X} = 0$

	0	0.1	0.2	0.3	0.4	0.5	0.6	0.7	0.8	0.9	1	...	1.5	...	3	...	3.5
0	HV	HV	HV	HV	HV	HV	HV	HV	HV	HV	HV	HV	HV	HV	HV	HV	HV
0.1	S	S	S	S	S	S	S	S	S	S	S	S	S	S	S	S	S
0.2	S	S	S	S	S	S	S	S	S	S	S	S	S	S	S	S	S
0.3	S	S	S	S	S	S	S	S	S	S	S	S	S	S	S	S	S
0.4	S	S	S	S	S	S	S	S	S	S	S	S	S	S	S	S	S
0.5	S	S	S	S	S	S	S	S	S	S	S	S	S	S	S	S	S
0.6	S	S	S	S	S	S	S	S	S	S	S	S	S	S	S	S	S
0.7	S	S	S	S	S	S	S	S	S	S	S	S	S	S	S	S	S
0.8	S	S	S	S	S	S	S	S	S	S	S	S	S	S	S	S	S
0.9	S	S	S	S	S	S	S	S	S	S	S	S	S	S	S	S	S
1	S	S	S	S	S	S	S	S	S	S	S	S	S	S	S	S	S
1.1	S	S	S	S	S	S	S	S	S	S	S	S	S	S	S	S	S
1.2	S	S	S	S	S	S	S	S	S	S	S	S	S	S	S	S	S
1.3	S	S	S	S	S	S	S	S	S	S	S	S	S	S	S	S	S
1.4	S	S	S	S	S	S	S	S	S	S	S	S	S	S	S	S	S
1.5	S	S	S	S	S	S	S	S	S	S	S	S	S	S	S	S	S
1.6	S	S	S	S	S	S	S	S	S	S	S	S	S	S	S	S	S
1.7	S	S	S	S	S	S	S	S	S	S	S	S	S	S	S	S	S
1.8	S	S	S	S	S	S	S	S	S	S	S	S	S	S	S	S	S
1.9	S	S	S	S	S	S	S	S	S	S	S	S	S	S	S	S	S
2	S	S	S	S	S	S	S	S	S	S	S	S	S	S	S	S	S

(D) $\theta^{\pi} = 15$, $\theta^{X} = 0$

FIGURE 2.7: Stability areas with mixed policies: varying QE reaction to inflation, θ^{π}.

The matrix is based on a sensitivity analysis of system stability for different configurations of the Taylor rule parameters (α^{π} in columns and α^{X} in rows). Each panel shows stability properties for a different value of θ^{π} while keeping $\theta^{X} = 0$. Each scenario is simulated over 10000 periods.

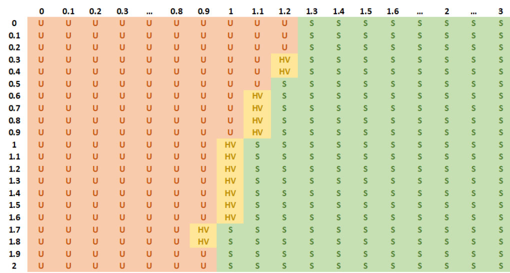

(A) $\theta^{\pi} = 0$, $\theta^{X} = 1.5$

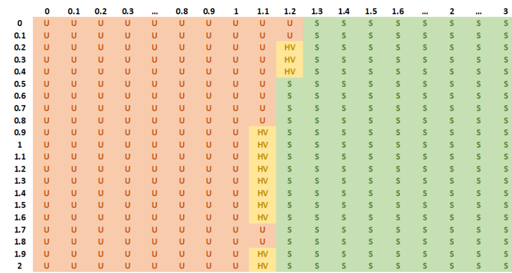

(B) $\theta^{\pi} = 0$, $\theta^{X} = 5$

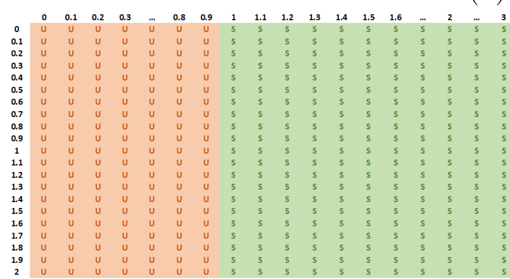

(C) $\theta^{\pi} = 0$, $\theta^{X} = 15$

FIGURE 2.8: Stability areas with mixed policies: varying QE reaction to output-gap, θ^{X}.
The matrix is based on a sensitivity analysis of system stability to different configurations of the Taylor rule parameters (α^{π} in columns and α^{X} in rows). Each panel shows stability properties for a different value of θ^{X} while keeping $\theta^{\pi} = 0$. Each scenario is simulated over 10000 periods.

Figure 2.9 provides further details on how conventional monetary policy can stabilise the long-term volatility of the system. Building on results shown in pane 2.7a in which QE does not react to economic developments ($\theta^{X} = \theta^{\pi} = 0$), the top pane shows the CB can absorb most of output-gap volatility through a soft intervention on this variable; values of α^{X} around 0.1 allow to exit a high-volatility environment and this is more evident when CB's react one by one to inflation movements. However, it seems the CB needs to react more than proportionally to inflation movements to curtail inflation variance - see the middle panel. Finally, the bottom panel suggests policymakers face a trade-off when minimizing these two variables.

To shed some light on the best policy mix, I follow De Grauwe (2011) assuming the CB optimises welfare by minimizing the overall volatility of the economic system. In practice, the CB chooses α^{X} and α^{π} to minimise a loss function depending on output-gap and inflation volatility:

$$L = std(\hat{\pi})P + std(\hat{x})(1 - P) \tag{2.95}$$

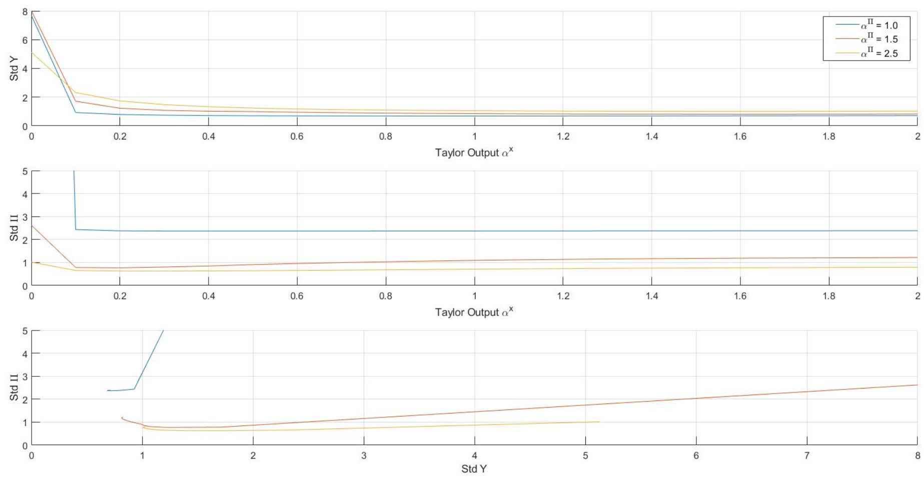

FIGURE 2.9: Taylor Rule parameters and volatility of endogenous variables for different values of θ^π. Simulated one scenario for 10000 periods while keeping $\theta^X = 0$.

where $0 < P < 1$ represents CB's preference for inflation stabilisation. When the CB minimises only one of the two standard deviations, the policy problem would lead to results shown the top-two panels of Figure 2.9. However, overall volatility reaches lower levels when the CB tries to stabilise both variables. The top panel of Figure 2.10 exhibits the case in which the CB has not a clear preference between output and inflation, and suggest that the minimum volatility is reached when the CB reacts heavily to both to output-gap ($\alpha^X = 1.2$) and inflation ($\alpha^\Pi = 2.5$). This result is qualitatively similar to what shown in the bottom panel where the CB prefers minimizing inflation volatility ($P = 0.75$) although in this case overall volatility is about 10% lower.

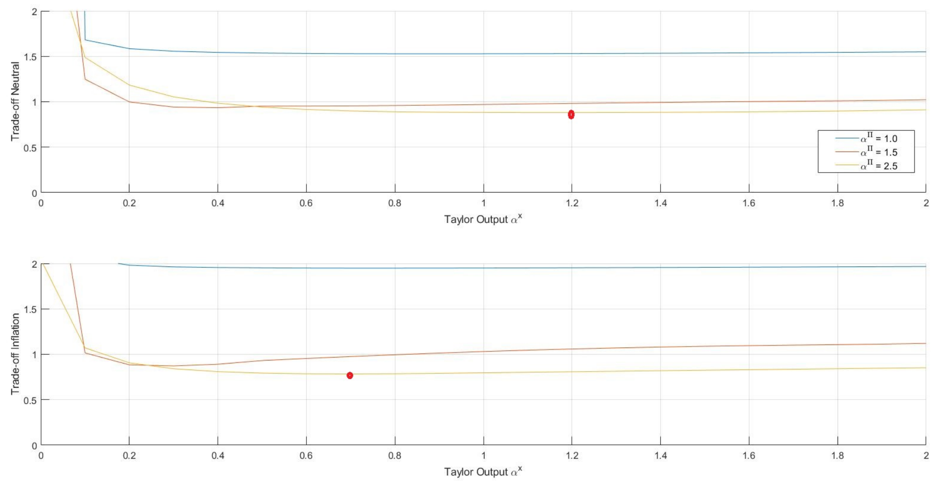

FIGURE 2.10: Taylor Rule parameters and loss function of endogenous variables for different values of α^π and α^X. In the top panel P=0.5 and in the bottom one P=0.75. Simulated one scenario for 10000 periods while keeping $\theta^\pi = \theta^X = 0$. Stability areas with mixed policies: varying QE reaction to inflation.
The matrix presents a grid search for different values of the standard Taylor rule (α^π in columns and α^X in rows) while keeping fixed values of the QE Taylor rule. Each scenario is simulated over 10000 periods.

2.5 Conclusions

This paper develops a Behavioural DSGE model to analyse quantitative easing under *bounded rationality*. Quantitative easing, in the form of long-term asset-purchases, was embedded through *portfolio adjustment costs* across bonds with different maturities modelled as perpetuities with geometrically decaying coupons *à la Woodford* (2001). By adjusting the quantity of long-term bonds in its balance-sheet, the Central Bank can reduce long-term interest rates and thereby influencing households' consumption decisions. The novelty of the paper is the study of long-term asset-purchase programs in a framework characterised by *heterogeneous expectations* and *Euler learning*. This implies agents' behaviour can differ depending on the rule adopted for forming expectations which is chosen on the basis of its past predictive performance as in canonical models with *reinforcement learning à la Brock and Hommes (1997)*.

Thanks to these features, the model is equipped to simulate state-dependent impulse responses, and possibly offer an explanation to the variety of empirical results on the effects of quantitative easing. In this framework, the pass-through of quantitative easing to the economy varies with economic sentiment and Central Bank credibility. The model generates waves of optimism and pessimism affecting the transmission of long-term interest rates changes to macroeconomic variables - *feedback channel*. The model suggests the short-run effects of asset purchases are expansionary and robust to different sentiment levels. However, their size and persistence vary with the state of the economy - as the variance across different scenarios is wide. The latter provide an interpretation for the different findings proposed by empirical literature suggesting the passthrough of long-term asset purchases depends on the state of the economy.

Furthermore, a Monte Carlo exercise suggests long-term asset purchases are likely to be a valid counter-cyclical measure. On average, the positive response of macroeconomic variables to policy actions is stronger either when extreme pessimism or optimism feature the state of the economy. As the output-gap and the sentiment indicator are highly correlated, one can infer this policy measures are suitable to stabilise the business cycle when it is far from its steady state in absolute value.

Moreover, the effectiveness of asset-purchase programs depends on central-bank credibility. The latter is endogenously generated by the model depending on how close inflation was to target over the recent past. In turn, this would result, on average, in higher impulse responses of inflation to a balance-sheet shock.

As in De Grauwe and Ji (2021), the model supports the relevance of a dual-mandate addressing directly both inflation and output-gap fluctuations to avoid economic uncertainty when agents form expectations using *reinforcement learning*. Although stabilizing inflation is crucial to avoid the system to become explosive, even a moderate intervention the output-gap is important to reduce the probability of high volatility episodes. By reacting to output-gap developments, the Central Bank can somehow curtail episodes of extreme optimism or pessimism and thereby reduce the risk of expectation-driven self-reinforcing mechanisms destabilizing the economy.

This model can be extended in several directions. These include the incorporation of forward-guidance as in Goy et al. (2020) to study how the latter can influence the term structure, uncertainty on the length of long-term asset purchase programs as in Hommes et al. (2018) to study the signalling effect of quantitative easing and in an open-economy environment as in De Grauwe and Ji (2020a) to analyse how the synchronisation of the sentiment indicator can influence the compression of the term structure. Finally, steady-states stability and system behaviour might be formalised as in Hommes and Lustenhouwer (2019). This is left for future research.

Chapter 3

Non-Linear Behavioural New Keynesian Models: Identification and Estimation

Abstract

This paper designs and estimates a non-linear New Keynesian (NK) Behavioural model with trend inflation, *heterogeneous expectations* and *bounded rational agents* forming expectations on the basis of *reinforcement learning* (Brock and Hommes, 1997). Novel identification tests for non-linear DSGE models show that the core parameters of the learning mechanism (i.e. the *intensity of choice* and the *memory parameters*) can only be identified with higher-order approximations while observing the proportion of agents adopting a specific forecasting rule. Thus, the model is estimated with Bayesian techniques by means of a second-order Extended Kalman filter (Gustafsson and Hendeby, 2012) -relying on results from *Chapter 1*- while expanding the information set with data from the *Survey of Consumers Expectations* from the *University of Michigan* to proxy the share of *näive* agents populating the economy. Given the combination of *fully rational* and *bounded-rational* agents, the *intensity of choice* parameter was estimated to be higher than usually assumed.

JEL Classification: C11, C18, C32, E32, E47, E52, E62, E70, O44
Keywords: DSGE modelling, rationality, endogenous growth, systems estimation, heterogeneity, unemployment, banking sector

3.1 Introduction

The assumption of fully informed rational expectations (FIRE) underpins the large majority of modern macroeconomic models. In standard linear dynamic stochastic general equilibrium (DSGE) models, the FIRE hypothesis implies agents to be taking decisions consistently with the actual structure of the model, while having timely access to the complete information set.

This modelling approach was recently subject to critics. On the one hand, the Great Financial Crisis showed that linear DSGE models are somewhat limited in reproducing the atypical patterns characterising macroeconomic data in turmoil periods (De Grauwe, 2012a; Ascari et al., 2015; Jump and Levine, 2019). On the other hand, a growing strand of literature relying on survey data (Branch, 2004; Pfajfar and Santoro, 2010; Coibion and Gorodnichenko, 2015) and on laboratory experiments (Assenza et al., 2021) somehow challenged the FIRE hypothesis at micro level.

With the aim of filling the gap between theory and empirical evidence, there was a proliferation of DSGE models endowed with various forms of bounded rationality. The issue is that the departure from rationality opens an infinite number of modelling options, making economists subject to the “wilderness" described in Sims (1980).

Among others, influential applications introduced *adaptive learning* (Evans and Honkapohja, 2001; Milani, 2007), *internal rationality* (Adam and Marcet, 2011; Deák et al., 2017b), *rational sunspot equilibria* (Jess and A., 1994; Ascari et al., 2019; Bianchi and Nicolò, 2021) and *cognitive discounting* (Gabaix, 2020).

The introduction of *reinforcement learning à la Brock and Hommes (1997)* represents an important response to the wilderness concern. This expectational mechanism in fact restricts the departure from rationality and excludes illogical behaviour by penalising poorly performing forecasting rules, while allowing for a random component of choice and a gradual adaptation of agents' behaviour.

This paper contributes to this strand of literature, pioneered by the work of Branch and McGough (2009) and De Grauwe (2012a), by bringing this family of Behavioural DSGE models to the data.[1] The reinforcement learning mechanism is

[1] This terminology is mainly due to De Grauwe's books (De Grauwe, 2012b; De Grauwe and Ji, 2020a) providing an extended treatment of the subject. However, the same term is also associated to recent DSGE models with cognitive discounting and representative agents illustrated in Gabaix (2020).

here characterised by three core parameters: *memory* parameters, ruling the importance of past forecast errors, the *intensity of choice*, indicating the sensitivity to changes in utility determined by the performance of the chosen forecast rule, and the *cost of being rational*. Two main challenges arise from such model: first, due to the deep interaction among the aforementioned parameters, their joint estimation is subject to serious identification issues; secondly, these parameters heavily affect the volatility of the system, thereby increasing the difficulty of tracking the dynamics of latent variables with direct inference. Therefore, estimating Behavioural DSGE models represents a quite challenging exercise from an econometric perspective, and the literature on this topic is still limited (see Liu and Minford (2014); Grazzini et al. (2017); Kukacka and Sacht (2021)).

The novelties of the paper are twofold. First, formal identification tests are applied on both a linear and a non-linear approximation of the Behavioural DSGE model with the aim of outlining the structural requirements for the estimation of the *reinforcement learning* parameters. For this exercise, a New Keynesian model with Calvo price-setting and trend inflation, similar to what illustrated in Ascari and Sbordone (2014), is extended to embed *heterogeneous expectations* and the *heuristic switching* mechanism as in canonical Behavioural DSGE models. In this framework, bounded rational agents cohabit with fully rational ones and are left free to correct their forecasting strategy depending on payoffs from past decisions.

Then, the methodology presented in Mutschler (2015, 2018) is applied to evaluate the rank criteria for the local identification of parameters in a non-linear DSGE model, given higher-order approximations and pruning (Schmitt-Grohé and Uribe, 2004b; Andreasen et al., 2018). Thus, the joint identification of the parameters describing the learning block of the model is tested under different hypotheses on the structure of the model and the observation set. The tests conclude that the learning rate of adaptive agents (i.e. the *speed of learning* under *adaptive expectations*), the *intensity of choice* and the memory parameters are jointly identifiable only in a non-linear framework while observing the share of agents adopting each forecasting rule. These results confirm the intuition suggested in Deák et al. (2017b) that *reinforcement learning* can influence agents' behaviour only in a higher-order approximation of the model. Moreover, this sheds light on the findings of Grazzini et al. (2017) and Kukacka and Sacht (2021), who could not jointly identify reinforcement learning parameters without observing the share of agents.

The second novelty of the paper is the use of survey-based measures to approximate the share of agents adopting a specific forecast rule to form expectations. Shares are approximated with the distribution of consumers' replies to the qualitative question on business activity from the *"Survey of Consumer Expectations"* held by the *University of Michigan*. In particular, respondents expecting *unchanged* business conditions are assumed to follow a *näive* or backward-looking rule and the information set is extended with survey data to estimate the Behavioural DSGE model, using Bayesian non-linear filtering techniques.[2] Finally, the ability of the Behavioural DSGE model in reproducing empirical moments is compared to that of a FIRE counterpart.

The paper is structured as follows. Section 3.2 reviews empirical research on DSGE models with *heterogeneous expectations*. Section 3.3 outlines the New Keynesian model with non-zero steady-state inflation under rational expectations, and then embeds the Brock-Hommes composite model with rational and bounded rational expectations. Section 3.4 shows the results of the identification tests, explains how observed time-series are mapped to model variables, presents parameters estimates based on *local-Gaussian* filtering techniques applied on a second-order Taylor approximation of the model and conclude with a validation exercise. Section 3.5 concludes and propose a road-map for future research.

3.2 Literature Review

There is a flourishing empirical literature on Bounded Rational DSGE models, covering several different learning mechanisms either with *homogeneous* or *heterogeneous expectations*. Comprehensive surveys on models with *homogeneous expectations* are provided in Hommes et al. (2019), mainly reviewing applications on *statistical learning*, and in Bianchi and Nicolò (2021), covering rational sunspots. This review will focus instead on models considering *heterogeneous expectations*, with particular attention devoted to empirical literature on *reinforcement learning*.

Empirical research on DSGE models with *heterogeneous expectations* mainly addressed the ability of alternative degrees of *bounded rationality* to outperform rational

[2]Even though expecting unchanged business conditions can be a fully rational choice, what matters for the model dynamics is that agents' expectations are in line with recent observations.

expectations models in fitting data in models characterised by fixed proportions of agents adopting specific expectations mechanisms (i.e. *hybrid expectations*).

Jang and Sacht (2016) estimate a work-horse NK model with *heterogeneous expectations* and exogenous (i.e. constant) shares of agents using the Simulated Method of Moments (SMM). The paper shows that the model specification with heterogeneous agents can reproduce second-order moments better than its FIRE analogue. Levine and Yang (2015) obtain similar results using direct inference by means of Bayesian estimation methods.

Deák et al. (2017b) extend this research framework to compare combinations of rational agents and agents with anticipated utility either with perfect or imperfect information (i.e. not observing shock processes). The paper finds the information set to be fundamental for selecting the form of *bounded rationality* with the highest fit. Surprisingly, a *rational expectation* model with *imperfect information* can reproduce sample moments similar to those of a model with *heterogeneous expectations* combining *anticipated utility* and *rational expectations* under *perfect information*. However, when *imperfect information* is introduced, the latter can fit the data slightly better than the original representative agent model with *rational expectations*.

Beqiraj et al. (2018) test the fit of a NK model with exogenous proportions of rational agents being either short-term (i.e. *naïve* agents) or long-term forecasters (i.e. *anticipated utility*). They conclude that a combination of rational and *naïve* agents improves the fit of the model, and estimate the share of rational agents in the best performing specification to be about 65%.

Similarly, Gelain et al. (2019) estimate a Smets-Wouters model with a mix of rational and bounded rational agents (i.e. *adaptive expectations*). In line with Deák et al. (2017b), the *heterogeneous expectations* model outperforms the fully rational one in a likelihood race while guaranteeing a similar matching of empirical moments in a validation exercise. However, the hybrid model is clearly superior to the fully rational one when it comes to out-of-sample exercises as it provides expectations which are closer to those of the Survey of Professional forecasters. Standard deviations of shocks and their persistence parameters narrow down in the hybrid specification, highlighting the ability of bounded rationality to intrinsically capture time-series persistence.

Finally, Jang and Sacht (2020) estimate a fully non-linear three-equation NK model with *reinforcement learning à la Brock-Hommes* using the simulated method of moments. However, the i*ntensity of choice*, the memory parameter and the cost for becoming "more rational" were calibrated.[3] Their results show that an economy populated by emotional forecasters, who predict future developments with a positive or negative average trend corrected by the volatility of consumption, delivers a slightly better match with US data than a RE model with habits and inflation indexation. On the contrary, a purely technical forecasting rule (e.g. a mix of fundamentalists and näives) better match Euro area data.

Although still limited, the literature on the estimation of models with endogenous shares of agents has recently been growing.

Grazzini et al. (2017) make the first attempt of estimating a fully non-linear Behavioural DSGE model using direct inference. They apply Bayesian estimation methods to estimate the parameters of the model developed in De Grauwe (2012a), where the fully non-linear reinforcement learning mechanism is embedded in a linear three-equations New Keynesian model. In this framework, agents can be either *näives* or *fundamentalists*, thereby generating a fully backward-looking system to be solved recursively. They fix the Taylor parameters and estimate 9 out of the 12 model parameters using two observables for the US economy: GDP deflator and output-gap. The prior of the *intensity of choice* parameter is a $\mathcal{B}(2, 2)$ and it is initialised at 5. The paper shows that the *intensity of choice* and the *memory parameters* are quite difficult to identify, with the former delivering a posterior mode not significantly different from that of the prior distribution and the latter being characterised by a flat posterior density. Interestingly, all the shocks standard deviations are estimated to be a lot smaller than under *rational expectations*. This is consistent with the intrinsic ability of *heuristic switching* models to endogenously generate business cycles through waves of optimism and pessimism.

Kukacka and Sacht (2021) obtain significant estimates of the *intensity of choice* parameter for both the US and the Euro area by applying novel simulated maximum likelihood methods on the De Grauwe (2012a) model with three different kinds of backward-looking forecasting rules: adaptive expectations, trend following, and a LAA (Learning Anchoring and Adjusting) heuristics. They obtain a low but significant value of the *intensity of choice* parameter, estimated to be slightly above 1 for the Euro area and between 0 and 1 for the US. In the main exercise, the *memory*

[3] The *intensity of choice* was set to be one and the *memory* parameters to be zero somehow in agreement with what suggested in Kukacka and Sacht (2021) - see below.

parameter is fixed to be zero. Nonetheless, Kukacka and Sacht (2021) find in a robustness exercise that a non-zero memory parameter deteriorate all estimates of the parameters underpinning the forecasting rules. This might be due to the similar role played by the parameters of the forecasting rules and of the *memory* parameters in capturing time-series auto-correlation.[4]

By contrast, Liu and Minford (2014) estimate the behavioural model by means of indirect inference on US data, and conclude that a simple three-equation model with reinforcement learning is worse than its fully rational counterpart.[5] Their methodology consist in estimating a VAR(1) model on actual data and on several different artificial data-sets generated by randomly varying parameters, either in a fully rational model or in a behavioural one. Estimated parameters coincide with those minimising the distance between the VAR coefficients estimated on actual data and those obtained from the artificial sample. The nice feature of this approach is the possibility to choose both the best parameters within a model specification, and the best model specification, which -in this case- only varies in the way expectations are modelled.

The results of these exercises have the limit of focusing on very simple models with three equations and only considering backward-looking agents. However, standard FIRE DSGE literature provides much more evolved models.

In this paper, I design a model embedding some of common features characterizing standard DSGE models, such as trend inflation and I allow for the presence of forward looking agents in order to evaluate the smallest possible deviation from the FIRE assumption. Moreover, the micro-foundation of the model distinguishes between households' and firms' expectations, thereby providing a flexible field to test an additional layer of heterogeneity.

[4]In a non-linear VAR framework, Cornea-Madeira et al. (2019) provide additional evidence that the switching mechanism is a valuable tool to assess whether the Phillips-curve is backward or forward-looking: the fit of their estimates improves when allowing agents to change towards the best performing rule. This study finds that the *intensity of choice* parameter is in line with theory by being positive and strongly significant. The estimates of the *intensity of choice* parameter is 5.040 when using actual macro-data for US and 1.995 when using US Survey of Professional Forecasters data. Interestingly, the share of *naïve* agents is dominating over the whole time span being roughly around 35 percent on average. Results are quite robust with an R^2 above the 80 percent and coefficients significant at the 1 percent level.

[5]Like Grazzini et al. (2017), they also estimate a simple backward-looking model with näives or fundamentalists agents, but they use real GDP, inflation and interest rates to disentangle parameters as in Kukacka and Sacht (2021).

Behavioural model estimates are validated against a non-linear FIRE NK model. Other studies compare the Behavioural DSGE model against a linear FIRE model thereby not allowing to distinguish between the effects purely related to the presence non-linearities from those generated by *bounded rationality.* By contrast, using a non-linear FIRE DSGE as a benchmark allows to better understand the role of the expectations-formation mechanism for eventual improvements in matching empirical moments.

Given the difficulties in jointly identifying the core *reinforcement learning* parameters, I apply formal identification tests for non-linear DSGE models as recently designed by Mutschler (2015, 2018). This helped understanding the potential for exploiting information from survey-based measures. Consequently, survey data on consumers' expectations is introduced to bridge the gap with the empirical literature and provide some evidence on their importance for matching empirical data.

3.3 The Full Non-linear Model

This section presents the New Keynesian DSGE model under *full information* and *rational expectations* (FIRE) to then introduce *heterogenous expectations* and *bounded rationality* in the form of *reinforcement learning à la Brock-Hommes* (1997). Under the FIRE hypothesis, agents can form model consistent expectations as they are assumed to know the structure of the model, including the value of parameters, and know the distribution of future shocks when forming expectations. Similar to Massaro (2013), heterogeneous expectations and the learning mechanism were embedded in accordance with *euler learning* assumptions (Evans and Honkapohja, 2001): (i) agents are aware of being identical and (ii) are able to observe the shock vector. Therefore, agents' behaviour varies only as result of the way of forming expectations.[6]

[6]Deák et al. (2017b) relax these assumptions to embed *internal rationality* (Adam and Marcet, 2011) and *anticipated utility* (Eusepi and Preston, 2011). This implies agents are fully rational with respect to their internal decisions, but do not have a model for predicting macroeconomic variables. They sharply distinguish between aggregate and internal quantities so that identical agents are not aware of this equilibrium property and they can maximise their utility over an infinite horizon without realising to be the representative agent. Finally, Jump and Levine (2019) define the analytical equilibrium conditions.

3.3.1 The Rational Expectation Model

The backbone of the model estimated in this paper is a small New Keynesian model with trend inflation, similar to the one developed in Ascari and Sbordone (2014), and extended with a fiscal policy shock.

The micro foundation foresees the three standard blocks of a representative agents model: households, firms and public sector. Households choose the optimal amounts of consumption, labour supply and financial assets to maximise their utility function over time. The production sector is composed by wholesale intermediate sector and retail sector, where firms in the retail sector are subject to Calvo pricing frictions when maximizing their profits.

Households

Household j chooses between consumption, $C_t^{(j)}$, and hours worked, $H_t^{(j)}$. The single-period utility $U_t^{(j)}$ of household j at time t is given by

$$U_t^{(j)} = U(C_t^{(j)}, H_t^{(j)}) = \log(C_t^{(j)}) - \kappa \frac{{H_t^{(j)}}^{1+\phi}}{1+\phi} \tag{3.1}$$

where k is a parameter scaling the disutility from supplying an additional unit of labour. In a stochastic environment, the value function of the representative household at time t is given by

$$V_t^{(j)} = \mathbb{E}_t \left[\sum_{s=0}^{\infty} \beta^s U_{t+s}^{(j)} \right] \tag{3.2}$$

with β being a discount factor. The household's problem at time t is to choose paths for consumption $\{C_t^{(j)}\}$, labour supply $\{H_t^{(j)}\}$ and holdings of financial assets $\{B_t^{(j)}\}$ to maximise the value function, $V_t^{(j)}$, described in equation (3.2) given its budget constraint

$$B_t^{(j)} = R_t B_{t-1}^{(j)} + W_t H_t^{(j)} + \Gamma_t - C_t^{(j)} - T_t \tag{3.3}$$

where $B_t^{(j)}$ is holdings of financial assets, R_t is the interest rate paid on assets held at the beginning of period t, W_t is the real wage rate, Γ_t are profits from wholesale and retail firms owned by households and T_t denotes taxes. W_t, R_t, Γ_t and T_t are all exogenous to household j.

The household's problem is solved by means of a Lagrangian auxiliary function:

$$\mathcal{L} = \mathbb{E}_t \Bigg[\sum_{s=0}^{\infty} \beta^s \Bigg\{ U_{t+s}^{(j)} + \lambda_{t+s}^{(j)} \left[R_{t+s} B_{t+s-1}^{(j)} + W_{t+s} H_{t+s}^{(j)} + \Gamma_{t+s} - C_{t+s}^{(j)} - T_{t+s} - B_{t+s}^{(j)} \right] \Bigg\} \Bigg] \quad (3.4)$$

The first-order conditions with respect to $\{C_{t+s}(j)\}$, $\{B_{t+s}^{(j)}\}$ and $\{H_{t+s}^{(j)}\}$ are

$$\{C_{t+s}^{(j)}\}: \quad \mathbb{E}_t \beta^s U_{C,t+s}(j) + \beta^s \lambda_{t+s}^{(j)} = 0$$

$$\{B_{t+s}^{(j)}\}: \quad \mathbb{E}_t \left[\beta^{s+1} \lambda_{t+s+1}^{(j)} R_{t+s+1} \right] - \beta^s \lambda_{t+s}^{(j)} = 0$$

$$\{H_{t+s}^{(j)}\}: \quad \mathbb{E}_t \left[\beta^s U_{H,t+s}^{(j)} + \beta^s \lambda_{t+s}^{(j)} W_{t+s} \right] = 0$$

Rearranging the first-order conditions we obtain:

$$1 = \mathbb{E}_t \left[\Lambda_{t,t+1}^{(j)} R_{t+1} \right] \quad (3.5)$$

$$W_t = -\frac{U_{H,t}^{(j)}}{U_{C,t}^{(j)}} \quad (3.6)$$

with

$$\Lambda_{t,t+1}^{(j)} = \beta \frac{U_{C,t+1}^{(j)}}{U_{C,t}^{(j)}} \quad (3.7)$$

$$U_{C,t} = \frac{1}{C_t} \quad (3.8)$$

$$U_{H,t} = -\kappa H_t^{\phi} \quad (3.9)$$

where $\Lambda_{t,t+1}^{(j)}$ is the real stochastic discount factor for household j over the interval $[t, t+1]$.

Firms in the Wholesale Sector

Wholesale firms employ a Cobb-Douglas production function to produce a homogeneous output

$$Y_t^W = F(A_t, H_t) = A_t H_t^{\alpha} \quad (3.10)$$

where A_t is total factor productivity. Profit-maximising demand for labour results in the first order condition

$$W_t = \frac{P_t^W}{P_t} F_{H,t} = \alpha \frac{P_t^W}{P_t} \frac{Y_t^W}{H_t} \tag{3.11}$$

Firms in the Retail Sector

The retail sector uses a homogeneous wholesale good to produce a basket of differentiated goods m for aggregate consumption

$$C_t = \left(\int_0^1 C_t(m)^{(\zeta-1)/\zeta} dm \right)^{\zeta/(\zeta-1)} \tag{3.12}$$

where ζ is the elasticity of substitution. Each retail firm produces only one good, and for each good m, the consumer chooses $C_t(m)$ at a price $P_t(m)$ to maximise (3.12) given total expenditure $\int_0^1 P_t(m)C_t(m)dm$. This results in a set of consumption demand equations for each differentiated good m with price $P_t(m)$ of the form

$$C_t(m) = \left(\frac{P_t(m)}{P_t} \right)^{-\zeta} C_t \Rightarrow Y_t(m) = \left(\frac{P_t(m)}{P_t} \right)^{-\zeta} Y_t \tag{3.13}$$

where $P_t = \left[\int_0^1 P_t(m)^{1-\zeta} dm \right]^{\frac{1}{1-\zeta}}$. P_t is the aggregate price index. C_t and P_t are Dixit-Stigliz aggregates (see Dixit and Stiglitz (1977)).

Each variety of retail good m is produced with wholesale production according to an iceberg technology

$$Y_t(m) = Y_t^W = A_t H_t(m)^\alpha \tag{3.14}$$

Following Calvo (1983), we assume that -in every period- there is a probability of $1-\xi$ that the price of each retail good m is set optimally to $P_t^0(m)$. If the price is not re-optimised, it is held fixed. Thus we can interpret $\frac{1}{1-\xi}$ as the average duration for which prices are left unchanged. For each retail producer m, given its real marginal cost MC_t, the objective is to choose $\{P_t^0(m)\}$ to maximise discounted profits

$$\mathbb{E}_t \sum_{k=0}^{\infty} \xi^k \frac{\Lambda_{t,t+k}}{P_{t+k}} Y_{t+k}(m) \left[P_t^0(m) - P_{t+k} MC_{t+k} \right] \tag{3.15}$$

subject to (3.13). The solution being

$$\mathbb{E}_t \sum_{k=0}^{\infty} \xi^k \frac{\Lambda_{t,t+k}}{P_{t+k}} Y_{t+k}(m) \left[P_t^0(m) - \frac{1}{(1-1/\zeta)} P_{t+k} MC_{t+k} \right] = 0 \tag{3.16}$$

which leads to

$$\frac{P_t^0(m)}{P_t} = \frac{1}{1-1/\zeta} \frac{\mathbb{E}_t \sum_{k=0}^{\infty} \xi^k \Lambda_{t,t+k} (\Pi_{t,t+k})^{\zeta} Y_{t+k} MC_{t+k}}{\mathbb{E}_t \sum_{k=0}^{\infty} \xi^k \Lambda_{t,t+k} (\Pi_{t,t+k})^{\zeta-1} Y_{t+k}} \tag{3.17}$$

where k periods ahead inflation is defined by

$$\Pi_{t,t+k} \equiv \frac{P_{t+k}}{P_t} = \frac{P_{t+1}}{P_t} \frac{P_{t+2}}{P_{t+1}} \cdot \cdot \frac{P_{t+k}}{P_{t+k-1}} = \Pi_{t+1} \Pi_{t+2} \cdot \cdot \Pi_{t+k}$$

Note that $\Pi_{t,t+1} = \Pi_{t+1}$ and $\Pi_{t,t} = 1$.

If we rewrite both numerator and denimonator of 3.17 in a recursive form as follows

$$\begin{aligned} J_t &= \frac{1}{1-\frac{1}{\zeta}} \mathbb{E}_t \sum_{k=0}^{\infty} \xi^k \Lambda_{t,t+k} \Pi_{t,t+k}^{\zeta} Y_{t+k} MC_{t+k} \\ &= \frac{1}{1-\frac{1}{\zeta}} Y_t MC_t + \xi \mathbb{E}_t \Lambda_{t,t+1} \Pi_{t,t+1}^{\zeta} J_{t+1} \end{aligned} \tag{3.18}$$

$$\begin{aligned} JJ_t &= \mathbb{E}_t \sum_{k=0}^{\infty} \xi^k \Lambda_{t,t+k} \Pi_{t,t+k}^{\zeta-1} Y_{t+k} \\ &= Y_t + \xi \mathbb{E}_t \Lambda_{t,t+1} \Pi_{t,t+1}^{\zeta-1} JJ_{t+1} \end{aligned} \tag{3.19}$$

then it can be expressed as

$$\frac{P_t^0(m)}{P_t} = \frac{J_t}{JJ_t} \tag{3.20}$$

By the law of large numbers the evolution of the price index is given by

$$P_{t+1}^{1-\zeta} = \xi P_t^{1-\zeta} + (1-\xi)(P_{t+1}^0)^{1-\zeta} \tag{3.21}$$

which can be written as

$$1 = \xi \Pi_t^{\zeta-1} + (1-\xi)\left(\frac{J_t}{JJ_t}\right)^{1-\zeta} \tag{3.22}$$

Price dispersion is defined as $\Delta_t^p = \int (P_t(m)/P_t)^{-\zeta}$. Assuming that the number of firms is large, we obtain the following dynamic relationship:

$$\begin{aligned}\Delta_t^p &= \xi \int_{not\ optimise} \left(\frac{P_{t-1}^0(m)}{P_{t-1}}\frac{P_{t-1}}{P_t}\right)^{-\zeta} + (1-\xi)\int_{optimise}\left(\frac{P_t^0(m)}{P_t}\right)^{-\zeta_p} \\ &= \xi \Pi_t^{\zeta}\Delta_{t-1}^p + (1-\xi)\left(\frac{P_t^0(m)}{P_t}\right)^{-\zeta} \\ &= \xi \Pi_t^{\zeta}\Delta_{t-1}^p + (1-\xi)\left(\frac{J_t}{JJ_t}\right)^{-\zeta} \end{aligned} \tag{3.23}$$

Profits

Total profits from retail and wholesale firms, Γ_t, are remitted to households. This is given in real terms by

$$\Gamma_t = \underbrace{Y_t - \frac{P_t^W}{P_t}Y_t^W}_{\text{retail}} + \underbrace{\frac{P_t^W}{P_t}Y_t^W - W_t H_t}_{\text{Wholesale}} = Y_t - \alpha \frac{P_t^W}{P_t}Y_t^W \tag{3.24}$$

using the first-order condition (3.11).

Closing the Model

The model is closed with a resource constraint over consumption C_t and government expenditure G_t

$$Y_t = C_t + G_t \tag{3.25}$$

and the government's budget constraint where government expenditure equals taxes T_t

$$G_t = T_t \tag{3.26}$$

Market clearing in the goods market requires that supply equals demand

$$\int_0^1 Y_t(m)dm = \int_0^1 \left(\frac{P_t(m)}{P_t}\right)^{-\zeta} Y_t dm = Y_t \Delta_t^p \tag{3.27}$$

Hence, in a symmetric equilibrium

$$Y_t = \frac{Y_t^W}{\Delta_t^p} \tag{3.28}$$

A monetary policy rule for the nominal interest rate is given by the following Taylor-type rule with a *forward-looking inflation target*

$$\begin{aligned}\log\left(\frac{R_{n,t}}{R_n}\right) =& \rho_r \log\left(\frac{R_{n,t-1}}{R_n}\right) + (1-\rho_r)\left(\theta_\theta \log\left(\frac{\mathbb{E}_t\Pi_{t+1}}{\Pi}\right) + \theta_y \log\left(\frac{Y_t}{Y}\right)\right) \\ &+ \log MPS_t\end{aligned} \tag{3.29}$$

where MPS_t is a monetary policy shock. The ex-ante nominal gross interest rate $R_{n,t}$ set at time t and the ex-post real interest rate, R_t are related by the Fischer equation

$$R_t = \frac{R_{n,t-1}}{\Pi_t} \tag{3.30}$$

Exogenous processes evolve according to:

$$\log A_t - \log A = \rho_A(\log A_{t-1} - \log A) + \epsilon_{A,t} \tag{3.31}$$

$$\log MS_t - \log MS = \rho_{MS}(\log MS_{t-1} - \log MS) + \epsilon_{MS,t} \tag{3.32}$$

$$\log MPS_t - \log MPS = \rho_{MPS}(\log MPS_{t-1} - \log MPS) + \epsilon_{MPS,t} \tag{3.33}$$

$$\log G_t - \log G = \rho_G(\log G_{t-1} - \log G) + \epsilon_{G,t} \tag{3.34}$$

3.3.2 Heterogeneous Expectations with Endogenous Proportions

To introduce heterogeneous expectations, this paper follows an *Euler Learning* approach by replacing all rational expectations terms, $\mathbb{E}_t X_{t+1}$, in the model described in Section 3.3 with a weighted average of different expectations,

$$\bar{\mathbb{E}}_t^* X_{t+1} = n_j \mathbb{E}_t X_{t+1} + (1-n_j)\mathbb{E}_t^* X_{t+1}; \quad j = h, f \tag{3.35}$$

where n_j is the share of representative agents adopting rational expectations and $\mathbb{E}_t^* X_{t+1}$ defines *bounded rational* expectations. Thus, heterogeneous expectations influence households behaviour when forecasting the marginal utility of consumption, $\bar{E}^*_{h,t}U_{C,t+1}$, and inflation, $\bar{E}^*_{h,t}\Pi_{t+1}$, and firms expectations on prices $E^*_{f,t}J_{t+1}$, $E^*_{f,t}JJ_{t+1}$ and $E^*_{f,t}\Pi_{t+1}$.

In this study, *bounded rationality* takes the form of *adaptive expectations* on contemporaneous variables:

$$\mathbb{E}^*_t X_{t+1} \quad = \quad \mathbb{E}^*_{t-1}X_t + (1-\lambda_1)(X_t - \mathbb{E}^*_{t-1}X_t)$$

As a result, *naive* expectations, according to which $\mathbb{E}^*_t X_{t+1} = X_t$, arise as a special case of (3.36) where the *speed of learning* parameter is null, $\lambda_1 = 0$. *Reinforcement learning à la Brock and Hommes (1997)* is embedded to allow the proportions of rational households ($n_{h,t}$) and firms ($n_{f,t}$) to endogenously evolve in response to model dynamics,

$$n_{j,t} = \frac{\exp(-\gamma\left(\Phi^{RE}_{j,t} + C^{RE,j}\right))}{\exp(-\gamma\left(\Phi^{RE}_{j,t} + C^{RE,j}\right) + \exp(-\gamma\Phi^{BR}_{j,t})}; \quad j = h, f \tag{3.36}$$

where $0 \leq \gamma < +\infty$ is the *intensity of choice* parameter determining the sensitivity of agents to changes in the relative utility of being rational, Φ_t, given an exogenous cost, $C^{RE,j}$. A value of γ close to zero makes agents almost indifferent between the two forecasting rules and the shares fluctuating around 0.5. On the contrary, large values of γ causes high volatility with all agents switching from one forecasting rule to the other for small changes in utility. The *cost of being rational* can be interpreted as the price that agents pay to widen their cognitive abilities and gathering information, and its effect is to reduce the attractiveness of full rationality. Moreover, it reduces the share of rational agents in steady state - see equation (3.38).

Utility is defined by a *fitness measure* for $j = h, f$,

$$\begin{aligned} \Phi^{RE}_{j,t} &= \mu^{RE}_j\Phi^{RE}_{j,t-1} + (1-\mu^{RE}_j)\Big(\text{weighted sum of forecast errors}\Big) \\ \Phi^{BR}_{j,t} &= \mu^{BR}_j\Phi^{BR}_{j,t-1} + (1-\mu^{BR}_j)\Big(\text{weighted sum of forecast errors}\Big) \end{aligned} \tag{3.37}$$

where the *memory* parameters, $0 \leq \mu_j \leq 1$, rule the importance of past errors. $\mu = 0$ means agents do not give importance to past errors, but they evaluate forecast rules only on the basis of their recent performance. Given the stochastic nature of endogenous variables, the latter case results in agents randomly choosing forecast rules.

In the steady state, forecast errors are null, hence it follows that the shares of agents in equilibrium, namely n_h and n_f reduce to

$$n_j = \frac{exp(-\gamma C^{RE,j})}{exp(-\gamma C^{RE,j}) + 1}\,;\; j = h, f \tag{3.38}$$

from which it is possible to derive the *cost of being rational*, $C^{RE,j}$, given n_j and γ

$$C^{RE,j} = -\frac{1}{\gamma}\log\frac{n_j}{1-n_j}\,;\; j = h, f \tag{3.39}$$

Finally, $C^{RE,j}$s are assumed to follow an AR(1) processes:

$$\log C_t^{RE,j} - \log C^{RE,j} = \rho_{C^{RE,j}}(\log C_{t-1}^{RE,j} - \log C^{RE,j}) + \epsilon_{C^{RE,j},t} \tag{3.40}$$

3.4 Empirical Analysis

This section presents the details of the empirical analysis. Measurement equations and the results of identification tests are described in Sections 3.4.1 and 3.4.2. Then, Section 3.4.3 illustrates the dataset used in Section 3.4.4 for estimating parameters of a non-linear approximation of the model. Finally, the empirical strategy is validated in Section 3.4.5.

3.4.1 Measurement Equations and Priors

Identification tests and the non-linear estimation of *reinforcement learning* parameters are based on five observable variables: output, hours worked, the nominal policy rate, the inflation rate and the share of rational agents. Concerning the latter, as households are also firms owners in this model, their shares are assumed to coincide, $n_t = n_t^h = n_t^f$.

When shares of rational agents are not observed, the model assumes only four observables and four shocks by excluding the shares of agents and the shock processes for the cost of being rational, respectively.

This ensures the number of shocks and observables to be the same and allows to back-out shocks with rational agents and perfect information.

The corresponding measurement equations are:

$$\texttt{dyobs} = \log\left((1+g)\frac{Y_t^c}{Y_{t-1}^c}\right) \tag{3.41}$$

$$\texttt{labobs} = \frac{H_t - H}{H} \tag{3.42}$$

$$\texttt{robs} = R_{n,t} - 1 \tag{3.43}$$

$$\texttt{pinfobs} = \Pi_t - 1 \tag{3.44}$$

$$\texttt{nobs} = n_t^h = n_t^f = n_t \tag{3.45}$$

$$\tag{3.46}$$

The steady state values of the observables are $\texttt{dyobs} = \log(1+g)$, $\texttt{labobs} = 0$, $\texttt{robs} = R_n - 1$, $\texttt{pinfobs} = \Pi - 1$ and $\texttt{nobs} = n$.

The model with endogenous proportion of agents under the assumption of a unique share of rational agents is characterised by 31 deep parameters:[7]

$$\begin{aligned}\boldsymbol{\theta} =&[\beta, \alpha, \zeta, g, \xi, \phi, k, \bar{g}, \bar{R}^n, \bar{\Pi}, \rho_r, \theta_\Pi, \theta_Y, \theta_{\Delta_Y},\\ &\rho_A, \rho_{MS}, \rho_{MPS}, \rho_G, \sigma_A, \sigma_{MS}, \sigma_{MPS}, \sigma_G,\\ &\lambda^{11h}, \lambda^{12h}, \lambda^{12f}, \lambda^{13f}, \gamma, \mu^{AE}, \mu^{RE}, \rho_{C^{RE}}, \sigma_{C^{RE}}]\end{aligned}$$

Some of the structural parameters are calibrated to match sample means while others are parameterised to match economically sensible criteria on the basis of related literature.

Knowing that the following relationships hold in steady-state,

$$\begin{aligned}\Pi &= \frac{\bar{\Pi}}{100} + 1\\ R_n &= \frac{\bar{R}_n}{100} + 1\\ g &= \frac{\bar{g}}{100}\end{aligned}$$

[7]The total number would increase to 36 assuming households and firms form expectations separately, as some parameters would duplicate: $\lambda^{11f}, \mu^{AE,h}, \mu^{RE,h}, \mu^{AE,F}, \mu^{RE,F}, \rho_{C^{RE,h}}, \sigma_{C^{RE,h}}, \rho_{C^{RE,F}}, \sigma_{C^{RE,F}}$.

the model is calibrated in accordance with sample averages by assigning empirical values to the inflation rate, $\bar{\Pi} = 3.196$, the annualised policy rate $\bar{R}_n = 1.24$ and by parametrising technological growth, $\bar{g} = 0.0039$, to match an annualised real GDP growth of 1.569. Hence, the steady state value of $\beta = 0.996$ is singled out by reorganising

$$R_n = \frac{\Pi}{\beta(1+g)^{-1}} = \frac{\bar{R}_n}{100} + 1 \tag{3.47}$$

as

$$\beta = \frac{\frac{\bar{\Pi}}{100} + 1}{\left(\frac{\bar{R}_n}{100} + 1\right)\left(1 + \frac{\bar{g}}{100}\right)^{-1}} \tag{3.48}$$

Following Deák et al. (2017b), the elasticity of substitution, ζ, and the production elasticity to labour, α, were set to 7 and 0.3, respectively. Parameter k in the utility function was calibrated to match a labour supply of 0.33 in steady state. Finally, government expenditure was set to match a 36 % share of GDP in steady state.

Priors shown in Table 3.1 are based on Gelain et al. (2019) who employ distributions from Smets and Wouters (2007) for structural parameters and from Levine et al. (2012) for adaptive expectations. Concerning heterogeneous expectations parameters, I follow Gelain et al. (2019) for the share of rational agents in the fixed proportion version of the model.

When moving to the non-linear version of the model with endogenous shares, sample means are used to calibrate the steady-state value of `nobs` $= n = 0.53$.

This allows to compute the steady-state value of the cost of being rational as:

$$C^{RE} = -\frac{1}{\gamma} \log \frac{n}{1-n} \tag{3.49}$$

The intensity of choice γ is assumed to be Γ-distributed as in Grazzini et al. (2017) so to reflect the implausibility of a negative γ as this would imply agents favour less precise forecast rules and this would be illogical. The memory parameters, μ^{AE} and μ^{RE}, range between 0 and 1 and are assumed to follow a $\mathcal{B}$ distribution.

Parameter		Prior Density	Distribution Mean	S.D./df
Calvo prices	ξ	$\mathcal{B}$	0.5	0.1
Labour Supply Elasticity	ϕ	$\mathcal{N}$	2.0	0.75
Interest rate rule				
Interest rate smoothing	ρ_r	$\mathcal{B}$	0.5	0.1
Inflation	θ_Π	$\mathcal{N}$	2.0	0.25
Output	θ_Y	$\mathcal{N}$	0.12	0.05
Output growth	θ_{Δ_y}	$\mathcal{N}$	0.12	0.05
Persistence in the AR(1) shock processes				
Technology	ρ_A	$\mathcal{B}$	0.5	0.2
Government spending	ρ_G	$\mathcal{B}$	0.5	0.2
Price mark-up	ρ_{MS}	$\mathcal{B}$	0.5	0.2
Monetary policy	ρ_{MPS}	$\mathcal{B}$	0.5	0.2
Standard deviation of shocks				
Technology	σ_A	Γ^{-1}	0.001	0.02
Government spending	σ_G	Γ^{-1}	0.001	0.02
Price mark-up	σ_{MS}	Γ^{-1}	0.001	0.02
Inflation target	σ_{MPS}	Γ^{-1}	0.001	0.02
Adaptive expectations - Speed of learning parameters				
HH - Marginal Utility	λ^{11h}	$\mathcal{B}$	0.5	0.2
HH - Inflation	λ^{12h}	$\mathcal{B}$	0.5	0.2
Firm - Numerator price F.O.C.	λ^{12f}	$\mathcal{B}$	0.5	0.2
Firm - Denominator price F.O.C.	λ^{13f}	$\mathcal{B}$	0.5	0.2
Heterogenous expectations				
B-H - Intensity of choice	γ	Γ	10	2.5
B-H - Memory adaptive	μ^{AE}	$\mathcal{B}$	0.5	0.2
B-H - Memory rational	μ^{RE}	$\mathcal{B}$	0.5	0.2
B-H - Persistence of Rationality Cost	$\rho_{C^{RE}}$	$\mathcal{B}$	0.5	0.2
B-H - Shock std of Rationality Cost	$\sigma_{c^{RE}}$	Γ^{-1}	0.001	0.02

Notation: std = standard deviation

Table 3.1: Parameters summary

3.4.2 Identification Tests based on Priors

Before starting with estimation attempts, it is important to understand which parameters can be identified given the structure of the model and the observables. The aim of this section is to check whether parameters lacking identification in a linear approximation of the model can be eventually identified when moving to a higher-order approximation.

In DSGE models, identification concerns with injectivity of two mappings: (i) from the structural parameters to the reduced form of the model (i.e. the uniqueness of solution), (ii) from the solution of the model to observed data (i.e. uniqueness of the probability distribution).

A DSGE model can be described as a system, $E_t\left(\mathbf{f}\left(z_t, z_{t-1}, z_{t+1}, \mathbf{u_t}|\theta\right)\right) = \mathbf{0}$, of n non-linear equations where z_t are endogenous variables, u_t are exogenous shocks and θ is a m-dimensional vector of deep parameters. In this paper, we estimate an order-i Taylor approximation of the model around its steady state, z^*, so that $z_t = \mathbf{f}^{\theta(i)}\left(z^*, z^*, z^*, \mathbf{0}|\theta\right) = \mathbf{0}$. Hence, a solution for this Taylor expansion is $z_t = \mathbf{h}^{\theta(i)}\left(z_{t-1}, u_t|\theta\right)$. In a linear approximation of the model around its steady-state, $z_t = z^* + h^\theta_z\left(z_{t-1} - z^*\right) + h^\theta_u\left(u_t\right)$, all equilibrium dynamics and steady-state properties for a given realisation of the parameter vector ` are determined by h^θ_z, $\Omega := h^\theta_u h^{\theta'}_u$ and z^*. The first injectivity problem consists in finding the parameters of $\mathbf{f}^{\theta(i)}$ influencing the solution of the system through h^θ_z, h^θ_u and z^*.

For estimation purposes, one needs to complement the model solution - which describes the transition equation - with measurement equations $y_t = \tilde{\mathbf{h}}^{\theta(i)}\left(x_t, u_t|\theta\right)$ where y_t are observables and x_t are state variables. This introduces the second injectivity problem on whether restrictions imposed from empirical moments indeed allow to identify those parameters entering the solution of the model.

Iskrev (2008, 2010) sets the necessary and sufficient condition for local identification of parameters from the reduced form of the first-order Taylor approximation of the model. Namely, the Jacobian matrix containing the derivatives of first and second-order moments entering the likelihood function must have full rank.

In this section, I study whether a higher-order Taylor expansion of the model provides a leeway to identify parameters not entering the reduced form of a linear approximation. Namely, given the below second-order Taylor expansion,

$$\begin{aligned} z_t = {} & z^* + h^\theta_z\left(z_{t-1} - z^*\right) + h^\theta_u\left(u_t\right) \\ & + \frac{1}{2}[h^\theta_{zz}\left(z_{t-1} - z^*\right) \otimes \left(z_{t-1} - z^*\right) + 2h^\theta_{xu}\left(z_{t-1} \otimes u_t\right) \\ & + 2h^\theta_{uu}\left(u_t \otimes u_t\right) + h^\theta_{\sigma\sigma}\sigma^2] \end{aligned} \tag{3.50}$$

I assess whether the additional restrictions imposed by h^{θ}_{zz}, h^{θ}_{xu}, h_{uu} and $h^{\theta}_{\sigma\sigma}\sigma^2$ help identifying the deep parameters of the model for a given set of observable variables. For this purpose, I apply the findings of Mutschler (2015, 2018) who extended Iskrev (2008)'s methodology to non-linear approximations of the system. Mutschler (2015) exploits the intrinsic linear structure of pruned higher-order Taylor approximations and, in the same spirit of Iskrev (2008), introduces rank conditions on the reduced form of the pruned system. The latter allow to study how parameters affect the higher-order moments (i.e. or the polispectra in the frequency domain) of the pruned model solution. Then, local identification is tested around the non-stochastic steady state evaluated at the prior mean. Technical details are presented in Appendix C.5.[8]

Table 3.2 reports the results of the identification analysis. When observing Y_t, Π_t, H_t and R^n_t, linear approximations allow to somehow identify the steady-state shares of rational agents in a model with fixed shares. This result is in line with Gelain et al. (2019) and Deák et al. (2017b) who find these parameters can be identified, even though identification is weak because of high collinearity between the shares and other parameters of the model. By contrast, this set-up is characterised by a complete lack of identification of reinforcement learning parameters.

Moving to a second order approximation is not sufficient to improve parameters identification. Although γ is identified through moment restrictions, it is collinear to $\mu^{AE,h}$ which is not identified. This result is consistent with what found in other studies. Grazzini et al. (2017) find it is not possible to identify these parameters using Y_t and Π_t (i.e. the prior for γ overlaps the associated posterior). Using SMM, Jang and Sacht (2016, 2020) conclude their estimates of the memory parameter were not significant on the basis of Y_t, Π_t and R^n_t. Similarly, Kukacka and Sacht (2021) calibrate the memory parameter equal to zero to reduce the computational burden and avoid joint-identification issues.[9]

Against this background, I have augmented the model by assuming it is possible to observe the shares of rational agents in populating the economy in each point

[8]Parameters identification is analysed with the identification toolbox implemented in Dynare 5.1.

[9]Kukacka and Sacht (2021) assessed the sensibility of estimates to different calibrations of the memory parameters by estimating the model on simulated data, and opted for a null value of the memory parameter because the overall estimation performance of the model tended to deteriorate when increasing its value.

in time. To guarantee invertibility of the system, one extra shock was added by modelling the costs of being rational - C_t^{RE} - as an AR(1) process.

Including observed shares allows to identify the core *reinforcement learning* parameters in a non-linear context. Testing a linear approximation of the model with observed shares, it is possible to only identify the intensity of choice parameter, but not the memory parameters. When moving to a second order approximation of the model, restrictions on higher-order moments (i.e. cumulants computed from the coefficients of higher-order Taylor expansions) allow to identify all parameters of the model. Looking at Figure 3.1, all parameters are identified in this framework. However, some parameters are more likely to influence the curvature of the posterior distribution, as standard New Keynesian model parameters, than others, as the cost of being rational parameters. As a result, comparing estimates of standard parameters obtained with the Behavioural model against those from a FIRE counterpart might help understanding whether parameters were correctly estimated.

Fixed Shares - not observed				
	Order 1			
Parameter	**Identified**	$\boldsymbol{\Delta_i \theta^i}$		
n^h	YES	12.8623		
n^f	YES	3.6132		
Endogenous shares - not observed				
	Order 1		**Order 2**	
Parameter	**Identified**	$\boldsymbol{\Delta_i \theta^i}$	**Identified**	$\boldsymbol{\Delta_i \theta^i}$
$\boldsymbol{\gamma}$	NO	-	YES	0.0002
$\boldsymbol{\mu^{AE,h}}$	NO	-	NO	-
$\boldsymbol{\mu^{RE,h}}$	NO	-	NO	-
Endogenous shares - observed				
	Order 1		**Order 2**	
Parameter	**Identified**	$\boldsymbol{\Delta_i \theta^i}$	**Identified**	$\boldsymbol{\Delta_i \theta^i}$
$\boldsymbol{\gamma}$	YES	0.9663	YES	0.2399
$\boldsymbol{\mu^{AE,h}}$	NO	-	YES	0.0205
$\boldsymbol{\mu^{RE,h}}$	NO	-	YES	0.0189
$\boldsymbol{\rho^{C^{RE,h}}}$	NO	-	YES	0.0060
$\boldsymbol{\sigma^{C^{RE,h}}}$	NO	-	YES	0.2000

Table 3.2: Identification tests.

Note: $\Delta_i \theta^i$ describes the identification strength of parameter θ^i based on the Fischer information matrix normalized by the value of the parameter at the prior mean θ^i (Iskrev, 2010). Jacobian matrices were computed analytically using sylvester equations. The tolerance level for selecting nonzero columns was set to 1e-08.

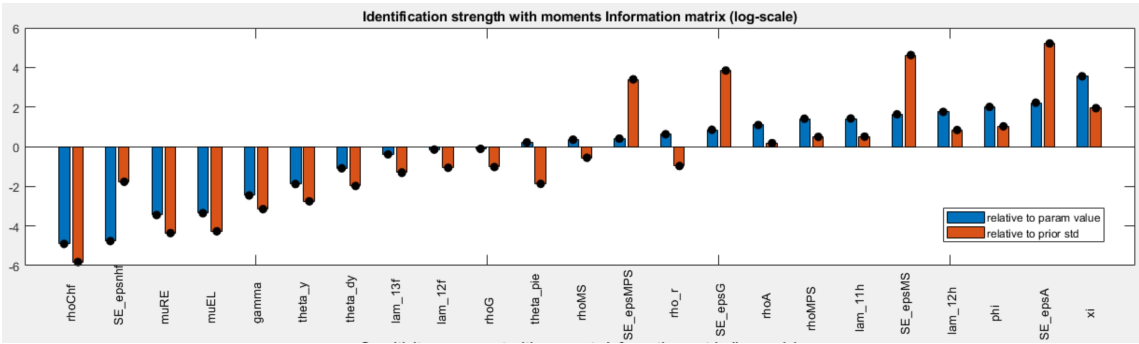

FIGURE 3.1: Identification strength for a second-order Taylor approximation with observed shares.
Blue bars present the log of $\Delta_i \theta^i$. Red bars are scaled by the prior standard deviation (Iskrev and Ratto, 2011).

3.4.3 Data

The main dataset is composed of quarterly frequency time-series for the US economy spanning over the period from 1984-Q1 to 2008-Q4. The observable variables include the inflation rate, growth in real GDP per capita, the monetary policy rate, hours worked per capita and a proxy for the share of rational agents. Further details on the sources, series keys and data transformations are exposed in the technical Appendix C.4.

All macroeconomic variables are seasonally adjusted and they are sourced from the FRED Database made available by the Federal Reserve Bank of St. Louis and the US Bureau of Labour Statistics. Real Gross Domestic Product is expressed in billions of chained 2012 Dollars. Following Smets and Wouters (2007), hours worked are adjusted to consider the limited coverage of the NFB sector compared to GDP: the index of average hours for the NFB sector is multiplied by the Civilian Employment (over 16 years old). Finally, aggregate real GDP and hours worked are expressed per capita, dividing the aggregate amounts by the population over 16 years old. Real GDP per capita is finally taken in first difference to match the measurement equation for output. Inflation is the first difference of the log of the implicit price deflator derived from GDP. For the policy rate, the FED fund rate is adjusted to be consistent with quarterly frequency data.

When extending the sample beyond the financial crisis, the FED rate is replaced with the Wu-Xia shadow interest rate (Wu and Xia, 2016; Wu and Zhang, 2019) to take into account for the zero lower bound.

Finding a good proxy for the shares of rational and bounded rational agents is certainly not an easy task. Nonetheless, survey data on expectations provide information on the dynamics characterizing the proportion of a agents following a specific rule.

First, one has to decide who are the reference agents and choose the most suitable survey, among those targeting professional forecasters, firms and consumers.

Even though surveys on professional forecasters are particularly rich of data, these are of very limited use since the Behavioural DSGE model estimated in this chapter is populated by households and firm owners only. Unfortunately, surveys on expectations of firms' owners are quite limited in number and long time-series are not available for the US (Coibion and Gorodnichenko, 2015).

Therefore, I have decided to use data from the *Survey of Consumer Expectations*, conducted by the University of Michigan since 1960. This is a source which was often used for testing the mechanisms underpinning the formation of households' expectations (Branch, 2004; Pfajfar and Santoro, 2010; Coibion and Gorodnichenko, 2015)- and provides *qualitative* and *quantitative* expectations on a number of economic indicators.

Second, one has to choose a survey indicator which is linked to the shares of agents and representative of the overall system dynamics.

In accordance with the theoretical literature on Behavioural DSGE models, I assume the evolution of the shares of forward- and backward-looking agents over time to co-move with the business cycle. For this reason, the share of *näive* agents is computed from the qualitative question on business activity expectations: *Would you say that at the present time business conditions are better or worse than they were a year ago?*. Respondents can choose among the following options: *"Better", "Worse", "Unchanged"*. The share of *näives* populating the economy is assumed to reflect the proportion of respondents reporting *"Unchanged"*. Although the latter might include a portion of rational agents actually thinking business activity will not vary over the next future, this indicator is still a good compromise for approximating the share of *näive* agents because what matters for model dynamics is the type of expectation itself (i.e. agents considering future output coincides with what currently observed).

For the estimation exercise presented in section 3.4.4, I assume households own firms and therefore their expectations coincide. This avoids arbitrary choices on how to distinguish between households and firms expectations and allows to use the total index. This series has also the advantage of starting back in 1960, thereby easing eventual robustness checks based on splitting the sample between *Great Moderation (1980-2008Q3)* and *Great Volatility (before 1980)*.

Figure 3.2 exhibits the series used to proxy rational households. This series is quite stable and cyclically fluctuates around 50%. Interestingly, the average share was slightly slower during the *Great Volatility* and tended to increase in recent periods.

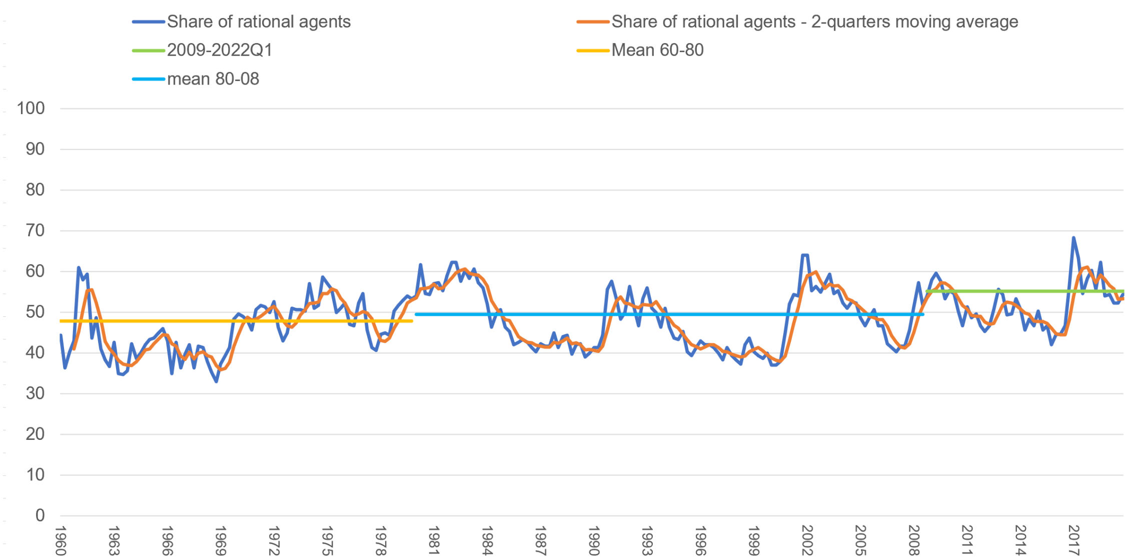

FIGURE 3.2: Proxy for the share of rational agents based on business conditions

Alternative approaches for modelling the shares of rational households and firms separately are proposed in Appendix C.7.

3.4.4 Estimation Results

This section presents estimates of a second-order approximation of the Behavioural New Keynesian (NK-BH) model based on the Extended Kalman filter developed by Gustafsson and Hendeby (2012) - see Appendix C.6 for technical details. A sample of five observables spanning between 1984-Q1 and 2008-Q4 was employed: real GDP per capita, the inflation rate, the FED policy rate and survey data on consumers' expectations from the University of Michigan *"Survey of Consumer Expectations"* to approximate the share of rational agents.

Although the main target of this exercise is to jointly estimate the *reinforcement learning* parameters of the model, namely, the *intensity of choice* and the memory parameters, estimates are compared against those obtained estimating a second-order Taylor expansion of the same model assuming rational expectations and full information (NK-RE) to better understand the relevance of information from survey data.

Table 3.3 shows the parameters values at their posterior mode and the respective standard deviation.

The Calvo parameter, ruling price stickiness, and the labour supply elasticity present similar values across the two model specifications. The former was estimated to be larger than its prior mean, 0.67 against 0.5, thereby implying that, on average, firms can adjust prices every three periods. The Frisch labour supply elasticity, defined as $1/\phi$, was estimated to be 0.29, a lower value with respect to what found in a linear context by Deák et al. (2017b).

The parameters of the Taylor rule, i.e. interest rate smoothing, inflation, output, and output growth, are qualitatively in line with similar studies. In accordance with the Taylor principle, the Central Bank responds more than proportionally to increases in the inflation rate. As in Deák et al. (2017b), the interest rate smoothing parameter decreases when moving from the NK-RE to the a model with heterogeneous expectations. However, differently from Deák et al. (2017b) who estimated a linear version of the model with fixed shares, I also observe a slight increase in the Taylor rule parameters related to output. Having introduced endogenous shares of agents, the Central Bank needs to adjust the policy rate more often and try to stabilise output to maintain economic confidence and avoid excessive volatility episodes.

As in Deák et al. (2017b) and Gelain et al. (2019), the introduction of bounded rationality in the form of hybrid expectations does not reduce, on balance, the persistence of shock processes. Technology, monetary policy and government spending shocks are more persistent than the price mark-up shock and the latter two capture most of the volatility. Similarly, in the case of Gelain et al. (2019), who estimated a linear Smets-and-Wouter's (2007) NK-model with hybrid expectations, bounded rationality translated into smaller habits and capital adjustments costs parameters, but it did not affect the inflation indexation ones.

Parameter		Prior Density	Prior Mean	Prior S.D./df	Post. Mode (1)	Post. S.D./df (2)	Post. Mode (3)	Post. S.D./df (4)
Calvo prices	ξ	$\mathcal{B}$	0.5	0.1	0.6798	0.0347	0.6703	0.0173
Labour Supply Elasticity	ϕ	$\mathcal{N}$	2	0.75	3.3553	0.5872	3.6267	0.427
Contract length	$1/(1-\xi)$				3.1230		3.0331	
Interest rate rule								
Interest rate smoothing	ρ_r	$\mathcal{B}$	0.5	0.1	0.5868	0.0655	0.2846	0.0763
Inflation	θ_Π	$\mathcal{N}$	2	0.25	2.5906	0.189	2.6558	0.1716
Output	θ_Y	$\mathcal{N}$	0.12	0.05	0.0793	0.03	0.0925	0.0215
Output growth	θ_{Δ_y}	$\mathcal{N}$	0.12	0.05	0.1415	0.0425	0.1469	0.0412
Persistence in the AR(1) shock processes								
Technology	ρ_A	$\mathcal{B}$	0.5	0.2	0.9887	0.010	0.9763	0.0117
Government spending	ρ_G	$\mathcal{B}$	0.5	0.2	0.97	0.0118	0.9973	0.0011
Price mark-up	ρ_{MS}	$\mathcal{B}$	0.5	0.2	0.45	0.0575	0.5423	0.0599
Monetary policy	ρ_{MPS}	$\mathcal{B}$	0.5	0.2	0.90	0.0154	0.8780	0.0136
Standard deviation of shocks								
Technology	σ_A	Γ^{-1}	0.001	0.02	0.0045	0.0003	0.005	0.0004
Government spending	σ_G	Γ^{-1}	0.001	0.02	0.026	0.0029	0.0391	0.0029
Price mark-up	σ_{MS}	Γ^{-1}	0.001	0.02	0.0186	0.0027	0.0213	0.0028
Monetary policy	σ_{MPS}	Γ^{-1}	0.001	0.02	0.002	0.0003	0.0043	0.0005
Adaptive expectations - Speed of learning parameters								
Marginal Utility	λ^{11h}	$\mathcal{B}$	0.5	0.1			0.9874	0.0095
Inflation	λ^{12h}	$\mathcal{B}$	0.5	0.2			0.3336	0.1353
Numerator price	λ^{12f}	$\mathcal{B}$	0.5	0.2			0.3528	0.0714
Denominator price	λ^{13f}	$\mathcal{B}$	0.5	0.2			0.7443	0.0904
Heterogenous expectations - Brock-Hommes parameters								
Intensity of choice	γ	Γ	10	2.5			16.4196	2.2824
Cost of rationality	$-\frac{1}{\gamma}\log\frac{n}{1-n}$						0.0755	
Memory adaptive	μ^{AE}	$\mathcal{B}$	0.5	0.2			0.9235	0.0543
Memory rational	μ^{RE}	$\mathcal{B}$	0.5	0.2			0.5993	0.0804
Rationality Cost - Persistence	$\rho_{C^{RE}}$	$\mathcal{B}$	0.5	0.2			0.9923	0.0037
Rationality Cost - Shock std	$\sigma_{c^{RE}}$	Γ^{-1}	0.001	0.02			0.0658	0.0103
Standard deviation of measurement errors								
Std Y^{obs}	$\sigma_{Y^{OBS}}$	Γ^{-1}	0.001	0.02	0.0014	0.0001	0.0006	0.0004
Std H^{obs}	$\sigma_{H^{OBS}}$	Γ^{-1}	0.001	0.02	0.0045	0.0004	0.0021	0.0012
Std Π^{obs}	$\sigma_{\Pi^{OBS}}$	Γ^{-1}	0.001	0.02	0.0077	0.0011	0.0014	0.0002
Std R_n^{obs}	$\sigma_{R_n^{obs}}$	Γ^{-1}	0.001	0.02	0.0004	0.0001	0.0011	0.0002
Std n_h^{obs}	$\sigma_{n_h^{obs}}$	Γ^{-1}	0.001	0.02			0.0200	0.0037
Log data density					-1707.49		-2267.85	

TABLE 3.3: Posterior mode

Estimates of the *speed of learning* parameters, λ^{11h}, λ^{12h}, λ^{12f}, λ^{13f} in Table 3.3, show that agents follow some form of adaptive expectations: all parameters have low positive values, indicating that backward-looking agents are not fully *näives* but form their expectations by correcting somewhat current observations by their forecast errors. The main exception is represented by the speed of learning parameter associated to marginal utility of consumption which is close to one, indicating agents do not adjust their expectations for current outcome.[10]

Turning to the core parameters of the reinforcement learning mechanism, the intensity of choice parameter is estimated to be 16.4. Such value is higher than in other studies (Kukacka and Sacht, 2021), likely due to the coexistence of adaptive learners -using current observations instead of lagged ones- and fully rational agents, who can quickly adjust their behaviour on the basis of recent changes in the fitness measure. On the contrary, the model of Kukacka and Sacht (2021) included three different kinds of backward-looking agents, who are not aware of the existence of different agent-types and heuristically adjust their behaviour.

Adaptive agents are also characterised by higher values of memory parameters with respect to rational agents, being 0.92 and 0.60, respectively. Lower values of the memory parameter mean that agents do not assign much weight to past errors and mostly consider newest available information when choosing their forecast rules. These estimated parameters suggest that while adaptive agents stick to longer-term memory for today's choices, rational agents are capable of dismantling pre-existing experience in favour of a fully rational information set.

The cost of being rational presents a strong persistence: intuitively, the cost of gathering information and gaining knowledge about the true mechanism of the economy is constant over time. Nevertheless, the standard deviation of the rationality cost shock is relatively high and seems to capture most of the system volatility.

3.4.5 Validating the Empirical Strategy

This section evaluates the ability of the estimated Behavioural New Keynesian (NK-BH) model to reproduce empirical moments. Given the different set of observables used to estimate the Behavioural and the FIRE New Keynesian (NK-RE) models, a

[10]Further robustness checks might consider using only a single *speed of learning* parameter for prices related expectations and assuming expectations on marginal utility to be fully rational in accordance with literature on internal rationality (Adam and Marcet, 2011).

comparison of the ability to replicate empirical moments can provide further insights on the value added by including survey measures and validating the empirical strategy. Following standard DSGE practice, I compare the ability of the two models in matching volatility and autocorrelations. Moreover, as non-linear models were proven to better match skewness and kurtosis, this section aims at understanding whether including *reinforcement learning* results in an improvement on the non-linear FIRE model.

Table 3.3 presents empirical moments computed over the estimation sample (1984Q1-2008Q4) and compares them with moments based on simulated data obtained from a third-order approximation of the model evaluated at the posterior mode.[11]

In general, both the non-linear NK-BH and the NK-RE produce higher volatility compared to what observed in the reference sample, with the only exception of hours worked.

This is particularly evident for growth in real GDP per capita for which the empirical standard deviation is roughly one-third of what generated by the models, but also for inflation which is characterised by half of the volatility produced by the NK-BH and two-thirds of the volatility resulting from the NK-RE.

Concerning the volatility of hours worked, actual data present higher volatility than what produced by the models. This might be the result of the low level of the estimated Frisch elasticity, $1/\phi$, being around 30% for both model types. Nonetheless, the *reinforcement learning* mechanism somehow compensates for the low volatility implied by bulk parameters of standard NK models, by halving the gap observed between data simulated with the NK-RE model and actual ones. Finally, the empirical standard deviation of the policy rate is in line with that produced by the NK-BH model.

Skewness and kurtosis are important measures to evaluate the ability of a model to reproduce the non-Gaussian features observed in empirical data in spite of using normally distributed shocks. A normal distribution is characterised by a skewness equal to zero and a kurtosis equal to three. Any divergence from these values implies non-Gaussianity. In particular, a positive skewness indicates higher (lower) probability mass to the right (left) of the distribution mean and a kurtosis above

[11] Simulations based on a second-order approximation of the model are qualitatively similar.

(below) three results in a distribution with more (less) density on the tails relative to a normal distribution.

The NK-BH always detects the direction which the distribution of actual data is skewed towards, whereas the NK-RE experiences some difficulties in replicating the skew of growth in real GDP per capita and inflation (which is positive but close to zero). The NK-BH is able to generate the negative skewness observed for growth in real GDP per capita, and - with the only exception of the nominal interest rate - the skewness produced with this model is always closer to the empirical one compared to that provided by the NK-RE.

Turning to kurtosis, results are less sharp, with the NK-RE providing a good match of growth in real GDP per capita and the NK-BH being better for hours worked per capita and inflation. Interestingly, the NK-BH always assigns more mass around the mean with respect to the NK-RE. Looking at the estimated parameters, this might be due to the lower value estimated for the persistence parameter of the Taylor Rule, ρ_r, compared to the NK-RE case which allows the Central Bank to reduce the frequency of extreme realisations of output and inflation.

	Std	Skew	Kurt	AR(1)
Y				
Data	0.54	-0.42	3.62	0.36
NK-RE	1.84	0.13	**3.09**	0.98
NK-BH	**1.68**	**-0.17**	2.61	**0.97**
H				
Data	1.98	0.43	1.90	0.99
NK-RE	0.87	0.13	3.06	0.95
NK-BH	**1.44**	**0.16**	**2.63**	**0.97**
π				
Data	0.23	0.51	2.74	0.84
NK-RE	**0.31**	0.07	3.05	0.71
NK-BH	0.38	**0.19**	**2.82**	**0.74**
R_n				
Data	0.60	0.13	2.60	0.95
NK-RE	0.43	**0.34**	**3.18**	**0.96**
NK-BH	**0.55**	0.67	**3.17**	0.91

TABLE 3.4: Empirical vs. simulated moments.

Looking at the ability of capturing time-series persistence, even though both models present some limits, the NK-BH performs slightly better than the NK-RE at reproducing the one-period autocorrelation. Table 3.4 shows that NK-BH better captures the AR(1) for hours worked and inflation, whereas the NK-RE better reproduces autocorrelation for the nominal interest rate. Both models overestimate autocorrelations for output. As exhibited in Figure 3.3, the autocorrelation for output is about three times larger than the empirical one when looking at the first lag and continue being very persistent until the 10th lag. Concerning other variables, the NK-BH better captures autocorrelation profile for the inflation rate and the NK-RE for the nominal interest rate. Regarding hours worked, the NK-BH generates autocorrelations which are closer to empirical ones over shorter lags, whereas the NK-RE is better over farther lags.

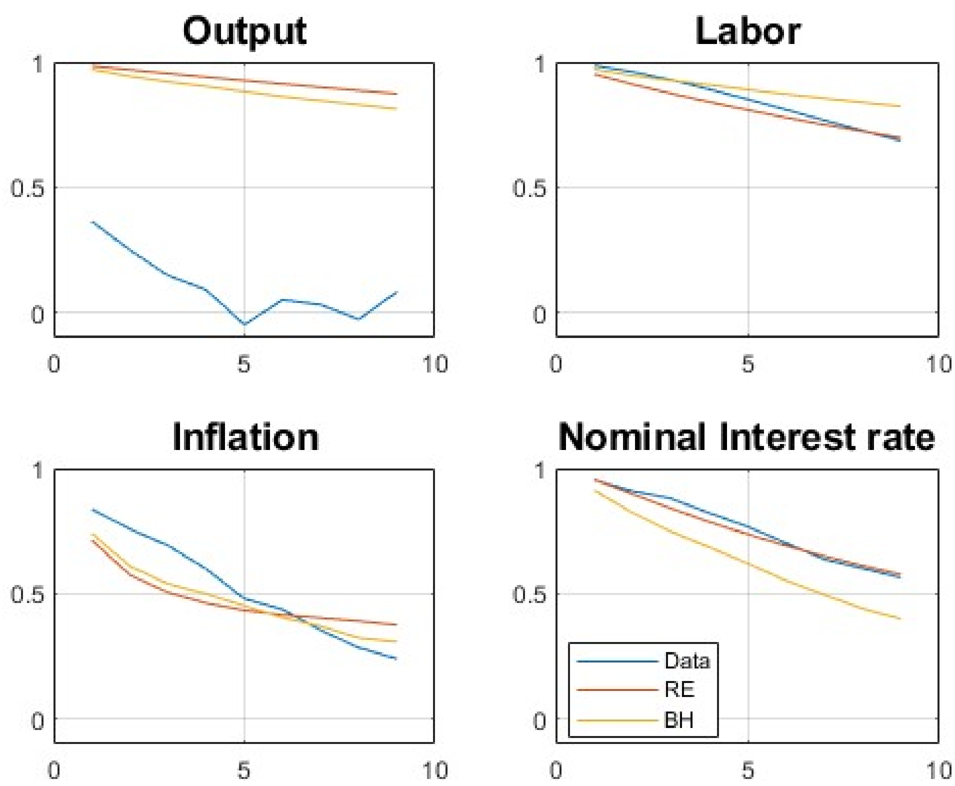

FIGURE 3.3: Autocorrelation function

3.5 Conclusions and Future Research

This paper designs and estimates a non-linear New Keynesian (NK) Behavioural model with trend inflation, heterogeneous expectations and bounded rational agents forming expectations on the basis of *reinforcement learning* (Brock and Hommes, 1997). Novel identification tests for non-linear DSGE models (Mutschler, 2015) show that the core parameters of the learning mechanism (i.e. the *intensity of choice* and the *memory parameters*) can only be jointly identified with higher-order approximations while including observations on the proportion of agents adopting a specific forecast rule. Thus, the model is estimated with Bayesian techniques applying a second-order Extended Kalman filter (Gustafsson and Hendeby, 2012) by expanding the information set with data from the *Survey of Consumers Expectations* from the *University of Michigan* to proxy the share of *näive* agents populating the economy.

Estimation results deliver a high value of the *intensity of choice* compared to what usually assumed in the literature. Furthermore, the *memory* parameters were found to be higher for backward-looking agents than for fully rational ones.

A possible explanation might reside in the presence of fully rational agents. This is an important difference with respect to the majority of other studies on DSGE models with *reinforcement learning* where usually all agents are endowed with *bounded rationality*. Fully rational agents can quickly adapt their behaviour by knowing the structure of the model, including the performance of other forecast rules. Additionally, they can timely update their information set and are able to understand whether past forecast errors might be of help. These theoretical insights are thus consistent with the estimated *intensity of choice* and *memory* parameters.

A validation exercise suggests that the Behavioural New Keynesian model outperforms the fully rational and fully informed counterpart in replicating key moments of the observed sample. On balance, it was able to better replicate volatility, skewness and kurtosis while providing a similar match of time series persistence.

In conclusion, this study bridges the gap between micro-level empirical evidence on expectations formation and standard DSGE models, thereby providing a complementary tool for testing policy measures.

Future research might focus on testing whether other forms of *bounded rationality* provide a better fit with the data or on testing alternative survey measures for checking the robustness of estimates - see appendix C.7 for an exploration of alternative indicators. The difficulty in matching empirical volatility and series autocorrelations, often affecting maximum likelihood estimators, suggests further refinements of model estimates might come from future research adopting endogenous priors for shocks based on second moments (Del Negro and Schorfheide, 2008). Then, structural parameters might be estimated with a two step-approach similar to Born and Pfeifer (2014) or Noh (2020)where part of the parameters are estimated on the basis of non-linear filtering techniques and part with the method of moments. The estimation exercise might be further refined using third-order Taylor expansions or higher, by means of stronger computing power. Moreover, one might study optimal policy design under *heterogenous expectations* and *reinforcement learning.*

Appendix A

Chapter 1: RBC model

A.1 RBC Zero-Growth Steady State Representation

The zero growth steady-state is:

$$U = \beta \left(log\left(C\right) + \psi \frac{\left(1-H\right)^{(1-\sigma)} - 1}{1-\sigma} \right) \tag{A.1}$$

$$Y = AK^{\alpha}H^{1-\alpha} \tag{A.2}$$

$$Y = AK^{\alpha}H^{1-\alpha} \tag{A.3}$$

$$K = K(1-\delta) + \mu I \tag{A.4}$$

$$C + K = Y + K(1-\delta) \tag{A.5}$$

which can be expressed in recursive form, knowing that A=1, μ=1 and H=0.33 in steady state:

$$K = H\left(\left(\frac{1}{\beta} - (1-\delta)\right) \left(\frac{1}{A\left(1-\alpha\right)}\right) \right)^{-\left(\frac{1}{\alpha}\right)} \tag{A.6}$$

$$Y = AK^{\alpha}H^{1-\alpha} \tag{A.7}$$

$$I = \frac{\delta K}{\mu} \tag{A.8}$$

$$C = Y + K(1-\delta) - K \tag{A.9}$$

$$\psi = \frac{\alpha}{C}\frac{Y}{H}\left(1-H\right)^{\sigma} \tag{A.10}$$

A.2 Laplace Approximation of the Posterior Density

The Laplace approximation is a Gaussian approximation of the likelihood $p(z|\theta)$ that can be reproduced from the second-order Taylor approximation of the log-posterior $h\left(\theta\right) \equiv log(p(z|\theta)) + log(p(\theta))$:

$$h\left(\theta\right) = h\left(\theta^{*}\right) - \frac{1}{2}\left(\theta-\theta^{*}\right)' h_{\theta\theta}\left(\theta-\theta^{*}\right) \tag{A.11}$$

where $\theta = \theta^{*}$ denotes the vector of parameters at the mode and $h_{\theta\theta} = \frac{\partial^{2}h(\theta)}{\partial\theta\partial\theta'}|_{\theta=\theta'}$ It follows that:

$$\begin{aligned}&(p(z|\theta, V(\theta_0, \xi_0, T)))p(\theta)\\ &\qquad\approx(p(z|\theta^{*}, V(\theta_0, \xi_0, T)))p(\theta^{*})exp\left(-\frac{1}{2}\left(\theta-\theta^{*}\right)' h_{\theta\theta}\left(\theta-\theta^{*}\right)\right)\end{aligned}$$

Where the the k stochastic variables are distributed according to a k-dimensional Gaussian distribution:

$$\frac{1}{\left(2\pi\right)^{\frac{k}{2}}} \mid h_{\theta\theta} \mid^{\frac{1}{2}} exp\left(-\frac{1}{2}\left(\theta-\theta^{*}\right)' h_{\theta\theta}\left(\theta-\theta^{*}\right)\right)$$

$$\int \frac{1}{\left(2\pi\right)^{\frac{k}{2}}} \mid h_{\theta\theta} \mid^{\frac{1}{2}} exp\left(-\frac{1}{2}\left(\theta-\theta^{*}\right)' h_{\theta\theta}\left(\theta-\theta^{*}\right)\right) d\theta = 1$$

Then:

$$\begin{aligned}p\left(z\right) &= \int p\left(z|\theta\right)p\left(\theta\right)\\ &\approx \int p\left(z|\theta^{*}\right)p\left(\theta^{*}\right)exp\left(-\frac{1}{2}\left(\theta-\theta^{*}\right)' h_{\theta\theta}\left(\theta-\theta^{*}\right)\right)d\theta\\ &= \left(2\pi\right)^{\frac{k}{2}} \mid h_{\theta\theta} \mid^{-\frac{1}{2}} p\left(z|\theta^{*}\right)p\left(\theta^{*}\right)\end{aligned}$$

which can be used to compare models for different parameters values:

$$\theta_i \sim N\left(\theta_i^*, [h_{\theta\theta}^{-1}]_{ii}\right) \tag{A.12}$$

A.3 Application with Flat Priors

Parameter	Actual	CKF	EKF	MGM	MGS	PF 300
α	0.67	0.6496	0.6634	0.666	0.6628	0.59
β	0.99	0.9856	0.9886	0.9892	0.9891	0.9471
σ	0.025	0.0298	0.0267	0.0262	0.0258	0.0359
ρ_z	2.75	2.5524	2.8645	2.9887	2.8706	54.6542
δ	0.95	0.9522	0.9516	0.9521	0.954	0.8152
ρ_M	0.72	0.9448	0.6585	0.6401	0.6458	0.3258
σ_M	0.06	0.0139	0.0691	0.0735	0.0712	0.0817
σ_Z	0.007	0.0063	0.0074	0.0074	0.0073	0.0092
σ_C	0.004	0.0046	0.0038	0.0038	0.0038	0.0045
σ_I	0.019	0.0046	0.0013	0.0014	0.0014	0.0273
σ_H	0.009	0.0091	0.009	0.0091	0.0091	0.0095
RMSE		10.5%	22.7%	21.6%	22.7%	25.7%
RMSE 10%		7.9%	12.6%	13.3%	15.4%	9.33%
RMSE 90%		13.4%	32.7%	33.1%	35.5%	42.8%
ARB		24%	19%	17%	19%	255%
Time		00:04:23	00:26:08	00:11:21	00:12:33	00:14:58
Log-Likelihood		-6198	-6229	-6227	-6227	-4270

Table A.1: Benchmark calibration with flat priors.
CKF: Cubature Kalman Filter; EKF: Full Second-order Extended Kalman Filter; MG-M: Approximation around the ergodic mean; MG-S: Approximation around the stochastic steady-state; SM-CKF: Sparse-matrix Cubature Kalman Filter;PF 300: Particle filter with 300 particles and systematic resampling. Observables: consumption, C, hours worked, H, investment, I. The experiment was run on 100 samples of 500 observations using CMAES algorithm to compute the mode, mh_replic=0. RMSE are normalised by the sample average of state variables. [10%,90%] are RMSEs at the 10^{th} and 90^{th} percentiles.

Parameter	Actual	CKF	EKF	MGM	MGS	PF 300
α	0.67	0.6638	0.6631	0.6708	0.6656	0.6706
β	0.99	0.9894	0.9893	0.9901	0.99	0.99
δ	0.025	0.0251	0.0254	0.0249	0.0253	0.0249
σ	0.05	0.0138	0.0427	0.1637	0.0889	0.0807
ρ_z	0.95	0.9511	0.9475	0.9468	0.9488	0.9503
ρ_M	0.72	0.9255	0.7193	0.7492	0.7484	0.72
σ_M	0.06	0.0171	0.0568	0.0578	0.0546	0.0435
σ_Z	0.035	0.0253	0.0348	0.0372	0.0354	0.0374
σ_C	0.0039	0.0069	0.004	0.0039	0.0039	0.0054
σ_I	0.019	0.0238	0.0021	0.0061	0.0076	0.0162
σ_H	0.0092	0.0102	0.009	0.0098	0.0097	0.0096
RMSE		36.0%	27.7%	28.1%	29.3%	24.0%
RMSE 10%		14.7%	19.9%	20.5%	20.7%	16.9%
RMSE 90%		31.2%	40.5%	40.8%	42.3%	28.5%
ARB		30.12%	17.79%	42.28%	48.14%	26.30%
Time		00:02:13	00:11:46	00:01:05	00:01:00	00:23:05
Log-Likelihood		-4686	-5008	-4815	-4816	-4879

TABLE A.2: Risky calibration with flat priors.
CKF: Cubature Kalman Filter; EKF: Full Second-order Extended Kalman Filter; MG-M: Approximation around the ergodic mean; MG-S: Approximation around the stochastic steady-state; SM-CKF: Sparse-matrix Cubature Kalman Filter; PF 300: Particle filter with 300 particles and systematic resampling. Observables: consumption, C, hours worked, H, investment, I. The experiment was run on 100 samples of 500 observations using CMAES algorithm to compute the mode, mh_replic=0. RMSE are normalised by the sample average of state variables. [10%,90%] are RMSEs at the 10^{th} and 90^{th} percentiles.

A.4 Application Benchmark Scenario with Flat Priors

Parameter	Actual	CKF	EKF	MGM	MGS	SM-CKF 300	PF 300
σ	2.75	2.85	2.7402	2.749	2.7468	2.9406	4.1269
ρ_z	0.95	0.9589	0.9509	0.951	0.9512	0.9505	0.8983
ρ_M	0.72	0.7918	0.6529	0.676	0.6676	0.9517	0.4672
σ_M	0.06	0.0384	0.0714	0.0682	0.0698	0.0231	0.0952
σ_Z	0.007	0.0063	0.0072	0.0072	0.0072	0.0068	0.0071
σ_C	0.004	0.0045	0.004	0.004	0.004	0.0043	0.0054
σ_I	0.019	0.0046	0.0016	0.0017	0.0016	0.0033	0.0045
σ_H	0.009	0.009	0.009	0.009	0.009	0.009	0.0089
RMSE		16.55%	23.19%	22.44%	22.13%	9.37%	32.02%
RMSE 10%		12.8%	15.4%	17.8%	14.6%	7.8%	11.5%
RMSE 90%		21.4%	29.7%	25.7%	26.2%	11.2%	60.4%
ARB		19.79%	18.77%	17.66%	18.12%	25.3%	42.71%
Time		00:03:01	00:08:59	00:01:00	00:01:02	00:03:08	00:08:58
Log-Likelihood		-6208	-6242	-6240	-6240	-6214	-6202

Table A.3: Benchmark calibration with informative priors on 100 observations and α, β and δ fixed. CKF: Cubature Kalman Filter; EKF: Full Second-order Extended Kalman Filter; MG-M: Approximation around the ergodic mean; MG-S: Approximation around the stochastic steady-state; SM-CKF: Sparse-matrix Cubature Kalman Filter; PF 300: Particle filter with 300 particles and systematic resampling. Observables: consumption, C, hours worked, H, investment, I. The experiment was run on 100 samples of 100 observations using CMAES algorithm to compute the mode, mh_replic=0. RMSE are normalised by the sample average of state variables. [10%,90%] are RMSEs at the 10^{th} and 90^{th} percentiles.

A.5 Application Benchmark Scenario with α, β and δ Fixed

Parameter	Actual	CKF	EKF	MGM	MGS	SM-CKF 300	PF 300
σ	2.75	2.8542	2.7248	2.7312	2.7287	2.9316	2.7248
ρ_z	0.95	0.959	0.9516	0.9517	0.9519	0.9498	0.9516
ρ_M	0.72	0.7885	0.6532	0.6759	0.6674	0.9509	0.6532
σ_M	0.06	0.0387	0.0709	0.0677	0.0693	0.0231	0.0709
σ_Z	0.007	0.0063	0.0072	0.0072	0.0072	0.0068	0.0072
σ_C	0.004	0.0046	0.004	0.004	0.004	0.0044	0.004
σ_I	0.019	0.0046	0.0017	0.0018	0.0018	0.0034	0.0017
σ_H	0.009	0.009	0.009	0.009	0.009	0.009	0.009
RMSE		14.4%	26.52%	22.4%	21.82%	9.21%	22.89%
RMSE 10%		11.6%	18.8%	18.1%	15.4%	7.7%	19.1%
RMSE 90%		17.6%	35.1%	27.9%	29.1%	10.7%	29.3%
ARB		19.82%	18.1%	16.97%	17.44%	25.43%	18.1%
Time		00:01:50	00:09:07	00:01:03	00:01:08	00:03:02	00:16:41
Log-Likelihood		-6210	-6243	-6243	-6243	-6218	-6243

TABLE A.4: Benchmark calibration with informative priors on 500 observations and α, β and δ fixed.
CKF: Cubature Kalman Filter; EKF: Full Second-order Extended Kalman Filter; MG-M: Approximation around the ergodic mean; MG-S: Approximation around the stochastic steady-state; SM-CKF: Sparse-matrix Cubature Kalman Filter; PF300: Particle filter with 300 particles and systematic resampling. Observables: consumption, C, hours worked, H, investment, I. The experiment was run on 100 samples of 500 observations using CMAES algorithm to compute the mode, mh_replic=0. RMSE are normalised by the sample average of state variables. [10%,90%] are RMSEs at the 10^{th} and 90^{th} percentiles.

A.6 Application with the Symplex Algorithm

Parameter	Actual	ckf	ekf	mgm	mgs	GF300	PF300
σ	2.75	2.85	2.7407	2.75	2.75	2.9405	3.0753
ρ_z	0.95	0.9589	0.9509	0.95	0.95	0.9505	0.968
ρ_M	0.72	0.7918	0.6531	0.72	0.72	0.9517	0.7432
σ_M	0.06	0.0384	0.0714	0.06	0.06	0.0231	0.0634
σ_Z	0.007	0.0063	0.0072	0.007	0.007	0.0068	0.0077
σ_C	0.004	0.0045	0.004	0.004	0.004	0.0043	0.0044
σ_I	0.019	0.0046	0.0016	0.019	0.019	0.0033	0.008
σ_H	0.009	0.009	0.009	0.009	0.009	0.009	0.0098
RMSE		13.13%	18.81%	19.04%	20.62%	8.65%	21.86%
ARB		19.79%	18.78%	.%	.%	25.3%	16.12%
Time		00:05:12	00:16:01	00:00:12	00:00:11	00:12:46	00:03:04
Log-Likelihood		-6208	-6242	-6553	-6553	-6214	-6106

TABLE A.5: Benchmark calibration with informative priors and α,β and δ fixed. CKF: Cubature Kalman Filter; EKF: Full Second-order Extended Kalman Filter; MG-M: Approximation around the ergodic mean; MG-S: Approximation around the stochastic steady-state; GF300: Sparse-matrix Cubature Kalman Filter;PF300: Particle filter with 300 particles and systematic resampling. Observables: consumption, C, hours worked, H, investment, I. The experiment was run on 100 samples of 500 observations using Matlab Symplex algorithm modified by the Dynare team to compute the mode, mh_replic=0. The optimisation was run in two steps, the first with a more global step size and the second with a more local step size by initialising the algorithm at the mode of the first step. RMSE are normalised by the sample average of state variables,

Appendix B

Chapter 2

B.1 The Full Non-linear Model

This appendix presents the details of the full non-linear system of equations composing the model.

The representative household behave following a separable utility function:

$$U_t = \log\left(C_t\right) - \frac{1}{1+\frac{1}{\varphi}}\, {L_t}^{1+\frac{1}{\varphi}} \tag{B.1}$$

$$U_t^C = \left(C_t\right)^{-1} \tag{B.2}$$

$$U_t^L = -L_t^{\left(\frac{1}{\varphi}\right)} \tag{B.3}$$

leading to the following first order conditions:

C:

$$\lambda_t = U_t^C \tag{B.4}$$

L:

$$\frac{-U_t^L}{\lambda_t} = W_t \tag{B.5}$$

B^S:

$$\begin{aligned} &1 + \phi^{LH} \frac{k^{LH}}{B_t^{LH}} \left(k^{LH} \frac{B_t^S}{B_t^{LH}} - 1 \right) = \\ &\frac{\lambda_{t+1}\beta}{\lambda_t} \left(\frac{R_t^S}{\pi_{t+1}} \right) \end{aligned} \tag{B.6}$$

B^{LH}:

$$1-\phi^{LH}\frac{k^{LH}B_t^S}{(B_t^{LH})^2}\left(k^{LH}\frac{B_t^S}{B_t^{LH}}-1\right)= \\ \frac{\mu_{t+1}\beta}{\mu_t}\left(\frac{R_{t+1}^L}{\pi_{t+1}}\right) \tag{B.7}$$

where

$$k^{LH}=\frac{B^{LH}}{B^S} \tag{B.8}$$

is household's preferred ratio of long-term to short-term bonds in equilibrium. The budget constraint features the following portfolio adjustment costs:

$$AC_t^L=\frac{\phi^{LH}}{2}\left(k^{LH}\frac{B_t^S}{B_t^{LH}}-1\right)^2 \tag{B.9}$$

Firms operate in a standard monopolistic competition environment characterised by a Calvo lottery where the price of firms adjusting prices in time t is

$$\frac{P_t^*}{P_t}=\frac{J_t}{JJ_t} \tag{B.10}$$

and JJ_t and J_t are computed by optimizing firms profits

$$JJ_t-\xi E_t\left[\Lambda_{t,t+1}\pi_{t+1}^{\varepsilon-1}JJ_{t+1}\right]=Y_t \tag{B.11}$$

$$J_t-\xi E_t\left[\Lambda_{t,t+1}\pi_{t+1}^{\varepsilon}J_{t+1}\right]=(\frac{\varepsilon}{\varepsilon-1})Y_tMC_tz_t^u \tag{B.12}$$

with

$$\log z_t^u=\phi_u\log z_{t-1}^u+{\epsilon^u}_t \tag{B.13}$$

Then, the average price in t can be expressed as

$$1=\xi\pi_t^{\varepsilon-1}+(1-\xi)\left(\frac{J_t}{JJ_t}\right)^{1-\varepsilon} \tag{B.14}$$

with price dispersion defined as

$$\Delta_t^P=\xi\pi_t^{\varepsilon}\Delta_{t-1}^P\,(1-\xi)\left(\frac{J_t}{JJ_t}\right)^{-\varepsilon} \tag{B.15}$$

For each retail producer, wages are equal to real marginal costs:

$$W_t = MC_t A_t = \frac{P_t^W}{P_t} \tag{B.16}$$

The intermediate sector faces the following productivity function:

$$Y_t^W = L_t\, A_t \tag{B.17}$$

The stochastic discount factor between t-1 and t is:

$$\Lambda_{t-1,t} = \beta \frac{\lambda_t}{\lambda_{t-1}} \tag{B.18}$$

Total output is equal to output divided dispersion.

$$Y_t = \frac{Y_t^W}{\Delta_t^P} \tag{B.19}$$

However, as inflation is assumed to be zero at the steady state, price dispersion does not affect total output. Finally, technology is assumed to follow a standard AR(1) process.

$$\log A_t = \phi_A \log A_{t-1} + {\epsilon^A}_t \tag{B.20}$$

Government: Government budget constraint:

$$B_t^S + B_t^{LT} = R_{t-1}^S B_{t-1}^S + R_t^L B_{t-1}^{LT} + GT_t \tag{B.21}$$

Total bonds in the economy:

$$Z_t = B^S + B^{LT} \tag{B.22}$$

Total long-term bonds held by the Central Bank:

$$B_t^{LCB} = B_t^{LT}\, W_t^B \tag{B.23}$$

Total long-term bonds held by households:

$$B_t^{LH} = B_t^{LT} \left(1 - W_t^B\right) \tag{B.24}$$

Total short-term bonds:

$$B_t^S = B^S > 0 \tag{B.25}$$

Total long-term bonds:

$$B_t^{LT} = B_t^{LH} + B_t^{CB} = B^{LT} > 0 \tag{B.26}$$

Balance-sheet shock:

$$\log W_t^B = -\left(\theta_\Pi \, \log \tilde{E}_t\{\pi_{t+1}\} \, + \theta_X \, \log \tilde{E}_t\{\hat{X}_{t+1}\}\right) + \log z_t^B \tag{B.27}$$

$$\log z_t^B = \phi_B \log z_{t-1}^B + \epsilon^B{}_t \tag{B.28}$$

$$GT_t = GT + \alpha_B \left(B_t^{LT} - B^{LT}\right) = GT \tag{B.29}$$

Long-term interest rates:

$$R_t^L = \frac{\left(1 + \chi Q_t^L\right)}{Q_{t-1}^L} \tag{B.30}$$

Central Bank:
Taylor rule on short-term interest rates:

$$R_t^S = \alpha^\pi \log \tilde{E}\{\pi_{t+1}\} + \alpha^X \log \tilde{E}\{\hat{X}_{t+1}\} + \epsilon_t^R \tag{B.31}$$

Resource constraint of the economy:

$$Y_t = C_t + GT_t + AC_t^L \tag{B.32}$$

B.2 The Zero-growth Steady State

This section presents the steady-state value of equations from Appendix B.1.
Utility function:

$$U = log\,(C) - \frac{1}{1+\frac{1}{\varphi}}\, L^{1+\frac{1}{\varphi}} \tag{B.33}$$

$$U^C = C^{-1} \tag{B.34}$$

$$U^L = -L^{\frac{1}{\varphi}} \tag{B.35}$$

Household FOCs:
C:

$$\lambda = U^C \tag{B.36}$$

L:

$$\frac{-U^L}{\lambda} = W \tag{B.37}$$

B^S:

$$R^S = \frac{\pi}{\beta} \tag{B.38}$$

B^{LH}:

$$R^L = \frac{\pi}{\beta} \tag{B.39}$$

$$k^{LH} = \frac{B^{LH}}{B^S} \tag{B.40}$$

Portfolio adjustment costs:

$$AC^L = \frac{\phi^L}{2}\left(k^{LH}\frac{B^S}{B^{LH}} - 1\right)^2 = 0 \tag{B.41}$$

Firm's problem:

$$\Delta^P = \xi\pi^{\varepsilon}\Delta^P + (1-\xi)\left(\frac{J}{JJ}\right)^{-\varepsilon} \tag{B.42}$$

$$Y^W = LA \tag{B.43}$$

$$Y = \frac{Y^W}{\Delta^P} \tag{B.44}$$

$$\Lambda = \beta\frac{\lambda}{\lambda} = \beta \tag{B.45}$$

$$JJ\left(1 - \xi E_t\left[\Lambda\pi^{\varepsilon-1}\right]\right) = Y \tag{B.46}$$

$$J\left(1 - \xi E_t\left[\Lambda\pi^{\varepsilon}\right]\right) = (\frac{\varepsilon}{\varepsilon-1})YMC \tag{B.47}$$

$$1 = \xi\pi^{\varepsilon-1} + (1-\xi)\left(\frac{J}{JJ}\right)^{1-\varepsilon} \tag{B.48}$$

$$W = MCA \tag{B.49}$$

$$\frac{P^W}{P} = MC \tag{B.50}$$

$$log\,(A) = \phi_A\, log\,(A) \tag{B.51}$$

$$log\,(z^u) = \phi_{z^u}\, log\,(z^u) \tag{B.52}$$

Consolidated Government-=Central Bank:

$$B^S + B^{LT} = R^S B^S + R^L B^{LT} + GT \tag{B.53}$$

$$Z = B^S + B^{LT} \tag{B.54}$$

$$W^B = \frac{B^{LCB}}{B^{LT}} \tag{B.55}$$

$$B^{LH} = B^{LT}\left(1 - W^B\right) \tag{B.56}$$

$$B^S = B^S > 0 \tag{B.57}$$

$$B^{LT} = B^{LH} + B^{LCB} > 0 \tag{B.58}$$

Balance-sheet shock:

$$\log W^B = -\left(\,\theta_\Pi\, \log \pi + \theta_X \log X\right) \tag{B.59}$$

$$\log z^B = \phi_B \log z^B \tag{B.60}$$

$$GT = GT + \alpha_B\left(B^{LT} - B^{LT}\right) = GT \tag{B.61}$$

$$R^L = \frac{1 + \chi q^L}{\chi q^L} \tag{B.62}$$

$$R_t^S = \alpha^\pi\,(\pi) + \alpha^X\,(X) \tag{B.63}$$

Resource constraint of the economy:

$$\begin{aligned} Y &= C + GT + AC^L \\ &= C + GT \end{aligned} \tag{B.64}$$

B.3 Steady State in Recursive Form

The zero-growth steady state can be expressed in recursive form as:

$$Y = 1; \tag{B.65}$$

$$A = 1 \tag{B.66}$$

$$z^u = \frac{1}{1 - \phi_{z^u}} \tag{B.67}$$

$$z^B = \frac{1}{1 - \phi_{z^B}} \tag{B.68}$$

$$Z = 1 \tag{B.69}$$

$$\pi = 1 \tag{B.70}$$

$$\Lambda = \beta \tag{B.71}$$

$$AC^L = \frac{\phi^{LH}}{2} \left(K^{LH} \frac{B^S}{B^{LH}} - 1 \right)^2 = 0 \tag{B.72}$$

$$JJ = \frac{Y}{(1 - \xi \Lambda \pi^{\varepsilon - 1})}; \tag{B.73}$$

$$J = JJ \left[\frac{(1 - \xi \pi^{\varepsilon - 1})}{(1 - \xi)} \right]^{\frac{1}{1-\varepsilon}} \tag{B.74}$$

$$MC = \left(\frac{\varepsilon - 1}{\varepsilon} \right) \frac{J}{Y} (1 - \xi \Lambda \pi^{\varepsilon}) \tag{B.75}$$

$$\frac{P^*}{P} = \frac{J}{JJ} \tag{B.76}$$

$$\frac{P^W}{P} = MC \tag{B.77}$$

$$W = MCA \tag{B.78}$$

$$\Delta^P = \frac{(1 - \xi)}{(1 - \xi \pi^{\varepsilon})} \left(\frac{J}{JJ} \right)^{-\varepsilon} \tag{B.79}$$

$$Y^W = Y \Delta^P \tag{B.80}$$

$$L = \frac{Y^W}{A} \tag{B.81}$$

$$U^L = -L^{(1/\varphi)}; \tag{B.82}$$

$$\lambda = -\frac{U^L}{W} \tag{B.83}$$

$$U^C = \frac{\lambda}{(1-\gamma\beta)} \tag{B.84}$$

$$C = U^{C-1}; \tag{B.85}$$

$$U = log\,(C) - \frac{L^{(1+(1/\varphi))}}{1+1/\varphi} \tag{B.86}$$

$$R^S = \frac{\pi}{\beta} \tag{B.87}$$

$$GT = Y - C \tag{B.88}$$

$$B^{LT} = 0.5; \tag{B.89}$$

$$B^S = 1 \tag{B.90}$$

$$W^B = 0 \tag{B.91}$$

$$B^{LCB} = W^B B^{LT} \tag{B.92}$$

$$R^L = \frac{\pi}{\beta} \tag{B.93}$$

$$q^L = \frac{\chi}{\left(\frac{\pi}{\beta} - 1\right)} \tag{B.94}$$

$$GT = \left(B^S + B^{LT}\right) - \left(R^L B^{LT} - R^S B^S\right) \tag{B.95}$$

$$B^{LH} = (1-X)B^{LT} \tag{B.96}$$

$$Z = B^S + B^{LT}; \tag{B.97}$$

$$k^{LH} = \frac{B^{LH}}{B^S}; \tag{B.98}$$

B.4 Log-linearisation

Linearisation at the zero-inflation steady state $\pi = 1$.

The marginal utility of consumption is

$$U_t^C = (C_t)^{-1} \tag{B.99}$$

Using total differentiation yields:

$$\hat{U}_t^C = -\hat{C}_t \tag{B.100}$$

The marginal utility of labour is

$$U_t^L = -L_t^{(\frac{1}{\varphi})} \tag{B.101}$$

Using total differentiation yields:

$$\hat{U}_t^L = (\frac{1}{\varphi})\hat{L}_t \tag{B.102}$$

Household FOCs:

Household's first-order condition for consumption,

$$\lambda_t = U_t^C \tag{B.103}$$

can be linearised to:

$$\hat{\lambda}_t = \hat{U}_t^C \tag{B.104}$$

Similarly, the first-order condition for labour

$$\frac{-U_t^L}{\lambda_t} = W_t \tag{B.105}$$

becomes:

$$\hat{U}_t^L - \hat{\lambda}_t = \hat{W}_t \tag{B.106}$$

For short-term bonds

$$\begin{aligned} & 1 + \phi^{LH} \frac{k^{LH}}{B_t^{LH}} \left(k^{LH} \frac{B_t^S}{B_t^{LH}} - 1 \right) \\ = & \\ & \frac{\lambda_{t+1}\beta}{\lambda_t} \left(\frac{R_t^S}{\pi_{t+1}} \right) \end{aligned} \tag{B.107}$$

one obtains:

$$\frac{\phi^{LH}}{B^S}\left(\hat{B}_t^S - \hat{B}_t^{LH}\right) = \\ \hat{R}_t^S + \hat{\lambda}_{t+1} - \hat{\pi}_{t+1} - \hat{\lambda}_t \tag{B.108}$$

Finally, for long-term bonds

$$1 - \phi^{LH}\frac{k^{LH}B_t^S}{(B_t^{LH})^2}\left(k^{LH}\frac{B_t^S}{B_t^{LH}} - 1\right) \\ \frac{\lambda_{t+1}\beta}{\lambda_t}\left(\frac{R_{t+1}^L}{\pi_{t+1}}\right) \tag{B.109}$$

the log-linearised version is:

$$-\frac{\phi^{LH}}{B^{LH}}\left(\hat{B}_t^S - \hat{B}_t^{LH}\right) = \\ R_{t+1}^L - \hat{\pi}_{t+1} + \hat{\lambda}_{t+1} - \hat{\lambda}_t \tag{B.110}$$

The production function

$$Y_t^W = L_t\, A_t \tag{B.111}$$

becomes:

$$\hat{Y}_t^W = \hat{L}_t + \hat{A}_t \tag{B.112}$$

The discount factor

$$\Lambda_{t-1,t} = \beta\frac{\lambda_t}{\lambda_{t-1}} \tag{B.113}$$

can be linearised as

$$\hat{\Lambda}_{t-1,t} = \hat{\lambda}_t - \hat{\lambda}_{t-1} \tag{B.114}$$

Equations from (B.10) to (B.15) can be linearised and combined to form a standard Phillips-curve:

$$\hat{\pi}_t = \beta\hat{\pi}_{t+1} + \frac{(1-\chi)\,(1-\beta\chi)}{(\chi)}\hat{MC}_t \tag{B.115}$$

Log-linearizing

$$W_t = MC_t A_t \tag{B.116}$$

leads to

$$\hat{W}_t - \hat{A}_t = \hat{MC}_t \tag{B.117}$$

Shock processes become

$$\hat{A}_t = \phi_A \hat{A}_{t-1} + {\epsilon^A}_t \tag{B.118}$$

$$\hat{z}^u_t = \phi_{z^u} \hat{z}^u_{t-1} + \epsilon^u_t \tag{B.119}$$

Government:

Government budget constraint:

$$R^S_{t-1} B^S_{t-1} + R^L_t B^{LT}_{t-1} + GT_t = B^S_t + B^{LT}_t \tag{B.120}$$

$$R^S B^S \left(\hat{R}^S_{t-1} + \hat{B}^S_{t-1}\right) + B^{LT} R^L \left(\hat{R}^L_t + \hat{B}^{LT}_{t-1}\right) + GT\hat{GT}_t = B^S \hat{B}^S_t + B^{LT} \hat{B}^{LT}_t \tag{B.121}$$

$$\begin{aligned} Z_t &= B^S_t + B^{LT}_t \\ &= 0 \end{aligned} \tag{B.122}$$

$$B^{LCB}_t = B^{LT}_t W^B_t \tag{B.123}$$

$$B^{LCB} \hat{B}^{LCB}_t = B^{LT} \hat{B}^{LT}_t + W^B \hat{W^B}_t \tag{B.124}$$

$$B^{LH}_t = B^{LT}_t (1 - X_t) \tag{B.125}$$

$$B^{LH} \hat{B}^{LH}_t = B^{LT} \hat{B}^{LT}_t - B^{LT} X \left(\hat{B}^{LT}_t + \hat{W}^B_t\right) \tag{B.126}$$

$$GT\hat{GT}_t = 0 \tag{B.127}$$

$$R^L_t = \frac{\left(1 + \chi q^L_t\right)}{\chi q^L_t} \tag{B.128}$$

$$R^L \hat{R}_t^L = -\frac{\hat{q}_t^L}{q^L} \tag{B.129}$$

Central Bank:

Asset purchase decision rule:

$$\hat{W_t^B} = -\left(\theta_\Pi\, \tilde{E}_t\{\hat{\pi}_{t+1}\}\; + \theta_X\, \tilde{E}_t\{\hat{X}_{t+1}\}\right) + {z^B}_t \tag{B.130}$$

$$Z\hat{Z}_t = B^S \hat{B}_t^S + \hat{B}_t^{LT} \tag{B.131}$$

$$\hat{R}_t^S = \alpha^\pi \tilde{E}\left(\hat{\pi}_{t+1}\right) + \alpha^X \tilde{E}\left(\hat{X}_{t+1}\right) + \epsilon_t^R \tag{B.132}$$

Resource constraint of the economy:

$$Y_t = C_t + GT_t + AC_t^L \tag{B.133}$$

$$Y = \frac{C}{Y}\hat{C}_t + \frac{GT}{Y}\hat{GT}_t \tag{B.134}$$

B.5 Details on Aggregate Demand and Term Structure

This section clarifies details on the derivation of the term structure (2.72) and the aggregate demand equation (2.73) with on short- and long-term interest rates.

The term-structure results from the combination of linearised household's FOCs for short-term, (B.108), and long-term bonds, (B.110):

$$\hat{R}_t^S = \hat{C}_{t+1} - \hat{C}_t + \hat{\pi}_{t+1} + \frac{\phi^{LH}}{B^S}\left(\hat{B}_t^S - \hat{B}_t^{LH}\right) \tag{B.135}$$

$$\hat{R}_{t+1}^L = \hat{C}_{t+1} - \hat{C}_t + \hat{\pi}_{t+1} - \frac{\phi^{LH}}{B^{LH}}\left(\hat{B}_t^S - \hat{B}_t^{LH}\right) \tag{B.136}$$

By subtracting (B.135) from (B.136):

$$\hat{R}^{L}_{t+1} - \hat{R}^{S}_{t} = -\frac{\phi^{LH}\left(B^{S} + B^{LH}\right)}{B^{S}B^{LH}}\left(\hat{B}^{S}_{t} - \hat{B}^{LH}_{t}\right) \tag{B.137}$$

The aggregate demand equation can be expressed in three equivalent different ways depending on the purpose of the analysis. The staring point of the derivation resides in representative households' FOCs, (B.138), (B.139), (B.140) which in our simplified model with logarithmic utility in consumption and no habits become:

$$U^{C}_{t} = C^{-1}_{t} \tag{B.138}$$

$$\lambda_{t} = U^{C}_{t} \tag{B.139}$$

$$1 + \phi^{LH}\frac{k^{LH}}{B^{LH}_{t}}\left(k^{LH}\frac{B^{S}_{t}}{B^{LH}_{t}} - 1\right) = \frac{\lambda_{t+1}\beta}{\lambda_{t}}\frac{R^{S}_{t}}{\pi_{t+1}} \tag{B.140}$$

Combining (B.138) to (B.140), leads to:

$$1 + \phi^{LH}\frac{k^{LH}}{B^{LH}_{t}}\left(k^{LH}\frac{B^{S}_{t}}{B^{LH}_{t}} - 1\right) = \frac{C_{t}\beta}{C_{t+1}}\frac{R^{S}_{t}}{\pi_{t+1}} \tag{B.141}$$

Log-linearizing, we obtain an expression of the aggregate demand with explicit bonds:

$$\hat{R}^{S}_{t} = \hat{C}_{t+1} - \hat{C}_{t} + \hat{\pi}_{t+1} + \frac{\phi^{LH}}{B^{S}}\left(\hat{B}^{S}_{t} - \hat{B}^{LH}_{t}\right) \tag{B.142}$$

As government transfers are zero in steady state,then, $Y_t = C_t$, and:

$$\hat{Y}_{t} = \hat{Y}_{t+1} - \left(\hat{R}^{S}_{t} - \hat{\pi}_{t+1}\right) + \frac{\phi^{LH}}{B^{S}}\left(\hat{B}^{S}_{t} - \hat{B}^{LH}_{t}\right) \tag{B.143}$$

The second representation, which is the one used for my simulations, explicitly depends on long-term interest rate and it is obtained by rearranging (B.136)

$$\phi^{LH}\left(\hat{B}_t^S - \hat{B}_t^{LH}\right) = -B^{LH}\hat{R}_{t+1}^L + B^{LH}\hat{C}_{t+1} - B^{LH}\hat{C}_t + B^{LH}\hat{\pi}_{t+1} \tag{B.144}$$

and plugging it into (B.143):

$$\hat{Y}_t = \hat{Y}_{t+1} - \left(1 + \frac{B^{LH}}{B^S}\right)^{-1}\left[\left(\hat{R}_t^S - \hat{\pi}_{t+1}\right) + \frac{B^{LH}}{B^S}\left(\hat{R}_{t+1}^L - \hat{\pi}_{t+1}\right)\right] \tag{B.145}$$

or:

$$\hat{Y}_t = \hat{Y}_{t+1} - w_1\left(\hat{R}_t^S - \hat{\pi}_{t+1}\right) - w_2\left(\hat{R}_{t+1}^L - \hat{\pi}_{t+1}\right) \tag{B.146}$$

where, $w_1 = \frac{1}{1+\frac{B^{LH}}{B^S}}$ and $w_2 = \frac{\frac{B^{LH}}{B^S}}{1+\frac{B^{LH}}{B^S}}$ are the weights of short-term and long-term interest rates in the aggregate demand equation, respectively.

Finally, one might want to show the relationship between output and the term structure. This might be presented by plugging a rearranged (B.137)

$$\phi^{LH}\left(\hat{B}_t^S - \hat{B}_t^{LH}\right) = -\frac{B^S B^{LH}}{(B^S + B^{LH})}\left(\hat{R}_{t+1}^L - \hat{R}_t^S\right) \tag{B.147}$$

into (B.143):

$$\hat{Y}_t = \hat{Y}_{t+1} - \left(\hat{R}_t^S - \hat{\pi}_{t+1}\right) - \frac{B^{LH}}{(B^S + B^{LH})}\left(\hat{R}_{t+1}^L - \hat{R}_t^S\right)$$

telling that when the term structure between long- and short-term bonds narrows down there is a positive effect on output.

B.6 Comparison to Sims, Wu, Zhang Linear Four-Equations Model

In this section, I compare the four-equation model developed in Harrison (2017) and the one presented in Sims et al. (2020). Even though the former is a RANK (representative agent model) and theirs is a TANK (two agents model) one, the linearised version of the two models present only one relevant difference in the Phillips-Curve specification and in the presence of a credit market shock.

In Sims et al. (2020)' s framework, the quantitative easing shock directly enter the Phillips Curve whereas in Harrison (2017) its effects only influence inflation indirectly through aggregate demand. Sims et al. (2020) suggest this feature seems to be in line with empirical literature showing differences between standard monetary policy shocks and Central Bank balance-sheet shocks with the former having similar effects on output and inflation and the latter having a more limited impact on inflation. However, Harrison (2017) can be opportunely calibrated to obtain similar effects as shown by the generalised impulse responses in Figure B.1 below.

For completeness, the model of Sims et al. (2020) is reported:

$$\begin{aligned}\hat{Y}_t =& E_t\left(\hat{Y}_{t+1}\right) - \frac{1-z}{\sigma}\left(\hat{R}^S_t - E_t\left(\hat{\pi}_{t+1}\right)\right) \ldots \\ &\ldots - z\left[\bar{b}^{FI}\left(E_t\left(\theta_{t+1}\right)-\theta_t\right) + \bar{b}^{CB}\left(E_t\left(qe_{t+1}\right) - qe_t\right)\right]\end{aligned} \tag{B.148}$$

$$\hat{\pi}_t = \gamma\xi\hat{Y}_t - \frac{z\gamma\sigma}{1-z}\left[\bar{b}^{FI}\theta_t + \bar{b}^{CB}qe_t\right] + \beta E_t\left(\hat{Y}_{t+1}\right) \tag{B.149}$$

$$\hat{R}^S_t = \phi^{\pi}E_t\left(\hat{\pi}_{t+1}\right) + \phi^{Y}E_t\left(\hat{Y}_{t+1}\right) + \sigma^R\epsilon^R \tag{B.150}$$

$$qe_t = \rho_{qe}qe_{t-1} + \sigma^{qe}\epsilon^{qe}_t \tag{B.151}$$

$$\theta_t = \rho_\theta \theta_{t-1} + \sigma^\theta \epsilon_t^\theta \tag{B.152}$$

Following appendix B of Sims , Wu, Zhang's, I could rearrange equation (B.148) to have a representation of the model tracking long-term interest rate as shown for Harrison's model in appendix B.5 for Harrison's model. Equation (B.148) is substituted by:[1]

$$\hat{Y}_t = E_t\left(\hat{Y}_{t+1}\right) - \frac{1-z}{\sigma}\left(\hat{R}_t^S - E_t\left(\hat{\pi}_{t+1}\right)\right) - \frac{z}{\sigma}E_t\left(\hat{R}_{t+1}^L - E_t\left(\hat{\pi}_{t+1}\right)\right) \tag{B.153}$$

and

$$\hat{R}_{t+1}^L = E_t\left(\hat{\pi}_{t+1}\right) + \left[\bar{b}^{FI}\left(E_t\left(\theta_{t+1}\right) - \theta_t\right) + \bar{b}^{CB}\left(E_t\left(qe_{t+1}\right) - qe_t\right)\right] \tag{B.154}$$

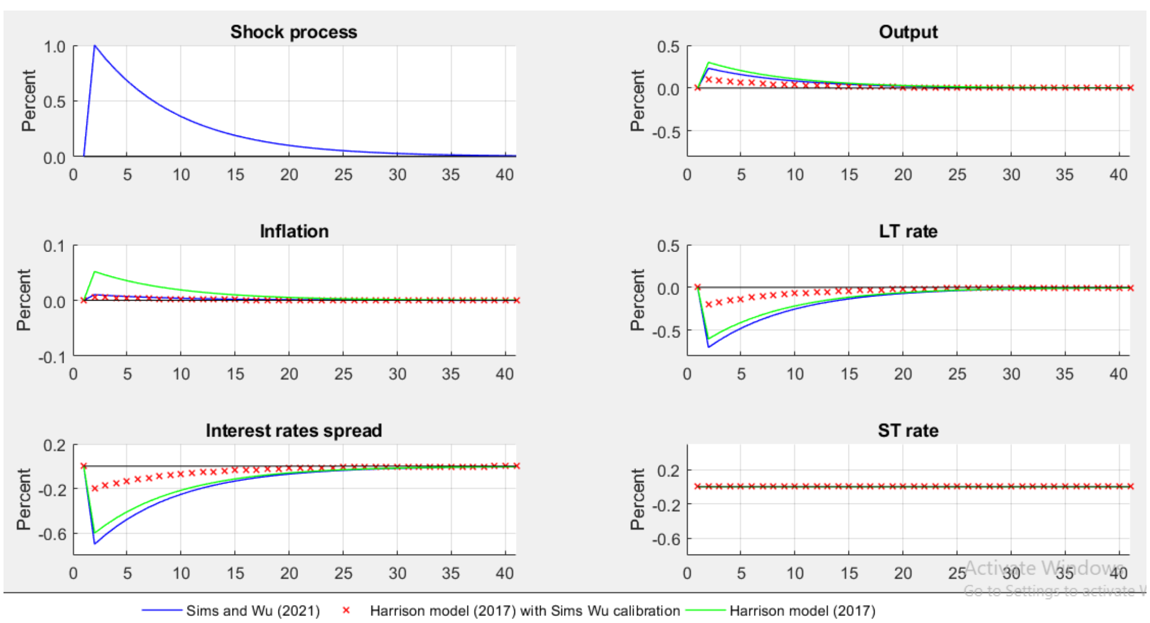

FIGURE B.1: Generalised impulse responses to a balance-sheet shock

[1]see equations B36-B38 at page 54

B.7 Determinacy Conditions under Rational Expectations with Forward-looking Taylor Rules

To study determinacy conditions the models needs to be written in form of difference equation. Rearranging equations while assuming rational expectations yields:

$$\begin{bmatrix} E_t\hat{\pi}_{t+1} \\ E_t\hat{X}_{t+1} \end{bmatrix} = \begin{bmatrix} \left(1-\alpha^X - w_3\theta^X\right) + \frac{\bar{k}}{\beta}\frac{(1-\alpha^\pi - w_3\theta^\pi)}{(1-\alpha^X - w_3\theta^X)} & \frac{-(1-\alpha^\pi - w_3\theta^\pi)}{\beta(1-\alpha^X - w_3\theta^X)} \\ \frac{1}{\beta}\left(1-\bar{k}\right) & \frac{1}{\beta} \end{bmatrix} \begin{bmatrix} \hat{\pi}_t \\ \hat{X}_t \end{bmatrix} = \Gamma \begin{bmatrix} \hat{\pi}_t \\ \hat{X}_t \end{bmatrix} \tag{B.155}$$

where $w_3 = V^{LH} w_2$.

As shown in Woodford (2003), determinacy is ensured by the following three conditions:

1. $\det(\Gamma) > 1$
2. det (Γ) - trace $(\Gamma) > 1$
3. $\det(\Gamma) + \text{trace}(\Gamma) > 1$

$$det\,(\Gamma) = \left(\frac{1}{\beta}\right)^2 \left[\frac{\left(1-\alpha^X - w_3\theta^X\right)^2 + \left(1-\alpha^\pi - w_3\theta^\pi\right)\bar{k}}{\left(1-\alpha^X - w_3\theta^X\right)}\right] \tag{B.156}$$

$$trace\,(\Gamma) = \frac{1}{\beta}\left[1 + \frac{\left(1-\alpha^Y - w_3\theta^X\right)^2 + \left(1-\alpha^\pi - w_3\theta^\pi\right)\bar{k}}{\left(1-\alpha^X - w_3\theta^X\right)}\right] \tag{B.157}$$

B.8 Additional Generalised Impulse Response

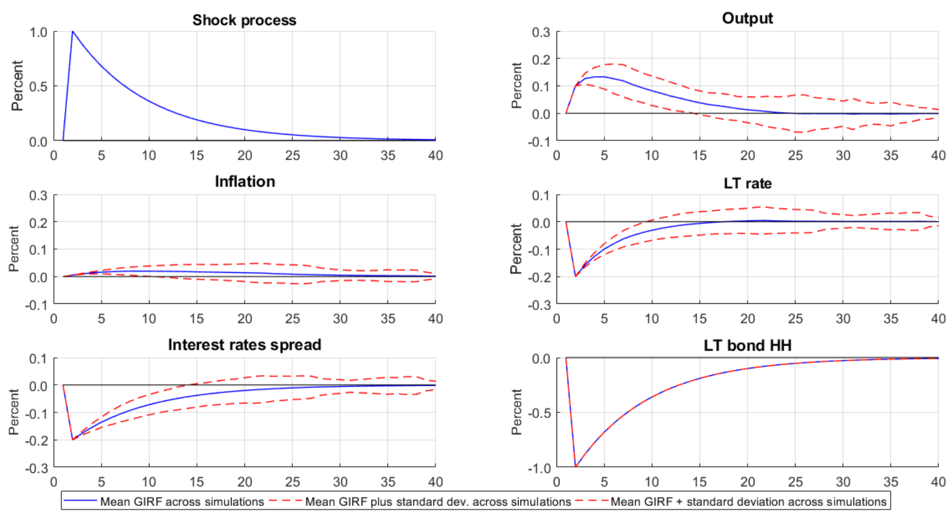

FIGURE B.2: Balance-sheet shock - persistence, only naives

Appendix C

Chapter 3

C.1 Equilibrium

A symmetric equilibrium is determined by the following equations:

$$U_t = \log(C_t) - \kappa \frac{H_t^{1+\phi}}{1+\phi} \tag{C.1}$$

$$V_t = \mathbb{E}_t \left[\sum_{s=0}^{\infty} \beta^s U_{t+s} \right] = U_t + \beta \mathbb{E}_t V_{t+1} \tag{C.2}$$

$$U_{C,t} = \frac{1}{C_t} \tag{C.3}$$

$$U_{H,t} = -\kappa H_t^{\phi} \tag{C.4}$$

$$\Lambda_{t,t+1} = \beta \frac{U_{C,t+1}}{U_{C,t}} \tag{C.5}$$

$$R_t = \frac{R_{n,t-1}}{\Pi_t} \tag{C.6}$$

$$1 = \mathbb{E}_t \left[\Lambda_{t,t+1} R_{t+1} \right] \tag{C.7}$$

$$W_t = -\frac{U_{H,t}}{U_{C,t}} \tag{C.8}$$

$$Y_t^W = A_t H_t^{\alpha} \tag{C.9}$$

$$W_t = \alpha \frac{P_t^W}{P_t} \frac{Y_t^W}{H_t} \tag{C.10}$$

$$MC_t = \frac{P_t^W}{P_t} \tag{C.11}$$

$$J_t = \frac{1}{1-\frac{1}{\zeta}} Y_t MC_t MS_t + \xi \mathbb{E}_t \Lambda_{t,t+1} \Pi_{t,t+1}^{\zeta} J_{t+1} \tag{C.12}$$

$$JJ_t = Y_t + \xi \mathbb{E}_t \Lambda_{t,t+1} \Pi_{t,t+1}^{\zeta-1} JJ_{t+1} \tag{C.13}$$

$$1 = \xi \Pi_t^{\zeta-1} + (1-\xi)\left(\frac{J_t}{JJ_t}\right)^{1-\zeta} \tag{C.14}$$

$$Y_t = \frac{Y_t^W}{\Delta_t^p} \tag{C.15}$$

$$\Delta_t^p = \xi \Pi_t^{\zeta} \Delta_{t-1}^p + (1-\xi)\left(\frac{J_t}{JJ_t}\right)^{-\zeta} \tag{C.16}$$

$$Y_t = C_t + G_t \tag{C.17}$$

$$\begin{aligned} \log\left(\frac{R_{n,t}}{R_n}\right) &= \rho_r \log\left(\frac{R_{n,t-1}}{R_n}\right) \\ &+ (1-\rho_r)\left(\theta_\theta \log\left(\frac{\mathbb{E}_t \Pi_{t+1}}{\Pi}\right) + \theta_y \log\left(\frac{Y_t}{Y}\right)\right) \\ &+ \log MPS_t \end{aligned} \tag{C.18}$$

$$\log A_t - \log A = \rho_A(\log A_{t-1} - \log A) + \epsilon_{A,t} \tag{C.19}$$

$$\log MS_t - \log MS = \rho_{MS}(\log MS_{t-1} - \log MS) + \epsilon_{MS,t} \tag{C.20}$$

$$\log MPS_t - \log MPS = \rho_{MPS}(\log MPS_{t-1} - \log MPS) + \epsilon_{MPS,t} \tag{C.21}$$

$$\log G_t - \log G = \rho_G(\log G_{t-1} - \log G) + \epsilon_{G,t} \tag{C.22}$$

where we have introduced a mark-up shock MS_t.

C.2 Stationary Equilibrium

Labour-augmenting technical progress parameter is decomposed into a cyclical component, A_t^c, and a deterministic trend $\bar{A}_t$:

$$\begin{aligned} A_t &= \bar{A}_t A_t^c \\ \bar{A}_t &= (1+g)\bar{A}_{t-1} \end{aligned}$$

Rewrite the equilibrium conditions as

$$U_t - \log(\bar{A}_t) = \log(C_t/\bar{A}_t) - \kappa \frac{H_t^{1+\phi}}{1+\phi} \tag{C.23}$$

$$V_t = U_t + \beta \mathbb{E}_t V_{t+1} \tag{C.24}$$

$$\bar{A}_t U_{C,t} = \frac{1}{C_t/\bar{A}_t} \tag{C.25}$$

$$U_{H,t} = -\kappa H_t^{\phi} \tag{C.26}$$

$$\Lambda_{t,t+1} = \frac{\beta}{\bar{A}_{t+1}/\bar{A}_t} \frac{\bar{A}_{t+1} U_{C,t+1}}{\bar{A}_t U_{C,t}} \tag{C.27}$$

$$R_t = \frac{R_{n,t-1}}{\Pi_t} \tag{C.28}$$

$$1 = \mathbb{E}_t \left[\Lambda_{t,t+1} R_{t+1} \right] \tag{C.29}$$

$$\frac{W_t}{\bar{A}_t} = -\frac{U_{H,t}}{\bar{A}_t U_{C,t}} \tag{C.30}$$

$$\frac{Y_t^W}{\bar{A}_t} = \frac{A_t}{\bar{A}_t} H_t^{\alpha} \tag{C.31}$$

$$\frac{W_t}{\bar{A}_t} = \alpha \frac{P_t^W}{P_t} \frac{Y_t^W / \bar{A}_t}{H_t} \tag{C.32}$$

$$MC_t = \frac{P_t^W}{P_t} \tag{C.33}$$

$$\frac{J_t}{\bar{A}_t} = \frac{1}{1 - \frac{1}{\zeta}} \frac{Y_t}{\bar{A}_t} MC_t MS_t + \xi \mathbb{E}_t \frac{\bar{A}_{t+1}}{\bar{A}_t} \Lambda_{t,t+1} \Pi_{t,t+1}^{\zeta} \frac{J_{t+1}}{\bar{A}_{t+1}} \tag{C.34}$$

$$\frac{JJ_t}{\bar{A}_t} = \frac{Y_t}{\bar{A}_t} + \xi \mathbb{E}_t \frac{\bar{A}_{t+1}}{\bar{A}_t} \Lambda_{t,t+1} \Pi_{t,t+1}^{\zeta-1} \frac{JJ_{t+1}}{\bar{A}_{t+1}} \tag{C.35}$$

$$1 = \xi \Pi_t^{\zeta-1} + (1-\xi) \left(\frac{J_t/\bar{A}_t}{JJ_t/\bar{A}_t} \right)^{1-\zeta} \tag{C.36}$$

$$\frac{Y_t}{\bar{A}_t} = \frac{Y_t^W / \bar{A}_t}{\Delta_t} \tag{C.37}$$

$$\Delta_t^p = \xi \Pi_t^{\zeta} \Delta_{t-1}^p + (1-\xi) \left(\frac{J_t/\bar{A}_t}{JJ_t/\bar{A}_t} \right)^{-\zeta} \tag{C.38}$$

$$\frac{Y_t}{\bar{A}_t} = \frac{C_t}{\bar{A}_t} + \frac{G_t}{\bar{A}_t} \tag{C.39}$$

$$\log\left(\frac{R_{n,t}}{R_n}\right) = \rho_r \log\left(\frac{R_{n,t-1}}{R_n}\right) + (1-\rho_r)\left(\theta_\theta \log\left(\frac{\Pi_t}{\Pi}\right) + \theta_y \log\left(\frac{Y_t}{Y}\right)\right) + \log MPS_t \tag{C.40}$$

$$\log A_t - \log A = \rho_A (\log A_{t-1} - \log A) + \epsilon_{A,t} \tag{C.41}$$

$$\log MS_t - \log MS = \rho_{MS} (\log MS_{t-1} - \log MS) + \epsilon_{MS,t} \tag{C.42}$$

$$\log MPS_t - \log MPS = \rho_{MPS} (\log MPS_{t-1} - \log MPS) + \epsilon_{MPS,t} \tag{C.43}$$

$$\log G_t - \log G = \rho_G (\log G_{t-1} - \log G) + \epsilon_{G,t} \tag{C.44}$$

Use change of variables to arrive to the following equilibrium conditions:[1]

$$U_t^c = \log(C_t^c) - \kappa \frac{H_t^{1+\phi}}{1+\phi} \tag{C.45}$$

$$V_t^c = U_t^c + \beta \mathbb{E}_t V_{t+1}^c \tag{C.46}$$

$$U_{C,t}^c = \frac{1}{C_t^c} \tag{C.47}$$

$$U_{H,t} = -\kappa H_t^{\phi} \tag{C.48}$$

$$\Lambda_{t,t+1} = \frac{\beta}{1+g} \frac{U_{C,t+1}^c}{U_{C,t}^c} \tag{C.49}$$

$$R_t = \frac{R_{n,t-1}}{\Pi_t} \tag{C.50}$$

$$1 = \mathbb{E}_t \left[\Lambda_{t,t+1} R_{t+1}\right] \tag{C.51}$$

$$W_t^c = -\frac{U_{H,t}}{U_{C,t}^c} \tag{C.52}$$

$$Y_t^{W,c} = A_t^c H_t^{\alpha} \tag{C.53}$$

$$W_t^c = \alpha \frac{P_t^W}{P_t} \frac{Y_t^{W,c}}{H_t} \tag{C.54}$$

$$MC_t = \frac{P_t^W}{P_t} \tag{C.55}$$

$$J_t^c = \frac{1}{1-\frac{1}{\zeta}} Y_t^c MC_t MS_t + \xi(1+g)\mathbb{E}_t \Lambda_{t,t+1} \Pi_{t,t+1}^{\zeta} J_{t+1}^c \tag{C.56}$$

$$JJ_t^c = Y_t^c + \xi(1+g)\mathbb{E}_t \Lambda_{t,t+1} \Pi_{t,t+1}^{\zeta-1} JJ_{t+1}^c \tag{C.57}$$

$$1 = \xi \Pi_t^{\zeta-1} + (1-\xi)\left(\frac{J_t^c}{JJ_t^c}\right)^{1-\zeta} \tag{C.58}$$

$$Y_t^c = \frac{Y_t^{W,c}}{\Delta_t^p} \tag{C.59}$$

$$\Delta_t^p = \xi \Pi_t^{\zeta} \Delta_{t-1}^p + (1-\xi)\left(\frac{J_t^c}{JJ_t^c}\right)^{-\zeta} \tag{C.60}$$

$$Y_t^c = C_t^c + G_t^c \tag{C.61}$$

$$\log\left(\frac{R_{n,t}}{R_n}\right) = \rho_r \log\left(\frac{R_{n,t-1}}{R_n}\right)$$

[1] The first equation is based on a hunch. Since the normalisation of utility is additive, we cannot have a different discount factor. However, we cannot derive the first equation above from (C.2). We can derive it starting from the definition $V_t^c = \mathbb{E}_t\left[\sum_{s=0}^{\infty} \beta^s U_{t+s}^c\right]$.

$$+ (1-\rho_r)\left(\theta_\theta \log\left(\frac{\Pi_t}{\Pi}\right) + \theta_y \log\left(\frac{Y_t^c}{Y^c}\right)\right) + \log MPS_t \tag{C.62}$$

$$\log A_t^c - \log A^c = \rho_A(\log A_{t-1}^c - \log A^c) + \epsilon_{A,t} \tag{C.63}$$

$$\log MS_t - \log MS = \rho_{MS}(\log MS_{t-1} - \log MS) + \epsilon_{MS,t} \tag{C.64}$$

$$\log MPS_t - \log MPS = \rho_{MPS}(\log MPS_{t-1} - \log MPS) + \epsilon_{MPS,t} \tag{C.65}$$

$$\log G_t^c - \log G^c = \rho_G(\log G_{t-1}^c - \log G^c) + \epsilon_{G,t} \tag{C.66}$$

This is a system of 22 equation in the following 22 "variables" (in order of appearance): V^c, U^c, C^c, H, Λ, R, W^c, U_H^c, U_C^c, $Y^{W,c}$, A^c, $\frac{P^W}{P}$, J^c, Y^c, MC, MS, Π, JJ^c, Δ^p, G^c, R_n, MPS.

C.3 Steady State

The exogenous variables have steady states $A^c = MS = MPS = 1$. Given the steady-state inflation rate Π and the steady-state nominal interest rate Rn, the steady-state values of the other variables can be computed as

$$\text{(C.49)} \Rightarrow \quad \Lambda = \frac{\beta}{1+g} \tag{C.67}$$

$$\text{(C.51)} \Rightarrow \quad R = \frac{1}{\Lambda} \tag{C.68}$$

$$\text{(C.58)} \Rightarrow \quad \frac{J^c}{JJ^c} = \left(\frac{1-\xi\Pi^{\zeta-1}}{1-\xi}\right)^{\frac{1}{1-\zeta}} \tag{C.69}$$

$$\text{(C.56), (C.57)} \Rightarrow \quad MC = \left(1-\frac{1}{\zeta}\right)\frac{J^c}{JJ^c}\frac{1-\xi\beta\Pi^\zeta}{1-\xi\beta\Pi^{\zeta-1}} \tag{C.70}$$

$$\text{(C.60)} \Rightarrow \quad \Delta^p = \frac{(1-\xi)\left(\frac{J^c}{JJ^c}\right)^{-\zeta}}{1-\xi\Pi^\zeta} \tag{C.71}$$

(C.54), using (C.47), (C.48),

$$\text{(C.52), (C.55), (C.59), (C.61)} \Rightarrow \quad H = \left(\frac{\alpha\Delta^p MC}{\kappa(1-gy)}\right)^{\frac{1}{1+\phi}} \tag{C.72}$$

$$\text{(C.53)} \Rightarrow \quad Y^{W,c} = (A^c H)^\alpha \tag{C.73}$$

$$\text{(C.59)} \Rightarrow \quad Y^c = \frac{Y^{W,c}}{\Delta} \tag{C.74}$$

$$G^c = gy * Y^c \tag{C.75}$$

$$(C.61) \Rightarrow \quad C^c = Y^c - G^c \tag{C.76}$$

$$(C.56) \Rightarrow \quad J^c = \frac{Y^c MCMS}{(1-\frac{1}{\zeta})(1-\xi\beta\Pi^{\zeta})} \tag{C.77}$$

$$(C.57) \Rightarrow \quad JJ^c = \frac{Y^c}{(1-\xi\beta\Pi^{\zeta-1})} \tag{C.78}$$

$$(C.45) \Rightarrow \quad U^c = \log(C^c) - \kappa\frac{H^{1+\phi}}{1+\phi} \tag{C.79}$$

$$(C.47) \Rightarrow \quad U^c_{C^c} = \frac{1}{C^c} \tag{C.80}$$

$$(C.48) \Rightarrow \quad U_H = -\kappa H^{\phi} \tag{C.81}$$

$$(C.55) \Rightarrow \quad \frac{P^W}{P} = MC \tag{C.82}$$

$$(C.54) \Rightarrow \quad W^c = \alpha\frac{P^W}{P}\frac{Y^{W,c}}{H} \tag{C.83}$$

$$(C.46) \Rightarrow \quad V^c = \frac{U^c}{1-\beta} \tag{C.84}$$

Finally we can define

$$\begin{aligned} CEquiv_t &= \mathbb{E}_t\left[\sum_{t=s}^{\infty}\beta^s U(1.01C_{t+s}, H_{t+s})\right] - \mathbb{E}_t\left[\sum_{t=s}^{\infty}\beta^s U(C_{t+s}, H_{t+s})\right] \\ &= \mathbb{E}_t\left[\sum_{t=s}^{\infty}\beta^s\left\{\log(1.01C^c_{t+s}) - \kappa\frac{H^{1+\phi}_{t+s}}{1+\phi} - \log(C^c_{t+s}) - \kappa\frac{H^{1+\phi}_{t+s}}{1+\phi}\right\}\right] \\ &= \log(1.01)\sum_{t=s}^{\infty}\beta^s = \frac{\log(1.01)}{1-\beta} \end{aligned} \tag{C.85}$$

The stationary version should be the same.

C.4 Data Sources and Transformations

Macroeconomic variables were retrieved from FRED portal by the Federal Reserve Bank of St. Louis: `https://fred.stlouisfed.org/`

Real Gross Domestic Product, Billions of Chained 2012 Dollars, Seasonally Adjusted Annual Rate [GDPC1]

Source: U.S. Department of Commerce, Bureau of Economic Analysis `https://fred.stlouisfed.org/series/GDPC1`

Gross Domestic Product - Implicit Price Deflator - Index 2012=100, Seasonally Adjusted [GDPDEF]
Source: U.S. Department of Commerce, Bureau of Economic Analysis
`https://fred.stlouisfed.org/series/GDPDEF`

U.S. Bureau of Labor Statistics, Employment Level [CE16OV]
Source: U.S. Department of Labor: Bureau of Labor Statistics
`https://fred.stlouisfed.org/series/CE16OV`

Nonfarm Business Sector: Average Weekly Hours Worked for All Employed Persons [PRS85006023]
Source: U.S. Bureau of Labor Statistics
`https://fred.stlouisfed.org/series/PRS85006023`

Population Level - 16 Years and Older - Not Seasonally Adjusted [CNP16OV or LNU00000000]
Source: U.S. Bureau of Labor Statistics
`https://fred.stlouisfed.org/series/CNP16OV`

Federal Funds Effective Rate [FEDFUNDS]
Source: Board of Governors of the Federal Reserve System (US)
`https://fred.stlouisfed.org/series/FEDFUNDS`
For the period after 2008Q4, it is extended with Shadow Interest Rate based on Wu and Xia (2016); Wu and Zhang (2019) as shown at `https://sites.google.com/view/jingcynthiawu/shadow-rates`.
Data was downloaded from: `https://www.atlantafed.org/cqer/research/wu-xia-shadow-federal-funds-rate`

Following Smets and Wouters (2007), raw data was transformed to map measurement equations in the following way:

$$\begin{aligned}
\texttt{dyobs} &= \Delta(LN((GDPC1)/CNP16OV)*100) \\
\texttt{labobs} &= LN((PRS85006023*index_CE16OV/100)/CNP16OV)*100 \\
&- mean_{[t:T]}(LN((PRS85006023*index_CE16OV/100)/CNP16OV)*100)
\end{aligned}$$

$$\begin{aligned} \texttt{pinfobs} &= LN(GDPDEF/GDPDEF(-1)) * 100 \\ \texttt{robs} &= FEDFUNDS/4 \end{aligned}$$

where the $\Delta = X_t^{obs} - X_{t-1}^{obs}$.

Concerning the shares of rational agents, data was collected from *"Table 26: Expected Change in Business Conditions in a Year"* from the *Survey of Consumers by the University of Michigan*: `https://data.sca.isr.umich.edu/subset/subset.php`

The reference qualitative question is: *"The question was: And how about a year from now, do you expect that in the country as a whole, business conditions will be better, or worse than they are at present, or just about the same"*. Possible replies are: *"Better"*, *"Same"*, *"Worse"*, *"Don't know"*. The *Don't know*s were equally distributed across other replies. Answer the *"Same"* was considered to be *näive* and the residual to be rational and `nobs` coincides with the rational group.

C.5 Higher-order Identification Test (Mutschler, 2015)

A DSGE model can be described as a system,

$$\begin{aligned} &E_t\left(\mathbf{f}\left(x_{t+1}, \mathbf{u_{t+1}}, y_{t+1}, x_t, \mathbf{u_t}, y_t|\theta\right)\right) = \mathbf{0} \\ &x_{t+1} = h(x_t, u_{t+1}, \sigma|\theta) \\ &y_{t+1} = g(x_t, u_{t+1}, \sigma|\theta) \end{aligned}$$

where x_t are states, y_t are controls, u_t are stochastic shocks, σ is a perturbation parameter and θ is a m-dimensional vector of deep parameters. It is assumed that all control variables are observables, $E(u_t) = 0$ and that $E(u_t u_t') = \sigma\eta\eta'$ is finite and there is no serial correlation. Moreover, u_t is nth-order white noise with finite higher-order moments with n being the order of approximation.

Under rational expectations the solution to this model is provided by policy functions h and g solving the system of equations f. By applying perturbation methods as in Schmitt-Grohé and Uribe (2004b) the solution around the non-stochastic steady state can be expressed as $x^* = h(x^*, 0, 0|\theta)$, $y^* = g(x^*, 0, 0|\theta)$, $u^* = 0$ and $f^* = h(x^*, y^*, u^*|\theta) = 0$. Then, Taylor expansions of order n can be evaluated in this point in closed form.

However, many applications have shown higher-order approximations are often explosive, even if the linear version of the model is stable. In response to this problem, *pruned* approximations of non-linear Taylor expansions were in introduced by Kim et al. (2008) and further generalised by Andreasen et al. (2018). The idea underpinning the pruning scheme consists in excluding from the policy functions all the elements of order higher than the approximation order.

For example, given the below second-order Taylor expansion,

$$\begin{aligned}\hat{x}_{t+1} = x^* + h_x^\theta \hat{x}_t + h_u^\theta (u_{t+1}) + \\ \frac{1}{2}\left[h_{xx}^\theta (\hat{x}_t \otimes \hat{x}_t) + 2h_{xu}^\theta \hat{x}_t \otimes u_{t+1} + 2h_{uu}^\theta (u_{t+1} \otimes u_{t+1}) + h_{\sigma\sigma}^\theta \sigma^2\right]\end{aligned} \tag{C.86}$$

where the Kronecker products in the second row can deliver elements of order higher than two. Then, the equivalent pruned system can be obtained by decomposing the state-vector into first-order ($\hat{x}_t^f$) and second-order ($\hat{x}_t^s$) effects ($\hat{x} = \hat{x}_t^f + \hat{x}_t^s$) and eliminate all higher-order effects by rewriting the system in the following way:

$$\hat{x}_{t+1}^f = x^* + h_x^\theta \hat{x}_t^f + h_u^\theta (u_{t+1}) \tag{C.87}$$

$$\begin{aligned}\hat{x}_{t+1}^s = h_x^\theta \hat{x}_t^s + \frac{1}{2}H_{xx}^\theta \left(\hat{x}_t^f \otimes \hat{x}_t^f\right) + \frac{1}{2}H_{xu}^\theta \left(\hat{x}_t^f \otimes u_{t+1}\right) \\ + \frac{1}{2}H_{ux}^\theta \left(u_{t+1} \otimes \hat{x}_t^f\right) + \frac{1}{2}H_{uu}^\theta (u_{t+1} \otimes u_{t+1}) + h_{\sigma\sigma}^\theta \sigma^2\end{aligned} \tag{C.88}$$

$$\begin{aligned}\hat{y}_{t+1} = g_x^\theta \left[\hat{x}_t^f + \hat{x}_t^s\right] + g_u^\theta u_{t+1} \frac{1}{2}G_{xx}^\theta \left(\hat{x}_t^f \otimes \hat{x}_t^f\right) + \frac{1}{2}G_{xu}^\theta \left(\hat{x}_t^f \otimes u_{t+1}\right) \\ + \frac{1}{2}G_{ux}^\theta \left(u_{t+1} \otimes \hat{x}_t^f\right) + \frac{1}{2}g_{uu}^\theta (u_{t+1} \otimes u_{t+1}) + g_{\sigma\sigma}^\theta \sigma^2\end{aligned} \tag{C.89}$$

where H_{xx} is an n_x x n_x^2 matrix ruling all second-order terms for the i-th state variable in the i-th row, and G_{xx} is an n_y x n_x^2 matrix ruling all second-order terms for the i-th control variable in the i-th row. H_{xu}, H_{ux}, G_{xu} and G_{ux} rule the relationship between states and shocks, and H_{uu}, G_{uu} provide information on second-order terms for the product of shocks. As a result, all elements of order higher than two (i.e. $\hat{x}_t^f \otimes \hat{x}_t^s$ and $\hat{x}_t^s \otimes \hat{x}_t^s$) are excluded.

Then, one can create an extended state vector $\tilde{z}_t := [(\hat{x}_t^f)', (\hat{x}_t^s)', (\hat{x}_t^f \otimes \hat{x}_t^f)']'$ and one can rewrite the second-order Taylor expansion as pruned state-space:

$$\tilde{z}_{t+1} = c + A\tilde{z}_t + B\Xi_{t+1} \tag{C.90}$$

$$\hat{y}_{t+1} = d + C\tilde{z}_t + B\Xi_{t+1} \tag{C.91}$$

with $A := \begin{bmatrix} h_x & 0 & 0 \\ 0 & h_x & \frac{1}{2}H_{xx} \\ 0 & 0 & h_x \otimes h_x \end{bmatrix}$, $B := \begin{bmatrix} h_u & 0 & 0 & 0 \\ 0 & \frac{1}{2}H_{uu} & \frac{1}{2}H_{ux} & \frac{1}{2}H_{xu} \\ 0 & h_u \otimes h_u & h_u \otimes h_x & h_x \otimes h_u \end{bmatrix}$,

$C := \begin{bmatrix} g_x & g_x & \frac{1}{2}G_{xx} \end{bmatrix}$, $D := \begin{bmatrix} g_u & \frac{1}{2}G_{uu} & \frac{1}{2}G_{ux} & \frac{1}{2}G_{xu} \end{bmatrix}$,

$\Xi_{t+1} := \begin{bmatrix} u_{t+1} \\ u_{t+1} \otimes u_{t+1} - vec(\Sigma) \\ u_{t+1} \otimes x_t^f \\ x_t^f \otimes u_{t+1} \end{bmatrix}$, $c := \begin{bmatrix} 0 \\ \frac{1}{2}H_{\sigma\sigma}\sigma^2 + \frac{1}{2}H_{uu}vec(\Sigma) \\ h_u \otimes h_u vec(\Sigma) \end{bmatrix}$, $d := \begin{bmatrix} \frac{1}{2}g_{\sigma\sigma}\sigma^2 + \frac{1}{2}G_{uu}vec(\Sigma) \end{bmatrix}$

Being linear in $\tilde{z}$, the pruned state-space can benefit of some properties of standard linear models. Andreasen et al. (2018) showed that if the first-order approximation of the model is stable, then also higher-order pruned state-space systems are stable. Moreover, if the first fourth-moment of u_t is finite, it can be shown that the pruned state-space has finite second moments. Mutschler (2015) shows that if u_t has finite eighth moment, the pruned state-space has finite fourth moments. Finally, it is important to notice that the distribution of Ξ_t is non-Gaussian even for Gaussian u_t and for this reason higher-order moments might contain additional information to identify model parameters.

In this context, Mutschler (2015, 2018) exploits restrictions introduced by cumulants (i.e. higher-order statistics based on the coefficients of the Taylor expansion of the log-moment generating function in the time domain). For the k-th order stationary and zero-mean process $\tilde{z}_t$ are provided by the n_z^k vectors $C_{k,z}$:

$$\mathcal{C}_{2,z}(t_1) := E[\tilde{z}_0 \otimes \tilde{z}_{t_1}]$$

$$\mathcal{C}_{3,z}(t_1,t_2) := E[\tilde{z}_0 \otimes \tilde{z}_{t_1} \otimes \tilde{z}_{t_2}]$$
$$\mathcal{C}_{4,z}(t_1,t_2,t_3) := E[\tilde{z}_0 \otimes \tilde{z}_{t_1} \otimes \tilde{z}_{t_2} \otimes \tilde{z}_{t_3}] - \mathcal{C}_{2,z}(t_1) \otimes \mathcal{C}_{2,z}(t_2 - t_3)$$
$$-P'_{n_z}(\mathcal{C}_{2,z}(t_2) \otimes \mathcal{C}_{2,z}(t_2 - t_3)) - P'_{n_z}(\mathcal{C}_{3,z}(t_3) \otimes \mathcal{C}_{2,z}(t_1 - t_2))$$

where $P_{n_z} = I_{n_z} \otimes U_{n_z^2 x n_z}$ and $U_{n_z^2 x n_z}$ is a $(n_z^3 x n_z^3)$ permutation matrix with unity entries in elements $[(i-1)n_z + j, (j-1)n_z^2]$,$i = 1,..,n_z^2$ and $j = 1,..,n_z$, and zero elsewhere. For the purpose of testing identification, cumulants are stacked into vectors and expressed in y terms (Mutschler, 2015):

$$m_2(\theta,T) = (\mathcal{C}_{2,y}(0)', ..., \mathcal{C}_{2,y}(T-1)')',$$
$$m_3(\theta,T) = (\mathcal{C}_{3,y}(0,0)', ..., \mathcal{C}_{3,y}(T-1,T-1)')',$$
$$m_4(\theta,T) = (\mathcal{C}_{4,y}(0,0,0)', ..., \mathcal{C}_{4,y}(T-1,T-1,T-1)')'$$

Iskrev (2010)'s moment-based criteria are extended to higher-order models. First, Mutschler (2015) defines the rank criteria to identify θ from the structure of the model.

In particular, $\theta_0 \in \Theta$ and $\theta_1 \in \Theta$ are considered observationally equivalent given a vector of observables $\{y_t\}$ if they generate the same four moments. Then, $\theta_0 \in \Theta$ is defined as locally identifiable from the first four moments of y_t, if there is an open neighborhood of θ_0 in which $\mu_y(\theta_0) = \mu_y(\theta_1)$, $m_2(\theta_0) = m_2(\theta_1)$, $m_3(\theta_0) = m_3(\theta_1)$, $m_4(\theta_0) = m_4(\theta_1)$ imply $\theta_0 = \theta_1$ for any $\theta_1 \in \Theta$.

Let $q \leqslant T$ and assume that $\bar{m}(\theta,q) := (\mu_y, m_2(\theta,q)', m_3(\theta,q)', m_2(\theta,q)')'$ is a continuously differentiable function of $\theta \in \Theta$. Let $\theta_0 \in \Theta$ be a regular point, $theta$ is then locally identifiable at a point θ_0 from the first four cumulants of y_t, if and only if $\bar{M}(\theta,q) := \frac{\partial \bar{m}(\theta_0,q)}{\partial(\theta')}$ has a full column rank equal to the number of parameters for $q \leqslant T$

C.6 Second Order Extended Kalman Filter (Gustafsson and Hendeby, 2012)

The Extended Kalman filter is based on the approximation of the non-linear transition equation with a Taylor series expansion along under the assumption that the filtering density is Gaussian - $p(\mathbf{s_t}|\mathbf{z_{1:t}}) \simeq N\left(s_t|\mathbf{m_t},\mathbf{Q_t}\right)$ [2].

The version exposed here is based on the second-order extended Kalman filter with additive errors in the measurement equation (Gustafsson and Hendeby, 2012; Holden, 2018).[3] For this paper, the Dynare implementation proposed in Holden (2018) is used as it allows to apply this filtering technique on a pruned system so to guarantee system stability.

The main advantage of the second-order Extended Kalman filter is the possibility of computing an exact closed form representation of mean and variance in a fashion similar to the linear Kalman filter. This should help both in the accuracy and speed of the algorithm and allows for a more stable computation of distributions moments. Given the generalized non-linear state-space representation with additive noise,

$$s_t = f\left(s_{t-1};\theta\right) + \varepsilon_t \qquad \varepsilon_t \sim N(0,\Sigma_\varepsilon) \tag{C.92}$$

$$z_t = g\left(s_t;\theta\right) + v_t \qquad v_t \sim N(0,\Sigma_v) \tag{C.93}$$

one can derive the moments characterising the prediction and updating steps.

The mean and the covariance matrix of the prediction step are:

$$\mathbf{m_{\bar{t}}} = \mathbf{f}(\mathbf{m_{t-1}}) + \frac{\mathbf{1}}{\mathbf{2}}\sum_{\mathbf{i}} \mathbf{e_i}\mathbf{tr}\left(\mathbf{F_{SS}^{(i)}}(\mathbf{m_{t-1}})\mathbf{Q_{t-1}}\right) \tag{C.94}$$

$$\begin{aligned}\mathbf{Q_{\bar{t}}} = {} & \mathbf{F_S}(\mathbf{m_{t-1}})\mathbf{Q_{t-1}}\mathbf{F_S^T}(\mathbf{m_{t-1}}) + \\ & + \frac{\mathbf{1}}{\mathbf{2}}\sum_{\mathbf{i,i'}} \mathbf{e_i}\mathbf{e_{i'}^T}\mathbf{tr}\left(\mathbf{F_{SS}^{(i)}}(\mathbf{m_{t-1}})\mathbf{Q_{t-1}}\mathbf{F_{SS}^{(i')}}(\mathbf{m_{t-1}})\mathbf{Q_{t-1}}\right) + \Sigma_{\epsilon,t-1}\end{aligned} \tag{C.95}$$

These can be used to build all the elements needed to recover the filtering distribution in the updating step:

[2] Alternatively, the non-linear dynamic can be approximated by means of statistical linearization (Stengel, 1994). This technique has the advantage of providing a more global approximation of the distribution but it often encounters issues due to very complex expectations to be computed in the prediction step of the filter - see Särkkä (2013) book for further details.

[3] Särkkä (2013) actually generalizes this algorithm to the case of non-additive noise.

$$\mathbf{h_t} = \mathbf{z_t} - \mathbf{g}(\mathbf{m_{\bar{t}}}) - \frac{\mathbf{1}}{\mathbf{2}} \sum_{\mathbf{i}} \mathbf{e_i} \mathbf{tr} \left(\mathbf{G_{SS}^{(i)}}(\mathbf{m_{\bar{t}}}) \mathbf{Q_{\bar{t}}} \right) \tag{C.96}$$

$$\begin{aligned} \mathbf{X_t} = {} & \mathbf{G_S}(\mathbf{m_{\bar{t}}}) \mathbf{Q_{\bar{t}}} \mathbf{G_S^T}(\mathbf{m_{\bar{t}}}) + \\ & + \frac{\mathbf{1}}{\mathbf{2}} \sum_{\mathbf{i},\mathbf{i'}} \mathbf{e_i} \mathbf{e_{i'}^T} \mathbf{tr} \left(\mathbf{G_{SS}^{(i)}}(\mathbf{m_{\bar{t}}}) \mathbf{Q_{\bar{t}}} \mathbf{G_{SS}^{(i')}}(\mathbf{m_{\bar{t}}}) \mathbf{Q_{\bar{t}}} \right) + \Sigma_{v,t} \end{aligned} \tag{C.97}$$

$$\mathbf{K_t} = Q_{\bar{t}} G_S^T(m_{\bar{t}}) X_t^{-1} \tag{C.98}$$

$$\mathbf{m_t} = m_{\bar{t}} + K_t h_t \tag{C.99}$$

$$\mathbf{Q_t} = Q_{\bar{t}} - K_t X_t K_t^T \tag{C.100}$$

with:

$$\mathbf{F_S}(\mathbf{m}) = \left. \frac{\partial \mathbf{f_j}(\mathbf{x}, \varepsilon)}{\partial \mathbf{s_j}} \right|_{[\mathbf{s}=\mathbf{m}, \varepsilon=0]} \tag{C.101}$$

$$\mathbf{G_S}(\mathbf{m}) = \left. \frac{\partial \mathbf{g_j}(\mathbf{s}, \mathbf{v})}{\partial \mathbf{s_j}} \right|_{[\mathbf{s}=\mathbf{m}, \mathbf{v}=\mathbf{0}]} \tag{C.102}$$

$$\mathbf{F_{SS}}(\mathbf{m}) = \left. \frac{\partial^{\mathbf{2}} \mathbf{f_i}(\mathbf{s})}{\partial \mathbf{s_j} \partial \mathbf{s_{j'}}} \right|_{[\mathbf{s}=\mathbf{m}]} \tag{C.103}$$

$$\mathbf{G_{SS}}(\mathbf{m}) = \left. \frac{\partial^{\mathbf{2}} \mathbf{g_i}(\mathbf{s})}{\partial \mathbf{s_j} \partial \mathbf{s_{j'}}} \right|_{[\mathbf{s}=\mathbf{m}]} \tag{C.104}$$

C.7 Michigan Survey Data - Alternative Shares Definitions

This section proposes alternative measures for approximating the proportion of rational and bounded rational agents by continuing the discussion exposed in section 3.4.3.

In case one would like to model the evolution of firms and households expectations separately, it is possible to exploit the income or education breakdowns (only starting in 1978).

For instance, one might approximate the share of *näive* firms by using number of *"Unchanged"* replies to the question on business expectations in the highest income or education quartile. By contrast, the share of *näive* households would result from the average share of the lowest three income quartiles. Then, the average value of the proxy for the share of rational households based on income quartiles is 4% and that of rational firms about 20%.

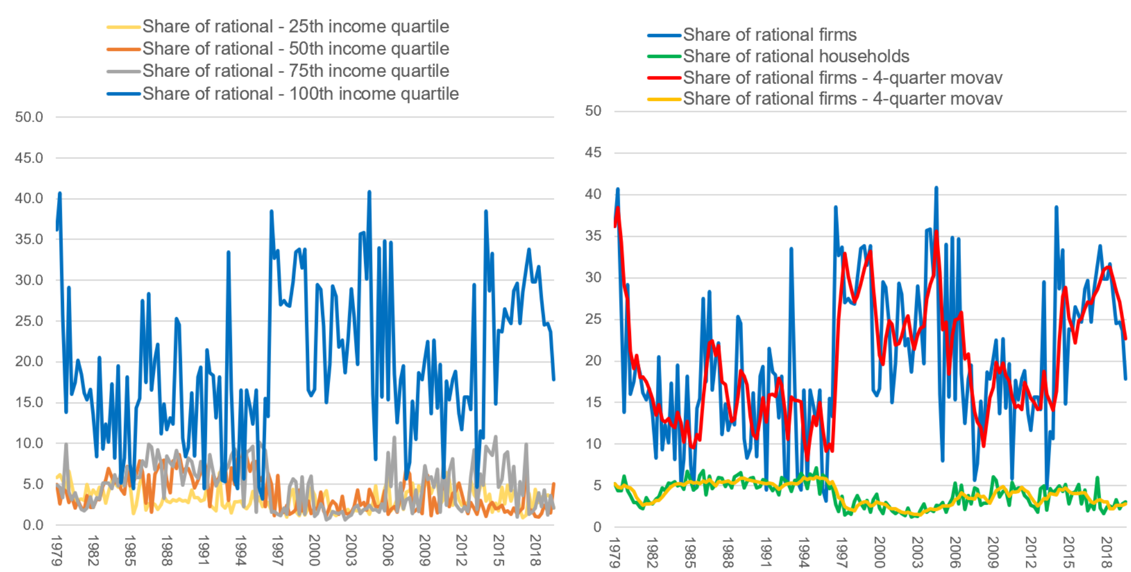

FIGURE C.1: Proxy for the share of rational agents based on business conditions by income

Alternatively, one might want to choose an indicator that is representative of the macroeconomic variables forecasted by model agents, namely inflation.

In building a proxy for the share of rational agents, I follow the findings of Pfajfar and Santoro (2010) who study how households form expectations across the different percentiles of the *quantitative* question on inflation. Specifically, they find agents adopt a rational-expectation rule in bins between the 55th and 63rd before 1988 and in bins between the 47th and the 50th. Moreover, results show households tend to be *näives* in lower percentiles and more *adaptive* in the highest ones.

Against this background, the share of rational agents might be approximated by the share of households reporting a qualitative answer in an interval corresponding to current value of median expectations. As shown in Figure C.2, the resulting series is a combination of the various qualitative time-series. To understand this with some examples, the value of median expectations was 10.2 percent in 1980-Q1, so the red line reports the share of households replying prices would grow "between 10 and 14 percent". Similarly, median inflation expectations were about 1.1 percent in 2001-Q4 so the red line reports the share of households replying between 1 and 2 percent.

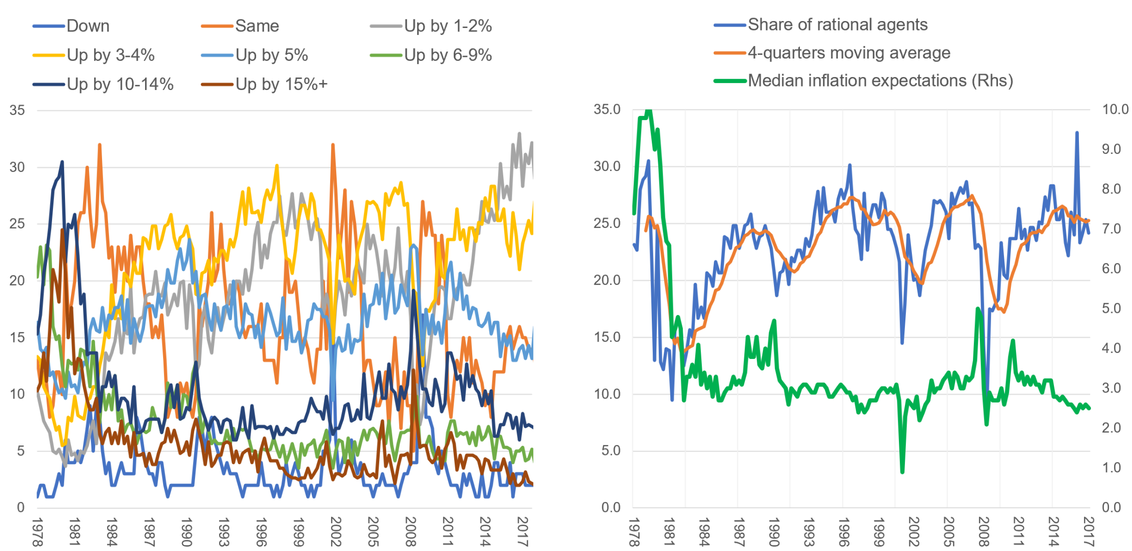

FIGURE C.2: Proxy for the share of rational agents based on qualitative inflation

As the model estimated in this paper assumes households and firms can choose different forecasting rules, I have applied the methodology presented above on a breakdown of replies by income. As shown in Figure C.1, the share of replies around the median is larger for households in the highest quartile whereas other quartiles present lower and similar values. Assuming the results of Pfajfar and Santoro (2010) can be extended to subgroups of the population, one can interpret the latter result in favour of a higher share of "more rational" households withing the highest income group.

Bibliography

Adam, K. and Marcet, A. (2011). Internal rationality, imperfect market knowledge and asset prices. *Journal of Economic Theory*, 146(3):1224–1252.

Adjemian, S. and Karame, F. (2016). Gaussian Particle Filtering with Dynare. 2017 meeting papers, MACFINROBODS.

Agliari, A., Massaro, D., Pecora, N., and Spelta, A. (2017). Inflation Targeting, Recursive Inattentiveness, and Heterogeneous Beliefs. *Journal of Money, Credit and Banking*, 49(7):1587–1619.

Aguiar, M. (2011). Comment on "On Graduation from Default, Inflation and Banking Crises: Elusive or Illusion?". In *NBER Macroeconomics Annual 2010, Volume 25*, pages 37–46. University of Chicago Press.

Alpanda, S. and Kabaca, S. (2020). International Spillovers of Large-Scale Asset Purchases. *Journal of the European Economic Association*, 18(1):342–391.

Altavilla, C. and Giannone, D. (2017). The effectiveness of non-standard monetary policy measures: Evidence from survey data. *Journal of Applied Econometrics*, 32:952–964.

Altavilla, C., Giannone, D., and Lenza, M. (2016). The Financial and Macroeconomic Effects of the OMT Announcements. *International Journal of Central Banking*, 12(3):29–57.

Altavilla, C., Lemke, W., Linzert, T., Tapking, J., and von Landesberger, J. (2021). Assessing the efficacy, efficiency and potential side effects of the ECB's monetary policy instruments since 2014. Occasional Paper Series 278, European Central Bank.

Amisano, G. and Tristani, O. (2010). Euro area inflation persistence in an estimated nonlinear DSGE model. *Journal of Economic Dynamics and Control*, 34(10):1837–1858.

Andreasen, M. (2010). How to Maximize the Likelihood Function for a DSGE Model. *Computational Economics*, 35(2):127–154.

Andreasen, M. M. (2013). Non-Linear DSGE Models And The Central Difference Kalman Filter. *Journal of Applied Econometrics*, 28(6):929–955.

Andreasen, M. M., Fernández-Villaverde, J., and Rubio-Ramírez, J. F. (2018). The Pruned State-Space System for Non-Linear DSGE Models: Theory and Empirical Applications. *Review of Economic Studies*, 85(1):1–49.

Andrieu, C., Doucet, A., and Punskaya, E. (2001). *Sequential Monte Carlo Methods for Optimal Filtering*, pages 79–95. Springer New York, New York, NY.

Andrés, J., López-Salido, J. D., and Nelson, E. (2004). Tobin's Imperfect Asset Substitution in Optimizing General Equilibrium. CEPR Discussion Papers 4336, C.E.P.R. Discussion Papers.

Angelini, P., Neri, S., and Panetta, F. (2011). Monetary and macroprudential policies. temi di discussione (economic working papers) 801, bank of italy. *Economic Research and International Relations Area.*

Arasaratnam, H. and Haykin, S. (2009). Cubature Kalman Filters. *Automatic Control, IEEE Transactions on*, 54:1254 – 1269.

Aruoba, S. B., Cuba-Borda, P., Higa-Flores, K., Schorfheide, F., and Villalvazo, S. (2021). Piecewise-Linear Approximations and Filtering for DSGE Models with Occasionally Binding Constraints. *Review of Economic Dynamics*, 41:96–120.

Ascari, G. (2004). Staggered prices and trend inflation: some nuisances. *Review of Economic dynamics*, 7(3):642–667.

Ascari, G., Bonomolo, P., and Lopes, H. F. (2019). Walk on the wild side: Temporarily unstable paths and multiplicative sunspots. *American Economic Review*, 109(5):1805–42.

Ascari, G., Castelnuovo, E., and Rossi, L. (2011). Calvo vs. Rotemberg in a trend inflation world: An empirical investigation. *Journal of Economic Dynamics and Control*, 35(11):1852–1867.

Ascari, G., Fagiolo, G., and Roventini, A. (2015). Fat-tail distributions and business-cycle models. *Macroeconomic Dynamics*, 19(2):465–476.

Ascari, G. and Ropele, T. (2009). Trend inflation, Taylor principle and indeterminacy. Temi di discussione (Economic working papers) 708, Bank of Italy, Economic Research and International Relations Area.

Ascari, G. and Sbordone, A. M. (2014). The macroeconomics of trend inflation. *Journal of Economic Literature*, 52(3):679–739.

Assenza, T., Heemeijer, P., Hommes, C., and Massaro, D. (2013). Individual Expectations and Aggregate Macro Behavior. Tinbergen Institute Discussion Papers 13-016/II, Tinbergen Institute.

Assenza, T., Heemeijer, P., Hommes, C., and Massaro, D. (2021). Managing self-organization of expectations through monetary policy: A macro experiment. *Journal of Monetary Economics*, 117:170–186.

Beck, R., Duca, I. A., and Stracca, L. (2019). Medium term treatment and side effects of quantitative easing: international evidence. Working Paper Series 2229, European Central Bank.

Beqiraj, E., Bartolomeo, G. D., Pietro, M. D., and Serpieri, C. (2018). Bounded-rationality and heterogeneous agents: Long or short forecasters? JRC Working Papers JRC111392, Joint Research Centre (Seville site).

Bernanke, B. S. (2020). The new tools of monetary policy. *American Economic Review*, 110(4):943–83.

Bianchi, F. and Nicolò, G. (2021). A generalized approach to indeterminacy in linear rational expectations models. *Quantitative Economics*, 12(3):843–868.

Binning, A. and Maih, J. (2015). Sigma point filters for dynamic nonlinear regime switching models. Working Papers No 4/2015, Centre for Applied Macro- and Petroleum economics (CAMP), BI Norwegian Business School.

Boehl, G., Goy, G., and Strobel, F. (2020). A structural investigation of quantitative easing. Working paper.

Boneva, L. M., Braun, R. A., and Waki, Y. (2016). Some unpleasant properties of loglinearized solutions when the nominal rate is zero. *Journal of Monetary Economics*, 84:216–232.

Bordalo, P., Gennaioli, N., Ma, Y., and Shleifer, A. (2020). Overreaction in Macroeconomic Expectations. *American Economic Review*, 110(9):2748–2782.

Born, B. and Pfeifer, J. (2014). Policy risk and the business cycle. *Journal of Monetary Economics*, 68(C):68–85.

Boswijk, H. P., Hommes, C. H., and Manzan, S. (2007). Behavioral heterogeneity in stock prices. *Journal of Economic Dynamics and Control*, 31(6):1938–1970. Tenth Workshop on Economic Heterogeneous Interacting Agents.

Branch, W., Carlson, J., Evans, G., and McGough, B. (2009). Monetary Policy, Endogenous Inattention and the Volatility Trade-off. *Economic Journal*, 119(534):123–157.

Branch, W. A. (2004). The Theory of Rationally Heterogeneous Expectations: Evidence from Survey Data on Inflation Expectations. *Economic Journal*, 114(497):592–621.

Branch, W. A. and McGough, B. (2009). A New Keynesian model with heterogeneous expectations. *Journal of Economic Dynamics and Control*, 33(5):1036–1051. Complexity in Economics and Finance.

Branch, W. A. and McGough, B. (2010). Dynamic predictor selection in a new Keynesian model with heterogeneous expectations. *Journal of Economic Dynamics and Control*, 34(8):1492–1508.

Breckenfelder, J., De Fiore, F., Andrade, P., Karadi, P., and Tristani, O. (2016). The ECB's asset purchase programme: an early assessment. Working Paper Series 1956, European Central Bank.

Brock, W. A. and Hommes, C. H. (1997). A rational route to randomness. *Econometrica*, 65(5):1059–1095.

Brock, W. A. and Mirman, L. J. (1972). Optimal economic growth and uncertainty: The discounted case. *Journal of Economic Theory*, 4(3):479–513.

Busetti, F., Delle Monache, D., Gerali, A., and Locarno, A. (2017). Trust, but verify. De-anchoring of inflation expectations under learning and heterogeneity. Working Paper Series 1994, European Central Bank.

Calvert Jump, R., Hommes, C., and Levine, P. (2019). Learning, heterogeneity, and complexity in the New Keynesian model. *Journal of Economic Behavior and Organization*, 166(C):446–470.

Calvo, G. A. (1983). Staggered prices in a utility-maximizing framework. *Journal of Monetary Economics*, 12(3):383–398.

Carlstrom, C. T., Fuerst, T. S., and Paustian, M. (2017). Targeting long rates in a model with segmented markets. *American Economic Journal: Macroeconomics*, 9(1):205–242.

Castelnuovo, E. and Pellegrino, G. (2018). Uncertainty-dependent effects of monetary policy shocks: A New-Keynesian interpretation. *Journal of Economic Dynamics and Control*, 93:277–296. Monetary and Fiscal Policy Stabilization amid a Debt Crisis.

Chen, H., Cúrdia, V., and Ferrero, A. (2012). The Macroeconomic Effects of Large-scale Asset Purchase Programmes. *Economic Journal*, 122(564):289–315.

Chopin, N., Jacob, P. E., and Papaspiliopoulos, O. (2013). SMC2: an efficient algorithm for sequential analysis of state space models. *Journal of the Royal Statistical Society: Series B (Statistical Methodology)*, 75(3):397–426.

Christiano, L. J. and Eichenbaum, M. (2012). Notes on linear approximations, equilibrium multiplicity and e-learnability in the analysis of the zero lower bound. *Manuscript, Northwestern University.*

Christiano, L. J., Eichenbaum, M., and Evans, C. L. (2005). Nominal rigidities and the dynamic effects of a shock to monetary policy. *Journal of political Economy*, 113(1):1–45.

Coeré, Benoit (2018). The persistence and signalling power of central bank asset purchase programmes. URL: `https://www.ecb.europa.eu/press/key/date/2018/html/ecb.sp180223.en.html`.

Coibion, O. and Gorodnichenko, Y. (2015). Information rigidity and the expectations formation process: A simple framework and new facts. *American Economic Review*, 105(8):2644–78.

Cornea-Madeira, A., Hommes, C., and Massaro, D. (2019). Behavioral Heterogeneity in U.S. Inflation Dynamics. *Journal of Business & Economic Statistics*, 37(2):288–300.

Cova, P. and Ferrero, G. (2015). The Eurosystem asset purchase programmes for monetary policy purposes. Questioni di Economia e Finanza (Occasional Papers) 270, Bank of Italy, Economic Research and International Relations Area.

Creel, M. and Kristensen, D. (2011). Indirect Likelihood Inference. Dynare Working Papers 8, CEPREMAP.

De Grauwe, P. (2011). Animal spirits and monetary policy. *Economic Theory*, 47(2/3):423–457.

De Grauwe, P. (2012a). Booms and busts in economic activity: A behavioral explanation. *Journal of Economic Behavior and Organization*, 83(3):484–501.

De Grauwe, P. (2012b). Lectures on behavioral macroeconomics. *Lectures on Behavioral Macroeconomics*, pages 1–136.

De Grauwe, P., Foresti, P., and Ji, Y. (2020). Animal Spirits and Fiscal Policy. *Journal of Economic Behavior and Organization*, 171:247–263.

De Grauwe, P. and Ji, Y. (2017). The International Synchronisation of Business Cycles: the Role of Animal Spirits. *Open Economies Review*, 28(3):383–412.

De Grauwe, P. and Ji, Y. (2019). Inflation targets and the zero lower bound in a behavioural macroeconomic model. *Economica*, 86(342):262–299.

De Grauwe, P. and Ji, Y., editors (2020a). *Behavioural Macroeconomics: Theory and Policy*. Oxford University Press.

De Grauwe, P. and Ji, Y. (2020b). Should central banks be forward-looking? CEPR Discussion Papers 14540, C.E.P.R. Discussion Papers.

De Grauwe, P. and Ji, Y. (2021). On the Use of Current or Forward-Looking Data in Monetary Policy: A Behavioural Macroeconomic Approach. CESifo Working Paper Series 8853, CESifo.

De Grauwe, P. and Macchiarelli, C. (2015). Animal spirits and credit cycles. *Journal of Economic Dynamics and Control*, 59(C):95–117.

Deák, S., Holden, T., and Mele, A. (2018). An advanced course on the science and art of DSGE Modelling. Technical report, University of Surrey – Summer School.

Del Negro, M. and Schorfheide, F. (2008). Forming priors for DSGE models (and how it affects the assessment of nominal rigidities). *Journal of Monetary Economics*, 55(7):1191–1208.

Dell'Ariccia, G., Rabanal, P., and Sandri, D. (2018). Unconventional Monetary Policies in the Euro Area, Japan, and the United Kingdom. *Journal of Economic Perspectives*, 32(4):147–72.

Demary, M. (2017). Yield curve responses to market sentiments and monetary policy. *Journal of Economic Interaction and Coordination*, 12(2):309–344.

Deák, S., Levine, P., Pearlman, J., and Yang, B. (2017a). Internal Rationality, Learning and Imperfect Information. School of Economics Discussion Papers 0817, School of Economics, University of Surrey.

Deák, S., Levine, P., Pearlman, J., and Yang, B. (2017b). Internal Rationality, Learning and Imperfect Information. School of Economics Discussion Papers 0817, School of Economics, University of Surrey.

Dixit, A. K. and Stiglitz, J. E. (1977). Monopolistic competition and optimum product diversity. *The American Economic Review*, 67(3):297–308.

D'Amico, S. and King, T. B. (2013). Flow and stock effects of large-scale treasury purchases: Evidence on the importance of local supply. *Journal of Financial Economics*, 108(2):425–448.

Eser, F. and Schwaab, B. (2016). Evaluating the impact of unconventional monetary policy measures: Empirical evidence from the ECB's Securities Markets Programme. *Journal of Financial Economics*, 119(1):147 – 167.

Eusepi, S. and Preston, B. (2011). Expectations, Learning, and Business Cycle Fluctuations. *American Economic Review*, 101(6):2844–2872.

Evans, G. and Honkapohja (2001). *Learning and Expectations in Macroeconomics.* Princeton University Press.

Falagiarda, M. (2013). Evaluating Quantitative Easing: A DSGE Approach. MPRA Paper 49457, University Library of Munich, Germany.

Falagiarda, M. and Reitz, S. (2015). Announcements of ECB unconventional programs: Implications for the sovereign spreads of stressed Euro area countries. *Journal of International Money and Finance*, 53(C):276–295.

Fernández-Villaverde, J., Gordon, G., Guerrón-Quintana, P., and Rubio-Ramirez, J. F. (2015). Nonlinear adventures at the zero lower bound. *Journal of Economic Dynamics and Control*, 57:182–204.

Fernández-Villaverde, J. and Rubio-Ramírez, J. F. (2007). Estimating macroeconomic models: A likelihood approach. *The Review of Economic Studies*, 74(4):1059–1087.

FernÃ¡ndez-Villaverde, J., Rubio-RamÃrez, J., and Schorfheide, F. (2016). Solution and Estimation Methods for DSGE Models. In Taylor, J. B. and Uhlig, H., editors, *Handbook of Macroeconomics*, volume 2 of *Handbook of Macroeconomics*, chapter 0, pages 527–724. Elsevier.

Fernández-Villaverde, J., Guerrón-Quintana, P., Rubio-Ramírez, J. F., and Uribe, M. (2011). Risk matters: The real effects of volatility shocks. *American Economic Review*, 101(6):2530–61.

Fernández-Villaverde, J. and Guerrón-Quintana, P. A. (2021). Estimating DSGE Models: Recent Advances and Future Challenges. *Annual Review of Economics*, 13(1):229–252.

Fernández-Villaverde, J. and Rubio-Ramírez, J. F. (2005). Estimating dynamic equilibrium economies: Linear versus nonlinear likelihood. *Journal of Applied Econometrics*, 20(7):891–910.

Friedman, B. M. and Woodford, M., editors (2010). *"DSGE Models for Monetary Policy Analysis", Handbook of Monetary Economics, Chapter 7, pages 285-367*, volume 3 of *Handbook of Monetary Economics*. Elsevier, 1 edition.

Gabaix, X. (2020). A Behavioral New Keynesian Model. *American Economic Review*, 110(8):2271–2327.

Gagnon, J., Raskin, M., Remache, J., and Sack, B. (2011a). The Financial Market Effects of the Federal Reserve's Large-Scale Asset Purchases. *International Journal of Central Banking*, 7(1):3–43.

Gagnon, J. E. (2016). Quantitative Easing: An Underappreciated Success. Policy Briefs PB16-4, Peterson Institute for International Economics.

Gagnon, J. E., Raskin, M., Remache, J., and Sack, B. P. (2011b). Large-scale asset purchases by the Federal Reserve: did they work? *Economic Policy Review*, 17(May):41–59.

Galì, J. (2008). Introduction to Monetary Policy, Inflation, and the Business Cycle: An Introduction to the New Keynesian Framework. In *Monetary Policy, Inflation, and the Business Cycle: An Introduction to the New Keynesian Framework*, Introductory Chapters. Princeton University Press.

Galì, J. (2015). *Monetary Policy, Inflation, and the Business Cycle: An Introduction to the New Keynesian Framework and Its Applications Second edition.* Number 10495 in Economics Books. Princeton University Press.

Gelain, P., Iskrev, N., J. Lansing, K., and Mendicino, C. (2019). Inflation dynamics and adaptive expectations in an estimated DSGE model. *Journal of Macroeconomics*, 59(C):258–277.

Gertler, M. and Karadi, P. (2011). A model of unconventional monetary policy. *Journal of Monetary Economics*, 58:17–34.

Gertler, M. and Karadi, P. (2013). QE 1 vs. 2 vs. 3. . . : A Framework for Analyzing Large-Scale Asset Purchases as a Monetary Policy Tool. *International Journal of Central Banking*, 9(1):5–53.

Geweke, J. (1999). Using simulation methods for Bayesian econometric models: inference, development, and communication. *Econometric Reviews*, 18(1):1–73.

Giovannini, M., Ratto, M., and Pfeifer, J. (2021). Efficient and robust inference of models with occasionally binding constraints. JRC Working Papers in Economics and Finance JRC124394, JRC.

Goy, G., Hommes, C., and Mavromatis, K. (2020). Forward Guidance and the Role of Central Bank Credibility under Heterogeneous Beliefs. *Journal of Economic Behavior and Organization.*

Grazzini, J., Richiardi, M. G., and Tsionas, M. (2017). Bayesian estimation of agent-based models. *Journal of Economic Dynamics and Control*, 77(C):26–47.

Gustafsson, F. and Hendeby, G. (2012). Some Relations Between Extended and Unscented Kalman Filters. *Signal Processing, IEEE Transactions on*, 60:545 – 555.

Hansen, N. and Kern, S. (2004). Evaluating the CMA Evolution Strategy on Multimodal Test Functions. In Yao, X., Burke, E. K., Lozano, J. A., Smith, J., Merelo-Guervós, J. J., Bullinaria, J. A., Rowe, J. E., Tiňo, P., Kabán, A., and Schwefel, H.-P., editors, *Parallel Problem Solving from Nature - PPSN VIII*, pages 282–291, Berlin, Heidelberg. Springer Berlin Heidelberg.

Harrison, R. (2011). Asset purchase policies and portfolio balance effects: A DSGE analysis. *Interest Rates, Prices and Liquidity: Lessons from the Financial Crisis*, pages 117–143.

Harrison, R. (2012). Asset purchase policy at the effective lower bound for interest rates. Bank of England working papers 444, Bank of England.

Harrison, R. (2017). Optimal quantitative easing. Bank of England working papers 678, Bank of England.

Herbst, E. and Schorfheide, F. (2015). *Bayesian estimation of DSGE models*. Princeton University Press.

Herbst, E. and Schorfheide, F. (2019). Tempered particle filtering. *Journal of Econometrics*, 210(1):26–44.

Hesse, H., Hofmann, B., and Weber, J. M. (2018). The macroeconomic effects of asset purchases revisited. *Journal of Macroeconomics*, 58(C):115–138.

Holden, T. (2017). Tractable estimation and smoothing of highly non-linear dynamic state-space models. `https://github.com/tholden/EST-NLSS/raw/master/EstimationPaper.pdf`.

Holden, T. (2018). Trends and cycles without balanced growth. `https://ec.europa.eu/research/participants/documents/downloadPublic?documentIds=080166e5bfb8cbbf&appId=PPGMS`.

Hommes, C. (2015). *Behavioral Rationality and Heterogeneous Expectations in Complex Economic Systems*. Number 9781107564978 in Cambridge Books. Cambridge University Press.

Hommes, C. and in 't Veld, D. (2017). Booms, busts and behavioural heterogeneity in stock prices. *Journal of Economic Dynamics and Control*, 80:101–124.

Hommes, C. and Lustenhouwer, J. (2019). Inflation targeting and liquidity traps under endogenous credibility. *Journal of Monetary Economics*, 107(C):48–62.

Hommes, C., Lustenhouwer, J., and Mavromatis, K. (2018). Fiscal consolidations and heterogeneous expectations. *Journal of Economic Dynamics and Control*, 87(C):173–205.

Hommes, C., Mavromatis, K., Ozden, T., and Zhu, M. (2019). Behavioral learning equilibria in the New Keynesian model. DNB Working Papers 654, Netherlands Central Bank, Research Department.

Honkapohja, S., Mitra, K., and Evans, G. W. (2011). Notes on Agents Behavioral Rules Under Adaptive Learning and Studies of Monetary Policy. CDMA Working Paper Series 201102, Centre for Dynamic Macroeconomic Analysis.

Iiboshi, H., Shintani, M., and Ueda, K. (2020). Estimating a Nonlinear New Keynesian Model with the Zero Lower Bound for Japan. Working Papers e154, Tokyo Center for Economic Research.

Iiboshi, H., Shintani, M., and Ueda, K. (2022). Estimating a Behavioral New Keynesian Model with the Zero Lower Bound. Carf working papers, Tokyo Center for Economic Research.

Iskrev, N. (2008). Evaluating the information matrix in linearized DSGE models. *Economics Letters*, 99(3):607–610.

Iskrev, N. (2010). Local identification in DSGE models. *Journal of Monetary Economics*, 57(2):189–202.

Iskrev, N. and Ratto, M. (2011). Identification analysis of DSGE models with DYNARE. JRC Working Papers 225149, MONFISPOL.

Ivashchenko, S. (2014). DSGE Model Estimation on the Basis of Second-Order Approximation. *Computational Economics*, 43(1):71–82.

Ivashchenko, S. (2016). Estimation and filtering of nonlinear MS-DSGE models. HSE Working papers WP BRP 136/EC/2016, National Research University Higher School of Economics.

Jang, T.-S. and Sacht, S. (2016). Animal Spirits and the Business Cycle: Empirical Evidence from Moment Matching. *Metroeconomica*, 67(1):76–113.

Jang, T.-S. and Sacht, S. (2020). Forecast heuristics, consumer expectations, and New-Keynesian macroeconomics: A Horse race. *Journal of Economic Behavior and Organization*.

Jess, B. and A., F. R. E. (1994). Indeterminacy and Increasing Returns. *Journal of Economic Theory*, 63(1):19–41.

Joyce, M., Tong, M., and Woods, R. (2011). The United Kingdom's quantitative easing policy: design, operation and impact. *Bank of England Quarterly Bulletin*, 51(3):200–212.

Julier, S. and Uhlmann, J. (2004). Unscented filtering and nonlinear estimation. *Proceedings of the IEEE*, 92:401 – 422.

Julier, S., Uhlmann, J., and Durrant-Whyte, H. (1995). A new approach for filtering nonlinear systems. In *Proceedings of 1995 American Control Conference - ACC'95*, volume 3, pages 1628–1632 vol.3.

Jump, R. C. and Levine, P. (2019). Behavioural New Keynesian models. *Journal of Macroeconomics*, 59(C):59–77.

Kabaca, S., Maas, R., Mavromatis, K., and Priftis, R. (2020). Optimal Quantitative Easing in a Monetary Union. Staff Working Papers 20-49, Bank of Canada.

Kapetanios, G., Mumtaz, H., Stevens, I., and Theodoridis, K. (2012). Assessing the economy-wide effects of quantitative easing. Bank of England working papers 443, Bank of England.

Kim, J., Kim, S., Schaumburg, E., and Sims, C. A. (2008). Calculating and using second-order accurate solutions of discrete time dynamic equilibrium models. *Journal of Economic Dynamics and Control*, 32(11):3397–3414.

Kim, J. and Ruge-Murcia, F. (2009). How much inflation is necessary to grease the wheels? *Journal of Monetary Economics*, 56(3):365–377.

Kim, J. and Ruge-Murcia, F. (2019). Extreme Events and Optimal Monetary Policy. *International Economic Review*, 60(2):939–963.

Kim, J.-Y. (2002). Limited information likelihood and Bayesian Analysis. *Journal of Econometrics*, 107:175–193.

Kliem, M. and Meyer-Gohde, A. (2022). (Un)expected monetary policy shocks and term premia. *Journal of Applied Econometrics*, 37(3):477–499.

Kollmann, R. (2015). Tractable Latent State Filtering for Non-Linear DSGE Models Using a Second-Order Approximation and Pruning. *Computational Economics*, 45(2):239–260.

Kollmann, R. (2017). Tractable likelihood-based estimation of non-linear DSGE models. *Economics Letters*, 161(C):90–92.

Kotecha, J. and Djuric, P. (2003). Gaussian sum particle filtering. *IEEE Transactions on Signal Processing*, 51(10):2602–2612.

Krishnamurthy, A. and Vissing-Jorgensen, A. (2011). The Effects of Quantitative Easing on Interest Rates: Channels and Implications for Policy. NBER Working Papers 17555, National Bureau of Economic Research, Inc.

Kukacka, J., Jang, T.-S., and Sacht, S. (2018). On the estimation of behavioral macroeconomic models via simulated maximum likelihood. Economics Working Papers 100372, Christian-Albrechts-University of Kiel, Department of Economics.

Kukacka, J. and Sacht, S. (2021). Estimation of Heuristic Switching in Behavioral Macroeconomic Models. Economics Working Papers 2021-01, Christian-Albrechts-University of Kiel, Department of Economics.

Kuttner, K. N. (2018). Outside the box: Unconventional monetary policy in the great recession and beyond. *Journal of Economic Perspectives*, 32(4):121–46.

Lan, H. and Meyer-Gohde, A. (2013a). Dynare add-on for Pruning in Perturbation DSGE Models. QM&RBC Codes, Quantitative Macroeconomics & Real Business Cycles.

Lan, H. and Meyer-Gohde, A. (2013b). Pruning in perturbation DSGE models: Guidance from nonlinear moving average approximations. Technical report, SFB 649 Discussion Paper.

Levine, P., Pearlman, J., Perendia, G., and Yang, B. (2012). Endogenous Persistence in an estimated DSGE Model Under Imperfect Information. *Economic Journal*, 122(565):1287–1312.

Levine, P. and Yang, B. (2015). A New Keynesian Behavioural Model with Individual Rationality and Heterogeneous Agents. School of economics discussion papers, CEF.

Lindé, J. and Trabandt, M. (2017). Should we use linearised models to calculate fiscal multipliers? European Economy - Discussion Papers 2015 - 064, Directorate General Economic and Financial Affairs (DG ECFIN), European Commission.

Liu, C. and Minford, P. (2014). Comparing behavioural and rational expectations for the US post-war economy. *Economic Modelling*, 43(C):407–415.

Mankiw, N. G., Reis, R., and Wolfers, J. (2004). Disagreement about Inflation Expectations. In *NBER Macroeconomics Annual 2003, Volume 18*, NBER Chapters, pages 209–270. National Bureau of Economic Research, Inc.

Massaro, D. (2013). Heterogeneous expectations in monetary DSGE models. *Journal of Economic Dynamics and Control*, 37(3):680–692.

Meyer-Gohde, A. (2014a). Dynare add-on for Risk-Sensitive Linear Approximations. QM&RBC Codes, Quantitative Macroeconomics & Real Business Cycles.

Meyer-Gohde, A. (2014b). Risky linear approximations. Technical report, SFB 649 Discussion Paper.

Miao, J. (2014). *Economic dynamics in discrete time*. MIT press.

Milani, F. (2007). Expectations, learning and macroeconomic persistence. *Journal of Monetary Economics*, 54(7):2065–2082.

Motto, R., Altavilla, C., and Carboni, G. (2015). Asset purchase programmes and financial markets: lessons from the Euro area. Working Paper Series 1864, European Central Bank.

Mumtaz, H. and Zanetti, F. (2013). The Impact of the Volatility of Monetary Policy Shocks. *Journal of Money, Credit and Banking*, 45(4):535–558.

Murray, L., Jones, E., and Parslow, J. (2012). On Disturbance State-Space Models and the Particle Marginal Metropolis-Hastings Sampler. *SIAM/ASA Journal on Uncertainty Quantification*, 1.

Muth, J. F. (1961). Rational expectations and the theory of price movements. *Econometrica*, 29(3):315–335.

Mutschler, W. (2015). Identification of DSGE models - The effect of higher-order approximation and pruning. *Journal of Economic Dynamics and Control*, 56:34 – 54.

Mutschler, W. (2018). Higher-order statistics for DSGE models. *Econometrics and Statistics*, 6:44 – 56. Statistics Of Extremes and Applications.

Noh, S. (2019). Posterior Inference on Parameters in a Nonlinear DSGE Model via Gaussian-Based Filters. *Computational Economics*.

Noh, S. (2020). The effects and origins of house price uncertainty shocks. *SSRN Electronic Journal*.

Pfajfar, D. and Santoro, E. (2010). Heterogeneity, learning and information stickiness in inflation expectations. *Journal of Economic Behavior and Organization*, 75(3):426–444.

Pitt, M. K. and Shephard, N. (1999). Filtering via simulation: Auxiliary particle filters. *Journal of the American Statistical Association*, 94(446):590–599.

Reis, R. (2021). Losing the inflation anchor. CEPR Discussion Papers 16664, C.E.P.R. Discussion Papers.

Rogers, J. H., Scotti, C., and Wright, J. H. (2018). Unconventional Monetary Policy and International Risk Premia. *Journal of Money, Credit and Banking*, 50(8):1827–1850.

Ruge-Murcia, F. (2012). Estimating nonlinear DSGE models by the simulated method of moments: With an application to business cycles. *Journal of Economic Dynamics and Control*, 36(6):914–938.

Ríos-Rull, J.-V., Schorfheide, F., Fuentes-Albero, C., Kryshko, M., and Santaeulàlia-Llopis, R. (2012). Methods versus substance: Measuring the effects of technology shocks. *Journal of Monetary Economics*, 59(8):826–846.

Sacht, S. (2014). Analysis of Various Shocks within the High-Frequency Versions of the Baseline New-Keynesian Model. Annual Conference 2014 (Hamburg): Evidence-based Economic Policy 100372, Verein für Socialpolitik / German Economic Association.

Särkkä, S. (2013). *Bayesian Filtering and Smoothing*. Cambridge University Press, USA.

Scalone, V. (2018). Estimating Non-Linear DSGEs with the Approximate Bayesian Computation: an application to the Zero Lower Bound. Working papers 688, Banque de France.

Schmitt-Grohé, S. and Uribe, M. (2004a). Optimal operational monetary policy in the Christiano-Eichenbaum-Evans model of the US business cycle. Technical report, National Bureau of Economic Research.

Schmitt-Grohé, S. and Uribe, M. (2004b). Solving dynamic general equilibrium models using a second-order approximation to the policy function. *Journal of economic dynamics and control*, 28(4):755–775.

Sims, C. A. (1980). Macroeconomics and reality. *Econometrica*, 48(1):1–48.

Sims, E. and Wu, C. (2020a). Are QE and Conventional Monetary Policy Substitutable? *International Journal of Central Banking*, 16(1):195–230.

Sims, E. and Wu, C. (2020b). Evaluating Central Banks' toolkit: Past, present, and future. *Journal of Monetary Economics*.

Sims, E., Wu, C., and Zhang, J. (2020). The Four Equation New Keynesian Model. Working paper.

Slobodyan, S. and Wouters, R. (2012). Learning in a Medium-Scale DSGE Model with Expectations Based on Small Forecasting Models. *American Economic Journal: Macroeconomics*, 4(2):65–101.

Smets, F. and Wouters, R. (2005). Comparing shocks and frictions in US and Euro area business cycles: a Bayesian DSGE Approach. *Journal of Applied Econometrics*, 20(2):161–183.

Smets, F. and Wouters, R. (2007). Shocks and Frictions in US Business Cycles: A Bayesian DSGE Approach. *American Economic Review*, 97(3):586–606.

Vats, D., Flegal, J. M., and Jones, G. L. (2019). Multivariate output analysis for Markov chain Monte Carlo. *Biometrika*, 106(2):321–337.

Wan, E. A. and van der Merwe, R. (2001). *The Unscented Kalman Filter*, chapter 7, pages 221–280. John Wiley and Sons.

Woodford, M. (2001). Fiscal Requirements for Price Stability. *Journal of Money, Credit and Banking*, 33(3):669–728.

Woodford, M. (2003). *Interest and Prices: Foundations of a Theory of Monetary Policy*. Princeton University Press.

Wu, J. C. and Xia, F. D. (2016). Measuring the Macroeconomic Impact of Monetary Policy at the Zero Lower Bound. *Journal of Money, Credit and Banking*, 48(2-3):253–291.

Wu, J. C. and Zhang, J. (2019). A shadow rate New Keynesian model. *Journal of Economic Dynamics and Control*, 107(C):1–1.

Yun, T. (1996). Nominal price rigidity, money supply endogeneity, and business cycles. *Journal of Monetary Economics*, 37(2-3):345–370.